AN ANALYSIS OF THE MITOCHONDRIAL FISSION FACTOR DRP1 ALONG WITH MITOCHONDRIAL PROTECTION GENES IN DROSOPHILA MODELS OF PARKINSON DISEASE

by

© AZRA HASAN B.Sc. M.Sc.

A Thesis submitted to the

School of Graduate Studies

in partial fulfillment of the requirements for the degree of

Doctor of Philosophy

Department of Biology

Memorial University of Newfoundland

October 2021

St. John's, Newfoundland and Labrador

Abstract

Parkinson disease (PD) is the second most common neurodegenerative disorder and is strongly associated with the accumulation of Lewy bodies and loss of dopaminergic (DA) neurons in the *substantia nigra* of brain. The pathophysiology includes bradykinesia, tremors, motor, autonomic and cognitive disorders. Mitochondrial dysfunction induced cellular stress and cell death is implicated as the cause of PD. Mitochondrial dysfunction causes unregulated mitochondrial dynamics (biogenesis to degradation), impaired metabolic functions, oxidative stress, loss of proteostasis and abnormal cell death. *Drp1* is crucial in mitochondrial dynamics and other functions, including apoptosis and mitophagy. To analyze the implication of altering the protein which affects mitochondrial health, I altered the expression of mitochondrial fission gene, *Drp1*; the transcription regulator, *Rbf*; mitophagy regulators *Pink1* and *parkin*, *Bcl-2* family genes *Buffy* and *Debcl,* Insulin receptor signalling genes *foxo* and *trbl* and increased disease risk gene *α-synuclein;* in DA neurons of Drosophila. I found that the altered expression of these key genes can have a beneficial, intermediate, and detrimental effect on the health of DA neurons as determined by lifespan and locomotor functions. Furthermore, I found that the overexpression and inhibition of *Drp1*, which encodes a mitochondrial fission protein, could suppress various PD like phenotypes in Drosophila.

Acknowledgements

I would like to thank my supervisor, Dr. Brian E. Staveley, for granting me the opportunity to pursue research as a doctoral student under his supervision. He has given me invaluable guidance and financial support during the degree. I would like to thank Dr. Suzanne Dufour and Dr. Julissa Roncal for their continuous support and advice as committee members. I would like to thank Dr. Dylan Goudie for his assistance with SEM imaging and members of Staveley lab for tremendous motivation and assistance throughout my doctorate. Additionally, I would like to thank the members of my examination committee for their valuable input. I would like to acknowledge support during this program from the Natural Sciences and Engineering Research Council of Canada (NSERC) Discovery Grant Program and the Aging Research Centre of Newfoundland and Labrador (ARC-NL) Research Grant Program to Dr. Brian E. Staveley, Memorial University of Newfoundland School of Graduate Studies Baseline Funding and Memorial University of Newfoundland Department of Biology Assistantships.

Heartfelt gratitude to my family, especially my parents, for giving me much-needed support and encouragement to fulfill all hopes and dreams. Finally, I would like to thank my partner for all the coffees, dinners, and love to finish this degree.

Dedication

This thesis is dedicated to my mother, she is always the source of strength to me.

Co-Authorship Statement

The following statement clarifies the roles played by the authors in the manuscript chapters of this thesis, 2 to 9 accordance with the requirements of the School of Graduate Studies. My role in the completion of these manuscript chapters is defined with respect to the following categories:

i) Design and identification of the research proposal

BES initiated the research project by setting the research goal to investigate the effects of altered expression of different mitochondrial genes in the Drosophila model of Parkinson disease. AH identified the mitochondrial fission gene as a prime candidate with critical review from BES. All experiments in Chapters 2,3,4,5,6,7,8, and 9 were initiated, conceived, and designed by AH with critical review provided by BES

ii) Practical aspects of the research: AH completed the generation of the recombinant double mutants. AH carried out all biometric analysis, longevity and survivorship assays. Chapter 7: Kayla Patten initiated the experiments of this chapter; however, later repeated by AH. AH carried out all experiments.

iii) Data analysis: AH collected and analyzed all data.

iv) Manuscript preparation: All manuscripts were prepared by AH with critical review from BES

Table of Contents

List of Figures

List of Tables

List of Abbreviations

AIF - Apoptosis-inducing factor

Ambra1 - Autophagy and Beclin 1 Regulator 1

ATF4 - Activating Transcription Factor 4

ATF6 - Activating Transcription Factor 6

Bcl-2 - B-cell lymphoma-2

Bax - Bcl2 Associated X, Apoptosis Regulator

BNIP3 - Bcl2 Interacting Protein 3

CHOP - transcriptional factor C/EBP homologous protein

Ddc - Dopa decarboxylase

DNM1L – Dynamin-1-like protein

Drp1 – Dynamin-related protein 1

dsRNA - double-stranded RNA

eIF - eukaryotic translational initiation factor

ER - Endoplasmic Reticulum

ERAD - ER-Assisted Degradation

ETC - Electron Transport Chain

Fis1- Mitochondrial fission 1 protein

Foxo - Forkhead box transcription factors

GMR – Glass Multiple Reporter

GWAS - Genome Wide Association Study

IGF-1 – Insulin-like Growth Factor-1

IMM – Inner mitochondrial membrane

IRE1α - Inositol-Requiring Transmembrane Kinase/Endoribonuclease 1

IP3Rs - Inositol 1,4,5-triphosphate Receptors

JNK - c-Jun-N-terminal kinase

LRRK2 - Leucine-rich repeat kinase 2

MFN - Mitofusin

miRNA – micro-RNA

MPPP - Desmethylprodine or 1-methyl-4-phenyl-4-propionoxypiperidine

MPTP - 1-methyl-4-phenyl-1,2,3,6-tetrahydropyridine

MOMP - Mitochondrial Outer Membrane Permeabilization

mtDNA – Mitochondrial DNA

OPA1 - Optic atrophy type 1

polyQ - polyglutamine

PERK - Protein Kinase RNA-like Endoplasmic Reticulum Kinase

PINK1- PTEN-induced kinase 1

PTP - Permeability Transition Pore

Rb - Retinoblastoma protein

pRb – phosphorylated Retinoblastoma protein

Rbf - Retinoblastoma family protein

ROCK - Rho-associated protein kinase

RNAi - RNA interference

ROS - Reactive Oxygen Species

SNpc - Substantia nigra pars compacta

siRNA - small interfering RNA

TNFα - Tumor Necrosis Factor alpha

TOR - Target of Rapamycin

UAS - Upstream Activator Sequence

UPR - Unfolded Protein Response

VPS - Vacuolar protein sorting

XBP-1 - X-box binding protein 1

6-OHDA - 6-hydroxydopamine or 2,4,5-trihydroxyphenethylamine

Chapter 1: Introduction and Overview

1.1 Ageing and Parkinson disease

Ageing is a complex biological process, commonly associated with a continuous decline in the ability of a cell, a tissue, or an organism to perform essential routine functions in an efficient manner. Theories of ageing suggest that the accumulation of molecules which have been damaged through the activities of reactive oxygen species (ROS) are primary cause of age-related decline (Harman 1991; Kirkwood and Kowald 2012; Sergiev et al. 2015). ROS production and the associated oxidative damage increase as organisms age (Lambert et al. 2007), while a reduced level of ROS production and oxidative damage can increase the organism's lifespan. Several cellular processes produce ROS; however, the electron transport chain (ETC) of mitochondria appears to be the leading site of the cellular production of ROS. (Murphy 2009). Consequently, the dysfunction of mitochondria is characterized by unregulated mitochondrial dynamics, including biogenesis and degradation of the organelle network, the loss of proteostasis, the impairment of metabolic function and the subsequent occurrence of abnormal cell death: all of which are hallmarks of ageing (Cui et al. 2012; Rottenberg and Hoek 2017). The association of ageing with Parkinson disease (PD) has been known for a long time, and ageing is considered a primary risk factor in developing PD and other neurodegenerative disorders (Sulzer 2007; Collier et al. 2011). Mitochondrial dysfunction plays a significant part in the onset of ageing and age-related neurodegenerative disorders.

The etiology of PD is multifactorial and involves the interplay of several genes identified to cause neurodegenerative disease and various environmental factors. PD is known as a “disease of older people” because only 4% of the cases are diagnosed prior to 50 years of age. The majority of PD symptoms involve impaired motor function, which includes resting tremors, bradykinesia or akinesia, muscular rigidity, and impaired balance; the non-motor symptoms include anxiety,

depression, and cognitive and sleep disorders. The pathophysiology of PD is characterized by the substantial loss of dopaminergic (DA) neurons in the substantia nigra pars compacta (SNpc) area of the human midbrain (Davie 2008; Lees et al. 2009), and presence of Lewy Bodies (LB) and Lewy neurites (LN) in the surviving neurons (Recasens and Dehay 2014). The LB and LN are comprised of the intracytoplasmic proteinaceous inclusions of abnormally phosphorylated α-synuclein, ubiquitin, and associated neurofilament proteins in nerve cells (Spillantini et al. 1997; Ghosh et al. 2017). Genes identified for familial PD encode mitochondrial proteins (e.g., PINK1, DJ-1, Omi/HtrA2 and POLG), organelle trafficking and vesicular fusion proteins (e.g., α-synuclein, and tau), ubiquitination pathway proteins (e.g., parkin and DJ-1), and oxidative stress proteins (Sulzer 2007). However, often cases of familial Parkinson have sporadic influences such as environmental factors which cause oxidative stress, mitochondrial dysfunction, and inflammation along with ageing (Calne and Langston 1983; Modi et al. 2016). These observations are supported by twin studies, which attempted to distinguish the risk associated with genetics and the environment in the onset of PD. (Domingo and Klein 2018; Balck et al. 2019). Further research will shed light on cause, diagnosis, and treatment of PD.

1.2 *Drosophila melanogaster*: a model organism for research into PD and ageing

Drosophila melanogaster is a versatile model organism that has been extensively used to study ageing and age-related disorders. The fundamental cellular pathways are highly conserved among all eukaryotes (Lander et al. 2001). As a model organism, *Drosophila melanogaster* provides several advantages due to its short lifespan, low maintenance, non-problematic breeding, and a large number of offspring. The neurodegeneration, mitochondrial protection, metabolic, and signalling pathways are evolutionarily conserved in Drosophila (Sun et al. 2013). Genetic

manipulation is easy, and mutant models of flies are readily available. The first report of a single gene mutation that extended the lifespan of an organism was the insulin signalling pathway (IGF-1) originally in worms and subsequently in flies and mouse models (Kimura et al. 1997; Tatar et al. 2001; Holzenberger et al. 2003). Drosophila have orthologous genes and a conserved IGF-1 pathway. The complex central nervous system of flies with neurons, glia cells, and protection of the blood-brain barrier is an asset to study neurons and neurodegenerative disorders (Cajal and Sanchez 1915; Sanes and Zipursky 2010). A confirmed neurodegenerative phenotype was observed in flies about a half-century ago: the brains of *drop-dead* (*drd*) mutants were determined to undergo an evident degeneration and had a shorter lifespan (Benzer 1971). The first PD model was established in flies by expressing the human *α-synuclein* gene in selective sets of neurons, which deteriorated the fly neurons in 20 to 30 days. The molecular analysis showed LB-like inclusions made by denatured cellular proteins (Feany and Bender 2000). *Drosophila melanogaster* has an orthologue for many of the genes being studied for ageing, and neurodegenerative disorders (Feany and Bender 2000). Flies provide a simple yet evolutionary-conserved model to study the array of fundamental processes inclusive in ageing and neurodegenerative disorders.

1.3 Molecular mechanism of ageing

The molecular hallmarks of ageing are genomic instability, telomerase attrition, epigenetic alteration, proteostasis loss, unregulated nutrient sensing, mitochondrial dysfunction, stem cell exhaustion, cellular senescence, and altered intercellular communication (López-Otín et al. 2013). These hallmarks are not due to individual malfunctioning mechanisms but due to the impairments

in multiple pathways. The various cellular pathways interact with each other like a web and contribute to the function and dysfunction of cells (Kowald and Kirkwood 1996). A lot of these pathways affect mitochondrial functioning, and mitochondrial dysfunction decreases their efficiency (López-Otín et al. 2013; Nicolson 2014). Ageing has been associated with mitochondrial dysfunction ranging from its biogenesis, recycling, mitophagy, dynamics, Unfolded Protein Response mitochondria (UPRmt), and mitochondrial DNA (mtDNA) mutation (Chistiakov et al. 2014; Diot et al. 2016; Shpilka and Haynes 2018). The molecular mechanism of ageing is complex and cannot be defined in one pathway, but the cumulative decline in the efficiency of cellular pathways and mitochondrial health has a significant role.

1.3.1 Theories of ageing

Broadly, there are two main categories of theories employed to explain the process of ageing: the first theorizes ageing because of the "wear and tear" on the cells, which accumulate over time and lose efficiency to repair themselves, leading to the accumulation of damage; the second postulates that ageing is a pre-programmed progression directed by inheritance and organismal DNA (Longo *et al.* 2005; Sergiev *et al.* 2015). The "wear and tear" theory proposes that the efficiency of a cell to perform functions decreases due to errors and damages accumulated over time. In 1954, Dr. Denham Harman outlined the free radical theory of ageing, which proposed oxidative damage of the macromolecules due to ROS as the cause of ageing (Harman 1991). Later accumulation of cross-linking protein has been identified in damaged cells, and further experimental evidence confirmed the role of cross-linking proteins in age-related changes (Bjorksten and Tenhu 1990). All the developments in the wear and tear theory unravel one of the possible mechanisms of ageing. The pre-programmed theory of ageing proposes a pre-programmed switch on and off

different genes as biological clocks progress. (Davidovic et al. 2010). Recent studies show that hormones regulate biological clocks through evolutionarily conserved pathways (van Heemst 2010; Diamanti-Kandarakis *et al.* 2017). Abundant studies show that the efficiency of the immune system peaks at puberty and declines with age (Fulop et al. 2014). This theory is categorized as a programmed theory of ageing, but continued research is required as the decreased efficiency of the immune system could be due to the accumulated wear and tear. The acceptance of the former theory is more than the latter (Jin 2010). A Genome-Wide Associate Studies (GWAS) of nonagenarians found a similar number of disease risk alleles of diabetes, cancer and cardiovascular disease as young controls (Beekman et al. 2010). One possibility is that the long-lived individuals have a much more efficient set of protective genes which contribute to the cellular defence mechanisms to counteract cellular stresses such as forkhead box O (foxo) (Broer et al. 2015; Martins et al. 2016). The combination of the two theories better explains the experimental evidence of ageing.

1.3.2 Historical molecular models of ageing

The first pathway that was found to influence ageing and doubled *C. elegans* lifespan is part of the IGFs signalling pathway. The lower IGF-1 signalling in IGF-1 knockouts and variants has been associated with longevity in mice models and humans (Holzenberger et al. 2003; Yuan et al. 2009; Tazearslan et al. 2012). Similarly, inhibition of TOR signalling increases the lifespan of both simple and complex eukaryotes (Jia et al. 2004; Harrison et al. 2009). TOR signalling regulates the metabolism and growth of cells in response to environmental cues such as calorie restriction. The IGF-1 and TOR signalling are district pathways in *C. elegans* but share common intermediates in complex eukaryotes (Balasubramanian and Longo 2016). Both pathways alter cellular resistance

towards different stresses. The dietary restriction increases mitochondrial respiration, inhibits different cellular pathways such as IGF-1 and mTOR, and increases lifespan. (Zid et al. 2009; Kapahi et al. 2017). Inhibition of respiration is another way to attain longevity in eukaryotes, contrary to the fact that respiration promotes longevity during calorie restriction (Copeland et al. 2009). Perhaps the longevity attained in these diverse situations is the result of two separate pathways.

1.4 Molecular mechanism of PD and neurodegenerative disease.

Pathologically, PD is characterized by degradation of DA neurons in SNpc and accumulation of LB and LN in nearby neurons (Davie 2008; Lees et al. 2009; Recasens and Dehay 2014). The LB and LN are the protein aggregates of malfunctioned neuronal proteins, mainly α-synuclein. The α-synuclein protein has a mitochondrial targeting signal and is found associated with complex1 in PD brain; when overexpressed, α-synuclein increases ROS production and reduces complex I efficiency (Devi et al. 2008). Additionally, the expression of *α-synuclein* in neurons causes mitochondrial fragmentation which leads to respiratory decline and cell death (Nakamura et al. 2011). Different forms of PD have been found to overexpress *α-synuclein*. The regulators of mitophagy Pink1 and parkin, loss of function also causes the parkinsonian phenotype (Cookson 2012). The Pink1 and parkin protein function is the same pathways and one can rescue others inhibition phenotype (Pickrell and Youle 2015). The loss of *Pink1* and *parkin* can be rescued by mitochondrial fusion gene expression or mitochondrial fission gene knockdown in human SH-SY5Y cells (Kathrin Lutz et al. 2009). The cause of PD highlights the loss of DA neurons due to oxidative stress caused by dysfunctional pathways such as accumulation of misfolded protein, dysfunctional protein clearance pathway, mitochondrial dysfunction, neuroinflammation, or genetic mutation.

1.4.1 Theories of PD

Multiple theories have been proposed for the cause or onset of PD. The onset of PD is dependent on multiple factors: genetics, lifestyle, and environment (Obeso et al. 2010; Kalia and Lang 2015; Collier et al. 2017). The mutation in *α-synuclein*, *Parkin, Pink1, LRRK2* (Leucine-rich repeat kinase 2)*,* and *DJ-1* genes have been associated with PD. The mutation and multiplication of *α-synuclein* gene leads to the formation of *α-synuclein* aggregates or fibrils, which interfere with the intracellular function (Kalia et al. 2013). Earlier theories focused on the correlation of ageing and PD and used ageing theories like free radical and neuromelanin to explain the onset of PD (Langston 1989). A similar theory proposed that environmental toxins damage the SNpc and cause loss of DA neurons (Langston 1989). Recently PD has been proposed to be a prion-like disease; the intracerebral injection of preformed *α-synuclein* fibrils or brain homogenate of mice expressing mutant *α-synuclein* triggered the clinical signs of early onset of PD (Luk et al. 2012; Mougenot et al. 2012; Walsh and Selkoe 2016). In 2003, Braak et al. proposed ascending and spreading disease theory for sporadic PD. Braak proposed an unknown pathogen causes PD, and once microbial molecules come in contact with enteric neurons, it triggers the aggregation of α-synuclein. The α-synuclein aggregates spread from peripheral nervous system towards the central nervous system (Braak et al. 2003). Various studies defy the idea of ascending gradient theory because some studies found that the α-synuclein accumulation is more prevalent in the spinal cord than the vagus nerve and gastro-intestinal tract (Kalaitzakis et al. 2008; Beach et al. 2010); and the degeneration of SNpc in the absence of LB and Lewy pathology presence in the vagal nucleus (Wakabayashi et al. 1999). Keeping this in mind, a threshold theory has come which proposed parallel degeneration of both the Central nervous system and peripheral nervous system

(Engelender and Isacson 2017). Experimental models and theories bring us closer to understand PD pathology.

1.4.2 Historical molecular models of PD.

PD is a neurodegenerative disease. Therefore, the molecular models of PD were primarily focused on the degeneration of DA neurons by different neurotoxins or genetic mutations. The 6-OHDA (6-hydroxydopamine or 2,4,5-trihydroxyphenethylamine) is a neurotoxin is a organic compound that is found to accumulate in patients suffering from PD. Exposure to neurotoxin is analogue to oxidative stress and respiratory inhibition (Schober 2004). Another neurotoxin was discovered accidentally when people ingested MPTP due to contamination in MPPP (Desmethylprodine). The people who accidentally ingested MPTP (1-methyl-4-phenyl-1,2,3,6-tetrahydropyridine) developed symptoms similar to PD (Langston et al. 1983). Agricultural pesticides and herbicides have been reported to increase PD risk in the exposed population. (Kamel 2013; Tinakoua et al. 2015). Exposure to these neurotoxins imitates the pathophysiology of PD.

The genetic mutations identified in familial PD is used to model the disease phenotype. The SNCA (α-synuclein) was the first mutant gene identified to be associated with PD, and the α- synuclein protein is an essential component of the LB aggregates (Spillantini et al. 1997; Polymeropoulos et al. 1997). A number of PD models, complete with distinctive PD pathophysiology, have been produced with loss-of-function or overexpressed versions of the α-synuclein gene (Magen and Chesselet 2010; Javed et al. 2016). The mutation in genes that encode the mitochondrial-associated proteins Pink1, Park, DJ-1 and Omi/HtrA2 in eukaryotic models produce phenotypes that mimic aspects of the disease (Sulzer 2007). Although the LRRK2 gene is altered in some familial forms of PD, only a few transgenic models successfully replicated PD (Niu et al. 2012; Blesa

and Przedborski 2014). Few models listed here, and numerous other PD models have been developed over time by altering different cellular pathways to study PD.

1.5 Factors affects ageing and neurodegenerative disease.

The molecular mechanisms and signal transduction pathways responsible for many aspects of ageing and neurodegenerative disease are quite diverse. Mitochondrial dysfunction, loss of proteostasis, calcium homeostasis, oxidative stress, DNA damage, unregulated nutrient sensing, inefficient autophagy, and apoptosis appear to be responsible for the comprehensive causes of ageing.

1.5.1 Mitochondrial dysfunction

Mitochondrial function has been studied extensively during the past few decades due to a clear relationship with ageing and age-related diseases. The mitochondrion is commonly known as the "powerhouse of the cell" as the prime site for aerobic respiration. The inner mitochondrial membrane (IMM) has an ETC comprised of four complexes: Complex I (NADH dehydrogenase), Complex II (succinate dehydrogenase); Complex III (cytochrome bc1 complex) and Complex IV (Cyt-c oxidase). These complexes reduce and oxidize simultaneously to transport electrons; these reactions are coupled with proton transfer across the membrane, thus creating an electrochemical proton gradient that drives ATP production. Mitochondria are vital in various cellular processes, other than ATP production; mitochondria sequester Ca^{2+} ions to keep the proper concentration of Ca^{2+} ions in the cytoplasm (Babcock and Hille 1998; Contreras et al. 2010); the production sites of many steroid hormones such as testosterone, estrogen, progesterone, and cortisol (Miller 2013). Mitochondria have a crucial role in producing the heme part of hemoglobin (O_2 and CO_2 carrier)

(Medlock et al. 2015); are essential regulator of programmed cell death, primarily intrinsic apoptosis (Green and Reed 1998; Wang and Youle 2009); required for signalling through ROS (Sena and Chandel 2012). Mitochondrial phosphatases and kinases regulate metabolism (McBride et al. 2006); active role in innate and adaptive immune response (Mills et al. 2017); and liver mitochondria have an enzyme that detoxifies ammonia (Esposti et al. 2012). In addition to being the powerhouses, mitochondria have a vital role in numerous cellular processes, specifically pathways responsible for cell death and cell survival.

1.5.1.1 Intrinsic Apoptosis

Apoptosis, or programmed cell death, is critical for normal cellular function to eliminate infected, damaged, or unwanted cells. Apoptosis is characterized by cell shrinkage, membrane budding, chromatin aggregation, nuclear fragmentation, loss of plasma membrane integrity, caspase activation, and apoptotic body formation (He et al. 2009). Apoptosis is vital for development, such as the formation of digits; defence mechanism against inflammation and cancerous cells; and senescence or ageing (Scheffler 2008). The signal that initiates the apoptotic cascade can be of two different types, extrinsic signals received on cell surface receptors, such as Fas or TNF receptors, and intrinsic non-receptor mediated signals received internally, such as damaged DNA or chromosome rearrangement. Intrinsic and extrinsic pathways share common intermediates, and either may influence one another (Igney and Krammer 2002). The mitochondria primarily regulate cell-autonomous or intrinsic apoptosis (Parsons and Green 2010). Caspases are enzymatic proteases that have an essential role in apoptosis. The caspases are constitutively expressed at a basal level as pro-caspases, activated once cleaved at specific aspartate residue (Parsons and Green 2010). The proteolytic cleavage occurs as a cascade of reactions to activate all pro-caspases

before they assemble into active proteases. The *ced9* mutation in *C. elegans* led to the characterization of the homologue the Bcl-2 (B-cell lymphoma-2) proto-oncogene (Hengartner & Horvitz, 1994). The caspases are activated by a Bcl-2 protein family, which can initiate or inhibit mitochondrial apoptotic progression. The whole family of a Bcl-2 genes are localized to the outer mitochondrial membrane (OMM) and cytoplasm (Hengartner and Robert Horvitz 1994). Bcl-2 family members are broadly classified as either pro-apoptotic such as Bcl-2, Bcl-xl, Mcl-k or anti-apoptotic such as Bad, Bak, Nix, Binp3 or Bax proteins depending on their function. To initiate apoptosis, Bax and Bak, the pro-apoptotic members of the Bcl-2 family, mediate mitochondrial outer membrane permeabilization (MOMP) (Hardwick and Soane 2013). The MOMP releases inter-mitochondrial space proteins such as Cyt-c, apoptosis-inducing factor (AIF), and endonuclease G, and increases the production of ROS (Galluzzi et al. 2012). The Cyt-c and Apaf activate caspase 9, which, in turn, initiates the apoptotic cascade to activate executioner caspases (Galluzzi et al. 2012). Cells are equipped with various mechanisms to establish homeostasis; however, if the damage is irreversible, intrinsic apoptosis is initiated to favour organismal survival.

Bcl-2 family protein in intrinsic apoptosis.

The signal required for the activation of caspases comes from the presence of Cyt-c, a protein present in the mitochondrial intermembrane space (IMS). In the cytosol, Cyt-c interacts with Apaf-1 to form a multimeric protein complex known as the “apoptosome” in the presence of ATP. The apoptosome acts to cleave the initiator pro-caspase, start the cascade of caspase activation and activating the executioner caspases 3 and 7 (Parsons and Green 2010). The Cyt-c independent pathway of apoptosis involves proteins mitochondrial IMS proteins such as Apoptosis-inducing factor (AIF) and endonuclease G. The release of Cyt-c by MOMP can occur by various mechanisms such as mitochondrial permeability transition pore (PTP) or Bcl-2 family protein assisted MOMP

(Gogvadze et al. 2006). Stress activates pro-apoptotic Bcl-2 family members such as Bax or Bak and forms the ion channel in the isolated mitochondrial outer membrane *in vitro* (Schlesinger et al. 1997). Before the monomeric Bax or Bak's oligomeric assembly, they are activated by either protein modification or Bid, another pro-apoptotic Bcl-2 family protein. The permeabilization of a mitochondrial outer membrane with the help of Bcl-2 family proteins releases IMS proteins such as Cyt-c and AIF into the cytosol (Green and Kroemer 2004). Bcl-2 family proteins plays central role in the progression of intrinsic apoptosis by MOMP.

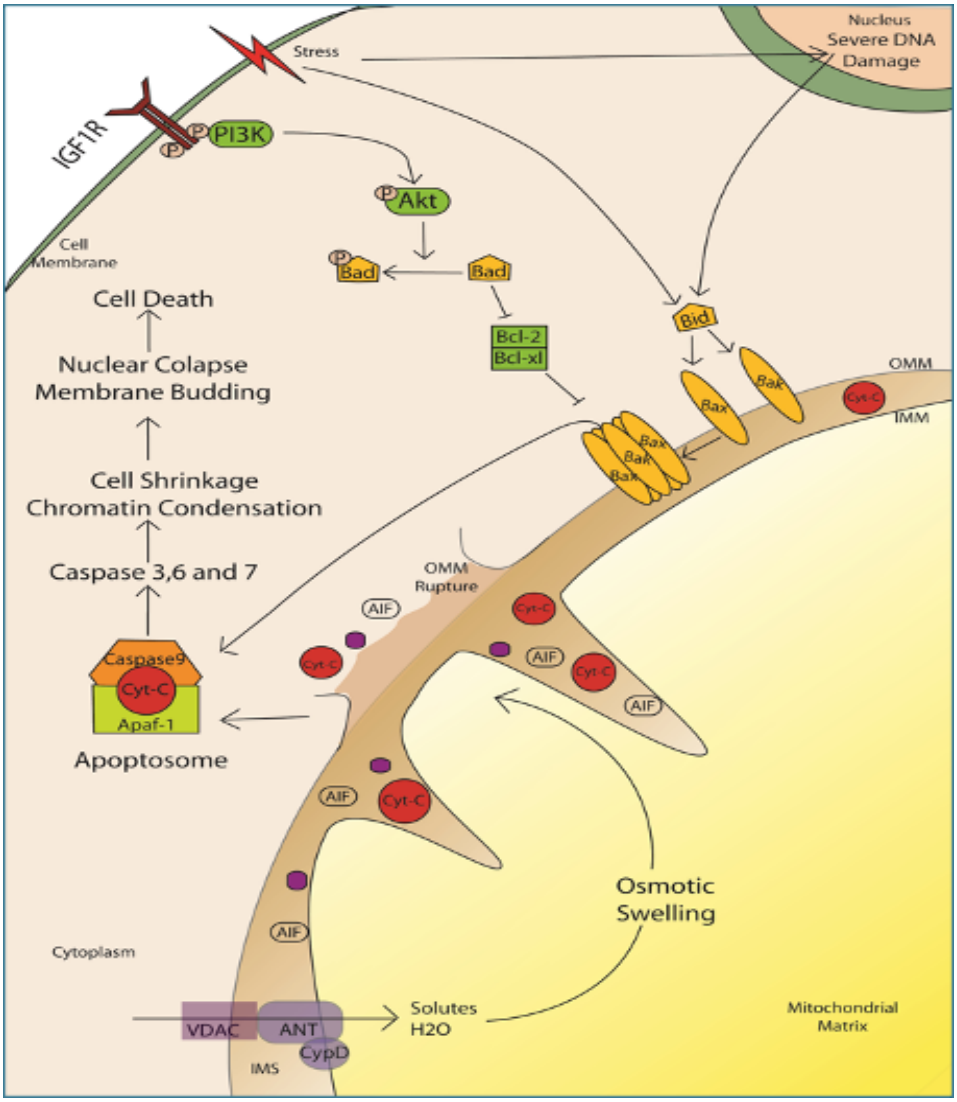

Figure 1.1 Intrinsic Pathway of Apoptosis. Mitochondria plays a central role in the intrinsic and extrinsic pathways of apoptosis. The formation of MOMP in OMM by the oligomerization of pro-apoptotic Bcl-2 family gene or PTP cause the release of inter mitochondrial membrane protein such as Cyt-c and AIF and triggers apoptosis. (This Figure is generated by author using Adobe Illustrator CS6)

1.5.1.3 Mitophagy – Pink and parkin.

Mitophagy alleviates the effect of dysfunctional mitochondria on the whole mitochondrial network and promotes cell survival. Autophagy is active consistently at a basal level to regulate the turnover of long-lived proteins and organelles. Recent studies have demonstrated a correlation between the process of mitophagy, ageing, and several age-related diseases

(Chistiakov et al. 2014). The role of cytosolic E3 ubiquitin ligase Parkin in the degradation of defective mitochondria has shed on its role in PD. The PTEN-induced putative kinase1 (Pink1)/Parkin pathway functions in the regulation of mitophagy (Bingol and Sheng 2016). In healthy mitochondria, Pink1 is imported, and its N-terminal mitochondrial signal sequence is cleaved and degraded by mitochondrial proteases. Successful Pink1 import signifies mitochondrial health. In unhealthy mitochondria, the Pink1 import fails, and protein starts to accumulate at the mitochondrial surface. Experimentally Pink1 accumulation on the surface can be triggered by mitochondrial depolarization, overexpression of misfolded mitochondrial proteins, or PINK1 overexpression. Accumulated Pink1 autophosphorylate and dimerize to activate its serine/threonine kinase activity (Okatsu et al. 2013; Aerts et al. 2015). The activated Pink1 phosphorylates ubiquitin, which then acts to recruit the Parkin (Koyano et al. 2014). Parkin performs the ubiquitination of OMM proteins and signals autophagosome assembly (Bingol and Sheng 2016). This implies that any disturbance in the Pink1/Parkin pathway affects mitochondrial quality and function.

The nucleation of the phagophore (Figure 1.2) starts with the assembly of Beclin-1, vacuolar sorting protein 34 (VPS34), and VPS15 protein (Kubli and Gustafsson 2012). Beclin1 and Ambra1 (Autophagy and Beclin 1 Regulator 1) are released from a close association of Bcl-2 family members proteins. Ambra1 activates the Beclin1-VPS34-VPS15 complex to allow the formation of the phagophore. Expansion of the phagophore is mediated by the ATG-12-ATG5-ATG16 and LC3 complex until the phagophore complex encircles the mitochondria. The mature autophagosome fuses with the lysosome to degrade the organelle or protein cargo. Loss of function of Parkin and Pink1 imitates the PD phenotype (Kawajiri et al. 2011 Rana et al. 2013; Githure and Staveley

2017d). Other than basal mitochondrial turnover, mitophagy is required under certain physiological (maturation of erythrocytes) or stress response (to eliminate damaged mitochondria) situations. There is enough evidence to show that increased autophagy delays ageing in flies and mammals by the mTOR pathway, as described earlier (Wu et al. 2013; Ulgherait et al. 2014). The rate of mitophagy markedly decreases by approximately 70% with age in mice (Sun et al. 2015). Moreover, Pink1 and parkin facilitate the Drp1 mediated mitochondrial fission prior to mitophagy. The parkin-mediated mitochondrial fission is partly independent of Pink1 and dependent on Drp1 phosphorylation (Buhlman et al. 2014). The autophagy of mitochondria or mitophagy is a cellular process that promotes the turnover of mitochondria.

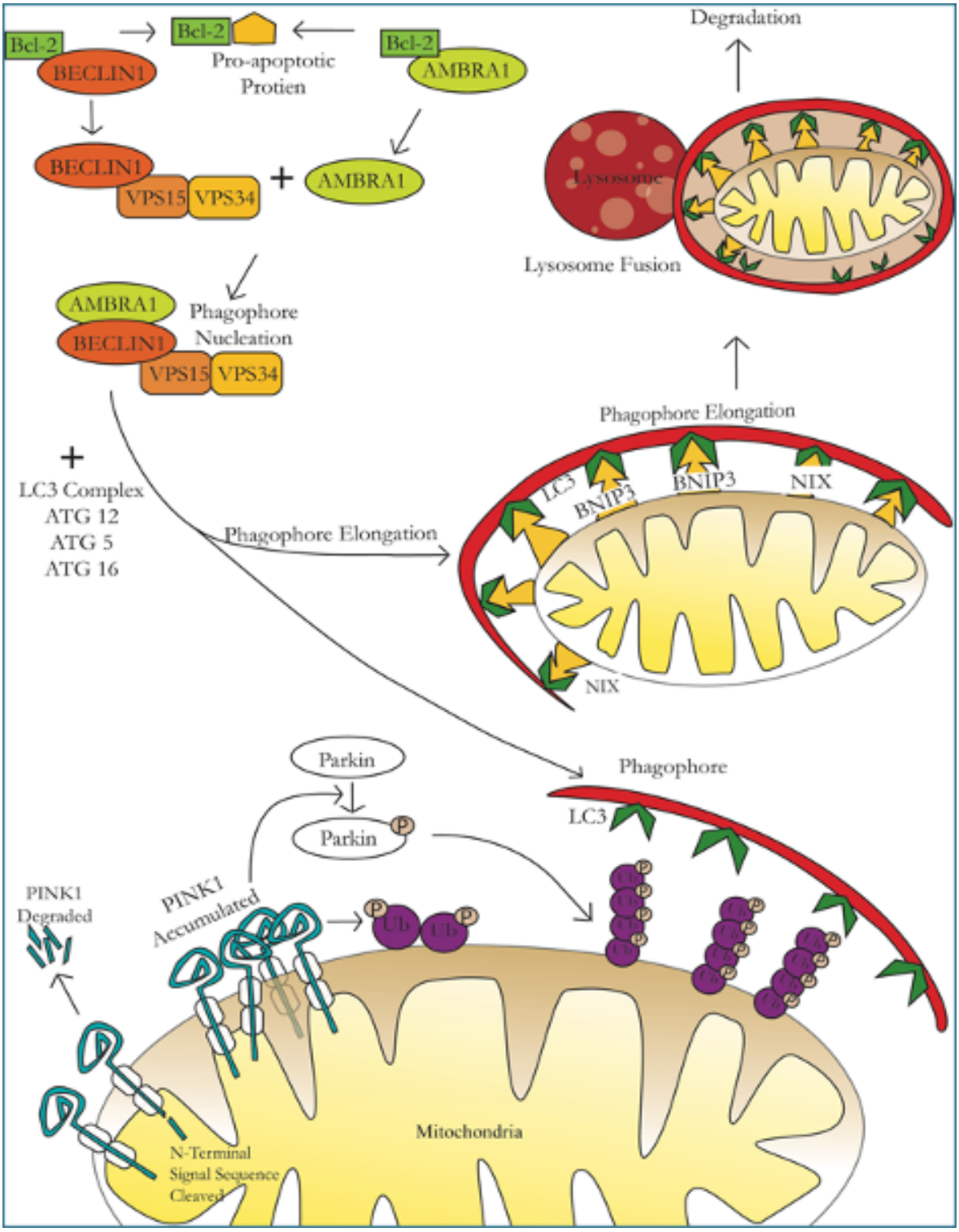

Figure 1.2 Autophagy of Mitochondria. Mitophagy is activated at the basal level in healthy cells, it can be ubiquitin-dependent or independent. The Pink1 and parkin proteins play central role in mitophagy regulation. (This Figure is generated by author using Adobe Illustrator CS6)

1.5.1.4 Mitochondrial dynamics *Drp1*

The regulation and maintenance of mitochondrial dynamics are important for maximizing mitochondrial function and health. Drp1 (Dynamin-related protein 1), a nuclear coded fission protein, which polymerises and forms a spiral structure around the outer membrane of mitochondrial tubule and utilises a GTPase activity to aid in the contraction and fragmentation of the mitochondrial tubules (Ingerman et al. 2005; Mears et al. 2011). The process of fusion is achieved by the activity of the mitofusin protein's position at the OMM with the help of SNARE proteins (Koshiba et al. 2004). The OPA1 mediates IMM fusion by a GTPase activity sequentially after OMM fusion (Song et al. 2009). The mitochondrial membrane potential partly regulates the fission and fusion of mitochondria. High membrane potential can promote fusion, while a low membrane potential acts to obstruct fusion (Twig et al. 2008). The mitochondrial fission and fusion are induced under very different circumstances.

Mitochondrial fission and fusion are regulated by a combination of factors and signal transduction pathways. The Bcl-2 family protein, Bax, present in cytosol, positively regulates mitochondrial fusion through interaction with MFN2 (Hoppins et al. 2011). Bax recruits the Drp1 protein to the OMM to promote mitochondria fragmentation in response to apoptotic stimuli (Frank et al. 2001; Wu et al. 2011). Bax has been found to co-localize with MFN2 and Drp1 on the OMM during the initiation of apoptosis (Karbowski et al. 2002). Bax does not act alone to induce Drp1 in the initiation of mitochondrial fragmentation, as Pink1 and parkin participate in the recruitment of Drp1 during mitophagy (Buhlman et al. 2014). Mitochondrial fission induced in response of UV irradiation may instigate apoptosis by recruiting Drp1. (Zhang et al. 2016). The role of Drp1 is important in one of the many of the processes that initiate apoptosis and the release of Cyt-c from

IMS (Clerc et al. 2014). Decreased mitochondrial fission leads to ageing due to the accumulation of damages in mitochondrial network (Lee et al. 2007). However, increased expression of Drp1 increases the ROS levels in mitochondria (Nagdas and Kashatus 2017). The overall influence of mitochondrial dynamics on cellular processes varies greatly.

1.5.1.4 Electron Transport Chain and Reactive Oxygen Species

ROS is a term used to collectively refer to the oxygen radicals, highly reactive oxygen containing molecules that possess unpaired electrons (Halliwell' and Cross 1994). ROS production ranges from 0.1 to 4% of the consumed oxygen in cell (Trifunovic and Larsson 2008). According to Denham Harman, free radical theory of ageing, ROS may cause oxidative damage, especially in mitochondria, and aid cell death (Kirkwood and Kowald 2012). Mitochondria have at least eleven sites where ROS production may occur, each with the distinct capacity to result in "electron leaking" (Wong et al. 2017). Both Complex I and Complex III of the ETC are subject to large changes in potential energy of electrons that may be lost to oxygen or H_2O_2 during the process of electron transfer. Coenzyme Q, which serves as an electron carrier from Complex I and II to Complex III, seems to play a primary role in the loss of electrons from the ETC (Raha et al. 2000; Muller et al. 2004; Hirst et al. 2008). Cells have ROS detoxifying enzymes such as SOD1, SOD2, monoamine oxidase, glutathione peroxidase, and catalase to minimise the damage (Andreyev et al. 2005; Bułdak et al. 2014; Edmondson 2014). Although cells have a number of approaches to minimise oxidative damage, oxidative stress can supersede the detoxifying capacity of cells to result in cellular damage.

The unstable nature of ROS may create changes to nearby molecules. Specially ROS can cause damage to mitochondrial DNA, lipids, proteins, and other macromolecules in mitochondria

primarily due to the proximity of these molecules to the mitochondrial site of origin (Wiseman and Halliwell 1996; Santos et al. 2018). Experimental evidence suggests that the reduction of negative influence upon cells through reduced ROS levels may be beneficial in the extension of the lifespan of the organism (Lambert et al. 2007; Cochemé et al. 2011). However, in a case of mito-hormesis, low levels of ROS result in beneficial effects, such as an increase in lifespan, and functions as a signalling molecule (Sena and Chandel 2012; Ristow and Schmeisser 2014). Hormesis is a biphasic response by the cell or organism to a substance or condition. It is characterized by a beneficial effect at low dosages and a toxic or inhibitory outcome at higher levels. Studies have shown that the scavenging of ROS during differentiation may retard the developmental processes, while an increase in the production of ROS may improve the developmental process (Owusu-Ansah and Banerjee 2009). The presence of ROS in the mitochondria seems to be a requirement in the activation of autophagy (Scherz-Shouval et al. 2007). The ROS cannot be labelled toxic since it is crucial in carrying out housekeeping steps like autophagy and apoptosis.

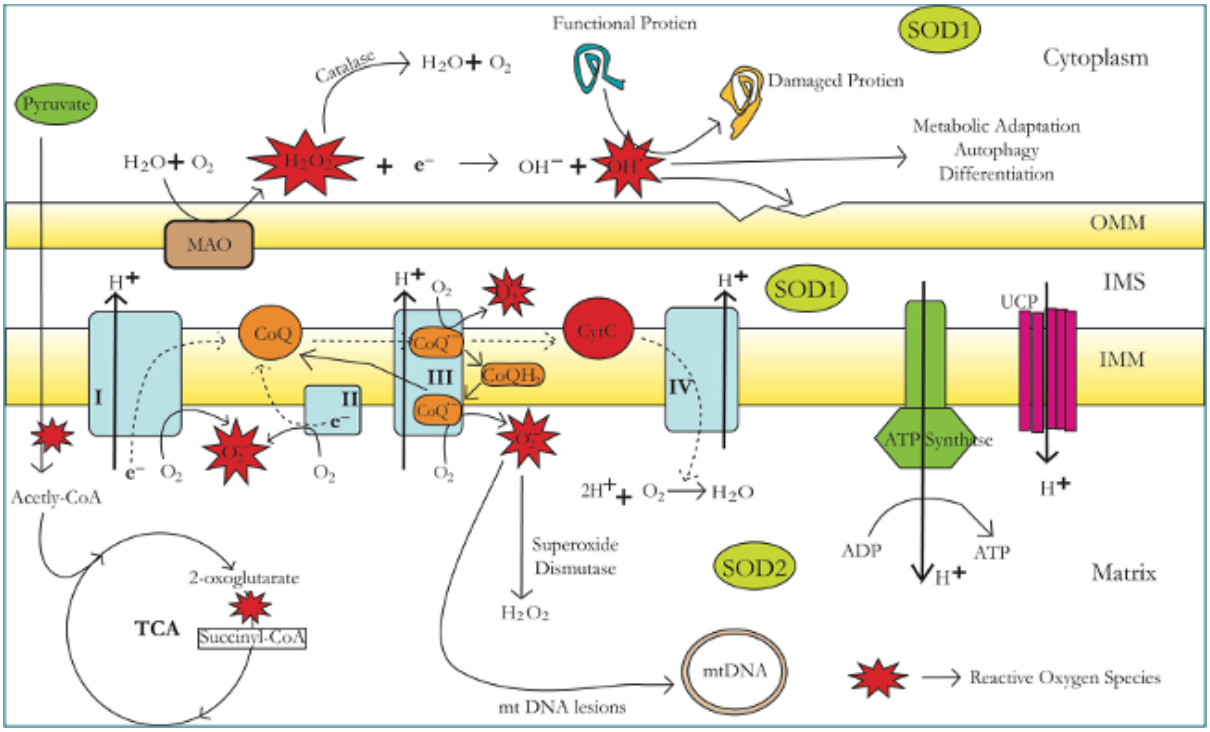

Figure 1.3 Mitochondrial reactive oxygen species production. Complex I and Complex III of ETC are prime producers of ROS in a cell. Lower amount of ROS helps metabolic adaptation, autophagy and differentiation, higher levels damage DNA, proteins and lipids. (This Figure is generated by author using Adobe Illustrator CS6)

1.5.1.5 Mitochondrial DNA

Mitochondrial DNA is highly polymorphic or heteroplasmic because mtDNA experiences various challenges, including alkylation, hydrolysis, formation of adducts, mismatched bases, DNA strand breaks, and oxidative damage (Alexeyev et al. 2013). The polymorphism of mtDNA is not always silent, and once the damage reaches a threshold level, the effect may produce apparent changes to the function of a cell. Notably, the integrity of mtDNA can exert an important influence upon neurodegenerative diseases and ageing (Trifunovic 2006; Reeve et al. 2008). Mutation in mtDNA accumulates over time and, in mice, the amount of mutation in the mtDNA correlates with advanced age (Trifunovic et al. 2004). The mutations and deletions are found in the mitochondrial ATP synthase, rRNA, tRNA, and ETC genes in the tissue of aged humans, rats, and rhesus monkeys

(Bua et al. 2006). The mtDNA mutations represent the clonal expansion of a primary mutational event that led toward impairment of mitochondrial functions (Fayet et al. 2002). Mitochondria evade the distress caused by mutant mtDNA by various maintenance processes, including mitochondrial biogenesis, mtDNA repair, and mitochondrial dynamics. The UPRmt is another stress response towards damaged mitochondrial genome (Martinus et al. 1996; Yoneda et al. 2004). The repair efficiency of DNA declines with age, such that it is 80% lower in 30-month-old rats when compared to 17-day old embryonic rats (Druzhyna et al. 2008). The SNpc neurons show a high level of mtDNA mutation, which contributes to the neuronal loss observed in PD (Bender et al. 2006). MtDNA can be explored as a diagnostic measure for ageing and PD.

1.5.3 Calcium homeostasis.

Calcium signalling is triggered by the uptake of calcium ions or their release from the Smooth Endoplasmic Reticulum (SER). Calcium is one of the most abundant elements in cells and upon various stimuli released in the cytosol through 1,4,5-triphosphate (IP_3R) and ryanodine receptors (RyR) Ca^{2+} channels (Berridge et al. 2003). Calcium takes part in cellular signalling functions like nerve impulse transmission, blood clotting, muscle contraction, proliferation, cell migration, hormone secretion, and transcription (Berridge et al. 2003). The precise control of calcium concentration is of utmost importance as high intracellular calcium concentrations can signal to initiate cell death pathways (Krebs 1998). The mitochondria-associated membranes (MAMs) or ER-mitochondria encounter structures (ERMES) are important in calcium transport and signalling between the ER and the mitochondria (Morciano et al. 2018). These regions have high calcium concentrations in cytosol and are impaired in many neurodegenerative diseases (Krebs et al. 2015). Mitochondria undergo PTP formation when exposed to high *in vitro* levels of calcium (Bernardi and Rasola 2007). The Krebs cycle enzymes, ATP/ADP exchange, apoptosis, and

autophagy are activated in response to elevated calcium concentrations in the mitochondrial matrix (Morciano et al. 2018). The ER and mitochondria protect cells from harmful cytosolic calcium concentration and help in maintaining homeostasis.

The dysregulation of calcium concentrations in various organelles contributes to ageing and neurodegenerative disease. The influx of calcium increases with age, and the buffering system is overwhelmed during sustained levels of calcium within ageing neurons and results in cognitive deficits (Oh et al. 2013). The mitochondrial calcium concentration is disturbed in the DA neuron of the PD model (Pink1 and LRRK2 loss of function). The high Ca^{2+} levels cause mitochondrial enlargement and neuronal death (Lee et al. 2018). The α-synuclein protein can act to form pores in the cellular membranes and can cause a calcium imbalance in the mitochondria (Ludtmann and Abramov 2018). When calcium ions bind to the C-terminus of α-synuclein protein, the excess Ca^{2+} can cause a conformation change and make α-synuclein prone to aggregation (Rcom-H'cheo-Gauthier et al. 2014; Lautenschläger et al. 2018). If calcium concentrations are disturbed in the cytosol, cellular signalling may be compromised (Fujita 2002). The inhibition of pro-apoptotic Bax and Bak facilitate Ca^{2+} intake of mitochondria, hence promotes apoptosis (Scorrano et al. 2003). An ER phosphatase, calcineurin, controlled by Ca^{2+} induces apoptosis by dephosphorylating (activating) a pro-apoptotic protein, Bad, thus enhance its dimerization with Bcl-xL and enhances PTP formation (Wang et al. 1999). Due to its important role, cells have devised various pathways to sustain calcium concentration.

1.5.4 Proteostasis

Proteostasis is homeostasis between the biogenesis, folding, trafficking, and degradation of cellular proteins. Despite the high fidelity of the proteostasis machinery, often proteins are

misfolded and are degraded by Unfolded protein response (UPS) (Ciechanover 2015). Moreover, due to high cellular disturbance, the number of misfolded proteins can increase exponentially. Cell monitors the protein requirements and the amount of misfolded proteins. If the accumulated proportion of misfolded protein exceeds a critical value, the cell signals to initiate the unfolded protein response (UPR) (Wang and Kaufman 2016). Activation of proteostasis systems depends on the location and the severity of the protein aggregates.

1.5.4.1 Ubiquitin proteasome system

A large portion of cellular proteins, synthesized on membrane-bound ribosomes of Rough Endoplasmic Reticulum (RER), are destined for ER, plasma membrane, Golgi, and lysosomes. The protein may undergo secondary and tertiary structure folding in addition to other post-translational modifications, which may happen with the assistance of chaperones and protein modification enzymes (Braakman and Bulleid 2011). The misfolded proteins may be ubiquitinated for subsequent degradation by the 26S proteasome (Smith et al. 2011). Three enzymes that mediate the ubiquitination action are ubiquitin-activating enzyme (E1), ubiquitin-conjugating enzyme (E2), and ubiquitin ligase (E3) (Ciechanover 2015). The E1 ubiquitin recognises E2, which transfers the ubiquitin molecule to the target protein with the help of E3 (Kwon and Ciechanover 2017). Polyubiquitination at specific Lys-residues is required for protein degradation; various ubiquitination's signal proteins for different fate (Dantuma and Bott 2014). Proteins targeted by polyubiquitination are recognised by the 26S proteasome and cleaved into short peptides. These peptide fragments are further cleaved by cellular aminopeptidase into amino acids (Bhattacharyya et al. 2014) to be made available for a number of processes, including protein translation. The UPS seems to act as the first line of defence against the misfolded protein.

The ERAD (ER-associated degradation) is a control system to clear the misfolded proteins from the ER. The pathway is conserved among all eukaryotes and utilises the UPS in the degradation of the misfolded protein (Smith et al. 2011). The mitochondria-associated degradation (MAD) pathway, utilises the UPS to retro-translocate matrix and IMM proteins for ubiquitination and subsequent degradation (Taylor and Rutter 2011). Ubiquitin is a part of inclusion body aggregates found in various neurodegenerative diseases. Inclusion bodies may sequester functioning cellular proteins to initiate neurodegenerative disease. Another hypothesis suggests that inclusion bodies act as a sink for misfolded proteins as a strategy to prevent cellular toxicity. Evidence suggests that the formation of an inclusion body is a protective mechanism against misfolded proteins (Dantuma and Bott 2014). The role of E3 ubiquitin ligase parkin in the pathology of PD further suggests that the involvement of the UPS in neurodegenerative diseases (Kawajiri et al. 2011). Although it is not yet established if the inclusion bodies function as a protective mechanism or result from UPS malfunction, the formation of these structures is a hallmark of ageing and neurodegenerative diseases.

1.5.4.2 Unfolded protein Response

The Unfolded Protein Response (UPR) is one of the essential stress responses associated with ageing, and this becomes activated in reaction to the accumulation of unfolded or misfolded proteins. The aggregates of misfolded protein can cause stress of both the endoplasmic reticulum and the mitochondria (Walter and Ron 2011; Bermales et al. 2012). ER stress initiates three signal transduction by IRE1 (Inositol requiring enzyme 1), ATF6 (Activating transcription factor 6) and PERK (protein kinase RNA line ER kinase) proteins located on the membrane of the ER (Wang and

Kaufman 2016). The IRE1 is transmembrane serine/threonine kinase, which can activate the RNase domain by dimerization, and splices the XBP1 mRNA to generates stable and active XBP1 transcription factor (Calfon et al. 2002). During ER stress, unfolded protein response controls chaperones, ERAD, protein translocation, and lipid synthesis genes expression (Hetz and Papa 2018). The ATF6α is a transmembrane protein with a b-zip transcription factor. The ATF6a is a transmembrane protein with a b-zip transcription factor. While ER stress, ATF6a translocates to the Golgi apparatus and cleaved by a protease to release the cytosolic domain of ATF6a. The ATF6a upregulates the transcription of ERAD and other UPR genes such as BiP and XBP1 to restore proteostasis in the ER (Hillary and Fitzgerald 2018). Lastly, PERK is a transmembrane kinase that oligomerizes and inhibits the protein translation in response to ER stress. PERK phosphorylates the eIF2α, which suppresses the transportation of initiator methionyl-tRNAi^{Met} (Liu et al. 2015). However, the expression of a protein with internal ribosomal entry sites is selectively increased, specifically ATF4. The ATF4 can enhance protein folding capacity, antioxidant response, and macroautophagy (Hetz and Papa 2018). Collectively these pathways enhance the degradation of misfolded protein and reduce overall protein synthesis.

The unfolded protein stress primarily involves, although it is not restricted to the ER. Mitochondria can undergo similar stress amid misfolded protein aggregation called UPR^{mt}. The mitochondrial protein translated in the cytosol are imported and then folded by mitochondrial chaperons (Neupert and Herrmann 2007). Due to impairment of ETC or other cellular stress, unfolded or misfolded protein precursors increase more than the folding capacity of chaperones (Cristina et al. 2009). The increase in unfolded proteins activates the CLPP-1 proteolytic complex, which degrades proteins into small peptides and transports them back to the cytosol (Haynes et al. 2007).

The mitochondrial import efficacy is decreased and affects ATFS-1 import into mitochondria (Jovaisaite et al. 2014). The ATFS-1 is another b-Zip transcription factor, which is typically imported and degraded into mitochondria. During mitochondrial stress, ATFS-1 is imported into the nucleus and initiates the transcription of the mitochondrial chaperones, proteases, antioxidants, glycolysis, and protective genes (Nargund et al. 2012). The ATFS-1 balances the gene expression with the folding capacity of mitochondria and suppresses the accumulation of Tri-carboxylic acid cycle (TCA) and OXPHOS transcripts (Nargund et al. 2015). UPR^{mt} helps to recover mitochondria and promotes cell survival.

When the UPR^{ER} response is insufficient to restore the protein homeostasis, apoptosis is initiated. The hyperactivation of PERK upregulates the transcription factor CHOP. The transcription factor, CHOP, inhibits anti-apoptotic proteins' expression and enhances the expression of pro-apoptotic Bcl-2 genes; Besides, increased protein synthesis causes oxidative stress (Urra et al. 2013). The hyperactivation of IRE1α cause ER-localised mRNA decay, which depletes cell-surface signalling protein and destabilises protein folding in ER (Urano et al. 2000; Han et al. 2009) and initiates the apoptotic signal by activating the JNK pathway (Hetz and Papa 2018). Interestingly, prolong activation of UPR^{mt} allows cells to keep defective mitochondrial DNA. A research group deleted 3.1kb of mtDNA encoding for 4 OXPHOS enzymes and created a heteroplasmic strain of *C. elegans*. The deleted mtDNA was maintained, compared to 60% of the total mtDNA (Tsang and Lemire 2002). Subsequent studies demonstrated that the knockdown (or deletion) of ATFS-1 or UPR^{mt} result in a dramatic reduction in deleterious mtDNA from 60% to 7%. The overexpression of ATFS-1 increases heteroplasmy from 60% to 73% (Lin et al. 2016). This suggests that UPR^{ER} and UPR^{mt} are beneficial, but prolonged activation could be harmful.

The UPR adapts to avoid stress and to minimize the damage caused to the cell by protein stress. The activity of the three signal transduction branches of the UPR^{ER} declines with increasing age (Taylor 2016). The overexpression of the mitochondrial matrix proteases increase lifespan substantially (Luce and Osiewacz 2009). The proteases, LON and Clp (CLPP), are essential to keep up the protein homeostasis in the mitochondrial matrix (Bezawork-Geleta et al. 2015). They are classic activators of UPR^{mt}, and a decline in their activity promotes ageing (Quirós et al. 2015). LON regulates the mitochondrial level of PINK1, a distinct regulatory pathway, which suggests cross-regulation between the two pathways (Thomas et al. 2014). The aggregation of unfolded or misfolded protein in neurons is a characteristic of neurodegenerative diseases like PD (Recasens and Dehay 2014). The UPR is important to prevent neurodegenerative diseases in animal models (Hetz and Mollereau 2014). Overall, UPR increases the efficiency of protein folding machinery and the upkeep of homeostasis.

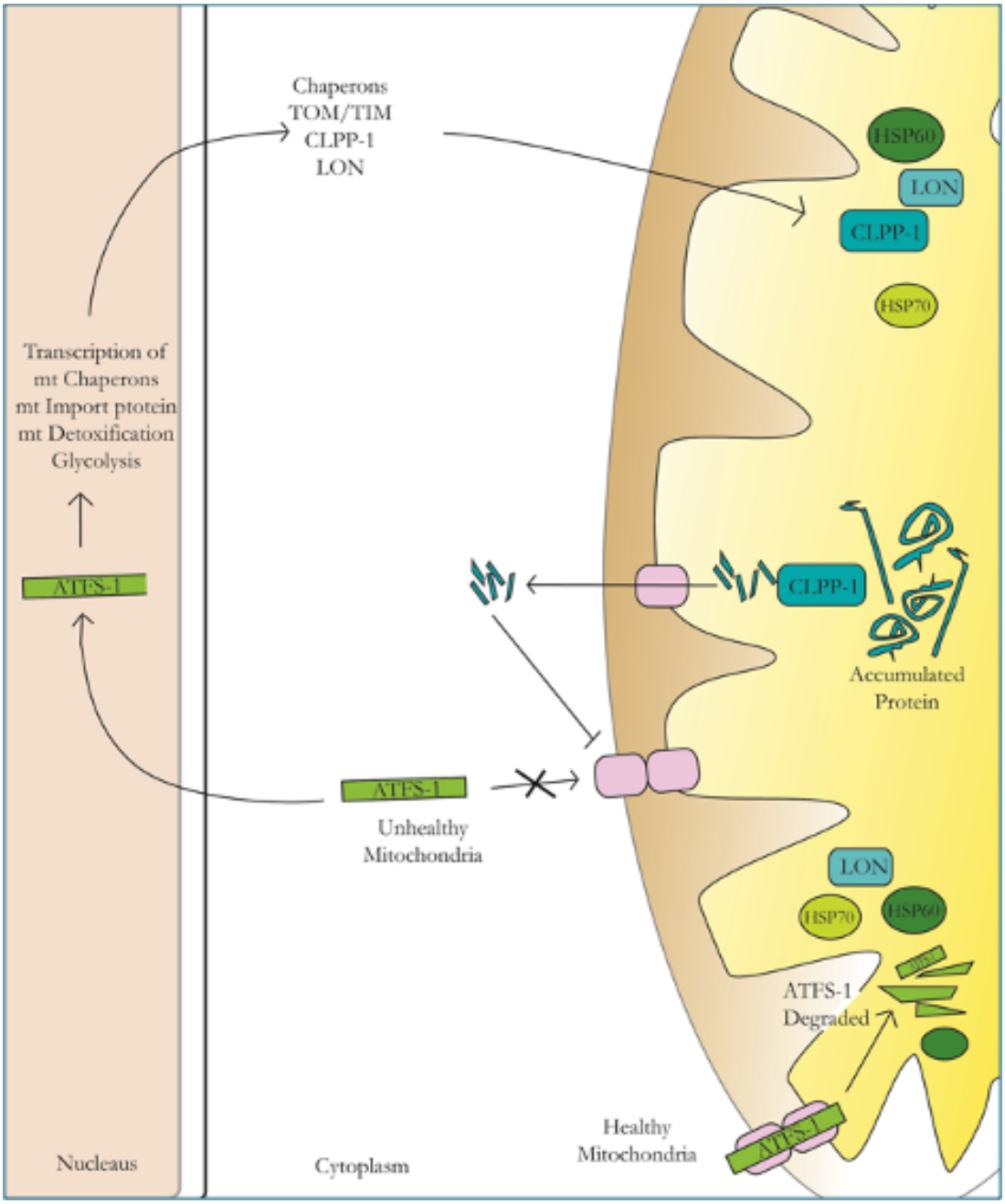

Figure 1.4 The Mitochondrial Unfolded Protein Response. The UPRmt is activated during unfolded protein stress and mitochondrial dysfunction, which upregulate the expression of mitochondrial chaperones, proteases, translocases, and glycolysis proteins, to relieve the mitochondrial stress. (This Figure is generated by author using Adobe Illustrator CS6)

1.5.5 The IGF-1 pathway

The insulin-like growth factors induce growth and differentiation by binding at specific Insulin-like

growth factor 1(IGF-1) receptors located at the cell outer surface. Once activated, IGF-1 receptors

can phosphorylate multiple downstream targets, including Akt (also known as Protein kinase B) (Vanhaesebroeck and Alessi 2000; Laviola et al. 2007). Akt protein overcomes cell cycle arrest (Kandel et al. 2002; Liu et al. 2014); regulates insulin metabolism and autophagy (Whiteman et al. 2002; Heras-Sandoval et al. 2014); and acts as a tumour suppressor (Manning and Toker 2017). The Akt can change the expression of genes through the activities of the foxo transcription factor. Foxo regulates glucose homeostasis, tumour suppression, autophagy, and resistance to oxidative stress (Martins et al. 2016). The IRS null mutant mice exhibited insulin resistance and lived ~16% longer (Selman et al. 2011); diminished IGF-1/IRS signalling increased lifespan in worms, flies, and mice (Holzenberger et al. 2003; Yuan et al. 2009; Tazearslan et al. 2012). Decreased IGF-1/IRS signalling activates downstream transcription factor foxo, which ameliorates different cellular stress. A GWAS study identified foxo for its association with longevity among the ~2.5 million SNPs (Broer et al. 2015). The foxo genes activate autophagy mechanisms in different cell types, including neurons (Martins et al. 2016). The autophagy mechanism is found to be dysfunctional in ageing and neurodegenerative disorders such as AD and PD (Heras-Sandoval et al. 2014). Likely reductions in IGF-1 signalling activities are beneficial for the cellular health of ageing cells.

Defects in the IRS pathway can disturb normal mitochondrial function (Cheng et al. 2010). Akt, the principal regulator of the IRS pathway, seems to prevent apoptosis through phosphorylation of the pro-apoptotic protein, Bad in mammals. The IRS pathway regulates mitochondrial biogenesis through the NAD^+/NADH ratio and the activated sirtuin-1/PGC1α pathway (Cheng et al. 2010). Akt phosphorylates and deactivates GSK3β, which in its active form deactivates anti-apoptotic Bcl-2 family proteins, Bcl-xL, and Mcl-1 (Maurer et al. 2006). The Akt regulated transcription factor foxo

triggers the expression of the Bcl-2 family proteins Bcl-xL, Bnip3, and Bim (Farhan et al. 2017). The IRS pathway has an active role in the maintenance of cellular homeostasis via Bcl-2 family protein.

1.6 Proteins involved in ageing and age-related disease progression

1.6.1 The Drp1, mitochondrial fission protein.

The mitochondria are dynamic, and the mitochondrial network is kept in part through proteins with GTPase activities: dynamin-related protein (Drp1) for fission, and Mitofusin-1 & 2 (Mfn1/2) for fusion (Chan 2006). The Drp1 protein is required for an array of processes from the maintenance of the mitochondria, peroxisomes, and the endoplasmic reticulum (ER) morphology (Koch et al. 2003, Pitts et al. 1999; Wikstrom et al. 2013) to the standard rate of cytochrome-c (Cyt-c) release and activation of caspase functions (Breckenridge et al. 2008). The role of Drp1 in apoptosis and mitophagy is not well understood, but it seems to depend upon interactions with proteins involved in a number of mitochondrial processes, such as the products of *Pink1 (PTEN-induced putative kinase 1)* and *parkin* in Cos-7 cells (Buhlman et al. 2014), and protein product of *Bax* (Karbowski et al. 2002; Yuan et al. 2007; Maes et al. 2019). Drp1 phosphorylation and localization on mitochondria increases by Akt activation, which results in "mito-fission" and escalates ROS production (Kim et al. 2016). *Drp1* loss of function can increase the nuclear translocation of the foxo transcription factor to enhance the expression of downstream targets (Favaro et al. 2019). Drp1 increases the mitochondrial fragmentation under nitrosative stress, due to the elevated production of nitric oxide, in primary cerebrocortical neuron culture (Yuan et al. 2007). Neurons are dependent on mitochondrial function for membrane excitability, synaptic plasticity, and neurotransmission (Kann and Kovács 2007). The synaptic regions of neurons are rich

in mitochondria (Vos et al. 2010). The crucial requirement of mitochondria is the intense need for ATP in synaptic transmission, fusion, and recycling of synaptic vesicle, to maintain the ionic environment at the synaptic membrane (Chan 2006; Vos et al. 2010). Drp1 controls mitochondrial fission and, as a vital consequence, mitochondrial and cellular health.

1.6.2 The E3 ubiquitin ligase Parkin.

The Parkin protein encoded by the *PARK* gene is an E3 ubiquitin ligase protein that serves as a component of the ubiquitin-proteasome degradation pathway. The four functional domains of the protein are well-conserved between the Drosophila and its human homologue (Haywood and Staveley 2004). Parkin is one of the proteins found altered in the familial form of PD. Parkin is found in the LB of both familial and sporadic PD forms (Schlossmacher et al. 2002). The parkin gene comprises an N-terminal Ubiquitin (Ub)-like domain, an Ub-parkin domain, a RING 1 domain, In-Between Ring fingers (IBR) and a RING 2 domain (Haywood and Staveley 2004; Olszewska and Lynch 2015). Parkin acts to mono- and polyubiquitinilate the substrate proteins (Von Coelln et al. 2004). Parkin substrates range from synphilin-1, an α-synuclein interacting protein, to cytoskeleton proteins (Panicker et al. 2017). In the past decade, extensive studies have revealed that the function of parkin is involved with another PD-associated protein, Pink1 (Thomas et al. 2014). Damaged and dysfunctional mitochondria can undergo a Pink1-parkin dependent process of mitophagy to upkeep cellular health and homeostasis. Loss of parkin in mitophagy has been implicated as a common cause in the onset of PD.

1.6.3 Bcl-2 family

The Bcl-2 family of proteins, first discovered as regulators of apoptosis, have been identified as regulators of a diverse selection of cell signalling pathways. Beyond the control of facets of cell death, these proteins control the calcium-dependent signalling mechanisms that act between the

mitochondria and the endoplasmic reticulum; the energy metabolism of the mitochondria; the cell cycle progression checkpoints; the unfolded protein response (UPR); various aspects of autophagy; and various aspects of mitochondrial dynamics (Danial et al. 2010). The Bcl-2 family proteins, Bcl-2, Bcl-XL, and Mcl-1 are located on the Inner Mitochondrial Membrane (IMM) and bind to Inositol 1,4,5-trisphosphate receptor (IP3R) and facilitate Ca^{2+} leakage from ER. The Bcl-2 and Bcl-xL proteins act to inhibit the progression of the cell cycle and mediate cellular survival and can be antagonised by the anti-apoptotic protein Bax (O'Reilly et al. 1996). The Bcl-2 protein can regulate mitochondrial respiration by binding to Cyt-c oxidase (COX) (Chen and Pervaiz 2010) to promote axonal growth in CNS neurons (Chen et al. 1997). The Bcl-xL protein can regulate the dynamics of synaptic vesicle membranes through interactions with Drp1 (Li et al. 2013). Bcl-xL, along with Mcl-1, may interact with the F1 F0 ATP synthase complex, and decrease ion leaks and increase ATP production if overexpressed (Alavian et al. 2011; Perciavalle et al. 2012). Mcl-1 may contribute in the organization of mitochondrial cristae, the efficiency of the ETC complexes and other attributes of mitochondrial dynamics (Perciavalle et al. 2012). Several BH3-only Bcl-2 family proteins like BAD, NOXA, BNIP3, and tBID regulate lipid and glucose metabolism (Giordano et al. 2005; Lowman et al. 2010; Glick et al. 2012; Ljubicic et al. 2015). The association of Bcl-2 family proteins in the regulation of different cellular processes signifies their importance in ageing and age-related disorders.

1.6.4 The Rbf1 transcription regulator.

The well-studied nuclear function of the retinoblastoma (Rb) protein is transcriptional regulation via interactions with the E2 transcription factor (E2F1). Both the overexpression or the inhibition of the *Rb* homologue in mice during development can have catastrophic effects, that include

lethality (Vooijs and Berns 1999; Lipinski and Jacks 1999). Interestingly, recent investigations into endogenous Rb protein activity have established direct interactions with mitochondria as the Rb protein: 1) can localize near the mitochondrial surface; 2) can induce the process of mitochondrial outer membrane permeabilization (MOMP); 3) can bind with the Bcl-2 family member Bax (*in vitro* and *in vivo*); 4) can induce apoptosis when in a form designed to be deficient of nuclear function and is targeted to mitochondria; and 5) can suppress tumourigenesis (Hilgendorf et al. 2013). The Rb protein is a crucial regulator of transcription and has a vital role in regulating cellular proliferation and apoptosis.

1.6.5 The α-synuclein protein

The *α-synuclein* gene encodes a 140 amino acid neuronal protein that is kept in a dynamic equilibrium between membrane-associated and free native conformation. The well-accepted function of the α-synuclein protein is in neurotransmission, specifically the facilitation of the clustering and docking of synaptic vesicles (Burré et al. 2010, 2014; Diao et al. 2013). The vesicle curvature and lipid composition increase the binding efficiency of α-synuclein by greater than 15 fold (Middleton and Rhoades 2010). The alteration of *α-synuclein* expression inhibits the process of vesicle recycling and re-clustering abilities (Nemani et al. 2010; Wang et al. 2014). In membrane-bound conformation, α-synuclein is associated with synaptic vesicles, mitochondria, endoplasmic reticulum, and Golgi membranes (Nakamura et al. 2008). The α-synuclein gene was first found to be associated with the familial form of PD. The histology of the PD brain shows an abnormal aggregation of proteins, LB. The α-synuclein is a major component of the LB. Although the conformations that are more susceptible to aggregation is still unclear (Miraglia et al. 2018). Furthermore, post-translational modifications of the *α-synuclein* gene, protein product increase the protein aggregation (Thomas and Beal 2011; Zhang et al. 2019a). These protein alterations

seem to cause the aggregation of insoluble proteins, which eventually cause neurotoxicity and PD pathology.

1.6.6 Trbl protein

The *trbl* homologues encode proteins that contain a highly conserved central domain, a non-conserved N-terminal domain, and a C-terminal domain with binding sites for *COP-1* and *MEK1*. The trbl gene has a central role in the insulin-receptor signalling pathway (Fischer et al. 2017). The levels of *trbl* expression increase during starvation and after exercise which can block the activation of *Akt* and can reduce tissue growth in diabetic mice and in human cell culture (Schwarzer et al. 2006; Lima et al. 2009; Fischer et al. 2017). In structure, the Trbl protein has the structure of a pseudokinase adaptor protein that contains a non-catalytic kinase region (Fischer et al. 2017). Pseudokinases are pseudo-enzymes that lack key catalytic residues and, therefore, are catalytically inactive (Jacobsen and Murphy 2017). While the general functions of pseudokinase proteins remain uncertain, the consensus is that these seem to function as mediators of protein interaction. The Trbl proteins are involved in cell signalling through the allosteric regulation of protein kinases. The trbl pseudokinase proteins are located in the nucleus and function primarily as adaptor proteins.

1.6.7 Foxo transcription factor

The foxo transcription factor help mitigates stress. Akt acts to phosphorylate the foxo protein to result in nuclear exclusion and thus suppression of downstream targets of transcriptional activities (Martins et al. 2016). The ageing process has been correlated to decreased levels of proteasomal activity, which can increase the accumulation of damaged protein in cells. Foxo plays a role in the

proteasome system by the encouraging the degradation of short-lived regulatory proteins (Murtaza et al. 2017). Additionally, foxo upregulates the production of ubiquitin ligases, the proteasome composition, the expression of autophagy and mitophagy genes, and the preparation of tissues to adapt to starvation conditions (Martins et al. 2016). Foxo can regulate the expression of *manganese superoxide dismutase* (*MnSOD*), *catalase* and *Gadd45* (Klotz et al. 2015). The conditional deletion of *foxo3A* leads to apoptosis and compromised regenerative potential in the hematopoietic system of mice (Miyamoto et al. 2007). The efficiency and number of adult stem cells are decreased on the onset of age-related diseases due to increased cellular stress, which can be rescued with antioxidant treatment (Martins et al. 2016). Foxo can interact with tumour suppressor p53 directly or indirectly and induce mitochondria-associated apoptosis (Wang et al. 2008; Farhan et al. 2017). The roles of foxo are diverse and may be poorly understood with concern to the maintenance of mitochondrial health.

1.7 Objective of the study.

The function of the Drp1 protein, other than as a mitochondrial fission factor in various pathways, is not well understood. In these studies, it is being explored under different conditions in order to enhance our understanding. To begin, I sought to investigate the effects of Drp1 upon the DA neurons and developing eyes of flies (Chapter 2). Further, I investigated the role of Drp1 in the parkin-induced Drosophila model of PD (Chapter 2). Additionally, I used the Drp1 induced novel PD-like phenotypic models to study the consequences of the alteration of the expression of the Bcl-2 family genes, Buffy and Debcl (Chapter 3), the transcription regulator, Rbf (Chapter 5), and IRS pathways regulator, trbl (Chapter 6), which are strongly associated with mitochondrial health and cell death pathways. I characterized the phenotype of altered expression of Rbf in Drosophila

DA neurons and attempted to rescue the phenotype by altering Buffy, Debcl or Drp1 (Chapter 4 and 5). Besides, I attempted to rescue the parkin-induced Drosophila model of PD by the overexpression of Rbf (Chapter 4). To further evaluate the role of Drp1, Bcl-2, Rbf and trbl, I altered their expression in the α-synuclein induced model of PD (Chapter 6 and 7). I characterized the phenotypes generated in response to the altered expression of trbl in Drosophila DA neurons and in the parkin-induced PD model (Chapter 7). To further understand the role of cell signalling and foxo in mitochondrial health, I inhibited the foxo expression in well-established parkin and α-synuclein; and novel Drp1 and Rbf Drosophila models of PD (Chapter 8). Additionally, I altered the expression of Drp1, Buffy, Debcl, Rbf, Pink1, parkin, trbl and foxo to see its effect on foxo overexpression-induced characteristics Drosophila eye phenotype. Exploring the role of Drp1 in established and novel PD models provided helpful information about the interaction between various mitochondrial proteins.

Bibliography

Aerts, L., Craessaerts, K., De Strooper, B., and Morais, V.A. 2015. PINK1 Kinase Catalytic Activity Is Regulated by Phosphorylation on Serines 228 and 402. J. Biol. Chem. **290**(5): 2798–2811. doi:10.1074/jbc.M114.620906.

Alavian, K.N., Li, H., Collis, L., Bonanni, L., Zeng, L., Sacchetti, S., Lazrove, E., Nabili, P., Flaherty, B., Graham, M., Chen, Y., Messerli, S.M., Mariggio, M.A., Rahner, C., McNay, E., Shore, G.C., Smith, P.J.S., Hardwick, J.M., and Jonas, E.A. 2011. Bcl-x L regulates metabolic efficiency of neurons through interaction with the mitochondrial F1 FO ATP synthase. Nat. Cell Biol. **13**(10): 1224–1233. Nature Publishing Group. doi:10.1038/ncb2330.

Alexeyev, M., Shokolenko, I., Wilson, G., and LeDoux, S. 2013. The maintenance of mitochondrial DNA integrity--critical analysis and update. Cold Spring Harb. Perspect. Biol. **5**(5): a012641. Cold Spring Harbor Laboratory Press. doi:10.1101/cshperspect.a012641.

Altintas, O., Park, S., and Lee, S.J. V. 2016. The role of insulin/IGF-1 signalling in the longevity of model invertebrates, C. elegans and D. melanogaster. BMB Rep. **49**(2): 81–92. The Biochemical Society of the Republic of Korea. doi:10.5483/BMBRep.2016.49.2.261.

Andreyev, A.Y., Kushnareva, Y.E., and Starkov, A.A. 2005. Mitochondrial metabolism of reactive oxygen species. Biochemistry. (Mosc). **70**(2): 200–14. Available from http://www.ncbi.nlm.nih.gov/pubmed/15807660 [accessed 7 December 2017].

Babcock, D.F., and Hille, B. 1998. Mitochondrial oversight of cellular Ca2+ signalling. Curr. Opin. Neurobiol. **8**(3): 398–404. Elsevier Current Trends. doi:10.1016/S0959-4388(98)80067-6.

Balasubramanian, P., and Longo, V.D. 2016. Growth factors,ageing and age-related diseases. Growth Horm. IGF Res. **28**: 66–68. Churchill Livingstone. doi:10.1016/j.ghir.2016.01.001.

Balck, A., Borsche, M., Kasten, M., Lohmann, K., Seibler, P., Brüggemann, N., and Klein, C. 2019. Discordance in monozygotic Parkinson's disease twins – continuum or dichotomy? Ann. Clin. Transl. Neurol.: acn3.775. doi:10.1002/acn3.775.

Beach, T.G., Adler, C.H., Sue, L.I., Vedders, L., Lue, L.F., White, C.L., Akiyama, H., Caviness, J.N., Shill, H.A., Sabbagh, M.N., and Walker, D.G. 2010. Multi-organ distribution of phosphorylated α-synuclein histopathology in subjects with Lewy body disorders. Acta Neuropathol. **119**(6): 689–702. Springer. doi:10.1007/s00401-010-0664-3.

Beekman, M., Nederstigt, C., Suchiman, H.E.D., Kremer, D., Van Der Breggen, R., Lakenberg, N., Alemayehu, W.G., De Craen, A.J.M., Westendorp, R.G.J., Boomsma, D.I., De Geus, E.J.C., Houwing-Duistermaat, J.J., Heijmans, B.T., and Slagboom, P.E. 2010. Genome-wide association study (GWAS)-identified disease risk alleles do not compromise human longevity. Proc. Natl. Acad. Sci. U. S. A. **107**(42): 18046–18049. National Academy of Sciences. doi:10.1073/pnas.1003540107.

Bender, A., Krishnan, K.J., Morris, C.M., Taylor, G.A., Reeve, A.K., Perry, R.H., Jaros, E., Hersheson, J.S., Betts, J., Klopstock, T., Taylor, R.W., and Turnbull, D.M. 2006. High levels of mitochondrial DNA deletions in substantia nigra neurons inageing and Parkinson disease. Nat. Genet. **38**(5): 515–517. doi:10.1038/ng1769.

Benzer, S. 1971. From the Gene to Behavior. JAMA J. Am. Med. Assoc. **218**(7): 1015–1022. doi:10.1001/jama.1971.03190200047010.

Bermales, S., Soto, M.M., and McCullagh, E. 2012, April 25. Unfolded protein stress in the endoplasmic reticulum and mitochondria: A role in neurodegeneration. Frontiers. doi:10.3389/fnagi.2012.00005.

Bernardi, P., and Rasola, A. 2007. Calcium and cell death: The mitochondrial connection. Subcell. Biochem. **45**: 481–506. Springer New York. doi:10.1007/978-1-4020-6191-2_18.

Berridge, M.J., Bootman, M.D., and Roderick, H.L. 2003, July 1. Calcium signalling: Dynamics, homeostasis and remodelling. doi:10.1038/nrm1155.

Bezawork-Geleta, A., Brodie, E.J., Dougan, D.A., and Truscott, K.N. 2015. LON is the master protease that protects against protein aggregation in human mitochondria through direct degradation of misfolded proteins. Sci. Rep. **5**: 17397. Nature Publishing Group. doi:10.1038/srep17397.

Bhattacharyya, S., Yu, H., Mim, C., and Matouschek, A. 2014, February 23. Regulated protein turnover: Snapshots of the proteasome in action. Nature Publishing Group. doi:10.1038/nrm3741.

Bingol, B., and Sheng, M. 2016. Mechanisms of mitophagy: PINK1, Parkin, USP30 and beyond. Free Radic. Biol. Med. **100**: 210–222. doi:10.1016/j.freeradbiomed.2016.04.015.

Bjorksten, J., and Tenhu, H. 1990. The crosslinking theory ofageing - Added evidence. Exp. Gerontol. **25**(2): 91–95. doi:10.1016/0531-5565(90)90039-5.

Blesa, J., and Przedborski, S. 2014. Parkinson's disease: Animal models and dopaminergic cell vulnerability. Front. Neuroanat. **8**(DEC). Frontiers Media S.A. doi:10.3389/fnana.2014.00155.

Braak, H., Del Tredici, K., Rüb, U., De Vos, R.A.I., Jansen Steur, E.N.H., and Braak, E. 2003. Staging of brain pathology related to sporadic Parkinson's disease. Neurobiol.ageing **24**(2): 197–211. Elsevier. doi:10.1016/S0197-4580(02)00065-9.

Braakman, I., and Bulleid, N.J. 2011. Protein Folding and Modification in the Mammalian Endoplasmic Reticulum. Annu. Rev. Biochem. **80**(1): 71–99. Annual Reviews. doi:10.1146/annurev-biochem-062209-093836.

Braschi, E., Goyon, V., Zunino, R., Mohanty, A., Xu, L., and McBride, H.M. 2010. Vps35 mediates vesicle transport between the mitochondria and peroxisomes. Curr. Biol. **20**(14): 1310–1315. doi:10.1016/j.cub.2010.05.066.

Breckenridge, D.G., Kang, B.-H., Kokel, D., Mitani, S., Staehelin, L.A., and Xue, D. 2008. Caenorhabditis elegans drp-1 and fis-2 regulate distinct cell-death execution pathways downstream of ced-3 and independent of ced-9. Mol. Cell **31**(4): 586–97. NIH Public Access. doi:10.1016/j.molcel.2008.07.015.

Broer, L., Buchman, A.S., Deelen, J., Evans, D.S., Faul, J.D., Lunetta, K.L., Sebastiani, P., Smith, J.A., Smith, A. V, Tanaka, T., Yu, L., Arnold, A.M., Aspelund, T., Benjamin, E.J., Jager, P.L. De, Eirkisdottir, G., Evans, D.A., Garcia, M.E., Hofman, A., Kaplan, R.C., Kardia, S.L.R., Kiel, D.P., Oostra, B.A., Orwoll, E.S., Parimi, N., Psaty, B.M., Rivadeneira, F., Rotter, J.I., Seshadri, S., Singleton, A., Tiemeier, H., Ferrucci, L., Gudnason, V., Harris, T.B., Karasik, D., Newman, A.B., Duijn, C.M. Van, and Murabito, J.M. 2015. GWAS of Longevity in CHARGE Consortium Confirms APOE and FOXO3 Candidacy. J. Gerontol. A. Biol. Sci. Med. Sci. **70**(1): 110–118. doi:10.1093/gerona/glu166.

Bua, E., Johnson, J., Herbst, A., Delong, B., McKenzie, D., Salamat, S., and Aiken, J.M. 2006. Mitochondrial DNA-deletion mutations accumulate intracellularly to detrimental levels in aged human skeletal muscle fibers. Am. J. Hum. Genet. **79**(3): 469–80. Elsevier. doi:10.1086/507132.

Buhlman, L., Damiano, M., Bertolin, G., Ferrando-Miguel, R., Lombès, A., Brice, A., and Corti, O. 2014. Functional interplay between Parkin and Drp1 in mitochondrial fission and clearance.

Biochim. Biophys. Acta - Mol. Cell Res. **1843**(9): 2012–2026. doi:10.1016/j.bbamcr.2014.05.012.

Bułdak, R.J., Bułdak, Ł., Kukla, M., Gabriel, A., and Żwirska-Korczala, K. 2014. Significance of selected antioxidant enzymes in cancer cell progression. Polish J. Pathol. **3**(3): 167–175. Termedia. doi:10.5114/pjp.2014.45779.

Burré, J., Sharma, M., and Südhof, T.C. 2014. α-Synuclein assembles into higher-order multimers upon membrane binding to promote SNARE complex formation. Proc. Natl. Acad. Sci. U. S. A. **111**(40): E4274–E4283. National Academy of Sciences. doi:10.1073/pnas.1416598111.

Burré, J., Sharma, M., Tsetsenis, T., Buchman, V., Etherton, M.R., and Südhof, T.C. 2010. α-Synuclein promotes SNARE-complex assembly in vivo and in vitro. Science (80-.). **329**(5999): 1663–1667. doi:10.1126/science.1195227.

Cajal, S. y, and Sanchez, D. 1915. Contribución al conocimiento de los centros nerviosos de los insectos.

Calfon, M., Zeng, H., Urano, F., Till, J.H., Hubbard, S.R., Harding, H.P., Clark, S.G., and Ron, D. 2002. IRE1 couples endoplasmic reticulum load to secretory capacity by processing the XBP-1 mRNA. Nature **415**(6867): 92–96. doi:10.1038/415092a.

Calne, D.B., and Langston, J.W. 1983. Aetiology of Parkinson's disease. Lancet (London, England) **2**(8365–66): 1457–9. doi:10.1016/s0140-6736(83)90802-4.

Chan, D.C. 2006, June 30. Mitochondria: Dynamic Organelles in Disease,ageing, and Development. Cell. doi:10.1016/j.cell.2006.06.010.

Chen, D.F., Schneider, G.E., Martinou, J.C., and Tonegawa, S. 1997. Bcl-2 promotes regeneration of severed axons in mammalian CNS. Nature **385**(6615): 434–439. doi:10.1038/385434a0.

Chen, L., Thiruchelvam, M.J., Madura, K., and Richfield, E.K. 2006. Proteasome dysfunction in aged human α-synuclein transgenic mice. Neurobiol. Dis. **23**(1): 120–126. Academic Press. doi:10.1016/j.nbd.2006.02.004.

Chen, Z.X., and Pervaiz, S. 2010. Involvement of cytochrome c oxidase subunits Va and Vb in the regulation of cancer cell metabolism by Bcl-2. Cell Death Differ. **17**(3): 408–420. doi:10.1038/cdd.2009.132.

Cheng, Z., Tseng, Y., and White, M.F. 2010. Insulin signalling meets mitochondria in metabolism. Trends Endocrinol. Metab. **21**(10): 589–598. doi:10.1016/j.tem.2010.06.005.

Chistiakov, D.A., Sobenin, I.A., Revin, V. V., Orekhov, A.N., and Bobryshev, Y. V. 2014. Mitochondrialageing and age-related dysfunction of mitochondria. Hindawi Publishing Corporation. doi:10.1155/2014/238463.

Ciechanover, A. 2015, April 23. The unravelling of the ubiquitin system. Nature Publishing Group. doi:10.1038/nrm3982.

Clerc, P., Ge, S.X., Hwang, H., Waddell, J., Roelofs, B.A., Karbowski, M., Sesaki, H., and Polster, B.M. 2014. Drp1 is dispensable for apoptotic cytochrome c release in primed MCF10A and fibroblast cells but affects Bcl-2 antagonist-induced respiratory changes. Br. J. Pharmacol. **171**(8): 1988–1999. John Wiley and Sons Inc. doi:10.1111/bph.12515.

Cochemé, H.M., Quin, C., McQuaker, S.J., Cabreiro, F., Logan, A., Prime, T.A., Abakumova, I., Patel, J. V, Fearnley, I.M., James, A.M., Porteous, C.M., Smith, R.A.J., Saeed, S., Carré, J.E., Singer, M., Gems, D., Hartley, R.C., Partridge, L., and Murphy, M.P. 2011. Measurement of H2O2 within living Drosophila duringageing using a ratiometric mass spectrometry probe targeted to the mitochondrial matrix. Cell Metab. **13**(3): 340–50. Elsevier.

doi:10.1016/j.cmet.2011.02.003.
Von Coelln, R., Dawson, V.L., and Dawson, T.M. 2004, October 30. Parkin-associated Parkinson's disease. Springer. doi:10.1007/s00441-004-0924-4.
Collier, T.J., Kanaan, N.M., and Kordower, J.H. 2011, June. Ageing as a primary risk factor for Parkinson's disease: Evidence from studies of non-human primates. doi:10.1038/nrn3039.
Collier, T.J., Kanaan, N.M., and Kordower, J.H. 2017.ageing and Parkinson's disease: Different sides of the same coin? Mov. Disord. **32**(7): 983–990. John Wiley and Sons Inc. doi:10.1002/mds.27037.
Contreras, L., Drago, I., Zampese, E., and Pozzan, T. 2010. Mitochondria: The calcium connection. Biochim. Biophys. Acta - Bioenerg. **1797**(6–7): 607–618. Elsevier. doi:10.1016/J.BBABIO.2010.05.005.
Cookson, M.R. 2012. Parkinsonism due to mutations in PINK1, Parkin, and DJ-1 and oxidative stress and mitochondrial pathways. Cold Spring Harb. Perspect. Med. **2**(9). Cold Spring Harbor Laboratory Press. doi:10.1101/cshperspect.a009415.
Copeland, J.M., Cho, J., Lo, T., Hur, J.H., Bahadorani, S., Arabyan, T., Rabie, J., Soh, J., and Walker, D.W. 2009. Extension of Drosophila Life Span by RNAi of the Mitochondrial Respiratory Chain. Curr. Biol. **19**(19): 1591–1598. doi:10.1016/j.cub.2009.08.016.
Cristina, D., Cary, M., Lunceford, A., Clarke, C., and Kenyon, C. 2009. A regulated response to impaired respiration slows behavioral rates and increases lifespan in Caenorhabditis elegans. PLoS Genet. **5**(4): e1000450. Public Library of Science. doi:10.1371/journal.pgen.1000450.
Cui, H., Kong, Y., and Zhang, H. 2012. Oxidative stress, mitochondrial dysfunction, andageing. J. Signal Transduct. **2012**: 646354. Hindawi. doi:10.1155/2012/646354.
Danial, N.N., Gimenez-Cassina, A., and Tondera, D. 2010. Homeostatic functions of BCL-2 proteins beyond apoptosis. Adv. Exp. Med. Biol. **687**: 1–32. Available from http://www.ncbi.nlm.nih.gov/pubmed/20919635 [accessed 10 January 2018].
Dantuma, N.P., and Bott, L.C. 2014, July 31. The ubiquitin-proteasome system in neurodegenerative diseases: Precipitating factor, yet part of the solution. Frontiers Research Foundation. doi:10.3389/fnmol.2014.00070.
Davidovic, M., Sevo, G., Svorcan, P., Milosevic, D.P., Despotovic, N., and Erceg, P. 2010. Old age as a privilege of the "selfish ones." International Society onageing and Disease.
Davie, C.A. 2008, June. A review of Parkinson's disease. doi:10.1093/bmb/ldn013.
Degli Esposti, D., Hamelin, J., Bosselut, N., Saffroy, R., Sebagh, M., Pommier, A., Martel, C., and Lemoine, A. 2012. Mitochondrial Roles and Cytoprotection in Chronic Liver Injury. Biochem. Res. Int. **2012**: 1–16. Hindawi. doi:10.1155/2012/387626.
Devi, L., Raghavendran, V., Prabhu, B.M., Avadhani, N.G., and Anandatheerthavarada, H.K. 2008. Mitochondrial import and accumulation of α-synuclein impair complex I in human dopaminergic neuronal cultures and Parkinson disease brain. J. Biol. Chem. **283**(14): 9089–9100. doi:10.1074/jbc.M710012200.
Diamanti-Kandarakis, E., Dattilo, M., Macut, D., Duntas, L., Gonos, E.S., Goulis, D.G., Gantenbein, C.K., Kapetanou, M., Koukkou, E., Lambrinoudaki, I., Michalaki, M., Eftekhari-Nader, S., Pasquali, R., Peppa, M., Tzanela, M., Vassilatou, E., and Vryonidou, A. 2017, June 1. Mechanisms in endocrinology:ageing and anti-Aging: A combo- Endocrinology overview. BioScientifica Ltd. doi:10.1530/EJE-16-1061.
Diao, J., Burré, J., Vivona, S., Cipriano, D.J., Sharma, M., Kyoung, M., Südhof, T.C., and Brunger, A.T.

2013. Native α-synuclein induces clustering of synaptic-vesicle mimics via binding to phospholipids and synaptobrevin-2/VAMP2. Elife **2013**(2). eLife Sciences Publications, Ltd. doi:10.7554/eLife.00592.

Diot, A., Morten, K., and Poulton, J. 2016, August 1. Mitophagy plays a central role in mitochondrial ageing. Springer New York LLC. doi:10.1007/s00335-016-9651-x.

Domingo, A., and Klein, C. 2018. Genetics of Parkinson disease. *In* Handbook of Clinical Neurology. Elsevier B.V. pp. 211–227. doi:10.1016/B978-0-444-63233-3.00014-2.

Douglas Green, A.R., and Reed, J.C. 1998. APOPTOSIS SPECIAL SECTION I. **281**(5381): 1309–1312. Available from http://www.jstor.org.qe2a-proxy.mun.ca/stable/pdf/2896429.pdf [accessed 6 December 2017].

Druzhyna, N.M., Wilson, G.L., and LeDoux, S.P. 2008. Mitochondrial DNA repair inageing and disease. Mech. Ageing Dev. **129**(7–8): 383–90. NIH Public Access. doi:10.1016/j.mad.2008.03.002.

Edmondson, D.E. 2014. Hydrogen peroxide produced by mitochondrial monoamine oxidase catalysis: biological implications. Curr. Pharm. Des. **20**(2): 155–60. Available from http://www.ncbi.nlm.nih.gov/pubmed/23701542 [accessed 26 December 2017].

Engelender, S., and Isacson, O. 2017, January 1. The Threshold Theory for Parkinson's Disease. Elsevier Ltd. doi:10.1016/j.tins.2016.10.008.

Farhan, M., Wang, H., Gaur, U., Little, P.J., Xu, J., and Zheng, W. 2017. FOXO signalling pathways as therapeutic targets in cancer. Ivyspring International Publisher. doi:10.7150/ijbs.20052.

Favaro, G., Romanello, V., Varanita, T., Andrea Desbats, M., Morbidoni, V., Tezze, C., Albiero, M., Canato, M., Gherardi, G., De Stefani, D., Mammucari, C., Blaauw, B., Boncompagni, S., Protasi, F., Reggiani, C., Scorrano, L., Salviati, L., and Sandri, M. 2019. DRP1-mediated mitochondrial shape controls calcium homeostasis and muscle mass. Nat. Commun. **10**(1): 2576. Nature Publishing Group. doi:10.1038/s41467-019-10226-9.

Fayet, G., Jansson, M., Sternberg, D., Moslemi, A.R., Blondy, P., Lombès, A., Fardeau, M., and Oldfors, A. 2002. Ageing muscle: clonal expansions of mitochondrial DNA point mutations and deletions cause focal impairment of mitochondrial function. Neuromuscul. Disord. **12**(5): 484–93. Available from http://www.ncbi.nlm.nih.gov/pubmed/12031622 [accessed 9 December 2017].

Feany, M.B., and Bender, W.W. 2000. A Drosophila model of Parkinson's disease. Nature **404**(6776): 394–398. Nature Publishing Group. doi:10.1038/35006074.

Fischer, Z., Das, R., Shipman, A., Fan, J.Y., Pence, L., Bouyain, S., and Dobens, L.L. 2017. A Drosophila model of insulin resistance associated with the human TRIB3 Q/R polymorphism. DMM Dis. Model. Mech. **10**(12): 1453–1464. Company of Biologists Ltd. doi:10.1242/dmm.030619.

Frank, S., Gaume, B., Bergmann-Leitner, E.S., Leitner, W.W., Robert, E.G., Catez, F., Smith, C.L., and Youle, R.J. 2001. The Role of Dynamin-Related Protein 1, a Mediator of Mitochondrial Fission, in Apoptosis. Dev. Cell **1**(4): 515–525. doi:10.1016/S1534-5807(01)00055-7.

Fujita, T. 2002, January 1. Chapter 2 Calcium homeostasis and signalling inageing. Elsevier. doi:10.1016/s1566-3124(02)10014-9.

Fulop, T., Witkowski, J.M., Pawelec, G., Alan, C., and Larbi, A. 2014. On the immunological theory ofageing. *In*ageing: Facts and Theories. S. Karger AG. pp. 163–176. doi:10.1159/000358904.

Galluzzi, L., Kepp, O., and Kroemer, G. 2012, December. Mitochondria: Master regulators of danger signalling. doi:10.1038/nrm3479.

Ghosh, D., Mehra, S., Sahay, S., Singh, P.K., and Maji, S.K. 2017. α-synuclein aggregation and its modulation. Int. J. Biol. Macromol. **100**: 37–54. Elsevier B.V. doi:10.1016/j.ijbiomac.2016.10.021.

Giordano, A., Calvani, M., Petillo, O., Grippo, P., Tuccillo, F., Melone, M.A.B., Bonelli, P., Calarco, A., and Peluso, G. 2005. tBid induces alterations of mitochondrial fatty acid oxidation flux by malonyl-CoA-independent inhibition of carnitine palmitoyltransferase-1. Cell Death Differ. **12**(6): 603–613. doi:10.1038/sj.cdd.4401636.

Githure, P.M., and Staveley, B.E. 2017. Overexpression of Buffy enhances the loss of parkin and suppresses the loss of Pink1 phenotypes in Drosophila. Genome **60**(3): 241–247. NRC Research Press. doi:10.1139/gen-2016-0165.

Glick, D., Zhang, W., Beaton, M., Marsboom, G., Gruber, M., Simon, M.C., Hart, J., Dorn, G.W., Brady, M.J., and Macleod, K.F. 2012. BNip3 regulates mitochondrial function and lipid metabolism in the liver. Mol. Cell. Biol. **32**(13): 2570–84. doi:10.1128/MCB.00167-12.

Gogvadze, V., Orrenius, S., and Zhivotovsky, B. 2006. Multiple pathways of cytochrome c release from mitochondria in apoptosis. Biochim. Biophys. Acta - Bioenerg. **1757**(5–6): 639–647. Elsevier. doi:10.1016/J.BBABIO.2006.03.016.

Green, D.R., and Kroemer, G. 2004. The pathophysiology of mitochondrial cell death. Science **305**(5684): 626–9. American Association for the Advancement of Science. doi:10.1126/science.1099320.

Halliwell ', B., and Cross1, C.E. 1994. Oxygen-derived Species: Their Relation to Human Disease and Environmental Stress. Available from https://www.ncbi.nlm.nih.gov/pmc/articles/PMC1566996/pdf/envhper00409-0012.pdf [accessed 23 December 2017].

Han, D., Lerner, A.G., Vande Walle, L., Upton, J.P., Xu, W., Hagen, A., Backes, B.J., Oakes, S.A., and Papa, F.R. 2009. IRE1α Kinase Activation Modes Control Alternate Endoribonuclease Outputs to Determine Divergent Cell Fates. Cell **138**(3): 562–575. Cell Press. doi:10.1016/j.cell.2009.07.017.

Hardwick, J.M., and Soane, L. 2013. Multiple functions of BCL-2 family proteins. Cold Spring Harb. Perspect. Biol. doi:10.1101/cshperspect.a008722.

Harman, D. 1991. Theageing process: Major risk factor for disease and death. Med. Sci. **88**: 5360–5363. Available from http://www.pnas.org/content/88/12/5360.full.pdf [accessed 22 December 2017].

Harrison, D.E., Strong, R., Sharp, Z.D., Nelson, J.F., Astle, C.M., Flurkey, K., Nadon, N.L., Wilkinson, J.E., Frenkel, K., Carter, C.S., Pahor, M., Javors, M.A., Fernandez, E., and Miller, R.A. 2009. Rapamycin fed late in life extends lifespan in genetically heterogeneous mice. Nature **460**(7253): 392–395. doi:10.1038/nature08221.

Haynes, C.M., Petrova, K., Benedetti, C., Yang, Y., and Ron, D. 2007. ClpP Mediates Activation of a Mitochondrial Unfolded Protein Response in C. elegans. Dev. Cell **13**(4): 467–480. doi:10.1016/j.devcel.2007.07.016.

Haywood, A.F.M., and Staveley, B.E. 2004, April 16. Parkin counteracts symptoms in a Drosophila model of Parkinson's disease. BMC Neurosci. doi:10.1186/1471-2202-5-14.

van Heemst, D. 2010. Insulin, IGF-1 and longevity. International Society onageing and Disease.

Hengartner, M. 0, and Robert Horvitz, H. 1994. C. elegans Cell Survival Gene ced-9 Encodes a Functional Homobg of the Mammalian Proto-Onoogene bcl-2. *In* Cell. Available from

https://ac-els-cdn-com.qe2a-proxy.mun.ca/0092867494905061/1-s2.0-0092867494905061-main.pdf?_tid=ffcd8de4-d5aa-48b1-acff-2dcfc2480d15&acdnat=1545606553_3d133f58128fe98154758e37f6231456 [accessed 23 December 2018].

Heras-Sandoval, D., Pérez-Rojas, J.M., Hernández-Damián, J., and Pedraza-Chaverri, J. 2014, December 1. The role of PI3K/AKT/mTOR pathway in the modulation of autophagy and the clearance of protein aggregates in neurodegeneration. Elsevier Inc. doi:10.1016/j.cellsig.2014.08.019.

Hetz, C., and Mollereau, B. 2014, April. Disturbance of endoplasmic reticulum proteostasis in neurodegenerative diseases. Nature Publishing Group. doi:10.1038/nrn3689.

Hetz, C., and Papa, F.R. 2018, January 18. The Unfolded Protein Response and Cell Fate Control. Cell Press. doi:10.1016/j.molcel.2017.06.017.

Hilgendorf, K.I., Leshchiner, E.S., Nedelcu, S., Maynard, M.A., Calo, E., Ianari, A., Walensky, L.D., and Lees, J.A. 2013. The retinoblastoma protein induces apoptosis directly at the mitochondria. Genes Dev. **27**(9): 1003–1015. Cold Spring Harbor Laboratory Press. doi:10.1101/gad.211326.112.

Hillary, R.F., and Fitzgerald, U. 2018, May 25. A lifetime of stress: ATF6 in development and homeostasis. BioMed Central Ltd. doi:10.1186/s12929-018-0453-1.

Hirst, J., King, M.S., and Pryde, K.R. 2008. The production of reactive oxygen species by complex I. Biochem. Soc. Trans. **36**(Pt 5): 976–80. Portland Press Limited. doi:10.1042/BST0360976.

Holzenberger, M., Dupont, J., Ducos, B., Leneuve, P., Géloën, A., Even, P.C., Cervera, P., and Le Bouc, Y. 2003. IGF-1 receptor regulates lifespan and resistance to oxidative stress in mice. Nature **421**(6919): 182–187. Nature Publishing Group. doi:10.1038/nature01298.

Hoppins, S., Edlich, F., Cleland, M.M., Banerjee, S., McCaffery, J.M., Youle, R.J., and Nunnari, J. 2011. The Soluble Form of Bax Regulates Mitochondrial Fusion via MFN2 Homotypic Complexes. Mol. Cell **41**(2): 150–160. NIH Public Access. doi:10.1016/j.molcel.2010.11.030.

Hulbert, A.J., Pamplona, R., Buffenstein, R., and Buttemer, W.A. 2007, October. Life and death: Metabolic rate, membrane composition, and life span of animals. doi:10.1152/physrev.00047.2006.

Ingerman, E., Perkins, E.M., Marino, M., Mears, J.A., McCaffery, J.M., Hinshaw, J.E., and Nunnari, J. 2005. Dnm1 forms spirals that are structurally tailored to fit mitochondria. J. Cell Biol. **170**(7): 1021–7. Rockefeller University Press. doi:10.1083/jcb.200506078.

Jacobsen, A. V., and Murphy, J.M. 2017, June 15. The secret life of kinases: Insights into noncatalytic signalling functions from pseudokinases. Portland Press Ltd. doi:10.1042/BST20160331.

Javed, H., Kamal, M., and Ojha, S. 2016. An Overview on the Role of α -Synuclein in Experimental Models of Parkinson's Disease from Pathogenesis to Therapeutics. CNS Neurol. Disord. - Drug Targets **15**(10): 1240–1252. Bentham Science Publishers Ltd. doi:10.2174/1871527315666160920160512.

Jia, K., Chen, D., and Riddle, D.L. 2004. The TOR pathway interacts with the insulin signalling pathway to regulate C. elegans larval development, metabolism and life span. Development **131**(16): 3897–3906. The Company of Biologists Ltd. doi:10.1242/dev.01255.

Jin, K. 2010. Modern biological theories ofageing. International Society onageing and Disease. doi:10.1093/jn/119.6.952.

Jovaisaite, V., Mouchiroud, L., and Auwerx, J. 2014. The mitochondrial unfolded protein response, a conserved stress response pathway with implications in health and disease. J. Exp. Biol. **217**(Pt 1): 137–43. Company of Biologists. doi:10.1242/jeb.090738.

Kalaitzakis, M.E., Graeber, M.B., Gentleman, S.M., and Pearce, R.K.B. 2008. The dorsal motor nucleus of the vagus is not an obligatory trigger site of Parkinson's disease: A critical analysis of α-synuclein staging. Neuropathol. Appl. Neurobiol. **34**(3): 284–295. John Wiley & Sons, Ltd. doi:10.1111/j.1365-2990.2007.00923.x.

Kalia, L. V., Kalia, S.K., McLean, P.J., Lozano, A.M., and Lang, A.E. 2013. α-synuclein oligomers and clinical implications for parkinson disease. Ann. Neurol. **73**(2): 155–169. doi:10.1002/ana.23746.

Kalia, L. V., and Lang, A.E. 2015, August 29. Parkinson's disease. Lancet Publishing Group. doi:10.1016/S0140-6736(14)61393-3.

Kamel, F. 2013, August 16. Paths from pesticides to Parkinson's. American Association for the Advancement of Science. doi:10.1126/science.1243619.

Kandel, E.S., Skeen, J., Majewski, N., Di Cristofano, A., Pandolfi, P.P., Feliciano, C.S., Gartel, A., and Hay, N. 2002. Activation of Akt/Protein Kinase B Overcomes a G2/M Cell Cycle Checkpoint Induced by DNA Damage. Mol. Cell. Biol. **22**(22): 7831–7841. American Society for Microbiology. doi:10.1128/mcb.22.22.7831-7841.2002.

Kann, O., and Kovács, R. 2007, February. Mitochondria and neuronal activity. Am J Physiol Cell Physiol. doi:10.1152/ajpcell.00222.2006.

Kapahi, P., Kaeberlein, M., and Hansen, M. 2017, October 1. Dietary restriction and lifespan: Lessons from invertebrate models. Elsevier Ireland Ltd. doi:10.1016/j.arr.2016.12.005.

Karbowski, M., Lee, Y.-J., Gaume, B., Jeong, S.-Y., Frank, S., Nechushtan, A., Santel, A., Fuller, M., Smith, C.L., and Youle, R.J. 2002. Spatial and temporal association of Bax with mitochondrial fission sites, Drp1, and Mfn2 during apoptosis. J. Cell Biol. **159**(6): 931–8. The Rockefeller University Press. doi:10.1083/jcb.200209124.

Kathrin Lutz, A., Exner, N., Fett, M.E., Schleke, J.S., Kloos, K., Lämmermann, K., Brunner, B., Kurz-Drexler, A., Vogel, F., Reichert, A.S., Bouman, L., Vogt-Weisenhorn, D., Wurst, W., Tatzelt, J., Haass, C., and Winklhofer, K.F. 2009. Loss of parkin or PINK1 function increases Drp1-dependent mitochondrial fragmentation. J. Biol. Chem. **284**(34): 22938–22951. doi:10.1074/jbc.M109.035774.

Kawajiri, S., Saiki, S., Sato, S., and Hattori, N. 2011. Genetic mutations and functions of PINK1. Trends Pharmacol. Sci. **32**(10): 573–580. Elsevier Current Trends. doi:10.1016/J.TIPS.2011.06.001.

Kim, D.I., Lee, K.H., Gabr, A.A., Choi, G.E., Kim, J.S., Ko, S.H., and Han, H.J. 2016. Aβ-Induced Drp1 phosphorylation through Akt activation promotes excessive mitochondrial fission leading to neuronal apoptosis. Biochim. Biophys. Acta - Mol. Cell Res. **1863**(11): 2820–2834. doi:10.1016/j.bbamcr.2016.09.003.

Kimura, K.D., Tissenbaum, H.A., Liu, Y., and Ruvkun, G. 1997. Daf-2, an insulin receptor-like gene that regulates longevity and diapause in Caenorhabditis elegans. Science (80-.). **277**(5328): 942–946. American Association for the Advancement of Science. doi:10.1126/science.277.5328.942.

Kirkwood, T.B.L., and Kowald, A. 2012. The free-radical theory of ageing - older, wiser and still alive: Modelling positional effects of the primary targets of ROS reveals new support.

BioEssays **34**(8): 692–700. doi:10.1002/bies.201200014.

Klotz, L.O., Sánchez-Ramos, C., Prieto-Arroyo, I., Urbánek, P., Steinbrenner, H., and Monsalve, M. 2015, December 1. Redox regulation of FoxO transcription factors. Elsevier B.V. doi:10.1016/j.redox.2015.06.019.

Koch, A., Thiemann, M., Grabenbauer, M., Yoon, Y., McNiven, M.A., and Schrader, M. 2003. Dynamin-like Protein 1 Is Involved in Peroxisomal Fission. J. Biol. Chem. **278**(10): 8597–8605. doi:10.1074/jbc.M211761200.

Koshiba, T., Detmer, S.A., Kaiser, J.T., Chen, H., McCaffery, J.M., and Chan, D.C. 2004. Structural basis of mitochondrial tethering by mitofusin complexes. Science (80-.). **305**(5685): 858–862. doi:10.1126/science.1099793.

Kowald, A., and Kirkwood, T.B. 1996. A network theory of ageing: the interactions of defective mitochondria, aberrant proteins, free radicals and scavengers in the ageing process. Mutat. Res. **316**(5–6): 209–36. doi:10.1016/s0921-8734(96)90005-3.

Koyano, F., Okatsu, K., Kosako, H., Tamura, Y., Go, E., Kimura, M., Kimura, Y., Tsuchiya, H., Yoshihara, H., Hirokawa, T., Endo, T., Fon, E.A., Trempe, J.-F., Saeki, Y., Tanaka, K., and Matsuda, N. 2014. Ubiquitin is phosphorylated by PINK1 to activate parkin. Nature **510**(7503): 162–166. Nature Publishing Group. doi:10.1038/nature13392.

Krebs, J. 1998. The role of calcium in apoptosis. doi:10.1023/A:1009226316146.

Krebs, J., Agellon, L.B., and Michalak, M. 2015, May 19. Ca2+ homeostasis and endoplasmic reticulum (ER) stress: An integrated view of calcium signalling. Academic Press Inc. doi:10.1016/j.bbrc.2015.02.004.

Kristiansen, M., Deriziotis, P., Dimcheff, D.E., Jackson, G.S., Ovaa, H., Naumann, H., Clarke, A.R., van Leeuwen, F.W.B., Menéndez-Benito, V., Dantuma, N.P., Portis, J.L., Collinge, J., and Tabrizi, S.J. 2007. Disease-Associated Prion Protein Oligomers Inhibit the 26S Proteasome. Mol. Cell **26**(2): 175–188. Elsevier. doi:10.1016/j.molcel.2007.04.001.

Kubli, D.A., and Gustafsson, Å.B. 2012. Mitochondria and mitophagy: the yin and yang of cell death control. Circ. Res. **111**(9): 1208–21. NIH Public Access. doi:10.1161/CIRCRESAHA.112.265819.

Kwon, Y.T., and Ciechanover, A. 2017, November 1. The Ubiquitin Code in the Ubiquitin-Proteasome System and Autophagy. Elsevier Ltd. doi:10.1016/j.tibs.2017.09.002.

Lambert, A.J., Boysen, H.M., Buckingham, J.A., Yang, T., Podlutsky, A., Austad, S.N., Kunz, T.H., Buffenstein, R., and Brand, M.D. 2007. Low rates of hydrogen peroxide production by isolated heart mitochondria associate with long maximum lifespan in vertebrate homeotherms.ageing Cell **6**(5): 607–618. Blackwell Publishing Ltd. doi:10.1111/j.1474-9726.2007.00312.x.

Lander, S., Linton, L.M., Birren, B., Nusbaum, C., Zody, M.C., Baldwin, J., Devon, K., Dewar, K., Doyle, M., FitzHugh, W., Funke, R., Gage, D., Harris, K., Heaford, A., Howland, J., Kann, L., Lehoczky, J., LeVine, R., McEwan, P., McKernan, K., Meldrim, J., Mesirov, J.P., Miranda, C., Morris, W., Naylor, J., Raymond, C., Rosetti, M., Santos, R., Sheridan, A., Sougnez, C., Stange-Thomann, N., Stojanovic, N., Subramanian, A., Wyman, D., Rogers, J., Sulston, J., Ainscough, R., Beck, S., Bentley, D., Burton, J., Clee, C., Carter, N., Coulson, A., Deadman, R., Deloukas, P., Dunham, A., Dunham, I., Durbin, R., French, L., Grafham, D., Gregory, S., Hubbard, T., Humphray, S., Hunt, A., Jones, M., Lloyd, C., McMurray, A., Matthews, L., Mercer, S., Milne, S., Mullikin, J.C., Mungall, A., Plumb, R., Ross, M., Shownkeen, R., Sims, S., Waterston, R.H., Wilson, R.K., Hillier, L.W., McPherson, J.D., Marra, M.A., Mardis, E.R., Fulton, L.A., Chinwalla,

A.T., Pepin, K.H., Gish, W.R., Chissoe, S.L., Wendl, M.C., Delehaunty, K.D., Miner, T.L., Delehaunty, A., Kramer, J.B., Cook, L.L., Fulton, R.S., Johnson, D.L., Minx, P.J., Clifton, S.W., Hawkins, T., Branscomb, E., Predki, P., Richardson, P., Wenning, S., Slezak, T., Doggett, N., Cheng, J.-F., Olsen, A., Lucas, S., Elkin, C., Uberbacher, E., Frazier, M., Gibbs, R.A., Muzny, D.M., Scherer, S.E., Bouck, J.B., Sodergren, E.J., Worley, K.C., Rives, C.M., Gorrell, J.H., Metzker, M.L., Naylor, S.L., Kucherlapati, R.S., Nelson, D.L., Weinstock, G.M., Sakaki, Y., Fujiyama, A., Hattori, M., Yada, T., Toyoda, A., Itoh, T., Kawagoe, C., Watanabe, H., Totoki, Y., Taylor, T., Umr-, C., Weissenbach, J., Heilig, R., Saurin, W., Artiguenave, F., Brottier, P., Bruls, T., Pelletier, E., Robert, C., Wincker, P., Smith, D.R., Doucette-Stamm, L., Ruben, M., Weinstock, K., Mei Lee, H., Dubois, J., Â Rosenthal, A., Platzer, M., Nyakatura, G., Taudien, S., Rump, A., Yang, H., Yu, J., Wang, J., Huang, G., Gu, J., Genome Technology Center, S., Davis, R.W., Federspiel, N.A., Pia Abola, A., Proctor, M.J., Human Genome Center, S., Myers, R.M., Schmutz, J., Dickson, M., Grimwood, J., Cox, D.R., Olson, M. V, Kaul, R., Raymond, C., Evans, G.A., Athanasiou, M., Schultz, R., Roe, B.A., Chen, F., Pan, H., Ramser, J., Lehrach, H., Reinhardt, R., Richard McCombie, W., de la Bastide, M., Dedhia, N., Blo È cker, H., Hornischer, K., Nordsiek, G., Agarwala, R., Aravind, L., Bailey, J.A., Bateman, A., Birney, E., Bork, P., Brown, D.G., Burge, C.B., Cerutti, L., Chen, H.-C., Church, D., Clamp, M., Copley, R.R., Doerks, T., Eddy, S.R., Eichler, E.E., Furey, T.S., Galagan, J., R Gilbert, J.G., Harmon, C., Hayashizaki, Y., Haussler, D., Hermjakob, H., Hokamp, K., Jang, W., Steven Johnson, L., Jones, T.A., Kasif, S., Kaspryzk, A., Kennedy, S., James Kent, W., Kitts, P., Koonin, E. V, Korf, I., Kulp, D., Lancet, D., Lowe, T.M., McLysaght, A., Mikkelsen, T., Moran, J. V, Mulder, N., Pollara, V.J., Ponting, C.P., Schuler, G., È rg Schultz, J., Slater, G., A Smit, A.F., Stupka, E., Szustakowki, J., Thierry-Mieg, D., Thierry-Mieg, J., Wagner, L., Wallis, J., Wheeler, R., Williams, A., Wolf, Y.I., Wolfe, K.H., Yang, S.-P., and Yeh, R.-F. 2001. Initial sequencing and analysis of the human genome International Human Genome Sequencing Consortium* The Sanger Centre: Beijing Genomics Institute/Human Genome Center. *In* NATURE. Available from www.nature.com [accessed 26 January 2020].

Langston, J., Ballard, P., Tetrud, J., and Irwin, I. 1983. Chronic Parkinsonism in humans due to a product of meperidine-analog synthesis. Science (80-.). **219**(4587): 979–980. American Association for the Advancement of Science (AAAS). doi:10.1126/science.6823561.

Langston, J.W. 1989. Current theories on the cause of Parkinson's disease. J. Neurol. Neurosurg. Psychiatry **52**(SUPPL): 13–17. BMJ Publishing Group. doi:10.1136/jnnp.52.Suppl.13.

Lautenschläger, J., Stephens, A.D., Fusco, G., Ströhl, F., Curry, N., Zacharopoulou, M., Michel, C.H., Laine, R., Nespovitaya, N., Fantham, M., Pinotsi, D., Zago, W., Fraser, P., Tandon, A., St George-Hyslop, P., Rees, E., Phillips, J.J., De Simone, A., Kaminski, C.F., and Schierle, G.S.K. 2018. C-terminal calcium binding of α-synuclein modulates synaptic vesicle interaction. Nat. Commun. **9**(1). Nature Publishing Group. doi:10.1038/s41467-018-03111-4.

Laviola, L., Natalicchio, A., and Giorgino, F. 2007. The IGF-I Signalling Pathway. *In* Current Pharmaceutical Design.

Lee, K.S., Huh, S., Lee, S., Wu, Z., Kim, A.K., Kang, H.Y., and Lu, B. 2018. Altered ER-mitochondria contact impacts mitochondria calcium homeostasis and contributes to neurodegeneration in vivo in disease models. Proc. Natl. Acad. Sci. U. S. A. **115**(38): E8844–E8853. National Academy of Sciences. doi:10.1073/pnas.1721136115.

Lee, S., Jeong, S.Y., Lim, W.C., Kim, S., Park, Y.Y., Sun, X., Youle, R.J., and Cho, H. 2007. Mitochondrial

fission and fusion mediators, hFis1 and OPA1, modulate cellular senescence. J. Biol. Chem. 282(31): 22977–22983. doi:10.1074/jbc.M700679200.

Lees, A.J., Hardy, J., and Revesz, T. 2009. Parkinson's disease. *In* www.thelancet.com. doi:10.1016/S0140-6736(09)60492-X.

Li, H., Alavian, K.N., Lazrove, E., Mehta, N., Jones, A., Zhang, P., Licznerski, P., Graham, M., Uo, T., Guo, J., Rahner, C., Duman, R.S., Morrison, R.S., and Jonas, E.A. 2013. A Bcl-x L -Drp1 complex regulates synaptic vesicle membrane dynamics during endocytosis. Nat. Cell Biol. 15(7): 773–785. doi:10.1038/ncb2791.

Lima, A.F., Ropelle, E.R., Pauli, J.R., Cintra, D.E., Frederico, M.J.S., Pinho, R.A., Velloso, L.A., and De Souza, C.T. 2009. Acute exercise reduces insulin resistance-induced TRB3 expression and amelioration of the hepatic production of glucose in the liver of diabetic mice. J. Cell. Physiol. 221(1): 92–97. J Cell Physiol. doi:10.1002/jcp.21833.

Lin, Y.-F., Schulz, A.M., Pellegrino, M.W., Lu, Y., Shaham, S., and Haynes, C.M. 2016. Maintenance and propagation of a deleterious mitochondrial genome by the mitochondrial unfolded protein response. Nature 533(7603): 416–419. Nature Publishing Group. doi:10.1038/nature17989.

Lipinski, M.M., and Jacks, T. 1999, December 20. The retinoblastoma gene family in differentiation and development. Nature Publishing Group. doi:10.1038/sj.onc.1203244.

Liu, P., Begley, M., Michowski, W., Inuzuka, H., Ginzberg, M., Gao, D., Tsou, P., Gan, W., Papa, A., Kim, B.M., Wan, L., Singh, A., Zhai, B., Yuan, M., Wang, Z., Gygi, S.P., Lee, T.H., Lu, K.P., Toker, A., Pandolfi, P.P., Asara, J.M., Kirschner, M.W., Sicinski, P., Cantley, L., and Wei, W. 2014. Cell-cycle-regulated activation of Akt kinase by phosphorylation at its carboxyl terminus. Nature 508(7497): 541–545. Nature Publishing Group. doi:10.1038/nature13079.

Liu, Z., Lv, Y., Zhao, N., Guan, G., and Wang, J. 2015, July 1. Protein kinase R-like ER kinase and its role in endoplasmic reticulum stress-decided cell fate. Nature Publishing Group. doi:10.1038/cddis.2015.183.

Ljubicic, S., Polak, K., Fu, A., Wiwczar, J., Szlyk, B., Chang, Y., Alvarez-Perez, J.C., Bird, G.H., Walensky, L.D., Garcia-Ocaña, A., and Danial, N.N. 2015. Phospho-BAD BH3 mimicry protects β cells and restores functional β cell mass in diabetes. Cell Rep. 10(4): 497–504. Elsevier. doi:10.1016/j.celrep.2014.12.056.

Longo, V.D., Mitteldorf, J., and Skulachev, V.P. 2005, November. Opinion: Programmed and altruistic ageing. Nature Publishing Group. doi:10.1038/nrg1706.

López-Otín, C., Blasco, M.A., Partridge, L., Serrano, M., and Kroemer, G. 2013. The Hallmarks ofageing Europe PMC Funders Group. Cell June 6(1536): 1194–121705. doi:10.1016/j.cell.2013.05.039.

Lowman, X.H., McDonnell, M.A., Kosloske, A., Odumade, O.A., Jenness, C., Karim, C.B., Jemmerson, R., and Kelekar, A. 2010. The Proapoptotic Function of Noxa in Human Leukemia Cells Is Regulated by the Kinase Cdk5 and by Glucose. Mol. Cell 40(5): 823–833. doi:10.1016/j.molcel.2010.11.035.

Luce, K., and Osiewacz, H.D. 2009. Increasing organismal healthspan by enhancing mitochondrial protein quality control. Nat. Cell Biol. 11(7): 852–858. Nature Publishing Group. doi:10.1038/ncb1893.

Ludtmann, M.H.R., and Abramov, A.Y. 2018, January 10. Mitochondrial calcium imbalance in Parkinson's disease. Elsevier Ireland Ltd. doi:10.1016/j.neulet.2017.08.044.

Luk, K.C., Kehm, V.M., Zhang, B., O'Brien, P., Trojanowski, J.Q., and Lee, V.M.Y. 2012. Intracerebral inoculation of pathological α-synuclein initiates a rapidly progressive neurodegenerative α-synucleinopathy in mice. J. Exp. Med. **209**(5): 975–988. The Rockefeller University Press. doi:10.1084/jem.20112457.

Maes, M.E., Grosser, J.A., Fehrman, R.L., Schlamp, C.L., and Nickells, R.W. 2019. Completion of BAX recruitment correlates with mitochondrial fission during apoptosis. Sci. Rep. **9**(1). Nature Publishing Group. doi:10.1038/s41598-019-53049-w.

Magen, I., and Chesselet, M.F. 2010. Genetic mouse models of Parkinson's disease. The state of the art. *In* Progress in Brain Research. Elsevier B.V. pp. 53–87. doi:10.1016/S0079-6123(10)84004-X.

Manning, B.D., and Toker, A. 2017. Leading Edge Review AKT/PKB Signalling: Navigating the Network. Cell **169**: 381–405. doi:10.1016/j.cell.2017.04.001.

Martins, R., Lithgow, G.J., and Link, W. 2016, April 1. Long live FOXO: Unraveling the role of FOXO proteins inageing and longevity. Blackwell Publishing Ltd. doi:10.1111/acel.12427.

Martinus, R.D., Garth, G.P., Webster, T.L., Cartwright, P., Naylor, D.J., Høj, P.B., and Hoogenraad, N.J. 1996. Selective Induction of Mitochondrial Chaperones in Response to Loss of the Mitochondrial Genome. Eur. J. Biochem. **240**(1): 98–103. Blackwell Publishing Ltd. doi:10.1111/j.1432-1033.1996.0098h.x.

Maurer, U., Charvet, C., Wagman, A.S., Dejardin, E., and Green, D.R. 2006. Glycogen synthase kinase-3 regulates mitochondrial outer membrane permeabilization and apoptosis by destabilization of MCL-1. Mol. Cell **21**(6): 749–760. doi:10.1016/j.molcel.2006.02.009.

McBride, H.M., Neuspiel, M., and Wasiak, S. 2006. Mitochondria: more than just a powerhouse. Curr. Biol. **16**(14): R551-60. Elsevier. doi:10.1016/j.cub.2006.06.054.

McLelland, G.L., Soubannier, V., Chen, C.X., McBride, H.M., and Fon, E.A. 2014. Parkin and PINK1 function in a vesicular trafficking pathway regulating mitochondrial quality control. EMBO J. **33**(4): 282–295. doi:10.1002/embj.201385902.

Mears, J.A., Lackner, L.L., Fang, S., Ingerman, E., Nunnari, J., and Hinshaw, J.E. 2011. Conformational changes in Dnm1 support a contractile mechanism for mitochondrial fission. Nat. Struct. Mol. Biol. **18**(1): 20–26. Nature Publishing Group. doi:10.1038/nsmb.1949.

Medlock, A.E., Shiferaw, M.T., Marcero, J.R., Vashisht, A.A., Wohlschlegel, J.A., Phillips, J.D., and Dailey, H.A. 2015. Identification of the Mitochondrial Heme Metabolism Complex. PLoS One **10**(8): e0135896. Public Library of Science. doi:10.1371/journal.pone.0135896.

Middleton, E.R., and Rhoades, E. 2010. Effects of curvature and composition on α-synuclein binding to lipid vesicles. Biophys. J. **99**(7): 2279–2288. Biophysical Society. doi:10.1016/j.bpj.2010.07.056.

Miller, W.L. 2013. Steroid hormone synthesis in mitochondria. Mol. Cell. Endocrinol. **379**(1–2): 62–73. Elsevier. doi:10.1016/J.MCE.2013.04.014.

Mills, E.L., Kelly, B., and O'Neill, L.A.J. 2017. Mitochondria are the powerhouses of immunity. Nat. Immunol. **18**(5): 488–498. Nature Publishing Group. doi:10.1038/ni.3704.

Miraglia, F., Ricci, A., Rota, L., and Colla, E. 2018, July 1. Subcellular localization of alpha-synuclein aggregates and their interaction with membranes. Wolters Kluwer Medknow Publications. doi:10.4103/1673-5374.235013.

Miyamoto, K., Araki, K.Y., Naka, K., Arai, F., Takubo, K., Yamazaki, S., Matsuoka, S., Miyamoto, T., Ito, K., Ohmura, M., Chen, C., Hosokawa, K., Nakauchi, H., Nakayama, K., Nakayama, K.I.,

Harada, M., Motoyama, N., Suda, T., and Hirao, A. 2007. Foxo3a Is Essential for Maintenance of the Hematopoietic Stem Cell Pool. Cell Stem Cell **1**(1): 101–112. Elsevier. doi:10.1016/j.stem.2007.02.001.

Modi, P., Mohamad, A., Phom, L., Koza, Z., Das, A., Chaurasia, R., Samadder, S., Achumi, B., Muralidhara, Pukhrambam, R.S., and Yenisetti, S.C. 2016. Understanding Pathophysiology of Sporadic Parkinson's Disease in Drosophila Model: Potential Opportunities and Notable Limitations. *In* Challenges in Parkinson's Disease. InTech. doi:10.5772/63767.

Morciano, G., Marchi, S., Morganti, C., Sbano, L., Bittremieux, M., Kerkhofs, M., Corricelli, M., Danese, A., Karkucinska-Wieckowska, A., Wieckowski, M.R., Bultynck, G., Giorgi, C., and Pinton, P. 2018, May 1. Role of Mitochondria-Associated ER Membranes in Calcium Regulation in Cancer-Specific Settings. Neoplasia Press, Inc. doi:10.1016/j.neo.2018.03.005.

Morrison, R.S., Kinoshita, Y., Johnson, M.D., Ghatan, S., Ho, J.T., and Garden, G. 2002. Neuronal survival and cell death signalling pathways. doi:10.1007/978-1-4615-0123-7_2.

Mougenot, A.L., Nicot, S., Bencsik, A., Morignat, E., Verchère, J., Lakhdar, L., Legastelois, S., and Baron, T. 2012. Prion-like acceleration of a synucleinopathy in a transgenic mouse model. Neurobiol.ageing **33**(9): 2225–2228. Elsevier. doi:10.1016/j.neurobiolaging.2011.06.022.

Muller, F.L., Liu, Y., and Van Remmen, H. 2004. Complex III Releases Superoxide to Both Sides of the Inner Mitochondrial Membrane. J. Biol. Chem. **279**(47): 49064–49073. doi:10.1074/jbc.M407715200.

Murphy, M.P. 2009. How mitochondria produce reactive oxygen species. Biochem. J. **417**(1): 1–13. Portland Press Ltd. doi:10.1042/BJ20081386.

Murtaza, G., Khan, A.K., Rashid, R., Muneer, S., Hasan, S.M.F., and Chen, J. 2017. FOXO Transcriptional Factors and Long-Term Living. Oxid. Med. Cell. Longev. **2017**: 1–8. Hindawi. doi:10.1155/2017/3494289.

Nagdas, S., and Kashatus, D.F. 2017. The Interplay between Oncogenic Signalling Networks and Mitochondrial Dynamics. Antioxidants **6**(2): 33. doi:10.3390/antiox6020033.

Nakamura, K., Nemani, V.M., Azarbal, F., Skibinski, G., Levy, J.M., Egami, K., Munishkina, L., Zhang, J., Gardner, B., Wakabayashi, J., Sesaki, H., Cheng, Y., Finkbeiner, S., Nussbaum, R.L., Masliah, E., and Edwards, R.H. 2011. Direct membrane association drives mitochondrial fission by the Parkinson disease-associated protein α-synuclein. J. Biol. Chem. **286**(23): 20710–20726. American Society for Biochemistry and Molecular Biology. doi:10.1074/jbc.M110.213538.

Nakamura, K., Nemani, V.M., Wallender, E.K., Kaehlcke, K., Ott, M., and Edwards, R.H. 2008. Optical reporters for the conformation of α-synuclein reveal a specific interaction with mitochondria. J. Neurosci. **28**(47): 12305–12317. doi:10.1523/JNEUROSCI.3088-08.2008.

Nargund, A.M., Fiorese, C.J., Pellegrino, M.W., Deng, P., and Haynes, C.M. 2015. Mitochondrial and nuclear accumulation of the transcription factor ATFS-1 promotes OXPHOS recovery during the UPRmt. Mol. Cell **58**(1): 123–133. Cell Press. doi:10.1016/j.molcel.2015.02.008.

Nargund, A.M., Pellegrino, M.W., Fiorese, C.J., Baker, B.M., and Haynes, C.M. 2012. Mitochondrial Import Efficiency of ATFS-1 Regulates Mitochondrial UPR Activation. Science (80-.). **337**(6094): 587–590. doi:10.1126/science.1223560.

Nemani, V.M., Lu, W., Berge, V., Nakamura, K., Onoa, B., Lee, M.K., Chaudhry, F.A., Nicoll, R.A., and Edwards, R.H. 2010. Increased Expression of α-Synuclein Reduces Neurotransmitter Release by Inhibiting Synaptic Vesicle Reclustering after Endocytosis. Neuron **65**(1): 66–79. doi:10.1016/j.neuron.2009.12.023.

Neupert, W., and Herrmann, J.M. 2007. Translocation of Proteins into Mitochondria. Annu. Rev. Biochem. **76**(1): 723–749. doi:10.1146/annurev.biochem.76.052705.163409.

Nicolson, G.L. 2014. Mitochondrial dysfunction and chronic disease: Treatment with natural supplements. Integr. Med. **13**(4): 35–43. InnoVision Communications. Available from /pmc/articles/PMC4566449/?report=abstract [accessed 29 December 2020].

Niu, J., Yu, M., Wang, C., and Xu, Z. 2012. Leucine-rich repeat kinase 2 disturbs mitochondrial dynamics via Dynamin-like protein. J. Neurochem. **122**(3): 650–658. John Wiley & Sons, Ltd. doi:10.1111/j.1471-4159.2012.07809.x.

O'Reilly, L.A., Huang, D.C., and Strasser, A. 1996. The cell death inhibitor Bcl-2 and its homologues influence control of cell cycle entry. EMBO J. **15**(24): 6979–90. Available from http://www.ncbi.nlm.nih.gov/pubmed/9003774 [accessed 28 February 2020].

Obeso, J.A., Rodriguez-Oroz, M.C., Goetz, C.G., Marin, C., Kordower, J.H., Rodriguez, M., Hirsch, E.C., Farrer, M., Schapira, A.H.V., and Halliday, G. 2010, June 23. Missing pieces in the Parkinson's disease puzzle. Nature Publishing Group. doi:10.1038/nm.2165.

Oh, M.M., Oliveira, F.A., Waters, J., and Disterhoft, J.F. 2013. Cellular/Molecular Altered Calcium Metabolism inageing CA1 Hippocampal Pyramidal Neurons. doi:10.1523/JNEUROSCI.5457-12.2013.

Okatsu, K., Uno, M., Koyano, F., Go, E., Kimura, M., Oka, T., Tanaka, K., and Matsuda, N. 2013. A Dimeric PINK1-containing Complex on Depolarized Mitochondria Stimulates Parkin Recruitment. J. Biol. Chem. **288**(51): 36372–36384. doi:10.1074/jbc.M113.509653.

Owusu-Ansah, E., and Banerjee, U. 2009. Reactive oxygen species prime Drosophila haematopoietic progenitors for differentiation. Nature **461**(7263): 537–541. doi:10.1038/nature08313.

Panicker, N., Dawson, V.L., and Dawson, T.M. 2017, September 15. Activation mechanisms of the E3 ubiquitin ligase parkin. Portland Press Ltd. doi:10.1042/BCJ20170476.

Perciavalle, R.M., Stewart, D.P., Koss, B., Lynch, J., Milasta, S., Bathina, M., Temirov, J., Cleland, M.M., Pelletier, S., Schuetz, J.D., Youle, R.J., Green, D.R., and Opferman, J.T. 2012. Anti-apoptotic MCL-1 localizes to the mitochondrial matrix and couples mitochondrial fusionÂ to respiration. Nat. Cell Biol. **14**(6): 575–583. doi:10.1038/ncb2488.

Pickrell, A.M., and Youle, R.J. 2015, January 21. The roles of PINK1, Parkin, and mitochondrial fidelity in parkinson's disease. Cell Press. doi:10.1016/j.neuron.2014.12.007.

Pinton, P., Ferrari, D., Magalhaes, P., Schulze-Osthoff, K., Di Virgilio, F., Pozzan, T., and Rizzuto, R. 2000. Reduced loading of intracellular Ca2+ stores and downregulation of capacitative Ca2+ influx in Bcl-2-overexpressing cells. J. Cell Biol. **148**(5): 857–862. The Rockefeller University Press. doi:10.1083/jcb.148.5.857.

Pitts, K.R., Yoon, Y., Krueger, E.W., and McNiven, M.A. 1999. The Dynamin-like Protein DLP1 Is Essential for Normal Distribution and Morphology of the Endoplasmic Reticulum and Mitochondria in Mammalian Cells. Mol. Biol. Cell **10**(12): 4403–4417. doi:10.1091/mbc.10.12.4403.

Polymeropoulos, M.H., Lavedan, C., Leroy, E., Ide, S.E., Dehejia, A., Dutra, A., Pike, B., Root, H., Rubenstein, J., Boyer, R., Stenroos, E.S., Chandrasekharappa, S., Athanassiadou, A., Papapetropoulos, T., Johnson, W.G., Lazzarini, A.M., Duvoisin, R.C., Di Iorio, G., Golbe, L.I., and Nussbaum, R.L. 1997. Mutation in the α-synuclein gene identified in families with Parkinson's disease. Science (80-.). **276**(5321): 2045–2047.

doi:10.1126/science.276.5321.2045.
Quirós, P.M., Langer, T., and López-Otín, C. 2015. New roles for mitochondrial proteases in health, ageing and disease. Nat. Rev. Mol. Cell Biol. **16**(6): 345–359. Nature Publishing Group. doi:10.1038/nrm3984.
Raha, S., Mceachern, G.E., Tomoko Myint, A., and Robinson, B.H. 2000. SUPEROXIDES FROM MITOCHONDRIAL COMPLEX III: THE ROLE OF MANGANESE SUPEROXIDE DISMUTASE. Available from https://ac.els-cdn.com/S0891584900003385/1-s2.0-S0891584900003385-main.pdf?_tid=6e24ac84-db81-11e7-a306-00000aab0f27&acdnat=1512673640_ddded510438e40c757a7797d9cf3d1c7 [accessed 7 December 2017].
Rana, A., Rera, M., and Walker, D.W. 2013. Parkin overexpression duringageing reduces proteotoxicity, alters mitochondrial dynamics, and extends lifespan. Proc. Natl. Acad. Sci. **110**(21): 8638–8643. doi:10.1073/pnas.1216197110.
Rcom-H'cheo-Gauthier, A., Goodwin, J., and Pountney, D.L. 2014, September 1. Interactions between calcium and alpha-synuclein in neurodegeneration. MDPI AG. doi:10.3390/biom4030795.
Recasens, A., and Dehay, B. 2014, December 18. Alpha-synuclein spreading in Parkinson's disease. Frontiers Media S.A. doi:10.3389/fnana.2014.00159.
Reeve, A.K., Krishnan, K.J., and Turnbull, D. 2008. Mitochondrial DNA mutations in disease,ageing, and neurodegeneration. *In* Annals of the New York Academy of Sciences. Blackwell Publishing Inc. pp. 21–29. doi:10.1196/annals.1427.016.
Ristow, M., and Schmeisser, K. 2014. Mitohormesis: Promoting Health and Lifespan by Increased Levels of Reactive Oxygen Species (ROS). Dose. Response. **12**(2): 288–341. SAGE Publications. doi:10.2203/dose-response.13-035.Ristow.
Rottenberg, H., and Hoek, J.B. 2017. The path from mitochondrial ROS toageing runs through the mitochondrial permeability transition pore.ageing Cell **16**(5): 943–955. Wiley-Blackwell. doi:10.1111/acel.12650.
Sanes, J.R., and Zipursky, S.L. 2010, April. Design Principles of Insect and Vertebrate Visual Systems. NIH Public Access. doi:10.1016/j.neuron.2010.01.018.
Santos, A.L., Sinha, S., and Lindner, A.B. 2018. The Good, the Bad, and the Ugly of ROS: New Insights onageing andageing-Related Diseases from Eukaryotic and Prokaryotic Model Organisms. doi:10.1155/2018/1941285.
Scheffler, I.E. 2008. Mitochondria. *In* Mitochondria. John Wiley & Sons, Inc., Hoboken, NJ, USA. pp. 441–462. doi:10.1002/9780470191774.index.
Scherz-Shouval, R., Shvets, E., Fass, E., Shorer, H., Gil, L., and Elazar, Z. 2007. Reactive oxygen species are essential for autophagy and specifically regulate the activity of Atg4. EMBO J. **26**(7): 1749–1760. doi:10.1038/sj.emboj.7601623.
Schlesinger, P.H., Gross, A., Yin, X.M., Yamamoto, K., Saito, M., Waksman, G., and Korsmeyer, S.J. 1997. Comparison of the ion channel characteristics of proapoptotic BAX and antiapoptotic BCL-2. Proc. Natl. Acad. Sci. U. S. A. **94**(21): 11357–62. National Academy of Sciences. Available from http://www.ncbi.nlm.nih.gov/pubmed/9326614 [accessed 16 December 2017].
Schlossmacher, M.G., Frosch, M.P., Gai, W.P., Medina, M., Sharma, N., Forno, L., Ochiishi, T., Shimura, H., Sharon, R., Hattori, N., Langston, J.W., Mizuno, Y., Hyman, B.T., Selkoe, D.J., and

Kosik, K.S. 2002. Parkin localizes to the Lewy bodies of Parkinson disease and dementia with Lewy bodies. Am. J. Pathol. **160**(5): 1655–1667. American Society for Investigative Pathology Inc. doi:10.1016/S0002-9440(10)61113-3.

Schober, A. 2004, October. Classic toxin-induced animal models of Parkinson's disease: 6-OHDA and MPTP. doi:10.1007/s00441-004-0938-y.

Schwarzer, R., Dames, S., Tondera, D., Klippel, A., and Kaufmann, J. 2006. TRB3 is a PI 3-kinase dependent indicator for nutrient starvation. Cell. Signal. **18**(6): 899–909. Cell Signal. doi:10.1016/j.cellsig.2005.08.002.

Scorrano, L., Oakes, S.A., Opferman, J.T., Cheng, E.H., Sorcinelli, M.D., Pozzan, T., and Korsmeyer, S.J. 2003. BAX and BAK regulation of endoplasmic reticulum Ca2+: A control point for apoptosis. Science (80-.). **300**(5616): 135–139. doi:10.1126/science.1081208.

Sebastián, D., Palacín, M., and Zorzano, A. 2017. Mitochondrial Dynamics: Coupling Mitochondrial Fitness with Healthyageing. Trends Mol. Med. **23**(3): 201–215. Elsevier Current Trends. doi:10.1016/J.MOLMED.2017.01.003.

Selman, C., Partridge, L., and Withers, D.J. 2011. Replication of extended lifespan phenotype in mice with deletion of insulin receptor substrate 1. PLoS One **6**(1). Public Library of Science. doi:10.1371/journal.pone.0016144.

Sena, L.A., and Chandel, N.S. 2012. Physiological roles of mitochondrial reactive oxygen species. Mol. Cell **48**(2): 158–67. NIH Public Access. doi:10.1016/j.molcel.2012.09.025.

Sergiev, P. V., Dontsova, O.A., and Berezkin, G. V. 2015. Theories ofageing: An ever-evolving field. Russian Federation Agency for Science and Innovation. doi:10.32607/20758251-2015-7-1-9-18.

Shpilka, T., and Haynes, C.M. 2018. The mitochondrial UPR: Mechanisms, physiological functions and implications in ageing. Nat. Rev. Mol. Cell Biol. **19**(2): 109–120. Nature Publishing Group. doi:10.1038/nrm.2017.110.

Smith, M.H., Ploegh, H.L., and Weissman, J.S. 2011, November 25. Road to ruin: Targeting proteins for degradation in the endoplasmic reticulum. American Association for the Advancement of Science. doi:10.1126/science.1209235.

Song, G., Ouyang, G., and Bao, S. 2005. The activation of Akt/PKB signalling pathway and cell survival Apoptosis Review Series. J. Cell. Mol. Med **9**(1): 59–71. Available from http://onlinelibrary.wiley.com/store/10.1111/j.1582-4934.2005.tb00337.x/asset/j.1582-4934.2005.tb00337.x.pdf?v=1&t=jc9wu4i7&s=ca01189af99364c57ff25e7a3aef148a82692bfb [accessed 10 January 2018].

Song, Z., Ghochani, M., McCaffery, J.M., Frey, T.G., and Chan, D.C. 2009. Mitofusins and OPA1 mediate sequential steps in mitochondrial membrane fusion. Mol. Biol. Cell **20**(15): 3525–3532. doi:10.1091/mbc.E09-03-0252.

Spillantini, M.G., Schmidt, M.L., Lee, V.M.Y., Trojanowski, J.Q., Jakes, R., and Goedert, M. 1997. α-synuclein in Lewy bodies [8]. doi:10.1038/42166.

Sugiura, A., McLelland, G.-L., Fon, E.A., and McBride, H.M. 2014. A new pathway for mitochondrial quality control: mitochondrial-derived vesicles. EMBO J. **33**(19): 2142–56. European Molecular Biology Organization. doi:10.15252/embj.201488104.

Sulzer, D. 2007, May. Multiple hit hypotheses for dopamine neuron loss in Parkinson's disease. doi:10.1016/j.tins.2007.03.009.

Sun, N., Yun, J., Liu, J., Malide, D., Liu, C., Rovira, I.I., Holmström, K.M., Fergusson, M.M., Yoo, Y.H.,

Combs, C.A., and Finkel, T. 2015. Measuring In Vivo Mitophagy. Mol. Cell **60**(4): 685–96. NIH Public Access. doi:10.1016/j.molcel.2015.10.009.

Sun, Y., Yolitz, J., Wang, C., Spangler, E., Zhan, M., and Zou, S. 2013.ageing studies in drosophila melanogaster. Methods Mol. Biol. **1048**: 77–93. Humana Press Inc. doi:10.1007/978-1-62703-556-9_7.

Tatar, M., Kopelman, A., Epstein, D., Tu, M.P., Yin, C.M., and Garofalo, R.S. 2001. A mutant Drosophila insulin receptor homolog that extends life-span and impairs neuroendocrine function. Science (80-.). **292**(5514): 107–110. American Association for the Advancement of Science. doi:10.1126/science.1057987.

Taylor, E.B., and Rutter, J. 2011. Mitochondrial quality control by the ubiquitin–proteasome system: Figure 1. Biochem. Soc. Trans. **39**(5): 1509–1513. doi:10.1042/BST0391509.

Taylor, R.C. 2016, October 1.ageing and the UPR(ER). Elsevier B.V. doi:10.1016/j.brainres.2016.04.017.

Tazearslan, C., Cho, M., and Suh, Y. 2012. Discovery of functional gene variants associated with human longevity: opportunities and challenges. J. Gerontol. A. Biol. Sci. Med. Sci. **67**(4): 376–83. doi:10.1093/gerona/glr200.

Thomas, B., and Beal, M.F. 2011, April 1. Molecular insights into Parkinson's disease. Faculty of 1000 Ltd. doi:10.3410/M3-7.

Thomas, R.E., Andrews, L.A., Burman, J.L., Lin, W.-Y., and Pallanck, L.J. 2014. PINK1-Parkin Pathway Activity Is Regulated by Degradation of PINK1 in the Mitochondrial Matrix. PLoS Genet. **10**(5): e1004279. Public Library of Science. doi:10.1371/journal.pgen.1004279.

Tinakoua, A., Bouabid, S., Faggiani, E., De Deurwaerdère, P., Lakhdar-Ghazal, N., and Benazzouz, A. 2015. The impact of combined administration of paraquat and maneb on motor and non-motor functions in the rat. Neuroscience **311**: 118–129. Elsevier Ltd. doi:10.1016/j.neuroscience.2015.10.021.

Trifunovic, A. 2006. Mitochondrial DNA and ageing. Biochim. Biophys. Acta - Bioenerg. **1757**(5–6): 611–617. doi:10.1016/j.bbabio.2006.03.003.

Trifunovic, A., and Larsson, N.-G. 2008. Mitochondrial dysfunction as a cause of ageing. J. Intern. Med. **263**(2): 167–178. Blackwell Publishing Ltd. doi:10.1111/j.1365-2796.2007.01905.x.

Trifunovic, A., Wredenberg, A., Falkenberg, M., Spelbrink, J.N., Rovio, A.T., Bruder, C.E., Bohlooly-Y, M., Gidlöf, S., Oldfors, A., Wibom, R., Törnell, J., Jacobs, H.T., and Larsson, N.-G. 2004. Premature ageing in mice expressing defective mitochondrial DNA polymerase. Nature **429**(6990): 417–423. doi:10.1038/nature02517.

Tsang, W.Y., and Lemire, B.D. 2002. Stable heteroplasmy but differential inheritance of a large mitochondrial DNA deletion in nematodes. Biochem. cell biol.: 645–654. doi:10.1139/O02-135.

Twig, G., Elorza, A., Molina, A.J.A., Mohamed, H., Wikstrom, J.D., Walzer, G., Stiles, L., Haigh, S.E., Katz, S., Las, G., Alroy, J., Wu, M., Py, B.F., Yuan, J., Deeney, J.T., Corkey, B.E., and Shirihai, O.S. 2008. Fission and selective fusion govern mitochondrial segregation and elimination by autophagy. EMBO J. **27**(2): 433–446. doi:10.1038/sj.emboj.7601963.

Ulgherait, M., Rana, A., Rera, M., Graniel, J., and Walker, D.W. 2014. AMPK Modulates Tissue and Organismalageing in a Non-Cell-Autonomous Manner. Cell Rep. **8**(6): 1767–1780. doi:10.1016/j.celrep.2014.08.006.

Urano, F., Wang, X.Z., Bertolotti, A., Zhang, Y., Chung, P., Harding, H.P., and Ron, D. 2000. Coupling

of stress in the ER to activation of JNK protein kinases by transmembrane protein kinase IRE1. Science (80-.). **287**(5453): 664–666. doi:10.1126/science.287.5453.664.

Urra, H., Dufey, E., Lisbona, F., Rojas-Rivera, D., and Hetz, C. 2013, December. When ER stress reaches a dead end. doi:10.1016/j.bbamcr.2013.07.024.

Vanhaesebroeck, B., and Alessi, D.R. 2000. The PI3K-PDK1 connection : more than just a road to PKB. *In* Biochem. J. Available from http://www2.ncbi.nlm.nih.gov/genbank/queryIform.html. [accessed 30 March 2020].

Vooijs, M., and Berns, A. 1999, September 20. Developmental defects and tumor predisposition in Rb mutant mice. doi:10.1038/sj.onc.1202999.

Vos, M., Lauwers, E., and Verstreken, P. 2010, September 22. Synaptic mitochondria in synaptic transmission and organization of vesicle pools in health and disease. Frontiers. doi:10.3389/fnsyn.2010.00139.

Wakabayashi, K., Toyoshima, Y., Awamori, K., Anezaki, T., Yoshimoto, M., Tsuji, S., and Takahashi, H. 1999. Restricted occurrence of Lewy bodies in the dorsal vagal nucleus in a patient with late-onset parkinsonism. J. Neurol. Sci. **165**(2): 188–191. Elsevier. doi:10.1016/S0022-510X(99)00101-X.

Walsh, D.M., and Selkoe, D.J. 2016, April 1. A critical appraisal of the pathogenic protein spread hypothesis of neurodegeneration. Nature Publishing Group. doi:10.1038/nrn.2016.13.

Walter, P., and Ron, D. 2011, November 25. The unfolded protein response: From stress pathway to homeostatic regulation. American Association for the Advancement of Science. doi:10.1126/science.1209038.

Wang, C., and Youle, R.J. 2009. The role of mitochondria in apoptosis*. Annu. Rev. Genet. **43**: 95–118. NIH Public Access. doi:10.1146/annurev-genet-102108-134850.

Wang, F., Marshall, C.B., Yamamoto, K., Li, G.Y., Plevin, M.J., You, H., Mak, T.W., and Ikura, M. 2008. Biochemical and Structural Characterization of an Intramolecular Interaction in FOXO3a and Its Binding with p53. J. Mol. Biol. **384**(3): 590–603. Academic Press. doi:10.1016/j.jmb.2008.09.025.

Wang, H.G., Pathan, N., Ethell, I.M., Krajewski, S., Yamaguchi, Y., Shibasaki, F., McKeon, F., Bobo, T., Franke, T.F., and Reed, J.C. 1999. Ca2+-Induced Apoptosis Through Calcineurin Dephosphorylation of BAD. Science (80-.). **284**(5412): 339–343. American Association for the Advancement of Science. doi:10.1126/science.284.5412.339.

Wang, L., Das, U., Scott, D.A., Tang, Y., McLean, P.J., and Roy, S. 2014. α-Synuclein multimers cluster synaptic vesicles and attenuate recycling. Curr. Biol. **24**(19): 2319–2326. Cell Press. doi:10.1016/j.cub.2014.08.027.

Wang, M., and Kaufman, R.J. 2016, January 20. Protein misfolding in the endoplasmic reticulum as a conduit to human disease. Nature Publishing Group. doi:10.1038/nature17041.

Wang, W., Wang, X., Fujioka, H., Hoppel, C., Whone, A.L., Caldwell, M.A., Cullen, P.J., Liu, J., and Zhu, X. 2016. Parkinson's disease-associated mutant VPS35 causes mitochondrial dysfunction by recycling DLP1 complexes. Nat. Med. **22**(1): 54–63. Nature Publishing Group. doi:10.1038/nm.3983.

Whiteman, E.L., Cho, H., and Birnbaum, M.J. 2002. Role of Akt/protein kinase B in metabolism. Trends Endocrinol. Metab. **13**(10): 444–51. doi:10.1016/s1043-2760(02)00662-8.

Wikstrom, J.D., Israeli, T., Bachar-Wikstrom, E., Swisa, A., Ariav, Y., Waiss, M., Kaganovich, D., Dor, Y., Cerasi, E., and Leibowitz, G. 2013. AMPK Regulates ER Morphology and Function in

Stressed Pancreatic β-Cells via Phosphorylation of DRP1. Mol. Endocrinol. **27**(10): 1706–1723. doi:10.1210/me.2013-1109.

Wiseman, H., and Halliwell, B. 1996. Damage to DNA by reactive oxygen and nitrogen species : role in inflammatory disease and progression to cancer. Biochem. J **313**: 17–29. Available from https://www.ncbi.nlm.nih.gov/pmc/articles/PMC1216878/pdf/8546679.pdf [accessed 7 December 2017].

Wong, H.-S., Dighe, P.A., Mezera, V., Monternier, P.-A., and Brand, M.D. 2017. Production of superoxide and hydrogen peroxide from specific mitochondrial sites under different bioenergetic conditions. J. Biol. Chem. **292**(41): 16804–16809. doi:10.1074/jbc.R117.789271.

Wu, J.J., Liu, J., Chen, E.B., Wang, J.J., Cao, L., Narayan, N., Fergusson, M.M., Rovira, I.I., Allen, M., Springer, D.A., Lago, C.U., Zhang, S., DuBois, W., Ward, T., deCabo, R., Gavrilova, O., Mock, B., and Finkel, T. 2013. Increased mammalian lifespan and a segmental and tissue-specific slowing ofageing after genetic reduction of mTOR expression. Cell Rep. **4**(5): 913–20. NIH Public Access. doi:10.1016/j.celrep.2013.07.030.

Wu, S., Zhou, F., Zhang, Z., and Xing, D. 2011. Bax is essential for Drp1-mediated mitochondrial fission but not for mitochondrial outer membrane permeabilization caused by photodynamic therapy. J. Cell. Physiol. **226**(2): 530–541. doi:10.1002/jcp.22362.

Xie, M., Doetsch, P.W., and Deng, X. 2015. Bcl2 inhibition of mitochondrial DNA repair. BMC Cancer **15**(1): 586. BioMed Central Ltd. doi:10.1186/s12885-015-1594-1.

Yoneda, T., Benedetti, C., Urano, F., Clark, S.G., Harding, H.P., and Ron, D. 2004. Compartment-specific perturbation of protein handling activates genes encoding mitochondrial chaperones. J. Cell Sci. **117**(Pt 18): 4055–66. The Company of Biologists Ltd. doi:10.1242/jcs.01275.

Yuan, H., Gerencser, A.A., Liot, G., Lipton, S.A., Ellisman, M., Perkins, G.A., and Bossy-Wetzel, E. 2007. Mitochondrial fission is an upstream and required event for bax foci formation in response to nitric oxide in cortical neurons. Cell Death Differ. **14**(3): 462–471. Cell Death Differ. doi:10.1038/sj.cdd.4402046.

Yuan, R., Tsaih, S.W., Petkova, S.B., de Evsikova, C.M., Xing, S., Marion, M.A., Bogue, M.A., Mills, K.D., Peters, L.L., Bult, C.J., Rosen, C.J., Sundberg, J.P., Harrison, D.E., Churchill, G.A., and Paigen, B. 2009.ageing in inbred strains of mice: Study design and interim report on median lifespans and circulating IGF1 levels.ageing Cell **8**(3): 277–287. doi:10.1111/j.1474-9726.2009.00478.x.

Zhang, J., Li, X., and Li, J. Da. 2019, April 18. The Roles of Post-translational Modifications on α-Synuclein in the Pathogenesis of Parkinson's Diseases. Frontiers Media S.A. doi:10.3389/fnins.2019.00381.

Zhang, Z., Liu, L., Wu, S., and Xing, D. 2016. Drp1, Mff, Fis1, and MiD51 are coordinated to mediate mitochondrial fission during UV irradiation-induced apoptosis. FASEB J. **30**(1): 466–476. FASEB. doi:10.1096/fj.15-274258.

Zid, B.M., Rogers, A.N., Katewa, S.D., Vargas, M.A., Kolipinski, M.C., Lu, T.A., Benzer, S., and Kapahi, P. 2009. 4E-BP Extends Lifespan upon Dietary Restriction by Enhancing Mitochondrial Activity in Drosophila. Cell **139**(1): 149–160. Elsevier. doi:10.1016/j.cell.2009.07.034.

Chapter 2: Alteration of expression of *Drp1* can increase longevity in Drosophila models of Parkinson Disease

A version of this chapter is submitted as: Hasan, A., and Staveley, B.E. 2021.

Abstract

Parkinson Disease (PD) and other neurodegenerative diseases have a significant relationship with mitochondrial dysfunction. The substantial effect of mitochondrial dynamics in PD has led us to study the role of the gene encoding the mitochondrial fission protein Drp1 in Drosophila models. *Drp1* is a member of the highly conserved, dynamin family of protein encoding genes. Drp1 is essential in maintaining the mitochondrial, peroxisomal, and endoplasmic reticulum (ER) dynamics and has been found to regulate processes during homeostasis and cell survival. The directed expression of *Drp1* in Drosophila neurons under the control of the *Ddc-Gal4* transgene decreases the lifespan and compromises climbing ability over time. The directed inhibition of *Drp1* causes little change in median lifespan but much decrease in locomotor or climbing abilities. Interestingly, the loss-of- parkin dependent Drosophila model of PD is rescued by the directed inhibition of *Drp1*. The compromised health-span of flies with directed overexpression and inhibition of *Drp1* has produced a new model for PD and can be used to further investigate the mechanism(s) underlying PD and other neurodegenerative diseases. The combined inhibition of both *Drp1* and *parkin* suppresses PD phenotypes and promotes survival.

Introduction

Mitochondria are critical organelles in the process of survival at the cellular level. Mitochondria accumulates damage over time, hence dysfunction, and contributes to ageing and eventually to the death of an organism (Harman 1991). Mitochondria is responsible for various aspects of energy homeostasis, oxidative stress, calcium handling, cell signalling, and cell survival (Galluzzi et al. 2012). Neurons are dependent on mitochondria for their excessive ATP requirement in membrane excitability, synaptic plasticity, and neurotransmission (Kann and Kovács 2007). The

central role of mitochondria in energy regulation and signalling implies that its dysfunction would have devastating effects upon cellular functions. Such is especially true for the nervous system because subtle signalling changes can have catastrophic consequences leading to neurodegenerative disease.

The shape and size of mitochondria are not fixed properties; mitochondrial morphology depends upon a number of factors, including stage of the cell cycle and cell type, and can change quite quickly in response to external stimuli or metabolic cues (Campello and Scorrano 2010). Changes to the mitochondrial network seem to differentially influence a number of signalling pathways (Hoitzing et al. 2015). Therefore, mitochondria undergo fission and fusion frequently in order to change their structure in response to the specific requirements of the cell, under a wide range of circumstances (Scott and Youle 2010). Mitochondrial fission allows segregation of damaged mitochondria components while the process of fusion facilitates the exchange of mitochondrial material vital in preserving homeostasis within the mitochondrial network (Twig et al. 2008; Twig and Shirihai 2011). Mitochondrial fusion helps compromised mitochondria, with highly damaged DNA and protein, to actively exchange components with other healthier mitochondria to decrease the severity of heteroplasmy, and help with functional complementation (Nakada et al. 2009; Chan 2012). Mitochondrial fission allows for the segregation of irreversibly damaged portions of the mitochondrial network and subsequent degradation (Twig et al. 2008). Mitochondrial fission necessarily requires *dynamin-related protein 1* (*Drp1*) and *FIS1* (Sebastián et al. 2017). Nevertheless, an explicit understanding of the factors promoting fission and fusion remains limited.

The *Drp1* gene encodes a dynamin family GTPase protein comprised of a characteristic Dynamin like protein family domain (Dynamin and Mx protein domains), a dynamin central domain, and a dynamin GTPase effector domain. While predominantly located in the cytoplasm, a small fraction is located upon the cytoplasmic surface of the mitochondrial tubules. Overexpression of *Drp1* causes mitochondrial fragmentation, whereas inhibition results in the elongation of the mitochondrial network (Twig et al. 2008; Twig and Shirihai 2011). Drp1 protein function is regulated by post-translational modification via phosphorylation, where a well-documented phosphorylation site, S616, promotes fission through an increase in activity. In contrast, phosphorylation of another site, S637, acts to lessen fission through reduced activity (Chang and Blackstone 2007a, 2007b; Cribbs and Strack 2007). Drp1 polymerizes to form a spiral structure around the mitochondrial tubule, and then utilizes its GTPase activity to constrict the tubule and eventually cause fragmentation of the mitochondria (Legesse-Miller et al. 2003; Ingerman et al. 2005; Lackner et al. 2009; Mears et al. 2011). Through its role in mitochondrial fission, *Drp1* controls mitochondrial morphology and function.

In addition to mitochondrial fission, Drp1 participates in peroxisomal fragmentation (Koch et al. 2003) and maintains the morphology and function of the Endoplasmic Reticulum (ER) (Wikstrom et al. 2013). Drp1 is required for a standard rate of Cyt-c release and caspase activation during programmed cell death (Breckenridge et al. 2008). The role of Drp1 in apoptosis is not clear, but the product of the *Bax* gene, a pro-apoptotic Bcl-2 family protein, has been found to co-localize with Drp1 at mitochondrial fission site in HeLa and Cos-7 mammalian cell lines (Karbowski et al.

2002). Drp1 increases the mitochondrial fragmentation under nitrosative stress in primary cerebrocortical neuron culture (Yuan et al. 2007). The Drp1 protein interacts with other proteins involved in a number of mitochondrial processes, such as protein product of *Bax* (Karbowski et al. 2002; Yuan et al. 2007; Maes et al. 2019), the products of *Pink1 (PTEN-induced putative kinase 1)* and *parkin* in Cos-7 cells (Buhlman et al. 2014). Mutation of the *Pink1* and *parkin* genes are among the most prominent causes of early onset of PD (Klein and Westenberger 2012). The roles of *Pink1* and *parkin* are vital to ubiquitin-dependent mitophagy (Pickrell and Youle 2015). The *Pink* and *parkin* loss of function mutation increase the mitochondrial localization of Drp1 in flies (Poole et al. 2010). The parkin protein ubiquitinates the Drp1 for proteasomal degradation, incriminate the Drp1 for dysregulated mitochondrial dynamics in parkin loss-of-function induced mitochondrial morphology in HeLa and SH-SY5Y cells (Wang et al. 2011). Number of stresses can increase the mitochondrial translocation of Drp1 in neurons and initiate apoptosis or mitophagy (Pradeep et al. 2014). Excessive activity of Drp1 increase mitochondrial fission and consequently promote cell death.

Here I propose that gain-of-function of *Drp1* results in a Parkinsonian-like phenotype. I use Drosophila to model Parkinson disease because it is an excellent model system to study of the genes and proteins that interact in PD (Staveley 2012; Xiong and Yu 2018). The inhibition of *Drp1* in the dopaminergic (DA) neurons of a mouse MPTP model of PD gives protection against mitochondrial translocation of p53 and the loss of DA neurons (Filichia et al. 2016). In my experiment, I used the *UAS-Gal4* system to direct and to inhibit the expression of the *Drp1* gene in Drosophila. The *Ddc-Gal4* transgene directs expression in DA and serotonergic neurons (Li et al.

2000; Riemensperger et al. 2013) and the *GMR-Gal4* transgene directs expression in the developing eye (Freeman 1996). We found overexpression of *Drp1* has toxic effects; although, its inhibition slightly improves the lifespan, the climbing ability over time is compromised. In an established *parkin-RNAi* model of PD (Githure and Staveley 2017), I directed and inhibited the expression of the *Drp1* gene. The PD -like phenotypes of *Ddc-Gal4 parkin-RNAi* were rescued by the expression of *Drp1-RNAi* transgenes. The strategy is to identify the basic mechanism in simple model organism and then further validate the finding in mammalian model organism.

Materials and methods

Bioinformatic analysis

Protein sequences were obtained from the National Center of Biotechnology Information (NCBI) database *(*https://www.ncbi.nlm.nih.gov/protein/). The conserved domains were identified using NCBI Conserved Domain Database *(*https://www.ncbi.nlm.nih.gov/cdd/*)*, and Eukaryotic Linear Motif *(*http://elm.eu.org/*).* Multiple sequence alignment was done using Clustal Omega *(*https://www.ebi.ac.uk/Tools/msa/clustalo/*)* to reveal the conservation of domains. The *Homo sapiens* Dynamin-1 like protein (DLP-1/Drp1) structure (PDB ID 4BEJ) was obtained from NCBI structure database *(*https://www.ncbi.nlm.nih.gov/structure/*)* and *Drosophila melanogaster Drp1* protein structure was developed using Phyre2 *(*http://www.sbg.bio.ic.ac.uk/phyre2/html/page.cgi?id=index*)* modeling tool. The final models were edited with the PyMOL software (https://pymol.org/2/) to highlight the N-terminus, C-terminus and LIR regions.

Drosophila stocks and media

The *Ddc-Gal4$^{4.3D}$(w[1118]; P{w[+mC]=Ddc-GAL4.L}4.3D); GMR-Gal4^{12}*; *UAS-lacZ^{4-1-2}*; *UAS-Drp1* (y[1] w[*]; P{w[+mC]=FLAG-FlAsH-HA-*Drp1*}3, Ki[1]); the *UAS-Drp1-RNAi1* (y[1] v[1]; P{y[+t7.7] v[+t1.8]=TRiP.JF02762}attP2}); and *UAS-Drp1-RNAi2* (y[1] v[1]; P{y[+t7.7] v[+t1.8]=TRiP.HMC03230}attP40) stocks were obtained from Bloomington Drosophila Stock Center at Indiana University, Bloomington, Indiana, USA. The *UAS-parkin-RNAi* line was obtained from Dr. B. Lu (Yang et al. 2003, 2006). The *Ddc-Gal4 parkin-RNAi* line was produced through standard methods (Githure M'angale and Staveley 2016). All flies were maintained on standard cornmeal/molasses/yeast/agar media treated with propionic acid and methylparaben to resist fungal growth. Stocks were maintained at room temperature (22° ± 3° C), whereas crosses and experiments were kept at 25°C.

Survival assay

Female virgins of the *Ddc-Gal4* and *Ddc-Gal4 UAS-parkin-RNAi* genotype were collected every 8 to 12 hours for several days. The confirmed virgin flies were then crossed with *UAS-lacZ, UAS-Drp1, UAS-Drp1-RNAi1* and *UAS-Drp1-RNAi2* males. Critical class male progeny were collected until approximately 250 flies of each genotype were obtained. To avoid over-crowding, the flies were maintained in cohorts of 25 or less per vial on standard media. Flies were scored every second day for viability and were transferred to new food every two to five days. Scoring continued until all flies had died (Todd and Staveley 2004, 2012). Longevity data were analyzed using GraphPad Prism version 8 statistical software (*graphpad.com*), and survival curves were compared by Mantel-Cox test. Significance were determined at 95% confidence level ($P \leq 0.05$). with Bonferroni correction.

Locomotor analysis

Approximately 70 male flies of the critical class were collected within a 24-hour period and maintained as cohorts of 10 flies in each vial. Media was replenished twice a week. The climbing assay was performed as previously described according to a standard protocol (Todd and Staveley 2004, 2012). Briefly, every week 50 males were assayed, in groups of 10, for their ability to climb a glass tube divided into 5 levels of 2 cm each. The climbing index was calculated for each week using GraphPad prism version 8 statistical software. The climbing curve was fitted using non-linear regression and determined at a 95% confidence interval ($P \leq 0.05$).

Biometric analysis of the *Drosophila melanogaster* eye

Female virgins of the *GMR-Gal4* genotype were collected every 8 to 12 hours for several days. The confirmed virgins were then crossed with the males of *UAS-lacZ, UAS-Drp1, UAS-Drp1-RNAi1* and *UAS-Drp1-RNAi2* genotypes. Critical class male progeny were collected for each genotype. The collected flies were kept as cohorts of 10 flies or less upon fresh media and allowed to age for 3 to 4 days. The flies were prepared for scanning electron microscopy following the standard protocol [35]. Ommatidia and interommatidial bristle counts were performed on 10 or more flies of each genotype using National Institute of Health (NIH) ImageJ software. The ommatidium area was calculated by measuring the area of 5 distinct ommatidial "rosettes" per fly eye and then dividing by 7 to determine the mean area of each ommatidium; done on 10 eyes of each genotype. The Biometric analysis was performed using GraphPad Prism version 8 statistical software. Significance were determined at 95% confidence level ($P > 0.05$).

Results

Drp1 is highly conserved between Homo sapiens and *Drosophila melanogaster*

The *D. melanogaster* Drp1 protein sequence was sourced from NCBI protein database, and the conserved sequences were identified using NCBI CDD. NCBI protein Blast of Drp1 protein of *D. melanogaster* (NP_608694.2) with the *H. sapiens,* identified dynamin-1-like protein (isoform 4) (NP_001265392.1), it is 65% identical with a bit score of 957. The multiple sequence alignment of the two proteins derived by Clustal Omega (Figure 2.1A) shows a highly conserved dynamin-like protein family domain, a dynamin central domain, and a dynamin GTPase effector domain. Two well-documented phosphorylation sites are identified; S606 and S627 in *dynamin-1-like protein* isoform 4 of *H. sapiens;* and S616 and T637 in *Drp1* of *D. melanogaster*. A template-based modeling of *D. melanogaster* Drp1 protein by use of a combination of empirically derived energy functions and physics-based simulated folding was produced using Phyre2. The modeled *D. melanogaster* Drp1 protein (i) and the *H. sapiens* Dynamin-1 like protein (ii) from the NCBI database share a near identical structure (Figure 2.1B). The amino-terminus region of the Drp1 protein is highly conserved and has a consensus LC3-interacting region (LIR) sequence for binding to the ATG8/LC3 protein as determined by the Eukaryotic Linear Motif (ELM) resource. As this protein structure is so highly conserved, it seems very likely that the functions are highly conserved.

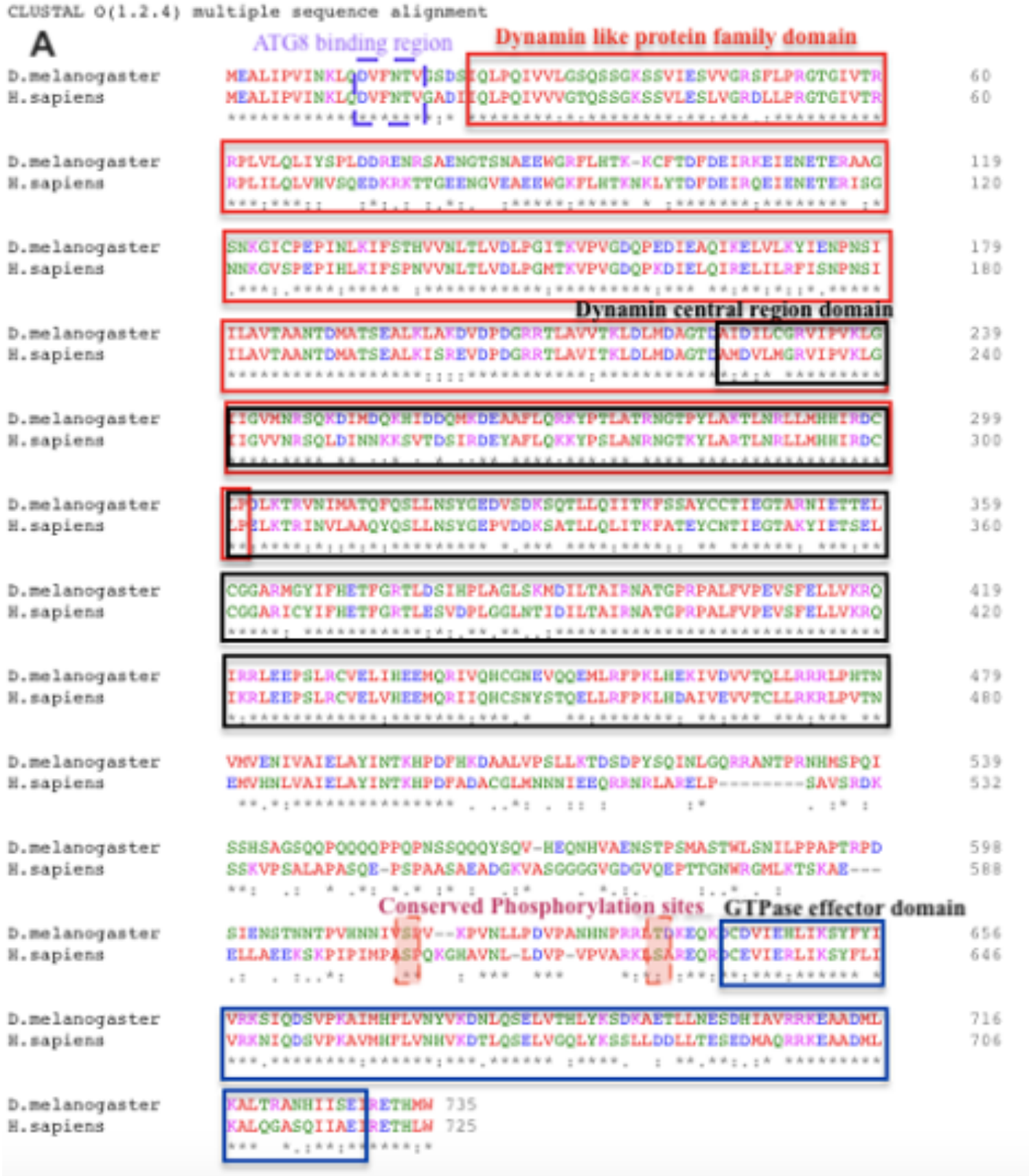
CLUSTAL O(1.2.4) multiple sequence alignment
A
ATG8 binding region
Dynamin like protein family domain
Dynamin central region domain
Conserved Phosphorylation sites
GTPase effector domain
D.melanogaster
H.sapiens

B (i)

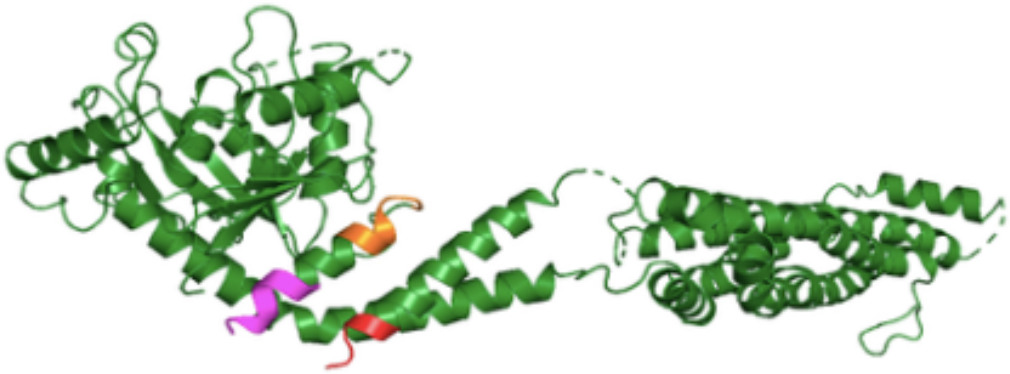

B (ii)

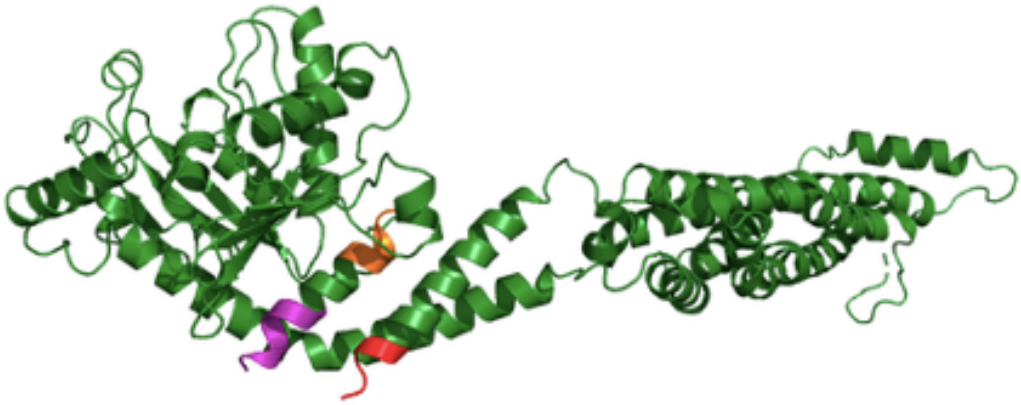

Figure 2.1 Drp1 is evolutionarily conserved in Drosophila. A. Clustal Omega multiple sequence alignment of D. melanogaster Drp1 (NP_608694.2) protein with the H. sapiens (NP_001265392.1) shows evolutionarily conserved domains identified using the NCBI Conserved Domain Database (CDD) and further confirmed by the Eukaryotic Linear Motif (ELM) resource. The two well documented phosphorylation sites are identified, S606 and S627 in dynamin-1-like protein (DLP-1) isoform 4 of H. sapiens; and S616 and T637 in Drp1 of D. melanogaster. The asterisks indicate the residues that are identical; the colons indicate the conserved substitutions; and the dots indicates the semi-conserved substitutions. Colour differences indicate the chemical nature of amino acids: red indicates small hydrophobic (includes aromatic) residues; blue indicates acidic; magenta indicates basic; and green indicates basic with hydroxyl or amine groups. **B (i).** The original Dynamin-1 like protein (DLP-1) structure of H. sapiens (NP_001265392.1) from the NCBI structure database. **B (ii).** The Phyre2 web portal for protein modelling, prediction and analysis mediated the development of a model of the Drp1 protein of D. melanogaster (NP_608694.2) from a 76% identical protein with a confidence of 100%. The N terminus is coloured in Magenta; C terminus is coloured in Red and a consensus ATG8 binding region at N terminus is coloured in orange.

The overexpression and inhibition of *Drp1* with *Ddc-Gal4$^{4.3D}$*

In these experiments, the control *Ddc-Gal4$^{4.3D}$; UAS-lacZ* critical class males were determined to have a median lifespan of 68 days (n=340). The overexpression of *Drp1* by the *Ddc-Gal4* transgene results in a decreased lifespan of 56 days in 314 flies, much lower compared to the control as determined by log-rank (Mantel-Cox) test with a P-value at <0.0001 (Figure 2.2A). Inhibition of *Drp1* by two distinct RNAi transgenes, via the *UAS-Drp1-RNAi1* and *UAS-Drp1-RNAi2* directed by the *Ddc-Gal4* transgene, results in median lifespans of 70 (n=377) and 72 days (n=323), respectively; very similar to the control (Figure 2.2A) as determined by log-rank (Mante-Cox) test with P-value 0.0566 and 0.0213. The non-linear fitting of the climbing curve shows that altering the *Drp1* expression have compromised the climbing ability phenotype compared to control at 95% CI (P- value <0.0001) (Figure 2.2B) (n=50).

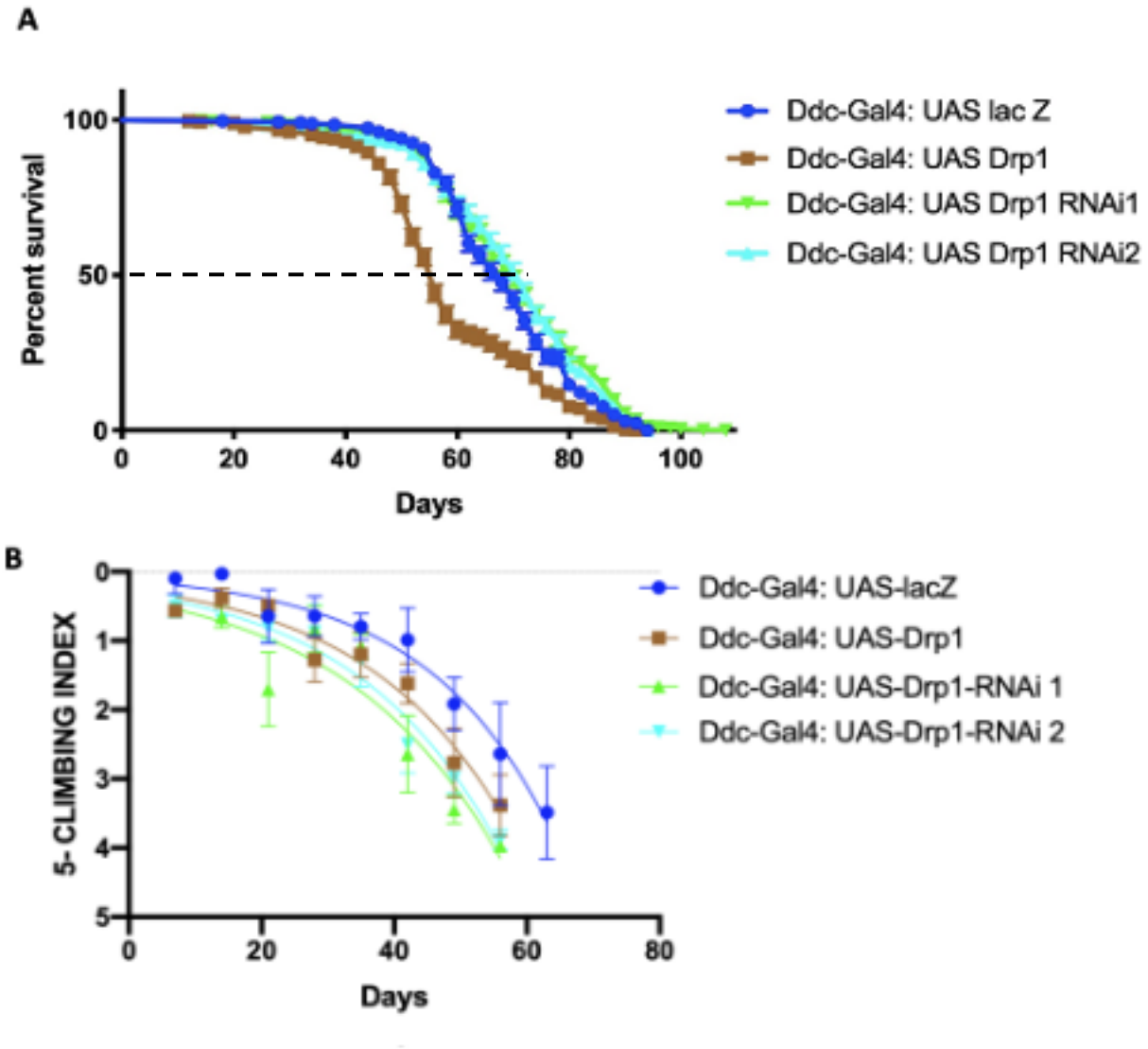

Figure 2.2 Altered *Drp1* expression under the control of *Ddc-Gal4$^{4.3D}$* influences the survival and climbing ability of flies. A). The GraphPad prism8 generated graph of the longevity assay for the expression of *Drp1, Drp1 RNAi's* under the control of *Ddc-Gal4* transgene. The directed expression results in decreased median lifespan of 56 days compared to 68 days of control calculated by Log-rank Mantel Cox test, with Bonferroni correction. The inhibition of Drp1 under the control of *Ddc-Gal4* transgene results in lifespan of 70 days with *UAS-Drp1-RNAi1* and 72 days with *UAS-Drp-RNAi2* compared to 68 days of control done by Log-rank Mantel Cox test, with Bonferroni correction. **B).** The GraphPad prism8 generated graph of the climbing abilities of flies with overexpression of *Drp1, Drp1 RNAi's* and control. The climbing ability of *Drp1* overexpression and *Drp1 RNAi's* flies have decreased compared to control as determined in nonlinear fitting of the climbing curve by 95% confidence interval (p-value <0.0001).

The altered co-expression of *Drp1* along with *parkin-RNAi* with *Ddc-Gal4$^{4.3D}$*

The loss of function of *parkin* has led to the establishment of a number of Drosophila models of PD. The *Ddc-Gal4$^{4.3D}$ parkin-RNAi UAS-lacZ* critical males were determined to have a median lifespan of 60 days (n=259). The overexpression of *UAS-Drp1* along with *UAS-parkin-RNAi* under the direction of the *Ddc-Gal4* transgene has a median life span of 58 days (n=258), similar to the control with a P-value of 0.0026. The inhibition of *Drp1* by the two *RNAi* transgenes, *UAS-Drp1-RNAi1^{JF02762}* and *UAS-Drp1-RNAi2^{HMC03230}*, results in much longer median lifespans of 84 (n=283) and 76 days (n=277) respectively, compared to the control (Figure 2.3A) as determined by log-rank (Mantel-Cox) test with a P-value at <0.0001. (Figure 2.3A). The overexpression of *Drp1* by *Ddc-Gal4* along with *parkin-RNAi* slightly increases the climbing ability over time. However, the locomotor activity of the critical classes with the directed expression of the *Drp1-RNAi transgenes* are rescued compared to control (Figure 2.3B).

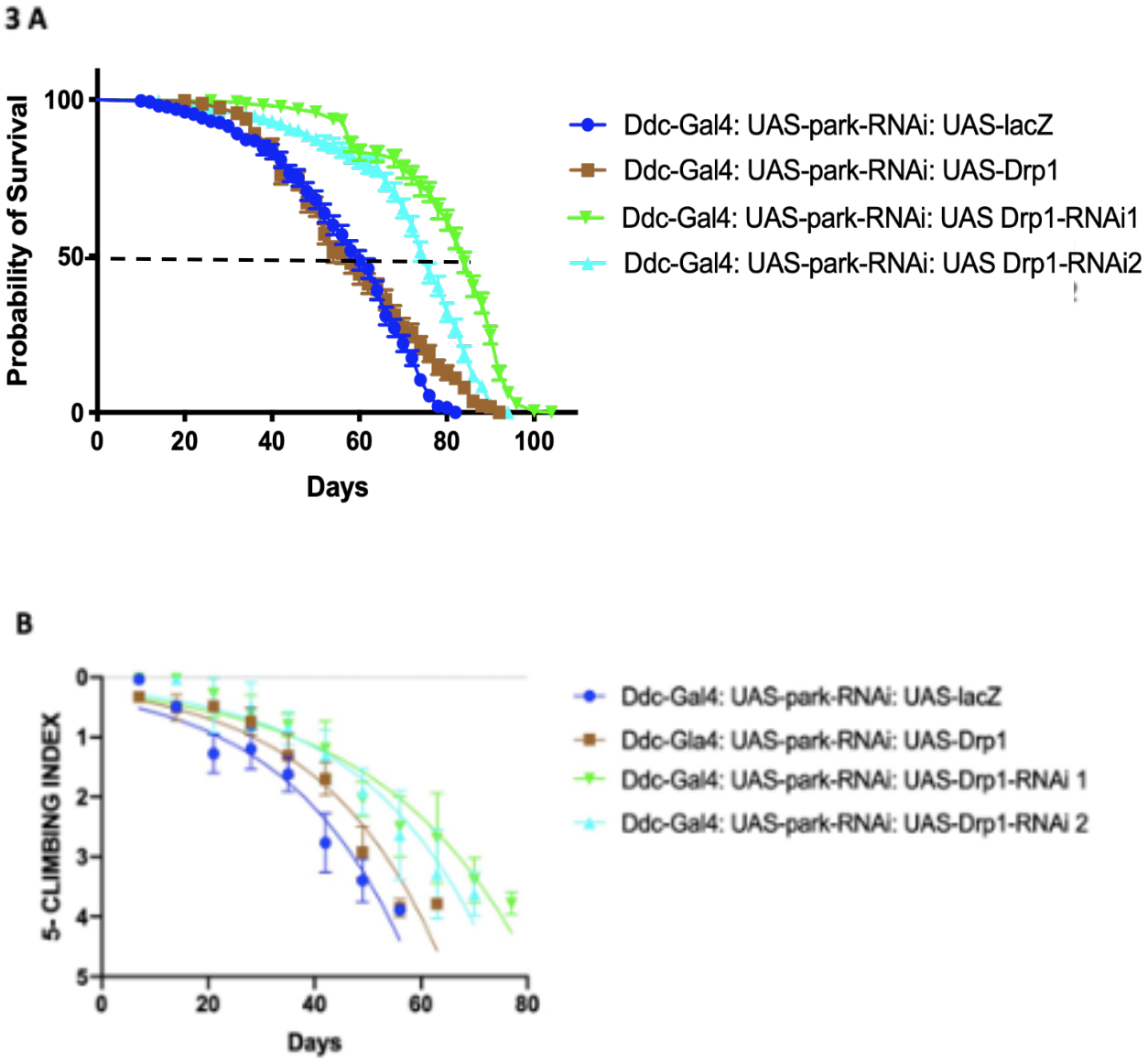

Figure 2.3. Altered *Drp1* expression when coupled with *Ddc-Gal4$^{4.3D}$ parkin-RNAi* influences the survival and climbing ability of flies. A). The graph of longevity assay generated by GraphPad prism8 with altered *Drp1* expression in *Ddc-Gal4 parkin-RNAi* expressing flies. The overexpression results in median lifespan of 58 days similar to 60 days of control (*lacZ/parkin-RNAi*) determined by Log-rank Mantel-Cox test, with Bonferroni correction. The inhibition of *Drp1* in neurons using *Ddc-Gal4* transgene along with *parkin-RNAi* results in increased lifespan of 84 days with UAS-*Drp1-RNAi1* and lifespan of 76 days with *UAS-Drp1-RNAi2* compared to 60 days of control done by Log-rank Mantel Cox test, with Bonferroni correction. **B)**. The GraphPad prism8 generated graph of the climbing abilities of flies with overexpression of *Drp1, Drp1 RNAi* and control. The climbing abilities of and *Drp1 RNAi* flies has rescued compared to control as determined in non-linear fitting of the climbing curve by 95% confidence interval.

Overexpression of *Drp1* during development of the eye decreases ommatidia and bristle number

The inhibition and overexpression of *Drp1*, directed by the *GMR-Gal4* transgene in the developing eye of flies affects development. The expression of *UAS-Drp1* and *UAS-Drp1-RNAi1* in developing eye directed by *GMR-Gal4* transgene results in higher mean number of ommatidia, 716.9 and 718.8, respectively compared to 703 for the *lacZ* control flies (Figure 2.4B) as determined by unpaired t-test with a P value of 0.0483 and 0.0484. The mean of interommatidial bristle produced through inhibition by the *UAS-Drp-RNAi1 and UAS-Drp1-RNAi2* transgene was higher at and 556.7 (P-value= 0.0406) and 578.7 (P-value=0.0023) compare to 536 of control flies as determined by an unpaired t-test. The mean number of interommatidial bristle for *UAS-Drp1* flies was 541.6 similar to 536 of control, as determined by an unpaired t-test (P-value= 0.6128). The ommatidia area of the control was 200um^2 per ommatidium, the overexpression of Drp1 has 213.7 um^2 (P value =0.0303) and the ommatidium area produced by the *UAS-Drp1-RNAi* ^{JF02762} and *UAS-Drp1-RNAi2*^{HMC03230} transgenes were 225 um^2 (0.0490) and 217 um^2 (P-value=0.0011), slightly increased compared to control as determined by unpaired t-test (Figure 2.4D).

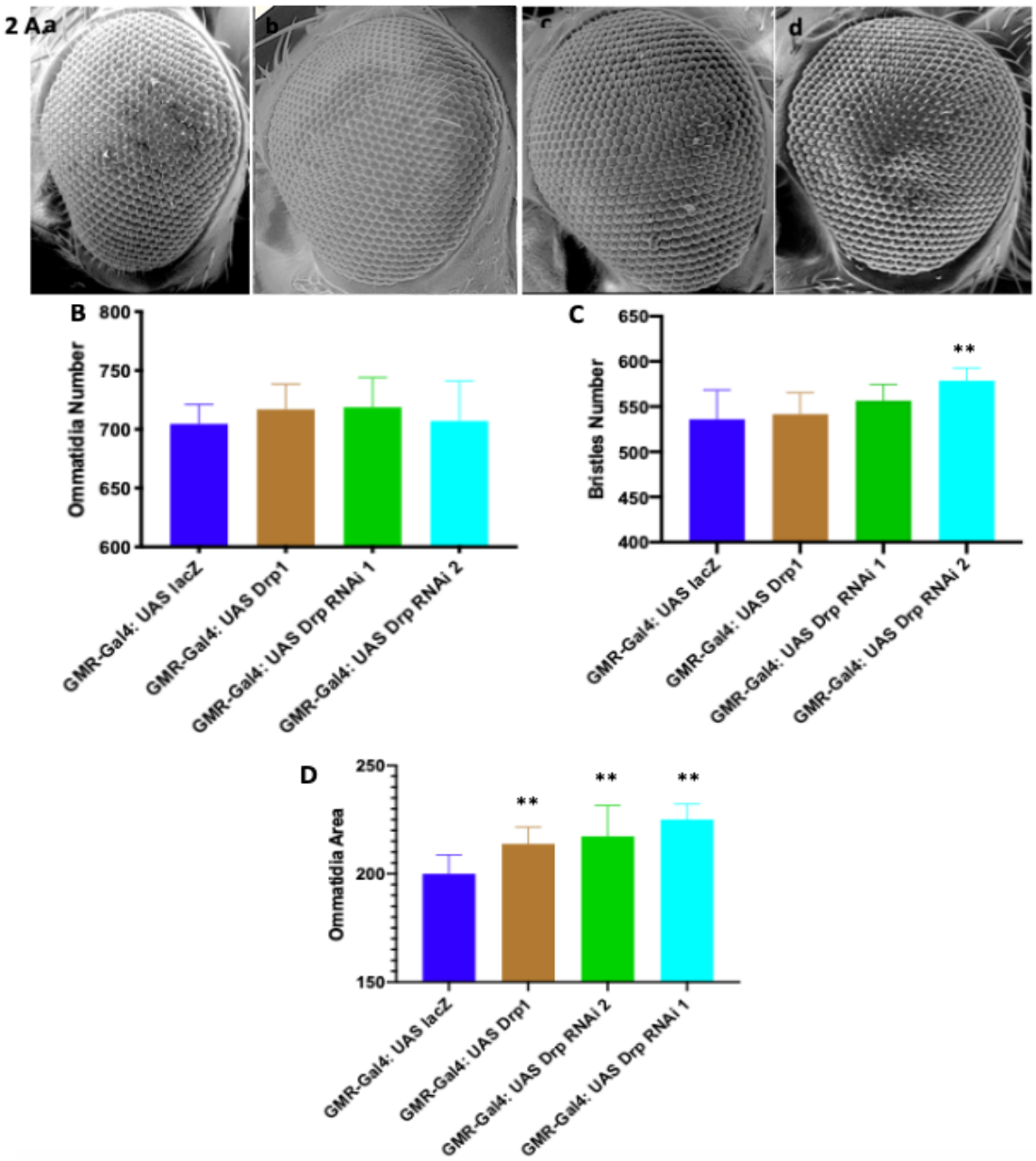

Figure 2.4 The phenotypic effects of altered *Drp1* expression in *D. melanogaster* eye. A). Scanning electron micrograph of the altered *Drp1* expression under the control of *GMR-Gal4* transgene. The genotypes are (a) *GMR-Gal4/UAS-lacZ* (Control); (b) *GMR-Gal4/UAS-Drp1*; (c) *GMR-Gal4/UAS-Drp1-RNAi1* (d) *GMR-Gal4/UAS-Drp1-RNAi2*. **B)**. The ommatidia number for control is 703±13.7, the inhibition and expression of Drp1 results in slight increase ommatidial count compared to control. **C**. The interommatidial bristle count for the control is 536±27.6 and the overexpression line has 541.6±24; inhibition lines have interommatidial bristle slightly more at mean value of 556.7±17.7 and 578±14. D. The ommatidium area of the *Drp1* expression transgene *GMR-Gal4 UAS-Drp1* and the inhibition transgenes *GMR-Gal4 UAS-Drp1-RNAi1* and *GMR-Gal4 UAS-Drp1-RNAi2* are slightly higher compared to control *(GMR-Gal4 UAS lacZ)*.

Discussion

The critical role of the structure of the mitochondria in the function of this organelle suggests that the product of the *Drp1* gene acts as an essential component in the regulation of a number of sub-cellular processes. Excessive mitochondrial fragmentation is associated with dysfunctional metabolic diseases and a "hyper-fused" mitochondrial network serves to protect from metabolic insult and autophagy (Wai and Langer 2016). In the skeletal muscle of mice, *Drp1* overexpression causes the severe impairment of post-natal muscle growth as the syntheses of protein is attenuated and growth hormone pathways are down regulated (Touvier et al. 2015). The high fat and high glucose diet cause excessive oxidative stress and mitochondrial fragmentation mediated by the Drp1 protein (Yu et al. 2006; Sun et al. 2020). These phenotypes are similar to the increased activity of Drp1 in COS and PC12 cells (Cribbs and Strack 2007). The effect of *Drp1* overexpression and consequently excessive mitochondrial fragmentation is toxic upon physiological processes.

The balance between mitochondrial fission and fusion is very delicate. *Drp1* is essential for embryonic development in mice such that homozygous mutants or knockout *Drp1* mice die during embryogenesis (Ishihara et al. 2009). The Drp1 protein assists in caspase-independent mitochondrial fission to amplify apoptosis (Oettinghaus et al. 2016). The acute overexpression and inhibition of the *Drp1* gene has shown similar phenotypes in mice (Favaro et al. 2019), most likely due to an extreme disruption in mitochondrial morphology. Besides an increase in *Drp1* expression in midlife can have beneficial effects on health-span of Drosophila (Rana et al. 2017), which confirms the sensitivity of the process towards cell death and cell survival outcome. In my experiments, the lifespan and climbing ability of flies that overexpress *Drp1* was significantly

decreased when compared to controls, which may be due to elevated oxidative stress beyond a threshold for a normal lifespan. The inhibition of *Drp1* in DA neurons through the directed expression of the *Drp1-RNAi's* results in a slight increase in lifespan but compromised the climbing ability. *Drp1* overexpression and inhibition, slightly influence the number of ommatidia, interommatidial bristles, and ommatidium area when expressed under the control of the *GMR-Gal4* transgene. The well-documented function of *Drp1* is the promotion of mitochondrial fission and the inhibition of mitochondrial fusion (Chang and Blackstone 2010). Mitochondria host a number of cellular processes, especially oxidative phosphorylation, and are thus under continuous cellular stress and require repair and replacement (Lambert and Brand 2009; Murphy 2009; Dan Dunn et al. 2015). The lower tolerance of mitochondria to fission, compared to fusion, suggests that a continuous network of mitochondria can survive greater injury due to a lower rate of mitophagy and a slower rate of mitochondrial biogenesis, up-to an optimum level. The overexpression of *Drp1* results in the excessive fragmentation of the mitochondria such that its efficiency can be diminished to the point that functional complementation by fellow mitochondria is negligible. Mitochondria can become a distinct burden for the cell to upkeep instead of being an efficient "powerhouse of the cell". Clearly, the level of *Drp1* expression plays a key role in cell survival.

The *parkin* gene is crucial to the function of *Pink1*-dependent mitochondrial mitophagy. The loss of the parkin protein is a cause of great cellular stress as a major mechanism that controls mitophagy is compromised with one potential result being the accumulation of non-functional mitochondria. Under normal circumstances, the *parkin*-encoded ubiquitin ligase recruits the Drp1

protein to mediate mitochondrial fragmentation during mitophagy (Buhlman et al. 2014; Wang et al. 2018). In mouse embryonic fibroblasts, loss of *parkin* does not produce visible effects upon the net number of mitochondria (Roy et al. 2016). Furthermore, the loss of *parkin* along with the loss of *Drp1* increases the number of mitochondria by threefold, which can be interpreted that *parkin* controls mitochondria fragmentation in a *Drp1* knockout background (Roy et al. 2016). Therefore, *parkin* may negatively regulate, the *Drp1*-independent mitochondrial division. Alternatively, parkin may direct the ubiquitination of mitochondrial Drp1 protein to lead its proteasomal mediated degradation (Poole et al. 2010) and, hence, the activity of Drp1 protein on mitochondria is higher in *Drp1-parkin* co-inhibition state as compared to the inhibition of Drp1 alone. In my experiments, the critical class flies that have the directed co-expression of *Drp1-RNAi* and *parkin-RNAi* inhibitory transgenes live longer than those that express *parkin-RNAi* and *Drp1-RNAi* under the *Ddc-Gal4* transgene individually; this novel result support the hypothesis that the basic mechanism of PD-like phenotypes may be conserved among mammals (Rappold et al. 2014; Filichia et al. 2016) and diptera. The rescue health-span signifies improved proteostasis, mitophagy, mitochondrial dynamics and health. This could be due to the establishment of an altered mitochondrial network to enhance homeostasis and benefit cellular health. Further study will be required to determine the relationship between *Drp1* and *parkin*. Regardless of the underlying mechanism, my work provides strong evidence of important therapeutic target for maintaining mitochondrial health.

	Genotype	Median lifespan	Lifespan Increased/ Decreased	Climbing Increase/ decrease
Control	*Ddc-Gal$^{4.3D;}$ lac Z*	68 days		
Experiment	*Ddc-Gal$^{4.3D;}$ UAS-Drp1*	56 days	Decreased <0.0001	Decreased <0.0001
	Ddc-Gal$^{4.3D;}$ UAS-Drp1-RNAi-1^{JF02762}	70 days	Similar to control	Decreased <0.0001
	Ddc-Gal$^{4.3D;}$ UAS-Drp1-RNAi-2^{HMC03230}	72 days	Similar to control	Decreased <0.0001
Control	*Ddc-Gal$^{4.3D;}$ UAS-park-RNAi; lacZ*	60 days		
Experiment	*Ddc-Gal$^{4.3D;}$ UAS-park-RNAi; UAS-Drp1*	58 days	Similar to control	Increased
	Ddc-Gal$^{4.3D;}$ UAS-park-RNAi; UAS-Drp1-RNAi-1^{JF02762}	84 days	Increased	Increased
	Ddc-Gal$^{4.3D;}$ UAS-park-RNAi; UAS-Drp1-RNAi-2^{HMC03230}	76 days	Increased	Increased

Table 2.1 Summary of the Results. The effect of the altered expression of *Drp1* directed by *Ddc-Gal4$^{4.3D}$* and altered expression of *Drp1* along with *parkin-RNAi* directed by *Ddc-Gal4$^{4.3D}$* transgene on median lifespan and climbing ability of the critical class male flies. The Cells with blue highlight denote control; Orange highlight denotes the decreased compared to control; Green highlights denote the increase compared to control, and yellow highlights denote the resulting longevity and climbing ability is very similar to control.

Conclusion

Although closely associated with cell death pathways in neurons, *Drp1* has not been identified as a major gene in the development of Parkinson disease. The overexpression of the *Drp1* gene in neurons can result in reduced survival over time and an age-dependent decline in locomotor ability. The inhibition of *Drp1* by the Drosophila *Ddc-Gal4* transgenes results in an age-dependent loss in climbing ability, phenotypes that are strongly associated with neuronal degeneration and Parkinson-like disease. Thus, the compromised climbing abilities in flies with directed inhibition of *Drp1* have produced a new model of Parkinson Disease which can be used to further the investigation of the mechanisms underlying PD and other neurodegenerative diseases. The co-inhibition of the *parkin* with *Drp1* results in the rescue of the phenotypes observed, thus it is possible that *Drp1* and parkin can participate in cellular pathways that promote cell death. Further studies are required to explore the interactions between *parkin* and *Drp1* in these neurons. Overall, my experiments contribute to the understanding of mitochondrial health and enhanced conditions of homeostasis.

Bibliography

Breckenridge, D.G., Kang, B.-H., Kokel, D., Mitani, S., Staehelin, L.A., and Xue, D. 2008. Caenorhabditis elegans drp-1 and fis-2 regulate distinct cell-death execution pathways downstream of ced-3 and independent of ced-9. Mol. Cell **31**(4): 586–97. NIH Public Access. doi:10.1016/j.molcel.2008.07.015.

Buhlman, L., Damiano, M., Bertolin, G., Ferrando-Miguel, R., Lombès, A., Brice, A., and Corti, O. 2014. Functional interplay between Parkin and Drp1 in mitochondrial fission and clearance. Biochim. Biophys. Acta - Mol. Cell Res. **1843**(9): 2012–2026. doi:10.1016/j.bbamcr.2014.05.012.

Campello, S., and Scorrano, L. 2010, September. Mitochondrial shape changes: Orchestrating cell pathophysiology. European Molecular Biology Organization. doi:10.1038/embor.2010.115.

Chan, D.C. 2012. Fusion and Fission: Interlinked Processes Critical for Mitochondrial Health. Annu. Rev. Genet. **46**(1): 265–287. doi:10.1146/annurev-genet-110410-132529.

Chang, C.-R., and Blackstone, C. 2007a. Cyclic AMP-dependent Protein Kinase Phosphorylation of

Drp1 Regulates Its GTPase Activity and Mitochondrial Morphology. J. Biol. Chem. **282**(30): 21583–21587. doi:10.1074/jbc.C700083200.

Chang, C.-R., and Blackstone, C. 2007b. Drp1 phosphorylation and mitochondrial regulation. EMBO Rep. **8**(12): 1088–9; author reply 1089-90. European Molecular Biology Organization. doi:10.1038/sj.embor.7401118.

Chang, C.R., and Blackstone, C. 2010. Dynamic regulation of mitochondrial fission through modification of the dynamin-related protein Drp1. *In* Annals of the New York Academy of Sciences. Blackwell Publishing Inc. pp. 34–39. doi:10.1111/j.1749-6632.2010.05629.x.

Cribbs, J.T., and Strack, S. 2007. Reversible phosphorylation of Drp1 by cyclic AMP-dependent protein kinase and calcineurin regulates mitochondrial fission and cell death. EMBO Rep. **8**(10): 939–44. European Molecular Biology Organization. doi:10.1038/sj.embor.7401062.

Dan Dunn, J., Alvarez, L.A., Zhang, X., and Soldati, T. 2015. Reactive oxygen species and mitochondria: A nexus of cellular homeostasis. Redox Biol. **6**: 472–485. Elsevier. doi:10.1016/J.REDOX.2015.09.005.

Favaro, G., Romanello, V., Varanita, T., Andrea Desbats, M., Morbidoni, V., Tezze, C., Albiero, M., Canato, M., Gherardi, G., De Stefani, D., Mammucari, C., Blaauw, B., Boncompagni, S., Protasi, F., Reggiani, C., Scorrano, L., Salviati, L., and Sandri, M. 2019. DRP1-mediated mitochondrial shape controls calcium homeostasis and muscle mass. Nat. Commun. **10**(1): 2576. Nature Publishing Group. doi:10.1038/s41467-019-10226-9.

Filichia, E., Hoffer, B., Qi, X., and Luo, Y. 2016. Inhibition of Drp1 mitochondrial translocation provides neural protection in dopaminergic system in a Parkinson's disease model induced by MPTP. Sci. Rep. **6**: 32656. Nature Publishing Group. doi:10.1038/srep32656.

Freeman, M. 1996. Reiterative use of the EGF receptor triggers differentiation of all cell types in the Drosophila eye. Cell **87**(4): 651–660. Cell Press. doi:10.1016/S0092-8674(00)81385-9.

Galluzzi, L., Kepp, O., and Kroemer, G. 2012, December. Mitochondria: Master regulators of danger signalling. doi:10.1038/nrm3479.

Githure M'angale, P., and Staveley, B.E. 2016. Bcl-2 homologue Debcl enhances a-synuclein-induced phenotypes in Drosophila. PeerJ. doi:10.7717/peerj.2461.

Githure, P.M., and Staveley, B.E. 2017. Overexpression of Buffy enhances the loss of parkin and suppresses the loss of Pink1 phenotypes in Drosophila. Genome **60**(3): 241–247. NRC Research Press. doi:10.1139/gen-2016-0165.

Harman, D. 1991. Theageing process: Major risk factor for disease and death. Med. Sci. **88**: 5360–5363. Available from http://www.pnas.org/content/88/12/5360.full.pdf [accessed 22 December 2017].

Hoitzing, H., Johnston, I.G., and Jones, N.S. 2015. What is the function of mitochondrial networks? A theoretical assessment of hypotheses and proposal for future research. BioEssays **37**(6): 687–700. doi:10.1002/bies.201400188.

Ingerman, E., Perkins, E.M., Marino, M., Mears, J.A., McCaffery, J.M., Hinshaw, J.E., and Nunnari, J. 2005. Dnm1 forms spirals that are structurally tailored to fit mitochondria. J. Cell Biol. **170**(7): 1021–7. Rockefeller University Press. doi:10.1083/jcb.200506078.

Ishihara, N., Nomura, M., Jofuku, A., Kato, H., Suzuki, S.O., Masuda, K., Otera, H., Nakanishi, Y., Nonaka, I., Goto, Y., Taguchi, N., Morinaga, H., Maeda, M., Takayanagi, R., Yokota, S., and Mihara, K. 2009. Mitochondrial fission factor Drp1 is essential for embryonic development and synapse formation in mice. Nat. Cell Biol. **11**(8): 958–966. Nature Publishing Group.

doi:10.1038/ncb1907.
Kann, O., and Kovács, R. 2007, February. Mitochondria and neuronal activity. Am J Physiol Cell Physiol. doi:10.1152/ajpcell.00222.2006.
Karbowski, M., Lee, Y.-J., Gaume, B., Jeong, S.-Y., Frank, S., Nechushtan, A., Santel, A., Fuller, M., Smith, C.L., and Youle, R.J. 2002. Spatial and temporal association of Bax with mitochondrial fission sites, Drp1, and Mfn2 during apoptosis. J. Cell Biol. **159**(6): 931–8. The Rockefeller University Press. doi:10.1083/jcb.200209124.
Klein, C., and Westenberger, A. 2012. Genetics of Parkinson's disease. Cold Spring Harb. Perspect. Med. **2**(1). Cold Spring Harbor Laboratory Press. doi:10.1101/cshperspect.a008888.
Koch, A., Thiemann, M., Grabenbauer, M., Yoon, Y., McNiven, M.A., and Schrader, M. 2003. Dynamin-like Protein 1 Is Involved in Peroxisomal Fission. J. Biol. Chem. **278**(10): 8597–8605. doi:10.1074/jbc.M211761200.
Lackner, L.L., Horner, J.S., and Nunnari, J. 2009. Mechanistic analysis of a dynamin effector. Science **325**(5942): 874–7. American Association for the Advancement of Science. doi:10.1126/science.1176921.
Lambert, A.J., and Brand, M.D. 2009. Reactive Oxygen Species Production by Mitochondria. *In* Methods in molecular biology (Clifton, N.J.). pp. 165–181. doi:10.1007/978-1-59745-521-3_11.
Legesse-Miller, A., Massol, R.H., and Kirchhausen, T. 2003. Constriction and Dnm1p Recruitment Are Distinct Processes in Mitochondrial Fission. Mol. Biol. Cell **14**(5): 1953–1963. doi:10.1091/mbc.e02-10-0657.
Li, H., Chaney, S., Forte, M., and Hirsh, J. 2000. Ectopic g-protein expression in dopamine and serotonin neurons blocks cocaine sensitization in Drosophila melanogaster. Curr. Biol. **10**(4): 211–214. Current Biology Ltd. doi:10.1016/S0960-9822(00)00340-7.
Maes, M.E., Grosser, J.A., Fehrman, R.L., Schlamp, C.L., and Nickells, R.W. 2019. Completion of BAX recruitment correlates with mitochondrial fission during apoptosis. Sci. Rep. **9**(1). Nature Publishing Group. doi:10.1038/s41598-019-53049-w.
Mears, J.A., Lackner, L.L., Fang, S., Ingerman, E., Nunnari, J., and Hinshaw, J.E. 2011. Conformational changes in Dnm1 support a contractile mechanism for mitochondrial fission. Nat. Struct. Mol. Biol. **18**(1): 20–26. Nature Publishing Group. doi:10.1038/nsmb.1949.
Murphy, M.P. 2009. How mitochondria produce reactive oxygen species. Biochem. J. **417**(1): 1–13. Portland Press Ltd. doi:10.1042/BJ20081386.
Nakada, K., Sato, A., and Hayashi, J.I. 2009, October. Mitochondrial functional complementation in mitochondrial DNA-based diseases. doi:10.1016/j.biocel.2009.05.010.
Oettinghaus, B., D'Alonzo, D., Barbieri, E., Restelli, L.M., Savoia, C., Licci, M., Tolnay, M., Frank, S., and Scorrano, L. 2016. DRP1-dependent apoptotic mitochondrial fission occurs independently of BAX, BAK and APAF1 to amplify cell death by BID and oxidative stress. Biochim. Biophys. Acta - Bioenerg. **1857**(8): 1267–1276. doi:10.1016/j.bbabio.2016.03.016.
Pickrell, A.M., and Youle, R.J. 2015, January 21. The roles of PINK1, Parkin, and mitochondrial fidelity in parkinson's disease. Cell Press. doi:10.1016/j.neuron.2014.12.007.
Poole, A.C., Thomas, R.E., Yu, S., Vincow, E.S., and Pallanck, L. 2010. The Mitochondrial Fusion-Promoting Factor Mitofusin Is a Substrate of the PINK1/Parkin Pathway. PLoS One **5**(4): e10054. Public Library of Science. doi:10.1371/journal.pone.0010054.
Pradeep, H., Sharma, B., and Rajanikant, G.K. 2014. Drp1 in Ischemic Neuronal Death: An Unusual

Suspect. Curr. Med. Chem. **21**(19): 2183–2189. Bentham Science Publishers Ltd. doi:10.2174/092986732166613122820351 3.

Rana, A., Oliveira, M.P., Khamoui, A. V., Aparicio, R., Rera, M., Rossiter, H.B., and Walker, D.W. 2017. Promoting Drp1-mediated mitochondrial fission in midlife prolongs healthy lifespan of Drosophila melanogaster. Nat. Commun. **8**(1): 1–14. Nature Publishing Group. doi:10.1038/s41467-017-00525-4.

Rappold, P.M., Cui, M., Grima, J.C., Fan, R.Z., De Mesy-Bentley, K.L., Chen, L., Zhuang, X., Bowers, W.J., and Tieu, K. 2014. Drp1 inhibition attenuates neurotoxicity and dopamine release deficits in vivo. Nat. Commun. **5**(1): 1–13. Nature Publishing Group. doi:10.1038/ncomms6244.

Riemensperger, T., Issa, A.R., Pech, U., Coulom, H., Nguyễn, M.V., Cassar, M., Jacquet, M., Fiala, A., and Birman, S. 2013. A Single Dopamine Pathway Underlies Progressive Locomotor Deficits in a Drosophila Model of Parkinson Disease. Cell Rep. **5**(4): 952–960. doi:10.1016/j.celrep.2013.10.032.

Roy, M., Itoh, K., Iijima, M., and Sesaki, H. 2016. Parkin suppresses Drp1-independent mitochondrial division. Biochem. Biophys. Res. Commun. **475**(3): 283–8. NIH Public Access. doi:10.1016/j.bbrc.2016.05.038.

Scott, I., and Youle, R.J. 2010. Mitochondrial fission and fusion. Essays Biochem. **47**: 85–98. NIH Public Access. doi:10.1042/BSE0470085.

Sebastián, D., Palacín, M., and Zorzano, A. 2017. Mitochondrial Dynamics: Coupling Mitochondrial Fitness with Healthyageing. Trends Mol. Med. **23**(3): 201–215. Elsevier Current Trends. doi:10.1016/J.MOLMED.2017.01.003.

Staveley, B.E. 2012. Successes of Modelling Parkinson Disease in Drosophila. *In* Mechanisms in Parkinson's Disease - Models and Treatments. InTech. pp. 233–250. doi:10.5772/18844.

Sun, Y., Ge, X., Li, X., He, J., Wei, X., Du, J., Sun, J., Li, X., Xun, Z., Liu, W., Zhang, H., Wang, Z.Y., and Li, Y.C. 2020. High-fat diet promotes renal injury by inducing oxidative stress and mitochondrial dysfunction. Cell Death Dis. **11**(10): 1–14. Springer Nature. doi:10.1038/s41419-020-03122-4.

Todd, A., and Staveley, B. 2012. Expression of Pink1 with α-synuclein in the dopaminergic neurons of Drosophila leads to increases in both lifespan and healthspan. Genet. Mol. Res. **11**(2): 1497–1502. doi:10.4238/2012.May.21.6.

Todd, A.M., and Staveley, B.E. 2004. Novel assay and analysis for measuring climbing ability in Drosophila. Drosoph. Inf. Serv. **87**: 101–108. Available from http://www.ou.edu/journals/dis/DIS87/4 - Techniques.pdf [accessed 6 October 2019].

Touvier, T., De Palma, C., Rigamonti, E., Scagliola, A., Incerti, E., Mazelin, L., Thomas, J.-L., D'Antonio, M., Politi, L., Schaeffer, L., Clementi, E., and Brunelli, S. 2015. Muscle-specific Drp1 overexpression impairs skeletal muscle growth via translational attenuation. Cell Death Dis. **6**(2): e1663. Nature Publishing Group. doi:10.1038/cddis.2014.595.

Twig, G., Elorza, A., Molina, A.J.A., Mohamed, H., Wikstrom, J.D., Walzer, G., Stiles, L., Haigh, S.E., Katz, S., Las, G., Alroy, J., Wu, M., Py, B.F., Yuan, J., Deeney, J.T., Corkey, B.E., and Shirihai, O.S. 2008. Fission and selective fusion govern mitochondrial segregation and elimination by autophagy. EMBO J. **27**(2): 433–446. doi:10.1038/sj.emboj.7601963.

Twig, G., and Shirihai, O.S. 2011, May 15. The interplay between mitochondrial dynamics and mitophagy. Mary Ann Liebert, Inc. doi:10.1089/ars.2010.3779.

Wai, T., and Langer, T. 2016. Mitochondrial Dynamics and Metabolic Regulation. Trends Endocrinol. Metab. **27**(2): 105–117. Elsevier Current Trends. doi:10.1016/J.TEM.2015.12.001.

Wang, H., Song, P., Du, L., Tian, W., Yue, W., Liu, M., Li, D., Wang, B., Zhu, Y., Cao, C., Zhou, J., and Chen, Q. 2011. Parkin Ubiquitinates Drp1 for Proteasome-dependent Degradation. J. Biol. Chem. **286**(13): 11649–11658. doi:10.1074/jbc.M110.144238.

Wang, Y., Tang, C., Cai, J., Chen, G., Zhang, D., Zhang, Z., and Dong, Z. 2018. PINK1/Parkin-mediated mitophagy is activated in cisplatin nephrotoxicity to protect against kidney injury. Cell Death Dis. **9**(11): 1113. Nature Publishing Group. doi:10.1038/s41419-018-1152-2.

Waterham, H.R., Koster, J., van Roermund, C.W.T., Mooyer, P.A.W., Wanders, R.J.A., and Leonard, J. V. 2007. A Lethal Defect of Mitochondrial and Peroxisomal Fission. N. Engl. J. Med. **356**(17): 1736–1741. Massachusetts Medical Society . doi:10.1056/NEJMoa064436.

Wikstrom, J.D., Israeli, T., Bachar-Wikstrom, E., Swisa, A., Ariav, Y., Waiss, M., Kaganovich, D., Dor, Y., Cerasi, E., and Leibowitz, G. 2013. AMPK Regulates ER Morphology and Function in Stressed Pancreatic β-Cells via Phosphorylation of DRP1. Mol. Endocrinol. **27**(10): 1706–1723. doi:10.1210/me.2013-1109.

Xiong, Y., and Yu, J. 2018, April 9. Modeling Parkinson's disease in Drosophila: What have we learned for dominant traits? Frontiers Media S.A. doi:10.3389/fneur.2018.00228.

Yang, Y., Gehrke, S., Imai, Y., Huang, Z., Ouyang, Y., Wang, J.W., Yang, L., Beal, M.F., Vogel, H., and Lu, B. 2006. Mitochondrial pathology and muscle and dopaminergic neuron degeneration caused by inactivation of Drosophila Pink1 is rescued by Parkin. Proc. Natl. Acad. Sci. U. S. A. **103**(28): 10793–10798. doi:10.1073/pnas.0602493103.

Yang, Y., Nishimura, I., Imai, Y., Takahashi, R., and Lu, B. 2003. Parkin suppresses dopaminergic neuron-selective neurotoxicity induced by Pael-R in Drosophila. Neuron **37**(6): 911–924. Cell Press. doi:10.1016/S0896-6273(03)00143-0.

Yu, T., Robotham, J.L., and Yoon, Y. 2006. Increased production of reactive oxygen species in hyperglycemic conditions requires dynamic change of mitochondrial morphology. Proc. Natl. Acad. Sci. U. S. A. **103**(8): 2653–8. National Academy of Sciences. doi:10.1073/pnas.0511154103.

Yuan, H., Gerencser, A.A., Liot, G., Lipton, S.A., Ellisman, M., Perkins, G.A., and Bossy-Wetzel, E. 2007. Mitochondrial fission is an upstream and required event for bax foci formation in response to nitric oxide in cortical neurons. Cell Death Differ. **14**(3): 462–471. Cell Death Differ. doi:10.1038/sj.cdd.4402046.

Chapter 3: Altered *Buffy* and *Debcl* expression suppresses *Drp1* gain and loss of function phenotypes in Drosophila

A version of this chapter is submitted as: Hasan, A., and Staveley, B.E. 2021.

Abstract

The Drp1 protein directly regulates mitochondrial dynamics and is crucial for apoptosis, autophagy and the maintenance of mitochondrial health. Mutations in *Drp1* can lead to mitochondrial dysfunction to promote the loss of neurons. The Drp1 protein can interact with members of the Bcl-2 family proteins in the initiation and progression of mitochondrial-induced apoptosis. The *Ddc-Gal4* transgene was exploited to direct the expression of *Drp1;* and the inhibition of *Drp1* function utilizing specific *RNAi* transgenes in neurons. The overexpression of *Drp1* under the control of *Ddc-Gal4*, in populations of neuronal cells that include dopamine-producing neurons, can severely reduce median lifespan and cause locomotor dysfunction. The phenotypes produced by overexpression of *Drp1* can be suppressed either when the pro-survival *Bcl-2* homologue *Buffy* is overexpressed or when the pro-cell death *Bcl-2* homologue *Debcl* is inhibited in these tissues. The inhibition of *Drp1* seems to compromise locomotor function throughout life but does not seem to affect longevity. The expression of pro-survival *Buffy* suppresses the compromised climbing phenotype induced by the loss of *Drp1* function while the median lifespan is reduced. The inhibition of *Buffy* expression acts to further decrease median lifespan and climbing ability compared to control. Alteration of the expression of *Drp1* acts to phenocopy a Parkinson Disease phenotype in Drosophila, while overexpression of *Buffy* can counteract these phenotypes to improve the overall health-span of the organism. Likely the pro-survival effect of Buffy can rescue the phenotypic effect due to the Drp1 induced excessive apoptosis.

Introduction

The dynamic nature of the mitochondria population is critical to the integrity of the subcellular network structures that this organelle maintains and to control the quality of mitochondrial proteins and other components (Wikstrom et al. 2013; Ikeda et al. 2015; Schmitt et al. 2018). In response to a series of molecular cues (Karbowski et al. 2002; Maes et al. 2019), the mitochondrial network participates in a delicate balance of continuous division and fusion processes (Lee et al. 2007). The mitochondrial fission protein Drp1 is a member of a GTPase family of proteins and functions in a manner similar to other dynamin protein family members (Ingerman et al. 2005; Chapter 2). The Drp1 monomers are localized to the cytoplasm and actively cycle on and off at the sites of division of the mitochondrial tubules. Blocking the GTPase activity of the Drp1 protein can act to inhibit the fission of the mitochondria (Suen et al. 2008). For the most part, the activation of the Drp1 protein is regulated through two very well-conserved phosphorylation sites (Chang and Blackstone 2007a, 2007b; Cribbs and Strack 2007). As well, Drp1 undergoes the distinct post-translational modification of SUMOylation to promote programmed cell death (Suen et al. 2008). The early events that occur during apoptosis include cristae remodeling, mitochondrial fragmentation, caspase activation and membrane "blebbing" or zeiosis (He et al. 2009). Fragmentation of mitochondria is invariably associated with the early stages of the process of intrinsic apoptosis (Suen et al. 2008). Drp1 downregulation directed by RNA-interference or by expression of a dominant-negative mutant form of *Drp1,* can slow the rate of mitochondrial fragmentation and the cascade of apoptotic events (Estaquier and Arnoult 2007; Wu et al. 2011; Wang et al. 2015). The activity of Drp1 promotes caspase-independent mitochondrial fission and cristae remodeling to amplify apoptosis instigated by either the activity of the pro-apoptotic

protein BID or by oxidative stress (Oettinghaus et al. 2016). Overall, the process of mitochondrial fission plays a multifaceted role in the amplification of the essential cellular process of apoptosis.

The roles of a number of mitochondrial fission and fusion proteins during apoptosis have been well studied. One such process involves the recruitment of the mitochondrial fission protein, Drp1, to the Mitochondrial Outer Membrane (MOM) by association with Outer Mitochondrial Membrane (OMM) proteins to promote fission (Chan 2012). The mechanism of Drp1 recruitment on MOM is not clearly understood; although this action is regulated by a post-translational modification process, specifically through protein phosphorylation (Cribbs and Strack 2007; Cereghetti et al. 2008). The activity of Drp1 is governed by the summation of the activity of several critical signalling pathways. Select Bcl-2 family proteins are essential in these pathways and act to protect the mitochondria through the regulation of mitophagy and apoptosis (Hardwick and Soane 2013). The Bcl-2 family proteins interact with Drp1, and Drp1 can promote apoptosis in Bcl-2 protein-dependent and independent manners (Cassidy-Stone et al. 2008; Oettinghaus et al. 2016). The two Bcl-2 family homologues in *Drosophila melanogaster* are *Buffy* (anti-apoptotic) and *Debcl* (pro-apoptotic). The Debcl protein can interacts with Drp1 in Drosophila to activate apoptosis via the JNK pathway (Clavier et al. 2015). The Bcl-2 family of proteins have up to four BH domains, BH1, BH2, BH3 and BH4 and the two Bcl-2 proteins in *D. melanogaster* have all four BH domains. The BH3 domains are critical for pro-apoptotic functions (Chittenden 2002). At one time, the BH4 domain was associated exclusively with the anti-apoptotic function of some Bcl-2 family proteins (Liu et al. 2016). The direct and indirect interaction of Bcl-2 family proteins and Drp1 is significant in the regulation of the balance between mitochondrial health and apoptosis.

The inhibition of *Drp1* has been shown to suppress *parkin (park)* mutant phenotypes (Chapter 2) which suggests a role for this protein in 1) in a pathway that regulates mitochondrial health and integrity and in 2) in interactions with mitochondrial proteins. The anticipated role of the mitochondria in PD pathogenesis has made the study of the interaction of *Drp1* and *Bcl-2* family genes important to the modelling of this disease in Drosophila. I utilized *Drosophila melanogaster* as a model organism to study the phenotypic effects of the interactions of these genes. In my experiments, I exploited the *UAS-Gal4* system to direct the expression and inhibition of the *Buffy* and *Debcl* in selected neuronal tissues using the *Ddc-Gal4* transgene. Here, I propose that the *Drp1* overexpression phenotype is due to excessive activities related to apoptosis and can be rescued by the appropriate regulation by anti-apoptotic Bcl-2 gene, *Buffy*. The phenotype produced in response to the expression of *Drp1-RNAi* is anticipated due to the diminishment of mitochondrial integrity and maybe rescued through modification of the responsible signalling pathway. The careful regulation of mitochondrial dynamics is important to control mitochondrial induced defects.

Material and Methods

Drosophila media and culture

All stocks were maintained on a standard media prepared from cornmeal/molasses/yeast/agar medium treated with propionic acid and methylparaben to resist fungal growth. Aliquots of media were poured into plastic vials, allowed to solidify, and refrigerated at 4°C until used. Stocks are kept at room temperature while crosses and experiments were carried out at 25°C. The *UAS-Drp1*

(y[1] w[*]; P{w[+mC]=FLAG-FlAsH-HA-Drp1}3, Ki[1]); the UAS-Drp1-RNAi1^{JF02762} (y[1] v[1]; P{y[+t7.7] v[+t1.8]=TRiP.JF02762}attP2}), UAS-Drp1-RNAi2^{HMC03230} (y[1] v[1]; P{y[+t7.7]v[+t1.8]=TRiP.HMC03230}attP40), the UAS-Buffy (w[*]; P{w[+mC]=UAS-Buffy.S}E1); UAS-Buffy-RNAi (w[*]; P{w[+mC]=UAS-Buffy.RNAi}3), UAS-Debcl^{EY05743} (y[1] w[67c23]; P{y[+mDint2] w[+mC]=EPgy2}Debcl[EY05743]), Ddc-Gal4$^{4.3D}$(w[1118]; P{w[+mC]=Ddc-GAL4.L}4.3D) and *UAS lacZ^{4-1-2}*; stocks were obtained from Bloomington Drosophila Stock Center at Indiana University, Bloomington, Indiana, USA. The *UAS-Debcl-RNAi^{v47515} (w1118; P{GD 1637}v47515)* was obtained from Vienna Drosophila Resource Center. The *Ddc-Gal4/CyO; UAS-Drp1/TM3, Ddc-Gal4/CyO; UAS-Drp1-RNAi /TM3*, derivative lines were generated using standard recombination methods (Githure and Staveley 2016) and used to overexpress or inhibit *Drp1* in the selected DA neurons using the *Ddc-Gal4$^{4.3D}$* transgene.

Ageing assay

Several crosses of virgin females and males were made, and a cohort of critical class males collected upon eclosion. At least 250 flies were aged per genotype in the cohorts of 25 or less per vial on fresh media, replenished every two-five day to avoid crowding. Flies were observed and scored every two days for the presence of deceased adults. As a rule, flies were considered dead when they did not display movement upon agitation (Todd and Staveley 2004, 2012). Longevity data were analyzed using GraphPad Prism version 8 statistical software (*graphpad.com*), and survival curves were compared by the Mantel-Cox test. Significance were determined at a 95% confidence level ($P \leq 0.05$) with Bonferroni correction.

Climbing assay

The 70 critical class male flies were collected within 24 hours and maintained as ten flies per each vial. The food was changed twice every week. Every week 50 males of each genotype were assayed, in groups of 10, for their ability to climb a glass tube divided into five levels of 2 cm each according to standard protocol (Todd and Staveley 2004, 2012). The climbing index was calculated for each week using GraphPad prism version 8 statistical software. The climbing curve was fitted using non-linear regression and determined at a 95% confidence interval ($P \leq 0.05$).

Results

Alteration of the expression of *Drp1* and *Drp1-RNAi* with the *Ddc-Gal4$^{4.3D}$* transgene

In these experiments, the control *Ddc-Gal4$^{4.3D}$; UAS-lacZ* critical class males were determined to have a median lifespan of 62 days (n = 308). The directed inhibition of *Drp1* by the *Ddc-Gal4* transgene results in a greater median lifespan of 70 days in 321 flies compared to the control as determined by log-rank (Mantel-Cox) test with P-value <0.0001 (Figure 3.1). In contrast, the directed expression of *Drp1* by the *Ddc-Gal4* transgene results in a reduced median lifespan of 56 days in 255 flies compared to the control as determined by log-rank (Mantel-Cox) test with P-value <0.0001 (Figure 3.1A). Furthermore, the *Ddc-Gal4 UAS-Drp1-RNAi UAS-lacZ* critical class males have a median lifespan of 70 days in 310 flies. The overexpression of *Drp1* along with *UAS-Drp1-RNAi* under the direction of the *Ddc-Gal4* transgene (*Ddc-Gal4; UAS-Drp1-RNAi; UAS-Drp1*) has a median lifespan of 64 days, similar to control (*Ddc-Gal4; UAS-lacZ*) with a P value of 0.0633 as determined by the Log-rank Mantel-Cox test with a Bonferroni correction (Figure 3.1A). The *Ddc-Gal4 UAS-Drp1 UAS-lacZ* critical class males have a median lifespan of 58 days in 294 flies. The

inhibition of *Drp1* along with *UAS-Drp1* under the direction of the *Ddc-Gal4* transgene (*Ddc-Gal4; UAS-Drp1; UAS-Drp1-RNAi*) has a median lifespan of 64 days (n=327), similar to control (*Ddc-Gal4; UAS-lacZ*) with a P value of 0.0582 as determined by the Log-rank Mantel-Cox test with a Bonferroni correction (Figure 3.1C). The non-linear fitting of the climbing ability curve shows the *Drp1* expression and inhibition both have compromised the climbing ability phenotype compared to control at 95% CI ($p < 0.0001$) (Figure 1B & D). The climbing ability curve of *Ddc-Gal4 UAS-Drp1-RNAi UAS-Drp1* and *Ddc-Gal4 UAS-Drp1 UAS-Drp1-RNAi* is very close to the control (*Ddc-Gal4; UAS-lacZ*) as determined by the non-linear fitting of the climbing curve at a 95% CI at P-value 0.2752 and 0.0589, respectively.

A)

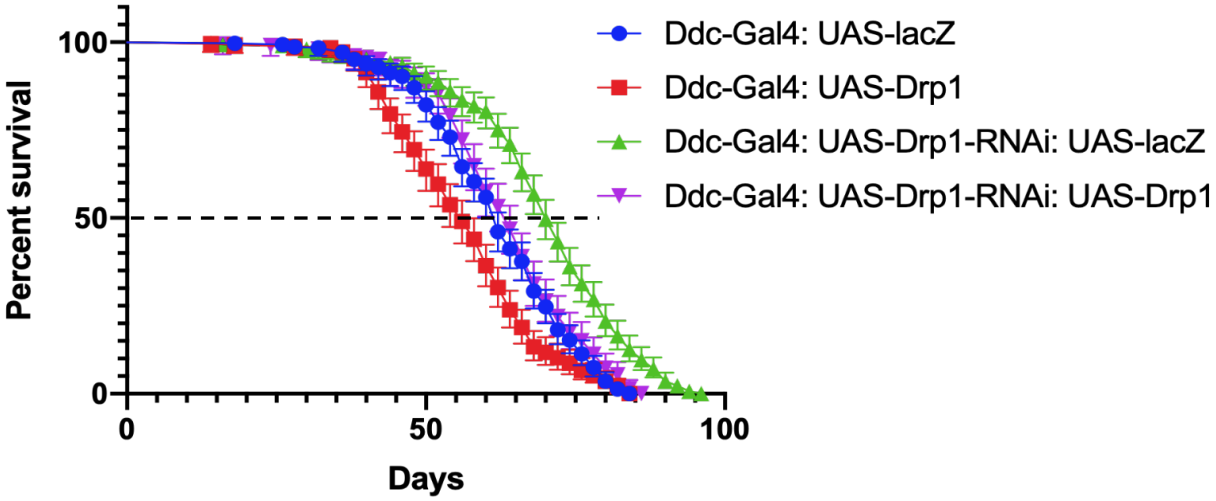
Percent survival
100
50
0
0
50
100
Days
Ddc-Gal4: UAS-lacZ
Ddc-Gal4: UAS-Drp1
Ddc-Gal4: UAS-Drp1-RNAi: UAS-lacZ
Ddc-Gal4: UAS-Drp1-RNAi: UAS-Drp1

B)

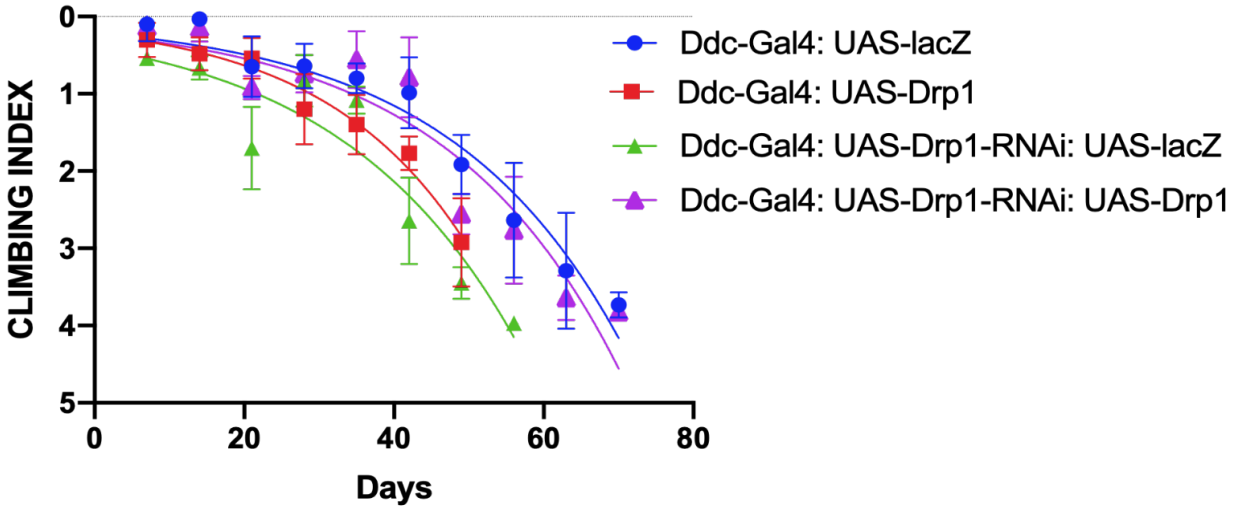
CLIMBING INDEX
0
1
2
3
4
5
0
20
40
60
80
Days
Ddc-Gal4: UAS-lacZ
Ddc-Gal4: UAS-Drp1
Ddc-Gal4: UAS-Drp1-RNAi: UAS-lacZ
Ddc-Gal4: UAS-Drp1-RNAi: UAS-Drp1

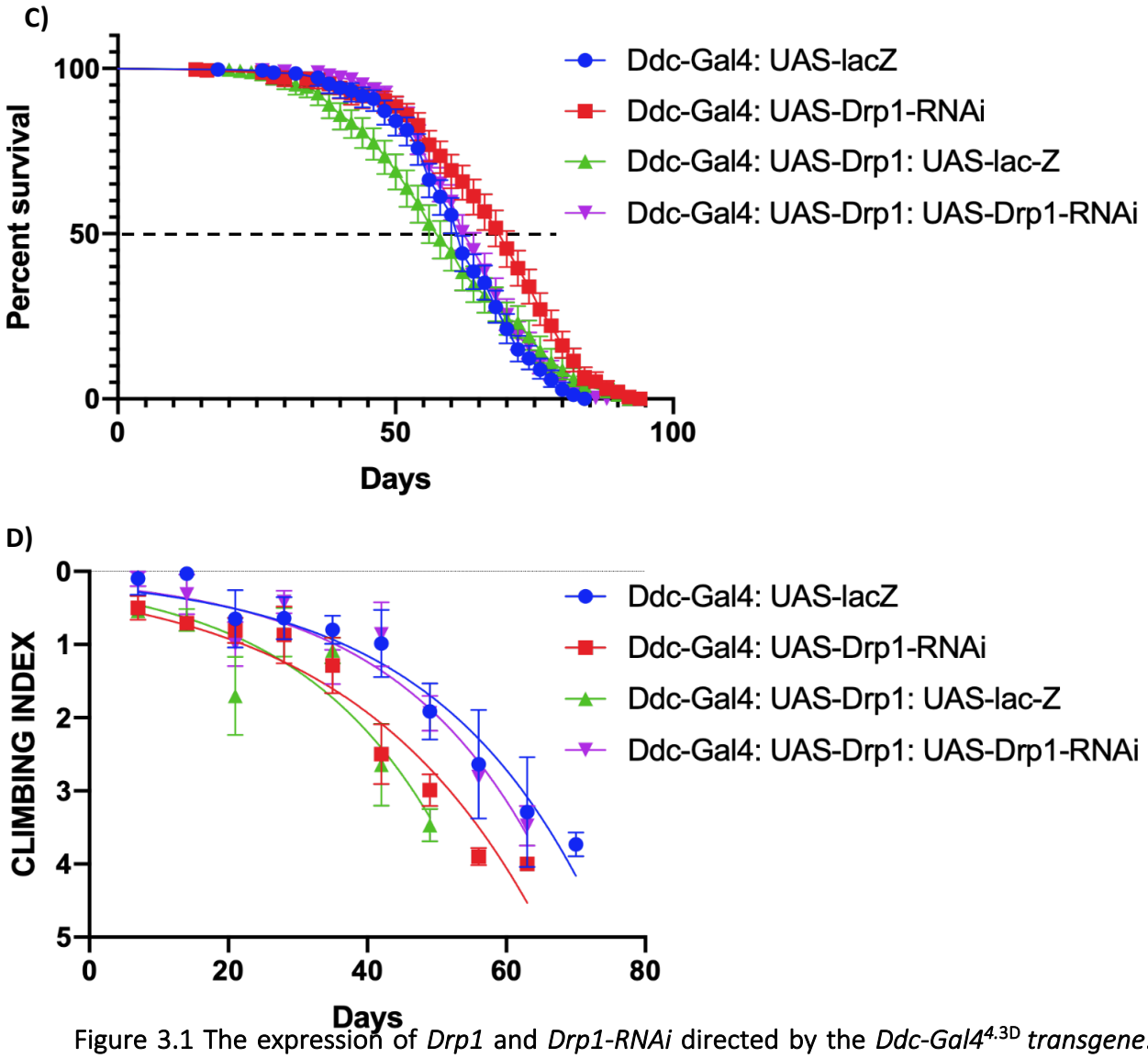

Figure 3.1 The expression of *Drp1* and *Drp1-RNAi* directed by the *Ddc-Gal4$^{4.3D}$ transgene*. **A)** In control, *Ddc-Gal4$^{4.3D}$ UAS-lacZ* critical class males resulted in a median life span of 62 days (n=308). Expression of *Drp1* in *Ddc-Gal4$^{4.3D}$* resulted in a median life span of 56 days (n=310), much lower than the *lacZ*-expressing control; expression of *Drp1* in *Ddc-Gal4$^{4.3D}$ UAS-Drp1-RNAi* resulted in a median life span of 64 days (n=250) very similar to control (Ddc/lacZ) as determined by the Log-rank Mantel-Cox test (p value=0.0633) with Bonferroni correction. The graph of the longevity assay was generated by GraphPad prism8. **B)** The *Ddc-Gal4$^{4.3D}$* flies express *UAS-lacZ in* control flies. The climbing abilities of *Ddc-Gal4$^{4.3D}$ UAS-Drp1* expressing flies have decreased compared to control as determined in the non-linear fitting of the climbing curve by a 95% confidence interval ($p<0.0001$). The flies' climbing ability expressing *Drp1* in *Ddc-Gal4$^{4.3D}$ UAS-Drp1-RNAi* transgene is similar to control as determined in the non-linear fitting of the climbing curve by a 95% confidence interval at P value=1.309. The graph of longevity assay was generated by GraphPad prism8 non-linear regression curve. **C)** In control, *Ddc-Gal4$^{4.3D}$ UAS-lacZ* critical class males resulted in a median life span of 62 days (n=308). Expression of *Drp1-RNAi* in *Ddc-Gal4$^{4.3D}$* resulted in a median life span of 70 days (n=321), much higher compared to the control; expression of *Drp1-RNAi* in *Ddc-Gal4$^{4.3D}$ UAS-Drp1* resulted in a median life span of 64 days (n=327), very similar to control (Ddc/lacZ) as

determined by the Log-rank Mantel-Cox test (p value=0.0582) with Bonferroni correction. The graph of the longevity assay was generated by GraphPad prism8. D) The *Ddc-Gal4*$^{4.3D}$ flies express *UAS-lacZ in* control flies. The climbing abilities of *Ddc-Gal4*$^{4.3D}$ *UAS-Drp1-RNAi* expressing flies have decreased compared to control as determined in the non-linear fitting of the climbing curve by a 95% confidence interval ($p<0.0001$). The flies' climbing ability expressing *Drp1-RNAi* in *Ddc-Gal4*$^{4.3D}$ *UAS-Drp1* transgene is similar to control (Ddc/lacZ) as determined in the non-linear fitting of the climbing curve by a 95% confidence interval at p value=0.0027. The graph of longevity assay was generated by GraphPad prism8 non-linear regression curve.

Altering the expression of *Buffy* and *Debcl* in combination with *Drp1* directed by the *Ddc-Gal4$^{4.3D}$* transgene

The control *Ddc-Gal4$^{4.3D}$; UAS-Drp1; UAS-lacZ* critical class males were determined to have a median lifespan of 58 days (n=282). The overexpression of *Buffy* along with *UAS-Drp1* under the direction of the *Ddc-Gal4* transgene (*Ddc-Gal4; UAS-Drp1; UAS-Buffy*) has a median lifespan of 68 days (n=255), much higher compared to control with a P value of <0.0001 as determined by log-rank (Mantel-Cox) test with a Bonferroni correction. The inhibition of *Buffy* along with *UAS-Drp1 under the direction of the Ddc-Gal4* transgene (*Ddc-Gal4; UAS-Drp1; UAS-Buffy-RNAi)* has a median lifespan of 52 days (n=274), much less compared to the control (Figure 3.2A) with a P value 0.0125 as determined by log-rank Mantel-Cox test with a Bonferroni correction. The overexpression of *Buffy* in neurons rescued the early onset of impairment in the climbing ability of *Ddc-Gal4; UAS-Drp1* flies. The non-linear fitting of the climbing curve shows *Buffy* overexpression has rescues the climbing ability defect compared to control at 95% CI (p <0.0001) (Figure 2B). The inhibition of *Buffy* by *Ddc-Gal4 UAS-Drp1; UAS-Buffy-RNAi* further contributes to loss of the climbing ability throughout the life of critical class flies compared to control at 95% CI at a P-value 0.0125 (n=50) (Figure 3.2B).

The overexpression of *Debcl* along with *UAS-Drp1* under the direction of *Ddc-Gal4* transgene *(Ddc-Gal4; UAS-Drp1; UAS-Debcl* ^{EY05743}) has a median lifespan of 60 days (n=331 flies), similar to the control (Figure 3.2A) with a P value at 0.0114 as determined by log-rank Mantel-Cox test with Bonferroni correction. The inhibition of *Debcl,* along with *UAS-Drp1 under the direction of the* Ddc-Gal4 transgene (*Ddc-Gal4; UAS-Drp1; UAS-Debcl-RNAi* ^{v47515}*) has a* median lifespan of 66 days (n=303), much higher compared to the control (Figure 3.2A) with a P value at 0.0004 as determined by log-rank Mantel-Cox test with Bonferroni correction. The non-linear fitting of the

climbing curve shows *Debcl* overexpression has no change in the climbing ability defect compared to control at 95% CI (p=0.3293) (Figure 3.2B). The inhibition of *Debcl* by *Ddc-Gal4 UAS-Drp1; UAS-Debcl-RNAi*^{v47515} has rescues the climbing ability throughout the life of critical class flies compared to control at 95% CI at a P-value 0.0057 (n=50) (Figure 3.2B).

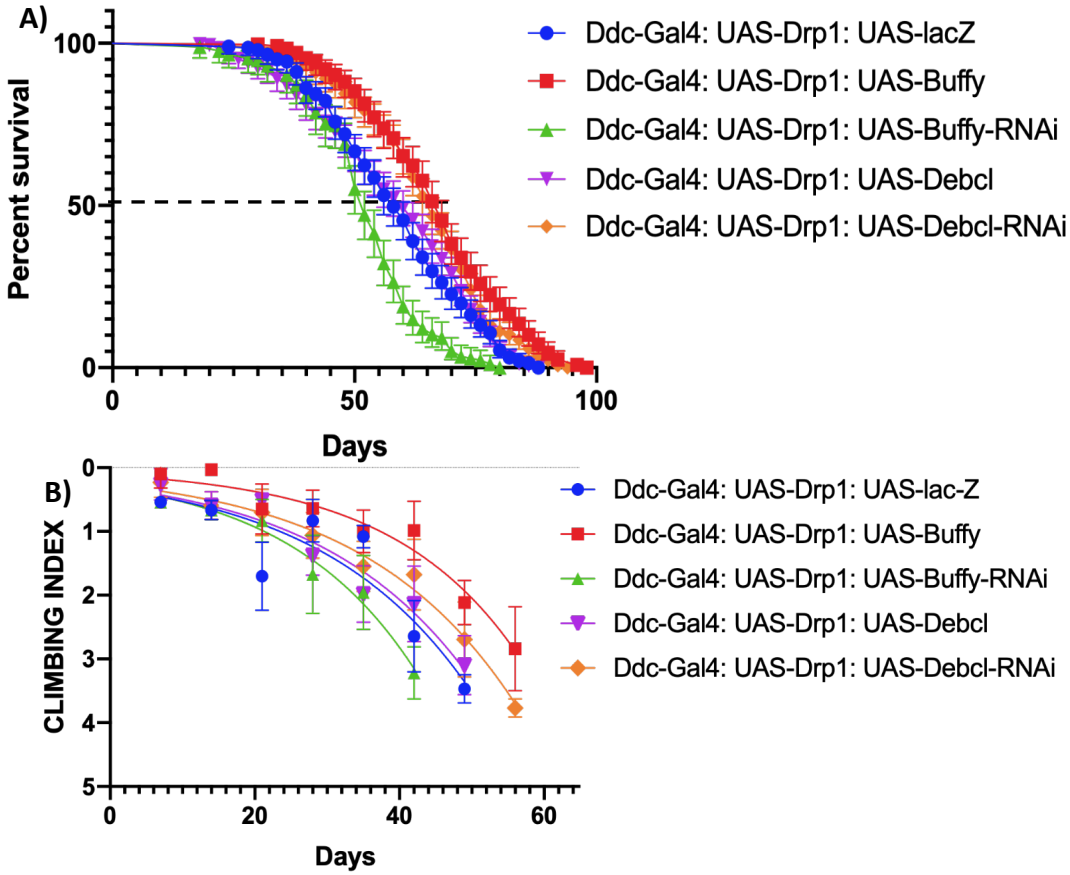

Figure 3.2 Altered expression of *Buffy* and *Debcl* with *UAS-Drp1* directed by the *Ddc-Gal4$^{4.3D}$* transgene. A. In control, *Ddc-Gal4$^{4.3D}$*; *UAS-Drp1 UAS-lacZ* critical class males resulted in a median life span of 58 days (n=282). The overexpression of *Buffy* results in a median lifespan of 68 days (n=375) compares to 58 days of control (P value=0.0002); the inhibition of *Buffy* directed by the *Ddc-Gal4$^{4.3D}$ UAS-Drp1* transgene results in the median lifespan of 52 (n=274), much less compared to control, determined by Log-rank Mantel-Cox test at P-value <0.0001, with Bonferroni correction. The overexpression of *Debcl^{EY05743}* results in a median lifespan of 60 days (n=331) similar to 58 days of control determined by Log-rank Mantel-Cox test at P-value 0.3293; the inhibition of *Debcl* directed by the *Ddc-Gal4 UAS-Drp1* transgene result in the median lifespan of 66 (n=303); much higher than control, determined by Log-rank Mantel-Cox test at P value 0.0057, with Bonferroni correction. **B** The GraphPad prism8 generated graph of the climbing abilities of *Ddc-Gal4 -Drp1* flies with the expression of *Buffy, Buffy-RNAi, Debcl^{EY05743}, Debcl-RNAi^{v47515}* and control. The climbing abilities of flies overexpressing *Buffy* have rescued compared to control as determined in the climbing curve's non-linear fitting by a 95% confidence interval (p<0.0001). The climbing ability of the flies was further weakened by the expression of *UAS-Buffy-RNAi* as determined in the non-linear fitting of the climbing curve by a 95% confidence interval at a p-value 0.0125 and 0.03293 respectively (n=50). The climbing abilities of flies expressing *Debcl-RNAi^{v47515}*has rescued compared to control as determined by the non-linear fitting of the climbing curve by a 95% confidence interval (p value=0.0057). The graph of longevity assay was generated by GraphPad prism8 non-linear regression curve.

Altering the expression of *Buffy* and *Debcl* along with *Drp1-RNAi* by *Ddc-Gal4$^{4.3D}$* transgene

The control *Ddc-Gal4$^{4.3D}$; UAS-Drp1-RNAi; UAS-lacZ* critical class males were determined to have a median lifespan of 70 days (n=323). The overexpression of *Buffy* along with *UAS-Drp1-RNAi* under the direction of the *Ddc-Gal4* transgene (*Ddc-Gal4; UAS-Drp1-RNAi; UAS-Buffy*) has a median lifespan of 64 days (n=308), much lower compared to control with a P value of <0.0001 as determined by log-rank (Mantel-Cox) test with a Bonferroni correction. The co-inhibition of *Buffy* and *Drp1 under the direction of the Ddc-Gal4* transgene (*Ddc-Gal4; UAS-Drp1-RNAi; UAS-Buffy-RNAi)* has a median lifespan of 62 days (n=273), much less compared to the control (Figure 3.3A) with a P value at <0.0001 as determined by log-rank Mantel-Cox test with a Bonferroni correction. The non-linear fitting of the climbing curve shows *Buffy* overexpression has rescued the climbing ability defect compared to control at 95% CI (p <0.0001) (Figure 2B). The inhibition of *Buffy* by *Ddc-Gal4 UAS-Drp1-RNAi; UAS-Buffy-RNAi* further contributes to loss of the climbing ability throughout the life of critical class flies compared to control at 95% CI at a P-value <0.0001 (n=50) (Figure 3.3B).

The overexpression of *Debcl* along with *UAS-Drp1-RNAi* under the direction of *Ddc-Gal4* transgene *(Ddc-Gal4; UAS-Drp1-RNAi; UAS-Debcl*^{EY05743}) has a median lifespan of 68 days (n=156 flies), similar to the control (Figure 2A) with a P value at 0.0003 as determined by log-rank Mantel-Cox test with Bonferroni correction. The inhibition of *Debcl,* along with *UAS-Drp1-RNAi* under the direction of the *Ddc-Gal4* transgene (*Ddc-Gal4; UAS-Drp1-RNAi; UAS-Debcl-RNAi ^{v47515})* results in a median lifespan of 72 days (n=321), higher compared to the control (Figure 3.3A) with a P value at 0.0211 as determined by log-rank Mantel-Cox test with Bonferroni correction. The non-linear fitting of the climbing curve shows *Debcl* overexpression has further increased the climbing ability defect compared to control at 95% CI (p=0.0004) (Figure 3B). The inhibition of *Debcl* by *Ddc-Gal4 UAS-*

Drp1-RNAi; UAS-Debcl-RNAi ^{v47515} has rescued the climbing ability throughout the life of critical class flies compared to control at 95% CI at a P-value 0.0211 (n=50) (Figure 3.3B).

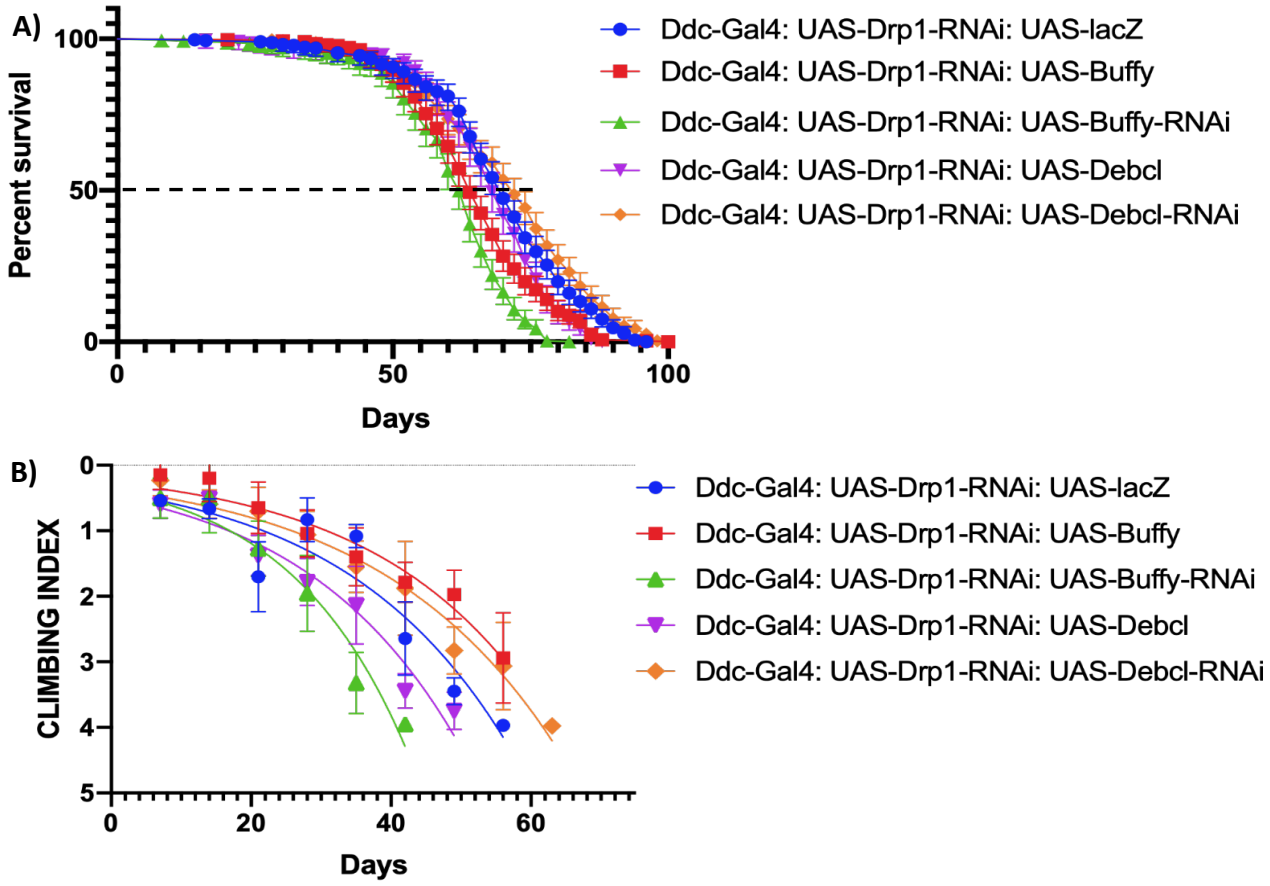

.

Figure 3.3 Altered expression of *Buffy* and *Debcl with UAS-Drp1-RNAi* directed by the *Ddc-Gal4*$^{4.3D}$ transgene. A. In control, *Ddc-Gal4*$^{4.3D}$; *UAS-Drp1* transgene results in the median lifespan of 62 (n=273), determined by Log-rank Mantel-Cox test at P-value <0.0001, with Bonferroni correction. The overexpression of *Debcl*^{EY05743} results in a median lifespan of 68 days (n=331) much higher compared to control as determined by Log-rank Mantel-Cox test at P-value 0.0003; the inhibition of *Debcl* directed by the *Ddc-Gal4; UAS-Drp1* transgene result in the median lifespan of 72 (n=303); similar to control, determined by Log-rank Mantel-Cox test at p-value 0.021, with Bonferroni correction. B The GraphPad prism8 generated graph of the climbing abilities of *Ddc-Gal4 UAS-Drp1* flies with the expression of *Buffy, Buffy-RNAi, Debcl*^{EY05743}, *Debcl-RNAi*^{v47515} and control. The

climbing abilities of flies overexpressing *Buffy* have rescued compared to control as determined in the climbing curve's non-linear fitting by a 95% confidence interval ($p<0.0001$). The climbing ability of the flies has further diminished through the expression of *UAS-Buffy-RNAi* and *UAS-Debcl*^{EY05743} as determined in the non-linear fitting of the climbing curve by a 95% confidence interval at a p-value 0.0004 and 0.0002 respectively (n=50). The climbing abilities of flies expressing *Debcl-RNAi*^{v47515}has rescued compared to control as determined by the non-linear fitting of the climbing curve by a 95% confidence interval (p value<0.0001). The graph of longevity assay was generated by GraphPad prism8 non-linear regression curve.

Discussion

The protein product of the *Drp1* gene is involved in the processes of mitochondrial fission, apoptosis, and mitophagy along with the participation of other mitochondrial protection proteins. In humans, the protein kinase PKA phosphorylates and inactivates the pro-apoptotic Bcl-2 family protein Bad (Virdee et al. 2000) and the mitochondrial fission protein Drp1 (Cereghetti et al. 2008) in a complex effort to promote cell survival. The co-expression of *Drp1-RNAi* along with *Drp1* overexpression in flies has resulted in the phenotypes that are similar to the control and suggests that these phenotypes are primarily due the changes in expression of Drp1. I investigated the effect of the altered expression of *Buffy* and *Debcl* upon *Drp1*-induced phenotypes in the dopaminergic (DA) neurons. The Bcl-2 family proteins assist the pro-fission activity of Drp1 in apoptotic cells of worms and mammals (Rolland and Conradt 2010). However, in non-apoptotic cells of mammals, Bcl-2 family proteins have both pro-fission and pro-fusion activity (Rolland and Conradt 2010). The overexpression of *Drp1* in selected neurons along with *Buffy* overexpression or *Debcl* inhibition has resulted in a much-increased lifespan and climbing ability over-time. In supportive experiments, *Buffy* inhibition and *Debcl* overexpression resulted in a shortened lifespan and impaired climbing ability over-time. The conclusion that *Buffy* functions as the antithesis of *Debcl* (Quinn et al. 2003) is anticipated by the phenotype. The rescue of the *Drp1* expression phenotype is in accordance with the role of Buffy as the guardian of mitochondria. As proteins, Buffy interacts with Debcl to inhibit Debcl-induced cell death (Quinn et al. 2003). At a molecular level, this could be due to the decrease in the activity of the Debcl protein, which cooperates with Drp1 to promote cell death (Clavier et al. 2015). The plausible interpretation is that a decrease in the pro-apoptotic signal helps to rescue the apoptotic phenotype generated by the overexpression of *Drp1*.

The involvement of the anti-apoptotic Bcl-2 family protein is an important aspect of mitochondrial protection. The pro-apoptotic Bcl-2 family protein assists in the permeabilization of the mitochondrial outer membrane to release proteins of the IMS, such as Cyt-c and AIF, into the cytosol, in turn to, initiate apoptosis (Green and Kroemer 2004). The pro-apoptotic Debcl protein acts to induces apoptosis through a caspase-independent mechanism that triggers the release of Cyt-C (Zhang et al. 2000) in a manner similar to activity of Drp1 (Oettinghaus et al. 2016). The overexpression of *Debcl* and *Drp1* together in selected neurons does not alter the phenotype generated by overexpression of *Drp1* without *Debcl*. This is not surprising as Drp1 and Debcl functions seem to cooperate to promote apoptosis (Clavier et al. 2015). Indeed, this and earlier studies have demonstrated that Drp1 can play various roles in mitochondrial fragmentation and apoptosis, to act in concert with anti- and pro-survival proteins, dependent upon the stimuli.

The directed inhibition of *Drp1* in a subset of neurons in *Drosophila melanogaster* results in an age-dependent loss in climbing ability, a phenotype strongly associated with the modelling of PD in flies. Like other genes with pro-survival characteristics, *Buffy* overexpression or *Debcl* inhibition seems to confer survival advantage by the restriction of the activity of cell death-promoting molecules. However, the overexpression of *Buffy* in neurons that co-express *Drp1-RNAi* led to a decrease in the median lifespan accompanied with a rescue of the impaired locomotor ability. The recovery in the age-dependent climbing ability over time may be evidence of a complicated regulatory relationship. The inhibition of *Drp1* in selected neurons with pro-survival *Buffy* reduced the climbing ability. A study shows *Drp1* inhibition reduces the total accumulation of pro-apoptotic

Bcl-2 protein, Bax, on mitochondria outer membrane in HeLa cell lines (Maes et al. 2019). This intermediate phenotype was not expected but may be important in the determination of the pathology of neurological diseases (Leuchter et al. 2014; Civelek and Lusis 2014). The overexpression of *Buffy* or inhibition of *Debcl* may have reduced further the mitochondrial fragmentation and the *Debcl*-induced apoptosis to a level that the consequence is a decrease in median lifespan. The inhibition of anti-apoptotic *Buffy* or overexpression of pro-apoptotic *Debcl* enhanced the loss of *Drp1*-induced phenotype. The interaction of Bax with Drp1 in mammals seems to evolve from the Debcl and Drp1 protein interactions during evolution. Drp1 protein interacts directly and indirectly with Bcl-2 family protein to facilitate MOMP in apoptotic cells (Rolland and Conradt 2010). Overall, I believe that I have established that anti-apoptotic activity of *Buffy* confers survival advantage to flies overexpressing *Drp1* and provides a partially rescued intermediate phenotype in flies with a loss of *Drp1* function.

	Genotype	Median Lifespan	Lifespan Increased/ Decreased	Climbing Increase/ Decrease
Control	*Ddc-Gal4$^{4.3D;}$ UAS-Drp1; UAS-lacZ*	58 days		
Experiment	*Ddc-Gal4$^{4.3D;}$ UAS-Drp1; UAS-Buffy*	68 days	Increased	Increased
	Ddc-Gal4$^{4.3D;}$ UAS-Drp1; UAS-Buffy-RNAi	52 days	Decreased	Decreased
	Ddc-Gal4$^{4.3D;}$ UAS-Drp1; UAS- Debcl^{EY05743}	60 days	Similar to control	Similar to control
	Ddc-Gal4$^{4.3D;}$ UAS-Drp1; UAS- Debcl-RNAi^{v47515}	66 days	Increased	Increased
Control	*Ddc-Gal4$^{4.3D;}$ UAS-Drp1-RNAi; UAS-lacZ*	70 days		
Experiment	*Ddc-Gal4$^{4.3D;}$ UAS-Drp1-RNAi; UAS-Buffy*	64 days	Decreased	Increased
	Ddc-Gal4$^{4.3D;}$ UAS-Drp1-RNAi; UAS-Buffy-RNAi	62 days	Decreased	Decreased
	Ddc-Gal4$^{4.3D;}$ UAS-Drp1-RNAi; UAS-Debcl^{EY05743}	68 days	Similar to control	Decreased
	Ddc-Gal4$^{4.3D;}$ UAS-Drp1-RNAi; UAS-Debcl-RNAi^{v47515}	72 days	Similar to control	Increased

Table 3.1 Summary of the Result. The effect of the altered expression of *Buffy* and *Debcl* genes directed by *Ddc-Gal4$^{4.3D}$ UAS-Drp1* and *Ddc-Gal4$^{4.3D}$ UAS-Drp1-RNAi* transgene on median lifespan and climbing ability of the critical class male flies. The Cells with blue highlight denote control; Orange highlight denotes the decreased compared to control; Green highlights denote the increase compared to control, and yellow highlights denote the resulting longevity and climbing ability is very similar to control.

Conclusions

Recent studies have recognized *Drp1* as a PD-candidate gene, *Drp1* seems to be associated with an increased risk of the disease (Filichia et al. 2016; Fan et al. 2019). My studies demonstrate that the overexpression and inhibition of the *Drp1* activity in selected neurons can phenocopy the PD-like symptoms in Drosophila and, therefore, may represent a novel model of PD. Importantly, the decrease in lifespan and age-dependent loss in climbing ability observed with overexpression of *Drp1* in flies is rescued either by overexpression of *Buffy* or by *Debcl* inhibition. The age-dependent loss of climbing ability in flies expressing *Drp1-RNAi* can be rescued by *Buffy* overexpression or *Debcl-RNAi*-directed inhibition. Future studies of these interactions will be required to chart out a pathway for *Drp1* and *Bcl-2* protein regulation in Drosophila and, importantly, the molecular changes associated with the loss-of-function of these proteins in the development and function of DA neurons.

Bibliography

Cereghetti, G.M., Stangherlin, A., Martins De Brito, O., Chang, C.R., Blackstone, C., Bernardi, P., and Scorrano, L. 2008. Dephosphorylation by calcineurin regulates translocation of Drp1 to mitochondria. Proc. Natl. Acad. Sci. U. S. A. **105**(41): 15803–15808. doi:10.1073/pnas.0808249105.

Chang, C.-R., and Blackstone, C. 2007a. Cyclic AMP-dependent Protein Kinase Phosphorylation of Drp1 Regulates Its GTPase Activity and Mitochondrial Morphology. J. Biol. Chem. **282**(30): 21583–21587. doi:10.1074/jbc.C700083200.

Chang, C.-R., and Blackstone, C. 2007b. Drp1 phosphorylation and mitochondrial regulation. EMBO Rep. **8**(12): 1088–9; author reply 1089-90. European Molecular Biology Organization. doi:10.1038/sj.embor.7401118.

Chittenden, T. 2002, September 1. BH3 domains: Intracellular death-ligands critical for initiating apoptosis. Cell Press. doi:10.1016/S1535-6108(02)00128-9.

Civelek, M., and Lusis, A.J. 2014, January 3. Systems genetics approaches to understand complex traits. Nature Publishing Group. doi:10.1038/nrg3575.

Clavier, A., Ruby, V., Rincheval-Arnold, A., Mignotte, B., and Guénal, I. 2015. The Drosophila retinoblastoma protein, Rbf1, induces a Debcl- and Drp1-dependent mitochondrial apoptosis. J. Cell Sci. **128**(17): 3239–49. The Company of Biologists Ltd. doi:10.1242/jcs.169896.

Cribbs, J.T., and Strack, S. 2007. Reversible phosphorylation of Drp1 by cyclic AMP-dependent protein kinase and calcineurin regulates mitochondrial fission and cell death. EMBO Rep. **8**(10): 939–44. European Molecular Biology Organization. doi:10.1038/sj.embor.7401062.

Estaquier, J., and Arnoult, D. 2007. Inhibiting Drp1-mediated mitochondrial fission selectively prevents the release of cytochrome c during apoptosis. Cell Death Differ. **14**(6): 1086–1094. Nature Publishing Group. doi:10.1038/sj.cdd.4402107.

Fan, R.Z., Guo, M., Luo, S., Cui, M., and Tieu, K. 2019. Exosome release and neuropathology induced by α-synuclein: New insights into protective mechanisms of Drp1 inhibition. Acta Neuropathol. Commun. **7**(1): 184. BioMed Central Ltd. doi:10.1186/s40478-019-0821-4.

Filichia, E., Hoffer, B., Qi, X., and Luo, Y. 2016. Inhibition of Drp1 mitochondrial translocation provides neural protection in dopaminergic system in a Parkinson's disease model induced by MPTP. Sci. Rep. **6**: 32656. Nature Publishing Group. doi:10.1038/srep32656.

Githure, P.M., and Staveley, B.E. 2016. Bcl-2 homologue Debcl enhances α-synuclein-induced phenotypes in Drosophila. PeerJ **2016**(9). PeerJ Inc. doi:10.7717/peerj.2461.

Gogvadze, V., Orrenius, S., and Zhivotovsky, B. 2006. Multiple pathways of cytochrome c release from mitochondria in apoptosis. Biochim. Biophys. Acta - Bioenerg. **1757**(5–6): 639–647. Elsevier. doi:10.1016/J.BBABIO.2006.03.016.

Green, D.R., and Kroemer, G. 2004. The pathophysiology of mitochondrial cell death. Science **305**(5684): 626–9. American Association for the Advancement of Science. doi:10.1126/science.1099320.

He, B., Lu, N., and Zhou, Z. 2009, December. Cellular and nuclear degradation during apoptosis. NIH Public Access. doi:10.1016/j.ceb.2009.08.008.

Ikeda, Y., Shirakabe, A., Maejima, Y., Zhai, P., Sciarretta, S., Toli, J., Nomura, M., Mihara, K., Egashira, K., Ohishi, M., Abdellatif, M., and Sadoshima, J. 2015. Endogenous Drp1 mediates mitochondrial autophagy and protects the heart against energy stress. Circ. Res. **116**(2): 264–

78. American Heart Association, Inc. doi:10.1161/CIRCRESAHA.116.303356.
Ingerman, E., Perkins, E.M., Marino, M., Mears, J.A., McCaffery, J.M., Hinshaw, J.E., and Nunnari, J. 2005. Dnm1 forms spirals that are structurally tailored to fit mitochondria. J. Cell Biol. 170(7): 1021–7. Rockefeller University Press. doi:10.1083/jcb.200506078.
Karbowski, M., Lee, Y.-J., Gaume, B., Jeong, S.-Y., Frank, S., Nechushtan, A., Santel, A., Fuller, M., Smith, C.L., and Youle, R.J. 2002. Spatial and temporal association of Bax with mitochondrial fission sites, Drp1, and Mfn2 during apoptosis. J. Cell Biol. 159(6): 931–8. The Rockefeller University Press. doi:10.1083/jcb.200209124.
Lee, S., Jeong, S.Y., Lim, W.C., Kim, S., Park, Y.Y., Sun, X., Youle, R.J., and Cho, H. 2007. Mitochondrial fission and fusion mediators, hFis1 and OPA1, modulate cellular senescence. J. Biol. Chem. 282(31): 22977–22983. doi:10.1074/jbc.M700679200.
Leuchter, A.F., Hunter, A.M., Krantz, D.E., and Cook, I.A. 2014. Intermediate phenotypes and biomarkers of treatment outcome in major depressive disorder. Dialogues Clin. Neurosci. 16(4): 525–537. Les Laboratoires Seriver. Available from www.brain.ucla.edu. [accessed 17 October 2020].
Liu, Z., Wild, C., Ding, Y., Ye, N., Chen, H., Wold, E.A., and Zhou, J. 2016, June 1. BH4 domain of Bcl-2 as a novel target for cancer therapy. Elsevier Ltd. doi:10.1016/j.drudis.2015.11.008.
Maes, M.E., Grosser, J.A., Fehrman, R.L., Schlamp, C.L., and Nickells, R.W. 2019. Completion of BAX recruitment correlates with mitochondrial fission during apoptosis. Sci. Rep. 9(1). Nature Publishing Group. doi:10.1038/s41598-019-53049-w.
Marie Hardwick, J., and Soane, L. 2013. Multiple functions of BCL-2 family proteins. Cold Spring Harb. Perspect. Biol. doi:10.1101/cshperspect.a008722.
Milani, M., Beckett, A.J., Al-Zebeeby, A., Luo, X., Prior, I.A., Cohen, G.M., and Varadarajan, S. 2019. DRP-1 functions independently of mitochondrial structural perturbations to facilitate BH3 mimetic-mediated apoptosis. Cell Death Discov. 5: 117. doi:10.1038/s41420-019-0199-x.
Oettinghaus, B., D'Alonzo, D., Barbieri, E., Restelli, L.M., Savoia, C., Licci, M., Tolnay, M., Frank, S., and Scorrano, L. 2016. DRP1-dependent apoptotic mitochondrial fission occurs independently of BAX, BAK and APAF1 to amplify cell death by BID and oxidative stress. Biochim. Biophys. Acta - Bioenerg. 1857(8): 1267–1276. doi:10.1016/j.bbabio.2016.03.016.
Quinn, L., Coombe, M., Mills, K., Daish, T., Colussi, P., Kumar, S., and Richardson, H. 2003. Buffy, a Drosophila Bcl-2 protein, has anti-apoptotic and cell cycle inhibitory functions. EMBO J. 22(14): 3568–79. European Molecular Biology Organization. doi:10.1093/emboj/cdg355.
Rolland, S.G., and Conradt, B. 2010, December. New role of the BCL2 family of proteins in the regulation of mitochondrial dynamics. NIH Public Access. doi:10.1016/j.ceb.2010.07.014.
Schmitt, K., Grimm, A., Dallmann, R., Oettinghaus, B., Restelli, L.M., Witzig, M., Ishihara, N., Mihara, K., Ripperger, J.A., Albrecht, U., Frank, S., Brown, S.A., and Eckert, A. 2018. Circadian Control of DRP1 Activity Regulates Mitochondrial Dynamics and Bioenergetics. Cell Metab. 27(3): 657-666.e5. Cell Press. doi:10.1016/j.cmet.2018.01.011.
Suen, D.F., Norris, K.L., and Youle, R.J. 2008, June 15. Mitochondrial dynamics and apoptosis. Cold Spring Harbor Laboratory Press. doi:10.1101/gad.1658508.
Todd, A., and Staveley, B. 2012. Expression of Pink1 with α-synuclein in the dopaminergic neurons of Drosophila leads to increases in both lifespan and healthspan. Genet. Mol. Res. 11(2): 1497–1502. doi:10.4238/2012.May.21.6.
Todd, A.M., and Staveley, B.E. 2004. Novel assay and analysis for measuring climbing ability in

Drosophila. Drosoph. Inf. Serv. 87: 101–108. Available from http://www.ou.edu/journals/dis/DIS87/4 - Techniques.pdf [accessed 6 October 2019].

Virdee, K., Parone, P.A., and Tolkovsky, A.M. 2000. Phosphorylation of the pro-apoptotic protein BAD on serine 155, a novel site, contributes to cell survival. Curr. Biol. 10(18): 1151–1154. Curr Biol. doi:10.1016/S0960-9822(00)00702-8.

Wang, P., Wang, P., Liu, B., Zhao, J., Pang, Q., Agrawal, S.G., Jia, L., and Liu, F.-T. 2015. Dynamin-related protein Drp1 is required for Bax translocation to mitochondria in response to irradiation-induced apoptosis. Oncotarget 6(26): 22598–612. Impact Journals, LLC. doi:10.18632/oncotarget.4200.

Wikstrom, J.D., Israeli, T., Bachar-Wikstrom, E., Swisa, A., Ariav, Y., Waiss, M., Kaganovich, D., Dor, Y., Cerasi, E., and Leibowitz, G. 2013. AMPK Regulates ER Morphology and Function in Stressed Pancreatic β-Cells via Phosphorylation of DRP1. Mol. Endocrinol. 27(10): 1706–1723. doi:10.1210/me.2013-1109.

Wu, S., Zhou, F., Zhang, Z., and Xing, D. 2011. Bax is essential for Drp1-mediated mitochondrial fission but not for mitochondrial outer membrane permeabilization caused by photodynamic therapy. J. Cell. Physiol. 226(2): 530–541. doi:10.1002/jcp.22362.

Zhang, H., Huang, Q., Ke, N., Matsuyama, S., Hammock, B., Godzik, A., and Reed, J.C. 2000. Drosophila Pro-apoptotic Bcl-2/Bax Homologue Reveals Evolutionary Conservation of Cell Death Mechanisms*. JBC Papers in Press. doi:10.1074/jbc.M002846200.

Chapter 4: The transcriptional regulator *Rbf* during healthy ageing in Drosophila: interactions with *park*in, *Buffy* and *Debcl*

Abstract

Mitochondrial health is maintained by mitochondrial proteins that counteract mitochondrial dysfunction caused by cellular stress due to the impairment of essential cellular pathways. The expression of Bcl-2 family genes, the ubiquitin ligase parkin and the transcription regulator Rbf/Rb has a significant role in mitochondrial and cellular survival. Under conditions of extreme cellular stress, mitochondria can act to promote apoptosis. The overexpression of Rbf in the dopaminergic neurons of Drosophila directed by Ddc-Gal4 can result in flies with a reduced median lifespan and impaired climbing ability over time: a novel Drosophila model of Parkinson Disease (PD). The inhibition of Rbf can lead to a premature reduction in locomotor ability compared to control. The overexpression of Rbf can rescue the neurodegenerative phenotypes induced due to the parkin loss of function. The expression of the pro-cell survival Bcl-2 family member Buffy and inhibition of the anti-apoptotic Debcl can rescue the longevity and impaired locomotor ability over time observed in the Rbf-RNAi induced model of PD. Overall, the alteration of expression of Rbf in selected neurons can produce a novel model of PD in Drosophila; the directed expression of Buffy can protect to counteract the Rbf-RNAi induced deficits in lifespan and climbing ability.

Introduction

Mitochondria is crucial in aerobic respiration and signalling processes. Poorly functioning mitochondria can contribute to a range of different pathologies, including AD, PD and other age-related neurodegenerative diseases (Perier and Vila 2012). The health of the mitochondrial population is dependent upon crucial cellular processes. Cells utilize a variety of diverse mechanisms to upkeep a healthy and efficient mitochondrial network, such as the mitochondrial unfolded protein response (UPRmt), Ubiquitin Proteasome System, mitophagy and other aspects of mitochondrial dynamics (Chan 2012; Jovaisaite et al. 2014; Sugiura et al. 2014). The protein

parkin is a key regulator of the ubiquitin-proteasome system and mitophagy; besides, its mutant variants are responsible for some familial forms of PD. The Parkin protein is a part of an E3 ubiquitin ligase complex that functions to target protein and organelles for degradation (Yoshii et al. 2011; Bingol and Sheng 2016). The loss of *parkin* gene activity is a common cause in the pathology of Parkinson disease. Loss of function of *parkin* can lead to the accumulation of substrates, such as Cyclin E, and the upregulation of the Akt pathway. Cyclin E phosphorylates the retinoblastoma (Rb) tumour suppressor protein, which then causes the release of the transcription factor E2F-1 (Höglinger et al. 2007; Feng et al. 2015). The unencumbered E2F-1 can trigger apoptosis in post-mitotic neurons, which is essentially the same as the death of dopaminergic (DA) neurons in PD patients (Höglinger et al. 2007; Feng et al. 2015). The Rb protein is a crucial regulator of cellular proliferation and apoptosis.

The well-studied nuclear function of the Rb protein is transcriptional regulation via E2F1. The overexpression or inhibition of the *Rb* homologue in mice throughout development can have catastrophic effects that include lethality (Vooijs and Berns 1999; Lipinski and Jacks 1999). Interestingly, the recent examination of endogenous Rb protein activity has established that it has direct interactions with mitochondria as the Rb protein: can localize to near the mitochondrial surface; induce the MOMP; bind with the Bcl-2 family member Bax (*in vitro* and *in vivo*); induce apoptosis when in a form designed to be deficient of nuclear function and is targeted to mitochondria; suppress tumourigenesis (Hilgendorf et al. 2013). In Drosophila, Rbf, the orthologue of Rb, can decrease the transcription of anti-apoptotic Bcl-2 family protein *Buffy* (Clavier et al. 2014) and promote the interaction of Debcl, the sole Drosophila pro-apoptotic Bcl-2 family protein

and Drp1, to promote apoptosis via JNK pathway by induction of the production of ROS (Clavier et al. 2015). Drp1 protein has a central role in mitochondrial quality control and mitochondrial apoptosis (Sebastián et al. 2017; Favaro et al. 2019). Altered forms of the Rb protein cause the cells to be sensitized with a predilection towards apoptosis (Ariss et al. 2018). The molecular mechanisms by which Rb/Rbf protein functions are under investigation.

The role of the Bcl-2 family proteins in the protection of the mitochondria is very well established. However, little is known about the contribution of *Rbf* to mitochondrial health. Here I propose that the phenotypes associated with the altered expression of *Rbf* are due to excessive apoptosis and can be rescued by the appropriate regulation of this process. I employed *Drosophila melanogaster* as a model organism to study the phenotypic effects of the interactions of these genes. In my experiments, I exploited the *UAS-Gal4* system to direct the expression and inhibition of the *Rbf* gene in selected neuronal tissues by *Ddc-Gal4* and, in supportive experiments, in the developing eye tissue via the *GMR-Gal4* transgenes. In our experiment the expression and inhibition of *Rbf* have led to toxic effects, compromised lifespan and the diminishment of the ability to climb overtime. Interestingly, the toxic effects of *Rbf* overexpression can act to rescue the toxic consequences of *parkin* inhibition. The toxic effects of *Rbf* inhibition can be rescued by the expression of the anti-apoptotic Bcl-2 family protein gene, *Buffy.*

Materials and Methods

Bioinformatic analysis

The *H. sapiens* and *D. melanogaster* protein sequences were obtained from the National Center of Biotechnology Information (NCBI) protein database *(https://www.ncbi.nlm.nih.gov/protein/)*. The conserved domains were identified through the use of the Eukaryotic Linear Motif *(http://elm.eu.org/)* and NCBI Conserved Domain Database *(https://www.ncbi.nlm.nih.gov/cdd/)*. Multiple sequence alignment was accomplished via the Clustal Omega on-line tool *(https://www.ebi.ac.uk/Tools/msa/clustalo/)* to reveal the conservation of domains. The nuclear localization signal was predicted with cNLS Mapper (*http://nls-mapper.iab.keio.ac.jp/cgi-bin/NLS_Mapper_form.cgi*) (Kosugi et al. 2009). The phosphorylation sites were identified using: KinasePhos (*http://kinasephos.mbc.nctu.edu.tw/index.php*) it computationally predicts phosphorylation site using HMM (Huang et al. 2005); PhosphositePlus (*https://www.phosphosite.org/homeAction*) and Eukaryotic Linear Motif (ELM) *(*http://elm.eu.org*/)*, it is a comprehensive information tool to study post-translational modifications (Hornbeck et al. 2015). The phosphorylation site found conserved between *D. melanogaster,* and *H. sapiens* were highlighted.

Drosophila stocks and media

The *GMR-Gal4^{12}*; *Ddc-Gal4$^{4.3D}$(w[1118]; P{w[+mC]=Ddc-GAL4.L}4.3D); UAS-lacZ$^{4-1-2;}$* the *UAS-Rbf1 (w[*]; P{w[+mC]=UAS-Rbf.D}II*); the *UAS-Rbf RNAi1^{HMS03004} (y[1] sc[*] v[1] sev[21]; P{y[+t7.7] v[+t1.8]=TRiP.HMS03004}attP2/TM3, Sb[1]);* the *UAS-Rbf RNAi2^{GL01293} (y[1] sc[*] v[1] sev[21]; P{y[+t7.7] v[+t1.8]=TRiP.GL01293}attP40)*; the *UAS-Buffy (w[*]; P{w[+mC]=UAS-Buffy.S}E1); UAS-Buffy-RNAi (w[*]; P{w[+mC]=UAS-Buffy.RNAi}3);* and *UAS-Debcl (y[1] w[67c23]; P{y[+mDint2] w[+mC]=EPgy2}Debcl[EY05743])*; stocks were obtained from Bloomington Drosophila Stock

Center at Indiana University, Bloomington, Indiana, USA. The UAS-Debcl-RNAi^{v47515} (w1118; P{GD 1637}v47515) stock were obtained from Vienna Drosophila Resource Center. The *UAS-parkin-RNAi* line was obtained from Dr. B. Lu (Yang et al. 2003, 2006). The *Ddc-Gal4 UAS-parkin-RNAi* and *Ddc-Gal4 UAS-Rbf-RNAi^{HMS03004}* transgene lines were produced through standard methods (Githure and Staveley 2016). All flies were maintained on standard cornmeal/molasses/yeast/agar media treated with propionic acid and methylparaben for fungal resistance. Stocks were maintained at room temperature of 22° ± 3° C, whereas crosses and experiments were kept at 25°C.

Survival assay

Several crosses of virgin females and males were made, and a cohort of critical class males collected upon eclosion Male progeny of critical class was collected from mating until approximately 250 flies of each genotype were obtained. The flies were maintained in cohorts of 25 or less per vial on standard media, to avoid over-crowding. Flies were scored every second day for viability and were transferred to new food every two to five days. The tally continued until all flies were observed to be dead (Todd and Staveley 2004, 2012). Longevity data were analyzed using GraphPad Prism version 8 statistical software (*graphpad.com*), and the Mantel-Cox test compared survival curves. Significance was determined at a 95% confidence level ($P \leq 0.05$) with Bonferroni correction.

Locomotor analysis

Approximately 70 male flies of the critical class were collected over 24 hours from the crosses similar to survival assay and maintained as cohorts of 10 flies in each vial. The media was changed twice a week. The climbing assay was performed as previously described according to a standard

protocol (Todd and Staveley 2004, 2012). Every week 50 males were assayed, in groups of 10, for their ability to climb a glass tube divided into five levels of 2 cm each. The climbing index was calculated for each week using GraphPad prism version 8 statistical software. The climbing curve was fitted using non-linear regression and determined at a 95% confidence interval ($P \leq 0.05$).

Biometric analysis of the *Drosophila melanogaster* eye

Female virgins of the *GMR-Gal4* genotype were collected every 8 to 12 hours for several days. The confirmed virgins were then crossed with the males of the following genotypes: *UAS-lacZ*, *UAS-Rbf1*, *UAS-Rbf2, UAS-Rbf-RNAi1* and *UAS-Rbf-RNAi2*. Critical class male progeny was collected from each genotype. The collected flies were kept as cohorts of 10 flies or less in each vial upon fresh media. Flies were allowed to age for three to four days and then frozen at -80°C. The flies were prepared for scanning electron microscopy following the standard protocol (Githure and Staveley 2017). Ommatidia and interommatidial bristle counts were performed on ten or more flies of each genotype using the National Institute of Health (NIH) ImageJ software. The Biometric analysis was performed using GraphPad Prism version 8 statistical software. Significance was determined at a 95% confidence level ($P \leq 0.05$) using unpaired t-test.

Result

Rbf is conserved between H. sapiens and D. melanogaster

The *D. melanogaster Rbf* (CAA65661.1) and the *H. sapiens,* retinoblastoma-like protein 1 (NP_899662.1) protein sequence were sourced from the NCBI protein database and the conserved sequences were identified using NCBI CDD. The multiple sequence alignment of the two proteins derived by Clustal Omega (Figure 1A) shows a highly conserved domain of the unknown function

(DUF3452), an RB-A and RB-B domain. The conserved phosphorylation sites identified using KinasePhos, PhosphoSitePlus and ELM and listed in Table1. Towards the amino-terminus region, a nuclear localization signal has been identified using cNLS Mapper and re-confirmed by Eukaryotic Linear Motif (ELM), which localized NLS in the overlapping region. The cNLS score of the sequence was 6.5, proteins with scores as high as 8, 9 and 10 are exclusively localized in nucleus; proteins with scores 1 and 2 are solely localized in the cytoplasm, and in-between scores are supposedly co-localized in nucleus and cytoplasm depending on their scores. As the amino acid sequence of these proteins is highly conserved, the cellular functions are likely to be nearly identical.

Phosphorylation site *D. melanogaster* /*H. sapiens*	Amino acid	Kinase	Identified using
85/74	Threonine	CK1	ELM
674/879	Tyrosine	EGFR	KinasePhos
700/938	Threonine	INSR	KInasePhos
742/980	Threonine/Serine	PKC and PKA	KinasePhos
749/988	Serine	CDK2	PhosphoSitePlus (Zhou et al. 2013)
771/1009	Serine	cdc2 and CDK2	KinasePhos; PhosphoSitePlus (Leng et al. 2002)

Table 4.1: List of the phosphorylation site found conserved between the Rbf/Rb protein sequence of *Homo sapiens* and *Drosophila melanogaster*. The phosphorylation sites were identified using KinasePhos and PhosphoSitePlus and ELM resources. The KinasePhos computationally predict the phosphorylation site using HMM. The PhosphoSitePlus is a comprehensive information resource to study and document post-translational modifications. The ELM scans user-submitted protein sequence and matches corresponding sequences could be false positive. The kinases found or predicted to do the phosphorylation are listed with the respective phosphorylation site.

Figure 4.1: Rbf/Rb evolutionarily is conserved between *D. melanogaster* and *H. sapiens*. Clustal Omega multiple sequence alignment of *D. melanogaster* Rbf (CAA65661.1) protein with the *H. sapiens* (NP_899662.1) shows evolutionarily conserved domains identified using the NCBI Conserved Domain Database (CDD) and further confirmed by the Eukaryotic Linear Motif (ELM) resource. The conserved domains, Nuclear localization Signals and phosphorylation sites found conserved between the two proteins are highlighted in different colours. The asterisks indicate the identical residues; the colons indicate the conserved substitutions; the dots indicate the semi-conserved substitutions. Colour differences indicate the chemical nature of amino acids: red indicates small hydrophobic (includes aromatic) residues; blue indicates acidic; magenta indicates basic; green indicates basic with hydroxyl or amine groups.

Alteration of the expression of *Rbf* with *Ddc-Gal4*

The directed expression and inhibition of *Rbf1* by the *Ddc-Gal4* transgene result in decreased lifespan compared to the control (Figure 4.2A). The overexpression of *Rbf* resulted in median lifespans of 42 days in 311 flies, which is significantly less than control. The inhibition of *Rbf* by two distinct RNAi transgenes, via the *UAS-Rbf-RNAi1* and *UAS-Rbf-RNAi2,* results in a reduced median lifespan of approximately 56 days in 250 flies compared to 68 days observed in control (Figure 2A) as determined by log-rank (Mantel-Cox) test at a P-value at <0.0001. The climbing ability of flies with altered *Rbf* expression is severely compromised as determined in the non-linear fitting of the climbing curve by 95% confidence interval (Figure 4.2B).

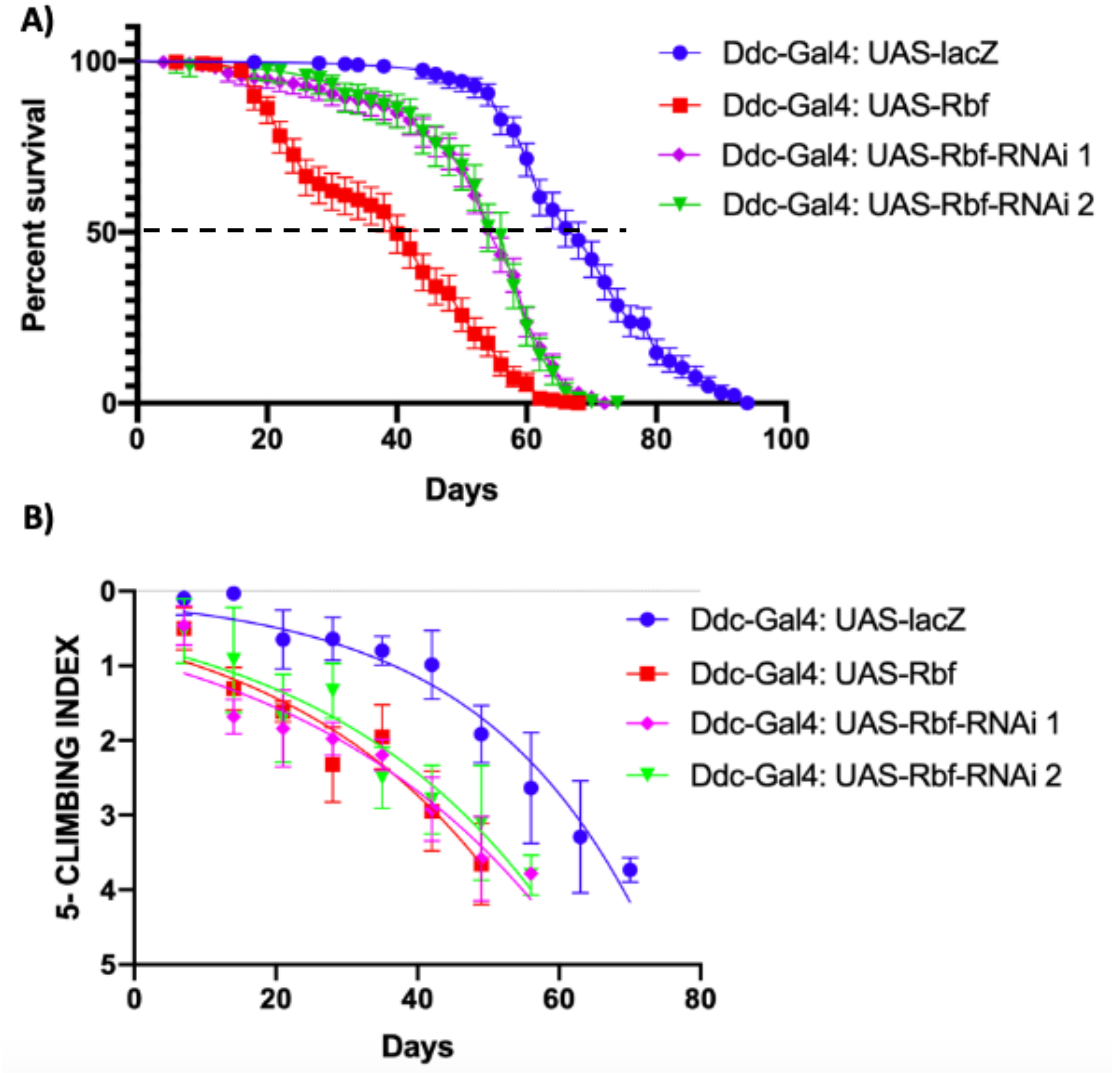

Figure 4.2: Altered *Rbf* expression under the control of *Ddc-Gal4$^{4.3D}$* influences the survival and climbing ability of flies. A). The GraphPad prism8 generated graph of the longevity assay for the directed expression of *Rbf, Rbf RNAi's* under the control of *Ddc-Gal4$^{4.3D}$* transgene. The overexpression results in decreased median lifespan of 40 days compared to 68 days of control calculated by the Log-rank Mantel-Cox test, with Bonferroni correction. The inhibition of *Rbf* under the control of the *Ddc-Gal4* transgene results in a decreased lifespan of 56 days with *UAS-Rbf-RNAi1*^{HMS03004} and *UAS-Rbf-RNAi2*^{GL01293} compares to 68 days of control done by Log-rank Mantel-Cox test, with Bonferroni correction. **B)**. The GraphPad prism8 generated graph of the climbing abilities of flies with overexpression of *Rbf, Rbf RNAi's* and control. The climbing ability of *Rbf* overexpression and *Rbf RNAi's* flies is significantly compromised compared to control as determined in the non-linear fitting of the climbing curve by a 95% confidence interval.

The directed expression of *Rbf* by the *Ddc-Gal4* transgene results in a decreased lifespan of 252 flies to 50 days compared to 68 days observed in control. The *Ddc-Gal4 UAS-Rbf-RNAi UAS-lacZ* critical class males have a lifespan of 60 days. The overexpression of *Rbf* in the *Ddc-Gal4 UAS-Rbf-RNAi* transgene has a median lifespan of 72 days in 272 flies, similar to 68 days of control done by Log-rank Mantel-Cox test, with Bonferroni correction (Figure 4.3A) as determined by log-rank (Mantel-Cox) test at a P value at <0.0001. The comparison of the climbing ability of flies shows an intermediate phenotype when *Rbf* is overexpressed along with *Rbf-RNAi*^{HMS03004} as determined in the non-linear fitting of the climbing curve by 95% confidence interval (Figure 4.3B).

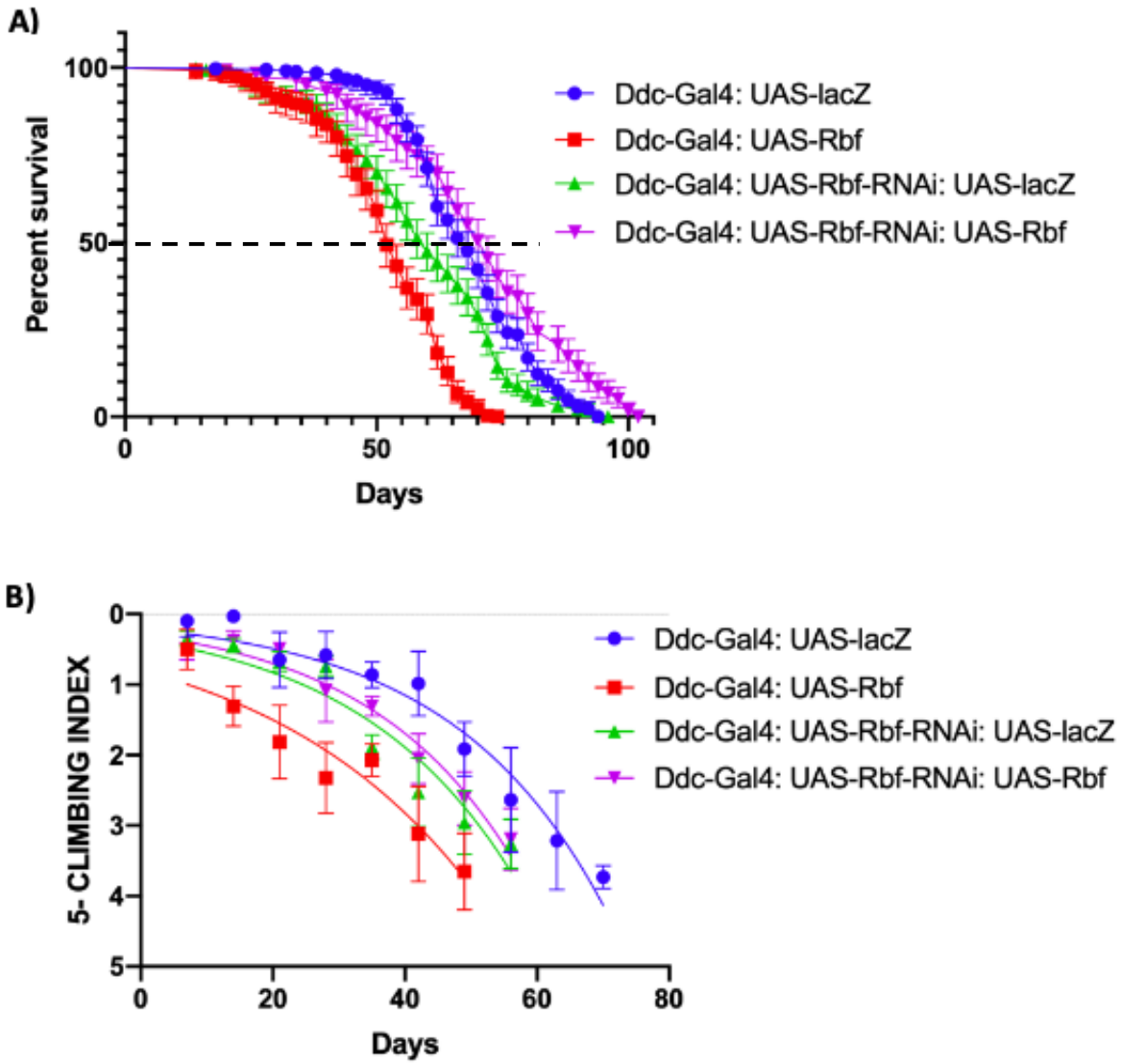

Figure 4.3: Directed co-expression of *Rbf* and *Rbf-RNAi* rescues diminished median lifespan A) The graph of longevity assay generated by GraphPad prism8 in *Ddc-Gal4/ UAS-lacZ; Ddc-Gal4/ UAS-Rbf; Ddc-Gal4 UAS-Rbf-RN ^{HMS03004}/ UAS-lacZ;* and *Ddc-Gal4* median *UAS-Rbf-RNAi^{HMS03004}/ UAS-Rbf*. The overexpression of *Rbf* resulted in a decreased lifespan of 50, and inhibition of *Rbf* resulted in a decreased lifespan of 60 days compared to 68 days of control done by the Log-rank Mantel-Cox test, with Bonferroni correction. The overexpression of *Rbf* in neurons using *Ddc-Gal4 Rbf-RNAi*^{HMS03004} transgene results in a lifespan of 72 days, similar to 68 days of control done by Log-rank Mantel-Cox test, with Bonferroni correction. **B)** The GraphPad prism8 generated graph of the climbing abilities of flies with expression *Rbf, Rbf-RNAi^{HMS03004}/lacZ, Rbf-RNAi^{HMS03004}/Rbf* and control. There is an intermediate phenotype when *Rbf* is overexpressed along with *Rbf-RNAi^{HMS03004}*, as determined in the non-linear fitting of the climbing curve by a 95% confidence interval.

The altered expression of *Rbf* influences the *Ddc-Gal4 Gal4$^{4.3D}$ UAS-parkin-RNAi* model of PD

The loss of function of the parkin has led to the establishment of several Drosophila models of PD. The *Ddc-Gal4 UAS-parkin-RNAi UAS-lacZ* critical males have a median lifespan of 60 days in 256 flies. Overexpression of *Rbf* in the *Ddc-Gal4 UAS-parkin-RNAi* expressing flies results in a much-increased median life span of 72 days (n=283) compared to the control, as determined by log-rank (Mantel-Cox) test at a P value at <0.0001. The *UAS-Rbf-RNAi1* transgene when expressed along with *UAS-parkin-RNAi* transgene, result in median lifespan of 50 (n=328) days much less compared to control flies (P-value=<0.0001) (Figure 4.4A). The *UAS-Rbf-RNAi2* transgene when expressed along with *Ddc-Gal4 parkin-RNAi*, results in a median life span of 58 days (n=308) (Figure 4.4A) similar to 60 days of control, as determined by log-rank (Mantel-Cox) test at a P-value at 0.8425. The overexpression of *Rbf* by *Ddc-Gal4* along with *parkin-RNAi* slightly ameliorates the decline in climbing ability over time. However, the locomotor activity of the critical classes with the directed expression of the *UAS-Rbf-RNAi* transgenes are decreased compared to control as determined in the non-linear fitting of the climbing curve by 95% confidence interval (Figure 4.4B).

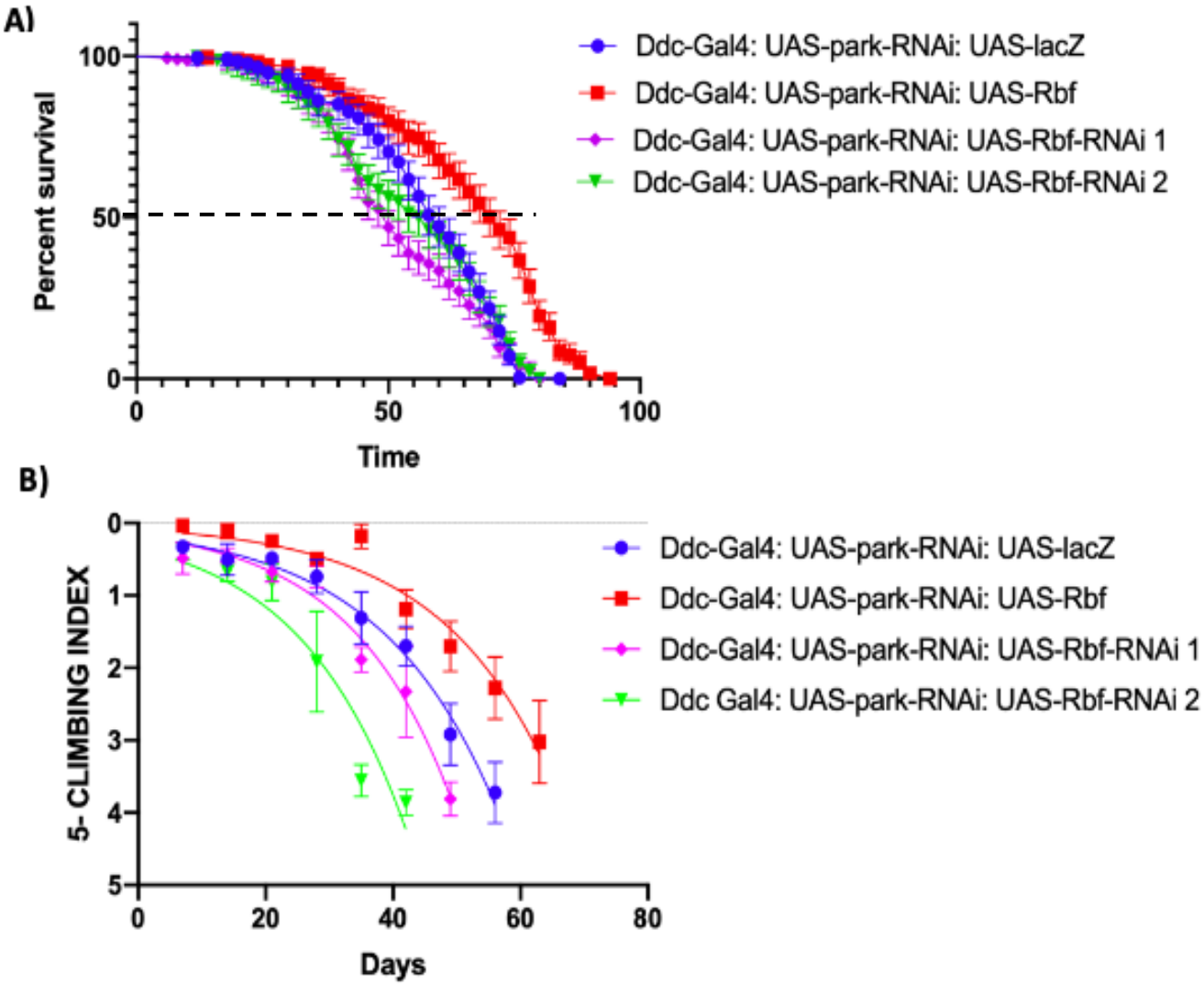

Figure 4.4: Altered expression of *Rbf* can enhance and suppress the *Ddc-Gal4 UAS-parkin-RNAi* model of PD. A. The graph of longevity assay generated by GraphPad prism8 with altered expression of *Rbf* in *Ddc-Gal4 parkin-RNAi* expressing flies. The overexpression of *Rbf* results in a median lifespan of 72 days compare to 60 days of control *(lacZ/parkin-RNAi*); the inhibition of *Rbf* by two distinct RNAi transgenes, via *UAS- Rbf-RNAi1*^{HMS03004} and *UAS-Rbf-RNAi2*^{GL01293} directed by the *Ddc-Gal4* transgene, result in the median lifespan of 50 and 58 days, respectively; similar to control, determined by Log-rank Mantel-Cox test, with Bonferroni correction. **B.** The GraphPad prism8 generated graph of the climbing abilities of *Ddc-Gal4 parkin-RNAi* flies with the expression of *Rbf, Rbf RNAi's* and control. The climbing ability of flies overexpressing *Rbf* have significantly increased compared to control as determined in the non-linear fitting of the climbing curve by a 95% confidence interval.

The altered co-expression of *Buffy* with *Rbf-RNAi* via *Ddc-Gal4*$^{4.3D}$

The loss of function of *Rbf* leads to compromised lifespan and climbing ability over time. The control *Ddc-Gal4; UAS-Rbf-RNAi; UAS-lacZ* critical class males have a median lifespan of 58 days (n=351). Overexpression of *Buffy* in the *Ddc-Gal4; UAS-Rbf-RNAi; UAS-Buffy* flies have a median lifespan of 88 days in 392 flies (P-value=<0.0001), which is significantly greater when compared to the controls. The inhibition of *Buffy* in the *Ddc-Gal4; UAS-Rbf-RNAi; UAS-Buffy-RNAi* critical class male flies have a median lifespan of 58 days in 275 flies which is very similar to the control (Figure 4.5A) as determined by log-rank (Mantel-Cox) test at a P value at 0.0007. The overexpression of *Buffy* in *Ddc-Gal4; UAS-Rbf-RNAi; UAS-Buffy flies* rescue the climbing ability defects over time. The inhibition of *Buffy* increases the loss of climbing ability throughout the life of critical class flies as determined in the non-linear fitting of the climbing curve by 95% confidence interval (Figure 4.5B).

The altered co-expression of *Debcl with Rbf-RNAi* via *Ddc-Gal4*

The *Ddc-Gal4; UAS-Rbf-RNAi; UAS-lacZ* critical class males have been demonstrated to have a lifespan of 58 days in the sample size of 351 flies and compromised climbing ability. Overexpression of *Debcl* in the *Ddc-Gal4; UAS-Rbf-RNAi; UAS-Debcl* critical class flies have a median lifespan of 54 days in 317 flies (P-value=0.0093), which is not very different from the *lacZ*-expressing controls. The inhibition of *Debcl* in the *Ddc-Gal4 UAS-Rbf-RNAi*; *UAS-Debcl-RNAi* expressing flies have a median lifespan of 64 days in 288 sample size, which is increased compared to control flies (Figure 4.5A) as determined by log-rank (Mantel-Cox) test at a P value at <0.0001. The overexpression of *Debcl* by *Ddc-Gal4 UAS-Rbf-RNAi; UAS-Debcl* results in an increase in impairment of the climbing ability defect over time. The inhibition of *Debcl* ameliorates the defects

in climbing abilities as determined in the non-linear fitting of the climbing curve by 95% confidence interval at a P-value= 0.0220 (Figure 4.5B).

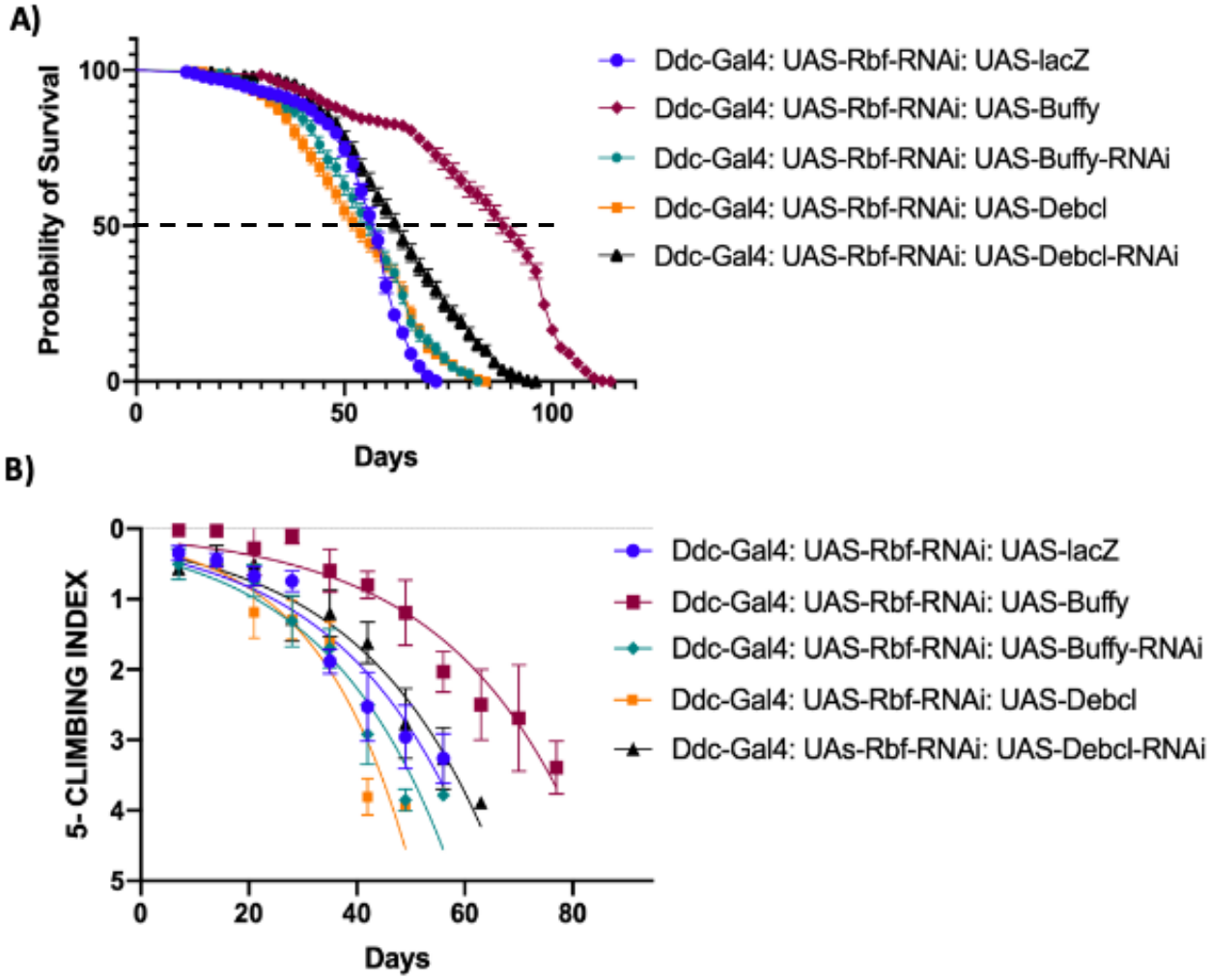

Figure 4.5: Altered expression of *Buffy* and *Debcl,* can suppress the *Ddc-Gal4$^{4.3D}$ UAS-Rbf-RNAi^{HMS03004}* potential model of PD. A. The graph of longevity assay generated by GraphPad prism8 with altered expression of *Buffy* and *Debcl* in *Ddc-Gal4 Rbf-RNAi^{HMS03004}* expressing flies. The overexpression of *Buffy* results in a median lifespan of 96 days compare to 58 days of control *(lacZ/Rbf-RNAi^{HMS03004}*); the inhibition of *Buffy* result in the median lifespan of 58 days similar to control, determined by Log-rank Mantel-Cox test, with Bonferroni correction. The overexpression of *Debcl^{EY05743}* in neurons using *Ddc-Gal4* transgene along with *Rbf-RNAi^{HMS03004}* results in a lifespan of 54 days similar to control and inhibition of *Debcl ^{EY05743}* resulted in the increased lifespan of 64 days compared to 58 days of control done by Log-rank Mantel-Cox test, with Bonferroni correction. **B.** The GraphPad prism8 generated graph of the climbing abilities of *Ddc-Gal4 Rbf-RNAi^{HMS03004}* flies with the expression of *Buffy, Buffy RNAi, Debcl ^{EY05743}, Debcl RNAi ^{v47515}* and control. The climbing abilities of *Buffy* flies have significantly increased compared to control as determined in the non-linear fitting of the climbing curve by a 95% confidence interval.

The overexpression and inhibition of *Rbf* during eye development

In complementary experiments, the inhibition and overexpression of *Rbf,* directed by the *GMR-Gal4* transgene in the neuron-rich developing eye of flies' influences development. The numbers of ommatidia are decreased with either overexpression or inhibition lines of *Rbf* analyzed in 15 flies of each group. The ommatidia count of *Rbf*, *Rbf-RNAi1*^{HMS03004} and *Rbf-RNAi2*^{GL01293} is 610, 664.2 and 670.6, respectively, compared to 704.4 for the *lacZ* control flies as shown in Figure 4.6B as determined by unpaired t-test with P values of 0.0198, 0.0677 and 0.8151. The mean of interommatidial bristle produced through inhibition by the *UAS-Rbf-RNAi1* and *UAS-Rbf-RNAi2* transgene was lower at 500.6 (P-value= 0.0320) and 498.1 (P-value=0.0.0296) compare to 536 of control flies as determined by an unpaired t-test. The mean number of interommatidial bristles for *UAS-Rbf* flies was 494.9 less compared to 536 of control, as determined by an unpaired t-test (P-value= 0.0.0128). The decrease in the interommatidial bristle number is consistent with the reduction of ommatidial numbers produced through overexpression and inhibition by the *Rbf and Rbf-RNAi* bearing transgenes compare to control (Figure 4.6B ii).

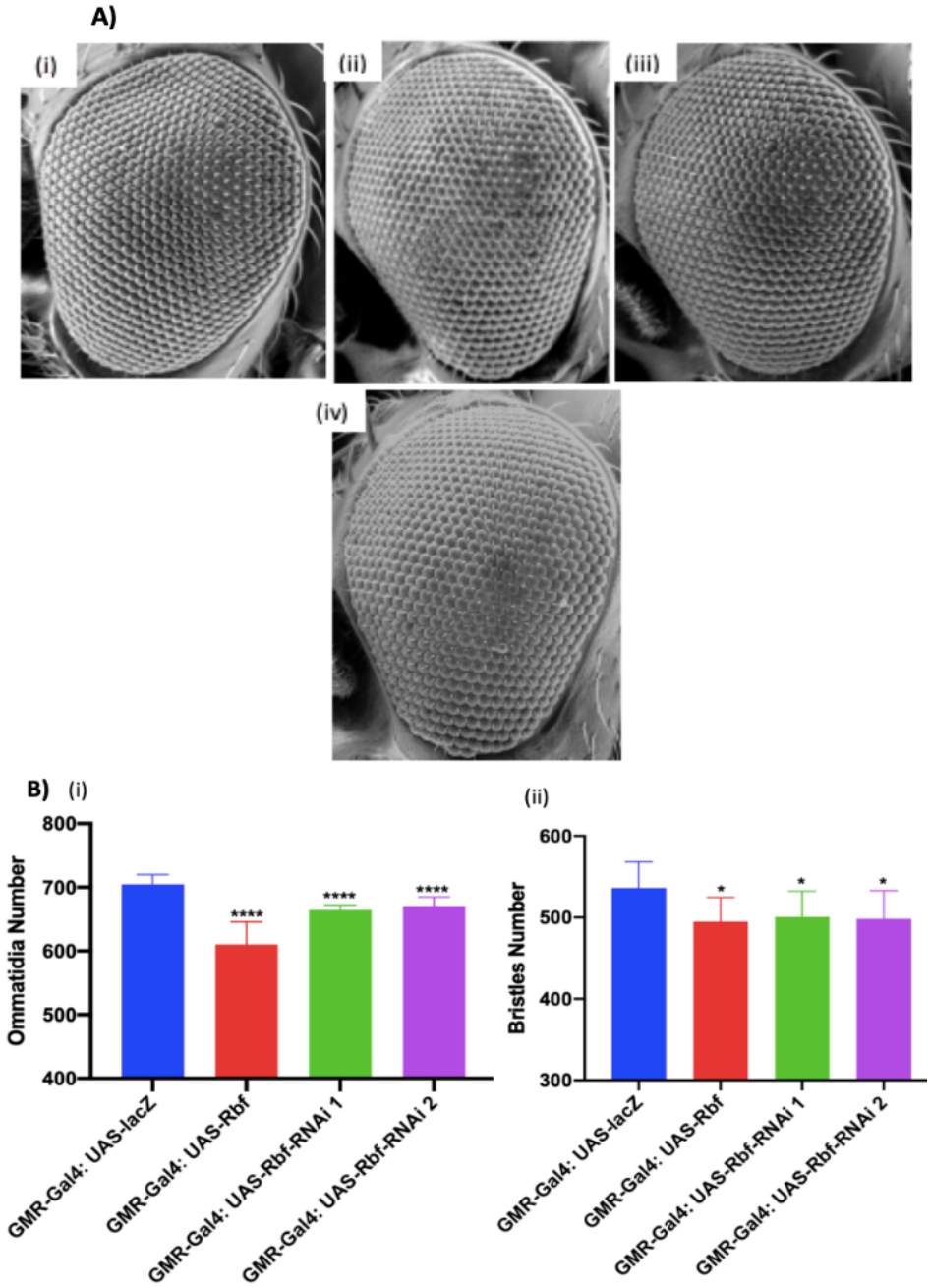

Figure 4.6: The phenotypic effects of altered *Rbf* expression in *D. melanogaster* eye. A. Scanning electron micrograph of the altered *Rbf* expression under the control of *GMR-Gal4* transgene. The genotypes are (a) *GMR-Gal4/UAS-lacZ* (Control); (b) *GMR-Gal4/UAS-Rbf*; (c) *GMR-Gal4/UAS-Rbf-RNAi1*^{HMS03004} (d) *GMR-Gal4/UAS-Rbf-RNAi2* ^{GL01293}. **B.** The ommatidia number for control is 704.4±15.4; the inhibition and expression of *Rbf* results in a decrease in ommatidial count compared to control. **C.** The interommatidial bristle count for the control is 536±32.5; the overexpression and RNAi inhibition lines (*GMR-Gal4 UAS-Rbf-RNAi1*^{HMS03004} and *GMR-Gal4 UAS-Rbf-RNAi2*^{GL01293}) results in a decrease interommatidial bristle count compared to control.

Discussion

The role of the protein products of the *Rbf/Rb* homologues is crucial. The *Rb* mutant mouse show reduced mitochondrial function from the TCA cycle to oxidative phosphorylation (Nicolay et al. 2015). The Rb protein is required for the activation of mitochondrial protein genes (Nicolay et al. 2015). Cells deficient in *Rb* are more sensitive to the damaging effects of ROS and require elevated levels of glutathione peroxidase to thrive (Nicolay et al. 2013). In my experiments, the flies with altered expression of *Rbf* display compromised longevity. The diminishment of the median lifespan of flies was more severe because of the overexpression of *Rbf* than with loss of function genotype. The cause could be due to the induction of apoptosis as observed with post-mitotic proliferating cells (Milet et al. 2010) or other consequences could be the overexpression of *pRb* acts to promote tumour progression (Shi et al. 2000). The differentiation defects due to loss of *pRb* can be rescued by normalizing mitochondrial activity with the help of PGC-1 alpha expression (Váraljai et al. 2015). The development of eyes compromised during *Rbf* overexpression, the eyes develop in a manner that reduces numbers of ommatidia and bristles as compared to control. Most likely, the overexpression of *Rbf* acts to promote apoptosis through transcription activation and regulation of the pro-apoptotic sub-cellular machinery. Interestingly novel results show *Rbf* overexpression rescues the *parkin*-inhibition phenotype. The *Rbf* induced protection could be due to its role in blocking the E2F1 transcription factor. Patients with PD demonstrate E2F1 activation in DA neurons and mediate neuronal death (Höglinger et al. 2007). Altering *Rbf* expression with parkin changes the dynamics of its phenotypic effects.

Here, I found that the inhibition of *Rbf* leads to consistently reduced longevity and loss of climbing ability phenotypes that, unexpectedly, are milder than those generated by the gain of *Rbf* function.

The *Rbf/Rb* mutants promote transcription of apoptosis genes in an *E2F1* dependent manner in eukaryotes (Moon et al. 2006; Milet et al. 2014). The inactivation of Rb protein allows E2F1 dependent transcription of pro-apoptotic genes, including *Apaf-1/PUMA* (Polager and Ginsberg 2009). Interestingly, *Rb* can contribute to neuronal apoptosis, both dependently and independently of E2F1 transcription activity (Andrusiak et al. 2012). The inhibition and overexpression phenotypes associated with *Rbf/Rb* is likely due to excessive apoptosis furthered through distinct sets of mechanisms.

The role of *Rbf* in transcription is well studied; however, the full understanding of a largely non-nuclear role of *Rbf*/*Rb* is limited. Research have established that endogenous *Rb* enhances *TNF-alpha* induced apoptosis. The function of Rb is dependent on a pro-apoptotic Bcl-2 family protein, Bax, which regulates mitochondrial intrinsic apoptosis (Hilgendorf et al. 2013). When the overexpression of the pro-apoptotic Bcl-2 family member, *Debcl*, was directed along with the inhibition of *Rbf1*, both the median lifespan and climbing ability over the life of the flies were severely compromised. However, the defects generated by the inhibition of *Rbf* was rescued by overexpression of the anti-apoptotic Bcl-2 family protein, *Buffy*. It is unclear if the rescue of the phenotype is due to the inactivation of the E2F1 apoptotic activity or a distinct anti-apoptotic activity of Buffy. The endogenous role of *Rb/Rbf* seems to promote apoptosis in non-mitotic cells with the help of Bcl-2 family protein. The nuclear role of regulating transcriptional factor E2F1 is very complex. However, the overall effect is dependent on the result of different pathways regulated by endogenous and nuclear Rbf protein. In my experiments, the inhibition of *Rbf* is beneficial when combined with overexpression of anti-apoptotic Bcl-2 protein.

	Genotype	Median lifespan	Lifespan Increased/ Decreased	Climbing Increase/ Decrease
Control	*Ddc-Gal$^{4.3D;}$ UAS-lac Z*	68 days		
Experiment	*Ddc-Gal$^{4.3D;}$ UAS-Rbf*	40 days	Decreased	Decreased
	Ddc-Gal$^{4.3D;}$ UAS-Rbf-RNAi1^{HMS03004}	56 days	Decreased	Decreased
	Ddc-Gal$^{4.3D;}$ UAS-Rbf-RNAi2 ^{GL01293}	56 days	Decreased	Decreased
Control	*Ddc-Gal$^{4.3D;}$ UAS-park-RNAi; lacZ*	60 days		
Experiment	*Ddc-Gal$^{4.3D;}$ UAS-park-RNAi; UAS-Rbf*	72 days	Increased	Increase
	Ddc-Gal$^{4.3D;}$ UAS-park-RNAi; UAS-Rbf-RNAi1^{HMS03004}	50 days	Decreased	Decreased
	Ddc-Gal$^{4.3D;}$ UAS-park-RNAi; UAS-Rbf-RNAi2 ^{GL01293}	58 days	Similar to control	Decreased
Control	*Ddc-Gal$^{4.3D;}$ UAS-Rbf-RNAi; UAS- lacZ*	58 days		
Experiment	*Ddc-Gal$^{4.3D;}$ UAS-Rbf-RNAi; UAS-Buffy*	89 days	Increased	Increased
	Ddc-Gal$^{4.3D;}$ UAS-Rbf-RNAi; UAS-Buffy-RNAi	58 days	Similar to control	Decreased
	Ddc-Gal$^{4.3D;}$ UAS-Rbf-RNAi; UAS-Debcl^{EY05743}	54 days	Similar to control	Decreased
	Ddc-Gal$^{4.3D;}$ UAS-Rbf-RNAi; UAS-Debcl-RNAi^{v47515}	64 days	Increased	Increased

Table 4.2: Summary of the Results. The effect of the directed expression of *UAS-Rbf* and *UAS-Rbf-RNAi* in the *Ddc-Gal4$^{4.3D}$* and *Ddc-Gal$^{4.3D;}$ UAS-parkin-RNAi* transgene on the median lifespan and climbing ability of the critical class male flies. The effect of the altered expression of *Buffy* and *Debcl* genes directed by *Ddc-Gal4$^{4.3D}$ UAS-Rbf-RNAi transgene* on median lifespan and climbing ability of the critical class male flies. The Cells with blue highlight denote control; Orange highlight denotes the decreased compared to control; Green highlights denote the increase compare to control and yellow highlights denote the resulting longevity and climbing ability is very similar to control.

Conclusion

The function of *Rbf* is mainly nuclear, but a small fraction of the protein tends to localize near mitochondria in the cytoplasm. The overexpression of *Rbf* gene in neurons results in reduced survival and an age-dependent decline in locomotor ability. The knockdown of *Rbf* in the *Ddc-Gal4* transgenes of Drosophila results in an age-dependent loss in locomotor function, phenotypes that are strongly associated with neuronal degeneration and Parkinson disease. Thus, the compromised climbing abilities in flies with directed inhibition of *Rbf* have produced a novel model of Parkinson Disease and can be used to investigate further the mechanisms underlying PD and other neurodegenerative diseases. The overexpression of *Rbf* rescue the *parkin* inhibition phenotype; the Rbf and parkin protein products may activate similar downstream targets for cell survival. Similarly, the anti-apoptotic *Bcl-2* proteins rescued the PD phenotypes induced by *Rbf* inhibition. Further studies are required to understand better the interaction between *parkin, Bcl-2* family members, and *Rbf* in these neurons. Overall, these experiments allow us to contribute to the understanding of mitochondrial health and enhanced conditions of homeostasis.

Bibliography

Andrusiak, M.G., Vandenbosch, R., Park, D.S., and Slack, R.S. 2012. The retinoblastoma protein is essential for survival of postmitotic neurons. J. Neurosci. **32**(42): 14809–14814. doi:10.1523/JNEUROSCI.1912-12.2012.

Ariss, M.M., Islam, A.B.M.M.K., Critcher, M., Zappia, M.P., and Frolov, M. V. 2018. Single cell RNA-sequencing identifies a metabolic aspect of apoptosis in Rbf mutant. Nat. Commun. **9**(1). Nature Publishing Group. doi:10.1038/s41467-018-07540-z.

Bingol, B., and Sheng, M. 2016. Mechanisms of mitophagy: PINK1, Parkin, USP30 and beyond. Free Radic. Biol. Med. **100**: 210–222. doi:10.1016/j.freeradbiomed.2016.04.015.

Chan, D.C. 2012. Fusion and Fission: Interlinked Processes Critical for Mitochondrial Health. Annu. Rev. Genet. **46**(1): 265–287. doi:10.1146/annurev-genet-110410-132529.

Clavier, A., Baillet, A., Rincheval-Arnold, A., Coléno-Costes, A., Lasbleiz, C., Mignotte, B., and Guénal, I. 2014. The pro-apoptotic activity of Drosophila Rbf1 involves dE2F2-dependent downregulation of diap1 and buffy mRNA. Cell Death Dis. **5**(9). Nature Publishing Group. doi:10.1038/cddis.2014.372.

Clavier, A., Ruby, V., Rincheval-Arnold, A., Mignotte, B., and Guénal, I. 2015. The Drosophila retinoblastoma protein, Rbf1, induces a Debcl- and Drp1-dependent mitochondrial apoptosis. J. Cell Sci. **128**(17): 3239–49. The Company of Biologists Ltd. doi:10.1242/jcs.169896.

Favaro, G., Romanello, V., Varanita, T., Andrea Desbats, M., Morbidoni, V., Tezze, C., Albiero, M., Canato, M., Gherardi, G., De Stefani, D., Mammucari, C., Blaauw, B., Boncompagni, S., Protasi, F., Reggiani, C., Scorrano, L., Salviati, L., and Sandri, M. 2019. DRP1-mediated mitochondrial shape controls calcium homeostasis and muscle mass. Nat. Commun. **10**(1): 2576. Nature Publishing Group. doi:10.1038/s41467-019-10226-9.

Feng, D.D., Cai, W., and Chen, X. 2015, October 26. The associations between Parkinson's disease and cancer: The plot thickens. BioMed Central Ltd. doi:10.1186/s40035-015-0043-z.

Githure, P.M., and Staveley, B.E. 2016. Bcl-2 homologue Debcl enhances α-synuclein-induced phenotypes in Drosophila. PeerJ **2016**(9). PeerJ Inc. doi:10.7717/peerj.2461.

Githure, P.M., and Staveley, B.E. 2017. Overexpression of Buffy enhances the loss of parkin and suppresses the loss of Pink1 phenotypes in Drosophila. Genome **60**(3): 241–247. NRC Research Press. doi:10.1139/gen-2016-0165.

Hilgendorf, K.I., Leshchiner, E.S., Nedelcu, S., Maynard, M.A., Calo, E., Ianari, A., Walensky, L.D., and Lees, J.A. 2013. The retinoblastoma protein induces apoptosis directly at the mitochondria. Genes Dev. **27**(9): 1003–1015. Cold Spring Harbor Laboratory Press. doi:10.1101/gad.211326.112.

Höglinger, G.U., Breunig, J.J., Depboylu, C., Rouaux, C., Michel, P.P., Alvarez-Fischer, D., Boutillier, A.L., DeGregori, J., Oertel, W.H., Rakic, P., Hirsch, E.C., and Hunot, S. 2007. The pRb/E2F cell-cycle pathway mediates cell death in Parkinson's disease. Proc. Natl. Acad. Sci. U. S. A. **104**(9): 3585–3590. National Academy of Sciences. doi:10.1073/pnas.0611671104.

Hou, S.T., Cowan, E., Walker, T., Ohan, N., Dove, M., Rasqinha, I., and MacManus, J.P. 2001. The transcription factor E2F1 promotes dopamine-evoked neuronal apoptosis by a mechanism independent of transcriptional activation. J. Neurochem. **78**(2): 287–297. doi:10.1046/j.1471-4159.2001.00402.x.

Huang, H.-D., Lee, T.-Y., Tzeng, S.-W., and Horng, J.-T. 2005. KinasePhos: a web tool for identifying

protein kinase-specific phosphorylation sites. Nucleic Acids Res. **33**(Web Server issue): W226-9. doi:10.1093/nar/gki471.

Jovaisaite, V., Mouchiroud, L., and Auwerx, J. 2014. The mitochondrial unfolded protein response, a conserved stress response pathway with implications in health and disease. J. Exp. Biol. **217**(Pt 1): 137–43. Company of Biologists. doi:10.1242/jeb.090738.

Kosugi, S., Hasebe, M., Tomita, M., and Yanagawa, H. 2009. Systematic identification of cell cycle-dependent yeast nucleocytoplasmic shuttling proteins by prediction of composite motifs. Proc. Natl. Acad. Sci. U. S. A. **106**(25): 10171–10176. National Academy of Sciences. doi:10.1073/pnas.0900604106.

Leng, X., Noble, M., Adams, P.D., Qin, J., and Harper, J.W. 2002. Reversal of Growth Suppression by p107 via Direct Phosphorylation by Cyclin D1/Cyclin-Dependent Kinase 4. Mol. Cell. Biol. **22**(7): 2242–2254. American Society for Microbiology. doi:10.1128/mcb.22.7.2242-2254.2002.

Lipinski, M.M., and Jacks, T. 1999, December 20. The retinoblastoma gene family in differentiation and development. Nature Publishing Group. doi:10.1038/sj.onc.1203244.

Milet, C., Rincheval-Arnold, A., Mignotte, B., and Guénal, I. 2010. The Drosophila retinoblastoma protein induces apoptosis in proliferating but not in post-mitotic cells. Cell Cycle **9**(1): 97–103. Taylor and Francis Inc. doi:10.4161/cc.9.1.10251.

Milet, C., Rincheval-Arnold, A., Moriéras, A., Clavier, A., Garrigue, A., Mignotte, B., and Guénal, I. 2014. Mutating RBF Can Enhance Its Pro-Apoptotic Activity and Uncovers a New Role in Tissue Homeostasis. PLoS One **9**(8): e102902. Public Library of Science. doi:10.1371/journal.pone.0102902.

Moon, N.-S., Di Stefano, L., and Dyson, N. 2006. A Gradient of Epidermal Growth Factor Receptor Signalling Determines the Sensitivity of rbf1 Mutant Cells to E2F-Dependent Apoptosis. Mol. Cell. Biol. **26**(20): 7601–7615. American Society for Microbiology. doi:10.1128/mcb.00836-06.

Nicolay, B.N., Danielian, P.S., Kottakis, F., Lapek, J.D., Sanidas, I., Miles, W.O., Dehnad, M., Tschöp, K., Gierut, J.J., Manning, A.L., Morris, R., Haigis, K., Bardeesy, N., Lees, J.A., Haas, W., and Dyson, N.J. 2015. Proteomic analysis of pRb loss highlights a signature of decreased mitochondrial oxidative phosphorylation. Genes Dev. **29**(17): 1875–1889. Cold Spring Harbor Laboratory Press. doi:10.1101/gad.264127.115.

Nicolay, B.N., Gameiro, P.A., Tschöp, K., Korenjak, M., Heilmann, A.M., Asara, J.M., Stephanopoulos, G., Iliopoulos, O., and Dyson, N.J. 2013. Loss of RBF1 changes glutamine catabolism. Genes Dev. **27**(2): 182–196. Cold Spring Harbor Laboratory Press. doi:10.1101/gad.206227.112.

Perier, C., and Vila, M. 2012. Mitochondrial biology and Parkinson's disease. Cold Spring Harb. Perspect. Med. **2**(2): a009332. Cold Spring Harbor Laboratory Press. doi:10.1101/cshperspect.a009332.

Peter V. Hornbeck, Bin Zhang, B.M., Jon M. Kornhauser, Vaughan Latham, and Elzbieta Skrzypek. 2015. PhosphoSitePlus, 2014: mutations, PTMs and recalibrations. Available from https://www.ncbi.nlm.nih.gov/pmc/articles/PMC4383998/ [accessed 11 March 2020].

Polager, S., and Ginsberg, D. 2009. p53 and E2f: partners in life and death. doi:10.1038/nrc2718.

Sebastián, D., Palacín, M., and Zorzano, A. 2017. Mitochondrial Dynamics: Coupling Mitochondrial Fitness with Healthyageing. Trends Mol. Med. **23**(3): 201–215. Elsevier Current Trends.

doi:10.1016/J.MOLMED.2017.01.003.
Shi, Y.Z., Hui, A.M., Li, X., Takayama, T., and Makuuchi, M. 2000. Overexpression of retinoblastoma protein predicts decreased survival and correlates with loss of p16INK4 protein in gallbladder carcinomas. Clin. Cancer Res. **6**(10): 4096–100. Available from http://www.ncbi.nlm.nih.gov/pubmed/11051262 [accessed 9 March 2020].
Sugiura, A., McLelland, G.-L., Fon, E.A., and McBride, H.M. 2014. A new pathway for mitochondrial quality control: mitochondrial-derived vesicles. EMBO J. **33**(19): 2142–56. European Molecular Biology Organization. doi:10.15252/embj.201488104.
Todd, A., and Staveley, B. 2012. Expression of Pink1 with α-synuclein in the dopaminergic neurons of Drosophila leads to increases in both lifespan and healthspan. Genet. Mol. Res. **11**(2): 1497–1502. doi:10.4238/2012.May.21.6.
Todd, A.M., and Staveley, B.E. 2004. Novel assay and analysis for measuring climbing ability in Drosophila. Drosoph. Inf. Serv. **87**: 101–108. Available from http://www.ou.edu/journals/dis/DIS87/4 - Techniques.pdf [accessed 6 October 2019].
Váraljai, R., Islam, A.B.M.M.K., Beshiri, M.L., Rehman, J., Lopez-Bigas, N., and Benevolenskaya, E. V. 2015. Increased mitochondrial function downstream from KDM5a histone demethylase rescues differentiation in pRB-deficient cells. Genes Dev. **29**(17): 1817–1834. Cold Spring Harbor Laboratory Press. doi:10.1101/gad.264036.115.
Vooijs, M., and Berns, A. 1999, September 20. Developmental defects and tumor predisposition in Rb mutant mice. doi:10.1038/sj.onc.1202999.
Yang, Y., Gehrke, S., Imai, Y., Huang, Z., Ouyang, Y., Wang, J.W., Yang, L., Beal, M.F., Vogel, H., and Lu, B. 2006. Mitochondrial pathology and muscle and dopaminergic neuron degeneration caused by inactivation of Drosophila Pink1 is rescued by Parkin. Proc. Natl. Acad. Sci. U. S. A. **103**(28): 10793–10798. doi:10.1073/pnas.0602493103.
Yang, Y., Nishimura, I., Imai, Y., Takahashi, R., and Lu, B. 2003. Parkin suppresses dopaminergic neuron-selective neurotoxicity induced by Pael-R in Drosophila. Neuron **37**(6): 911–924. Cell Press. doi:10.1016/S0896-6273(03)00143-0.
Yoshii, S.R., Kishi, C., Ishihara, N., and Mizushima, N. 2011. Parkin mediates proteasome-dependent protein degradation and rupture of the outer mitochondrial membrane. J. Biol. Chem. **286**(22): 19630–19640. J Biol Chem. doi:10.1074/jbc.M110.209338.
Zhou, H., Di Palma, S., Preisinger, C., Peng, M., Polat, A.N., Heck, A.J.R., and Mohammed, S. 2013. Toward a comprehensive characterization of a human cancer cell phosphoproteome. J. Proteome Res. **12**(1): 260–271. doi:10.1021/pr300630k.

Chapter 5: Rbf suppression of the phenotypes caused by *Drp1* gain of function in selected Drosophila neurons

A version of this chapter is submitted as: Hasan, A., and Staveley, B.E. 2021.

Abstract

Well known for its tumour-suppression transcriptional regulation activities, the Rb protein is a transcriptional regulator that plays a crucial role in cell-cycle regulation and apoptosis. In the past decade, research has established a cytosolic role and mitochondrial localization for this protein: Retinoblastoma protein seems to cooperate with Drp1 to regulate mitochondrial quality in a transcription-independent manner. Control of mitochondrial quality is vital for the assurance of cell survival, and the failure of this may result in mitochondrial dysfunction and, eventually, cell death. Here, the *UAS-Gal4* expression system was exploited to direct expression in neurons and achieved with the *Ddc-Gal4* transgene. Alteration of the expression of *Drp1* in neuronal populations of cells that include DA under the control of the *Ddc-Gal4* transgene produces a robust PD model with a severely reduced lifespan and locomotor dysfunction. The *Drp1* overexpression induced phenotypes are significantly suppressed when the Drosophila homologue of *Rbf* is overexpressed in these neurons. When *Drp1-RNAi* is expressed along with *Rbf*, this resulted in a similar increase in median lifespan coupled with a compromised locomotor ability. The *Rbf* overexpression suppresses both the *Drp1* overexpression and inhibition longevity phenotypes, to suggest a direct regulatory relationship between *Rbf* and *Drp1.* The inhibition of *Rbf* does not have a great effect upon the flies that overexpress or inhibit *Drp1*. Intriguingly, inhibition of the mitochondrial fission gene *Drp1* can act to rescue the longevity and impaired locomotor ability over time observed in the *Rbf-RNAi* induced model of PD. The *Rbf* overexpression may provide a survival advantage to the cells subjected to unregulated apoptotic stimuli.

Introduction

The retinoblastoma (*Rb/Rbf*) gene encodes a tumour suppressor protein that acts as a crucial transcriptional regulator of cell proliferation and apoptosis. The *Rb* gene was first identified as

tumour suppressor protein-encoding gene and was named so as mutant forms of the gene cause formation of a retinal cancer: retinoblastoma (Wen-Hwa et al. 1987). Since the initial discovery, the loss of function of *Rb*/*Rbf* has been linked to numerous types of human cancers (Linn et al. 2021; Du and Searle 2012). In humans, the Rb protein can bind to the E2F transcription factor and then act to suppress the transcription of the *cyclin* and *CDK* genes (Futatsugi et al. 2012). The *Rb/Rbf* activity predominantly depends on its phosphorylation status (Dyson 2016). Once, the inactivation of the Rb/Rbf protein was thought to be due to the inactivation of its catalytic site, but recent evidence found the movement of Rb from the nucleus to the cytoplasm can suppress its activity (Jiao et al. 2006, 2008). Further studies focused upon the cellular localization of Rb protein and found a fraction localizes in mitochondria regardless of the cell types – abnormal or not (Ferecatu et al. 2009). The Rb protein detected in mitochondria has been determined to suppress apoptosis in a manner that is independent of transcriptional regulator activity (Ferecatu et al. 2009; Hilgendorf et al. 2013). The Rb protein has been shown to interact with the pro-apoptotic Bcl-2 family protein, Bax, *in vivo* and can activate Bax to promote apoptosis (Hilgendorf et al. 2013). Apart from nuclear activity, mitochondrial localization suggests the existence of a cytosolic or mitochondrial function for the Rbf protein in eukaryotes.

The regulation of mitochondrial-mediated apoptosis with pro-apoptotic Bcl-2 protein(s) and Drp1 seems well conserved between Drosophila and humans. The Rb protein is found to interact with the Drp1 in mediation of mitochondrial-dependent cell death as induced by cadmium in hepatocytes (Zhang et al. 2019). The inhibition of Drp1 acts to counteract cell death induced by the localization of the Rb protein to the mitochondrial surface induced by $CdCl_2$ (Zhang et al. 2019).

Drp1 protein has a major role in mitochondrial quality control and mitochondrial apoptosis (Sebastián et al. 2017; Favaro et al. 2019). The overexpression of *Rbf* gene triggers apoptosis through the activation of the JNK pathway in *Drosophila melanogaster* (Milet et al. 2014). This *Rbf*-induced apoptosis requires the presence of the pro-apoptotic Bcl-2 family protein, Debcl, and the mitochondrial fission protein, Drp1, and is dependent upon mitochondrial fragmentation (Clavier et al. 2015). *Rbf* can act to suppress the transcription of *Buffy*, the anti-apoptotic *Bcl-2* family gene (Clavier et al. 2014) which promotes the interaction between Drp1 and Debcl (the sole pro-apoptotic Bcl-2 protein in flies) to induce apoptosis (Clavier et al. 2015). In contrast to the consequences of the overexpression of *Rbf*, flies deficient for *Rbf* are sensitive to apoptosis due to the upregulation of the apoptotic gene *hid* (Ariss et al. 2018). The localization of the Rbf protein to, or near, the mitochondria suggest that an influence upon the function of the Drp1 protein is of particular interest.

The processes that contribute to mitochondrial quality control are not isolated signalling pathways and are a network of interconnected activities that share a collection of common intermediate components at several levels. The mechanisms that contribute to mitochondrial dynamics maintain the homeostasis of the cell and assist in the function of the mitochondrial network. The UPR^{mt} transcription factor can induce the transcription of *Drp1* during periods of stress to promote mitophagy or the controlled degradation of select mitochondria (Nargund et al. 2015). The Drp1 protein can promote apoptosis in *C. elegans*, *D. melanogaster* and cell cultures (Jagasia et al. 2005; Goyal et al. 2007). The Drp1 protein can promote apoptosis in Bcl-2 protein-dependent and independent manners (Cassidy-Stone et al. 2008; Oettinghaus et al. 2016). The activities related

to transcription of the Rb/Rbf protein such as the regulation of metabolic pathways, control of oxidative phosphorylation and mediation of mitochondrial functions through the control of the very important E2F transcription factor seems well conserved in eukaryotes (Dyson 2016). Many mitochondrial activities are vital for the survival of cells and the assurance of the quality of mitochondria, and the failure of these processes results in phenotypes characterized by the dysfunction of mitochondria and subsequent cell death.

Little is known about the contribution of *Rbf* towards mitochondrial health and neurodegeneration. As I have demonstrated, both the overexpression and inhibition of *Drp1* act to phenocopy PD-like phenotype in Drosophila, the anticipated role of the mitochondria in PD pathogenesis suggest that the *Drp1*-induced model of PD (chapter 2) an attractive model for investigation of the role of *Rbf*. I utilized the *Drosophila melanogaster* as a model organism to study the phenotypic effects of *Rbf* and *Drp1* gene interaction. I examined the effects of over expression and inhibition of the expression of transcription regulator *Rbf* in selected neurons along with modified expression of *Drp1*. I propose that the *Drp1*-induced phenotypes can be modified by alteration of the expression of *Rbf.*

Materials and Methods

Drosophila media and culture

All stocks were maintained on a standard media prepared from cornmeal/molasses/yeast/agar medium treated with propionic acid and methylparaben to resist fungal growth. Aliquots of media were poured into plastic vials, allowed to solidify, and refrigerated at 4°C until used. Stocks are

kept at room temperature while crosses and experiments were carried out at 25°C. The *UAS-Rbf RNAi1*^{HMS03004} (y[1] sc[*] v[1] sev[21]; P{y[+t7.7] v[+t1.8]=TRiP.HMS03004}attP2/TM3, Sb[1]); the *UAS-Rbf RNAi2*^{GL01293} *(y[1] sc[*] v[1] sev[21]; P{y[+t7.7] v[+t1.8]=TRiP.GL01293}attP40); UAS-Rbf (w[*]; P{w[+mC]=UAS-Rbf.D}III); UAS-Drp1 (y[1] w[*]; P{w[+mC]=FLAG-FlAsH-HA-Drp1}3, Ki[1]);* the *UAS-Drp1-RNAi1*^{JF02762} *(y[1] v[1]; P{y[+t7.7] v[+t1.8]=TRiP.JF02762}attP2}); UAS-Drp1-RNAi2*^{HMC03230} *(y[1] v[1]; P{y[+t7.7] v[+t1.8]=TRiP.HMC03230}attP40); Ddc-Gal4*$^{4.36}$*(w[1118]; P{w[+mC]=Ddc-Gal4.L}Lmpt[4.36];* and *UAS-lacZ* stocks were obtained from Bloomington Drosophila Stock Center at Indiana University, Bloomington, Indiana, USA. The *Ddc-Gal4/CyO; UAS-Drp1/TM3, Ddc-Gal4/CyO; UAS-Drp1-RNAi /TM3*; *Ddc-Gal4/CyO; UAS-Rbf-RNAi /TM3* derivative lines were generated through the use of standard recombination methods (Githure and Staveley 2016) and used to overexpress and inhibit *Drp1* and inhibit *Rbf* in the selected DA neurons by use of the *Ddc-Gal4*$^{4.3D}$ transgene.

Ageing assay

Several crosses of virgin females and males were made, and a cohort of critical class males collected upon eclosion. At least 250 flies were aged per genotype in the cohorts of 25 or less per vial on fresh media, replenished every two-five days to avoid crowding. Flies were observed and scored every second day for the presence of deceased adults. As a rule, flies were considered dead when movement was not observed upon agitation [40]. Longevity data were analyzed with GraphPad Prism version 8 statistical software, and the Mantel-Cox test compared survival curves. Significance was determined at a 95% confidence level ($P \leq 0.05$) with Bonferroni correction.

Climbing assay

The 70 male flies of the critical class were collected within 24 hours and maintained as ten flies in each vial. The food was changed twice every week. Every week 50 males of each genotype were assayed, in groups of 10, for their ability to climb a glass tube divided into five levels of 2 cm each according to the established protocol (Todd and Staveley 2004, 2012). The climbing index was calculated for each week using GraphPad prism version 8 statistical software. The climbing curve was fitted using non-linear regression and determined at a 95% confidence interval ($P \leq 0.05$).

Results

Alteration of the expression of *Rbf* along with *Drp1* directed by the *Ddc-Gal4$^{4.3D}$* transgene

The overexpression of *Drp1* leads to a compromised lifespan and diminished climbing ability over time. In these experiments, the control *Ddc-Gal4$^{4.3D}$ UAS-Drp1 UAS-lacZ* critical males were determined to have a median lifespan of 58 days (n=282). The overexpression of *Rbf* in the *Ddc-Gal4 UAS-Drp1* critical class flies results in much increased median life span of 74 days (n=294) compared to control with a P-value at <0.0001 as determined by log-rank (Mantel-Cox) test. The two *UAS-Rbf-RNAi* transgenes, *UAS-Rbf-RNAi1 ^{HMS03004}* and *UAS-Rbf-RNAi2^{GL01293}*, when expressed along with *Ddc-Gal4 UAS-Drp1*, results in a median life span of 56 (n=253) and 60 days (n=280) (Figure 5.1A) similar to control with a P-value at 0.0012 and 0.3854, respectively, as determined by log-rank (Mantel-Cox) test. The non-linear fit of the climbing curve shows overexpression of *Rbf* by *Ddc-Gal4 UAS-Drp1* rescues the decline in climbing ability compared to control at 95% CI with P-value < 0.0001. The non-linear fitting of the climbing curve shows inhibition of *Rbf* by *Ddc-Gal4 UAS-Drp1; UAS-Rbf-RNAi1 ^{HMS03004}* and *Ddc-Gal4 UAS-Drp1; UAS-Rbf-RNAi ^{GL01293}* is very similar to the control flies at 95% CI with P-value at 0.3012 and 1.762 respectively (Figure 5.1B) (n=50).

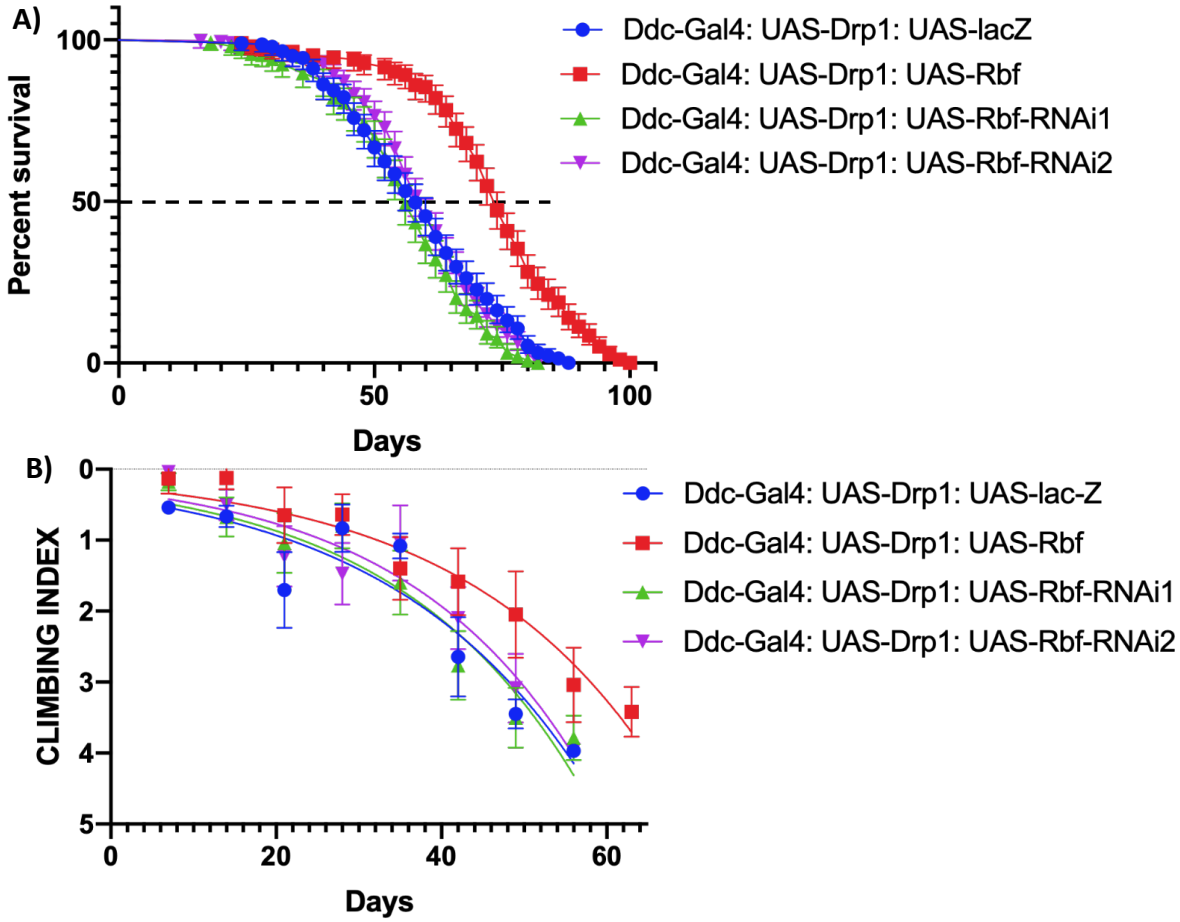

Figure 5.1: Altered expression of *Rbf* in the *Ddc-Gal4$^{4.3D}$ UAS-Drp1* model of PD. A. In the control, *Ddc-Gal4$^{4.3D}$ UAS-Drp1 UAS-lacZ* critical class males were determined to have a median life span of 58 days (n=282). The overexpression of *Rbf* along with *Drp1*, resulted in a median lifespan of 74 days (n=294), much higher than 58 days of control determined by the Log-rank Mantel-Cox test P-value of <0.0001, with Bonferroni correction. The inhibition of *Rbf* by two RNAi transgenes, *UAS-Rbf-RNAi1 ^{HMS03004}* and *UAS-Rbf-RNAi ^{GL01293}*, directed by the *Ddc-Gal4$^{4.3D}$* along with the *UAS-Drp1* transgene resulted in the median lifespans of 56 (n=266) and 60 days (n=263) similar to 58 days of control, determined by Log-rank Mantel-Cox test at P-value 0.0012 and 0.3854 respectively, with Bonferroni correction. The graph of longevity assay was generated by GraphPad prism8. **B.** The GraphPad prism8 generated a graph of the climbing abilities of *Ddc-Gal4 UAS-Drp1* flies that express *Rbf, Rbf-RNAi* and control. The abilities of flies that overexpress *Rbf* has improved compared to control as determined in the non-linear fitting of the climbing curve by a 95% confidence interval (p<0.0001). The abilities of flies expressing *UAS-Rbf-RNAi's* are very similar to control as determined in the non-linear fitting of the climbing curve by a 95% confidence interval with a p-value of 0.3012 and 1.762 (n=50). The graph of longevity assay was generated by GraphPad prism8 non-linear regression curve.

Alterion of the expression of *Rbf* along with *Drp1-RNAi* directed by *Ddc-Gal4*$^{4.3D}$

The *Ddc-Gal4*$^{4.3D}$ *UAS-Drp1-RNAi UAS-lacZ* critical males were determined to have a median lifespan of 70 days in 323 flies. Overexpression of *Rbf* in the *Ddc-Gal4 UAS-Drp1-RNAi* expressing flies results in the increased median life span of 74 days (n=275) compared to the control with a P-value of <0.0001 as determined by log-rank (Mantel-Cox) test. The two *UAS-Rbf-RNAi* transgenes, *UAS-Rbf-RNAi*^{HMS03004} and *UAS-Rbf-RNAi2*^{GL01293}, when expressed along with *Ddc-Gal4 UAS-Drp1-RNAi*, results in a median life span of 72 (n=253 flies) and 70 days (n=280 flies), respectively (Figure 5.2A) similar to control with P-value of 0.3679 and 1.1737 respectively, as determined by log-rank (Mantel-Cox) test. The non-linear fit of the climbing curve shows overexpression of *Rbf* by *Ddc-Gal4 UAS-Drp1-RNAi* further contributes to the loss of climbing ability throughout the life of critical class flies compared to control at 95% CI (P<0.0001). The non-linear fit of the climbing curve shows inhibition of *Rbf* by *Ddc-Gal4 UAS-Drp1; UAS-Rbf-RNAi1* ^{HMS03004} and *Ddc-Gal4 UAS-Drp1; UAS-Rbf-RNAi2* ^{GL01293} is very similar to the climbing ability of control flies at 95% CI with P-value at 0.0452 and 0.1229 respectively (Figure 5.2B) (n=50).

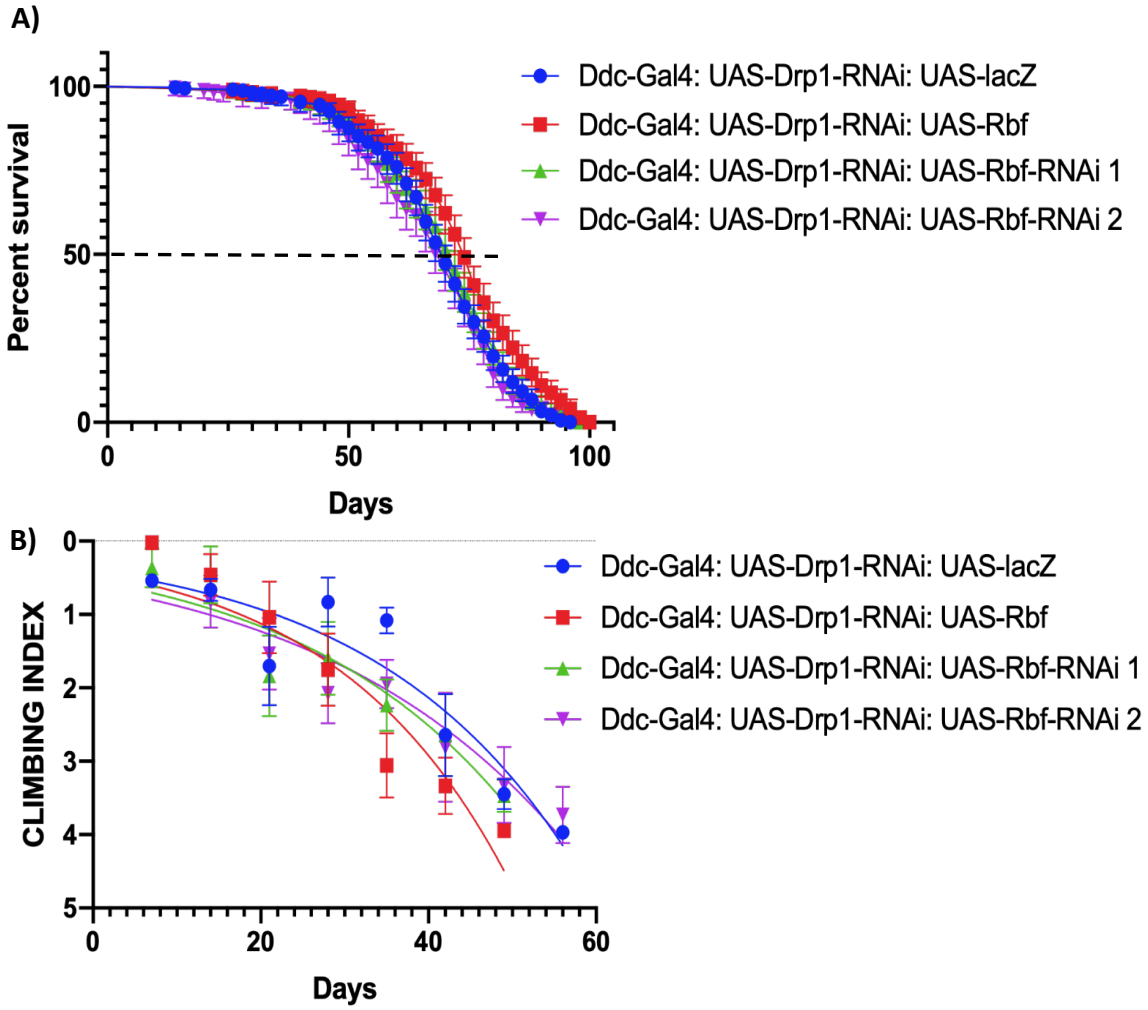

Figure 5.2: Altered expression of *Rbf* in the *Ddc-Gal4$^{4.3D}$UAS-Drp1-RNAi* model of PD. A. In the control, *Ddc-Gal4$^{4.3D}$ UAS-Drp1-RNAi UAS-lacZ* critical class males were determined to have a median life span of 70 days (n=323). The overexpression of *Rbf* , along with *UAS-Drp1-RNAi* , results in a median lifespan of 74 days (n=275), higher when compared to 70 days of control determined by the Log-rank Mantel-Cox test at P-value <0.0001, with Bonferroni correction. The inhibition of *Rbf* by two RNAi lines, *UAS-Rbf-RNAi1 ^{HMS03004}* and *UAS-Rbf-RNAi ^{GL01293}*, directed by the *Ddc-Gal4$^{4.36}$ UAS-Drp1-RNAi* transgene results in the median lifespan of 72 (n=266) and 70 days (n=263) similar to 70 days of control, determined by Log-rank Mantel-Cox test at P-value 0.3679 and 0.1737 respectively (n~250), with Bonferroni correction. The graph of longevity assay was generated by GraphPad prism8. **B.** The GraphPad prism8 generated a graph of the climbing abilities of *Ddc-Gal4 UAS-Drp1-RNAi* flies when expressing *Rbf, Rbf-RNAi's* and control. The climbing abilities of flies overexpressing *Rbf* has further compromised compared to control as determined in the non-linear fitting of the climbing curve by a 95% confidence interval (p<0.0001). The climbing abilities of flies expressing *UAS-Rbf-RNAi's* are very similar to control as determined in the non-linear fitting of the climbing curve by a 95% confidence interval with a p-value of 0.0452 and 0.1229 (n=50). The graph of longevity assay was generated by GraphPad prism8 non-linear regression curve.

The altered expression of the mitochondrial fission gene *Drp1 with Rbf-RNAi* via *Ddc-Gal4$^{4.3D}$*

In this experiment, the control *Ddc-Gal4$^{4.3D}$; UAS-Rbf-RNAi; UAS-lacZ* critical class males were determined to have a median lifespan of 58 days (n=351). The overexpression of *Drp1* along with the directed *RNAi* inhibition of *Rbf via Ddc-Gal4* results in flies with a similar median lifespan of 56 days with a sample size of 350 flies (P-value=0.0006). The inhibition of *Drp1* by either of two RNAi transgenes, *UAS-Drp1-RNAi1* and *UAS-Drp1-RNAi2*, results in greater median lifespans of 66 days (n =313) and 76 days (n=322), increased compared to the control (Figure 5.3A) as determined by log-rank (Mantel-Cox) test at a P value at <0.0001. The overexpression of *Drp1* in *Ddc-Gal4 Rbf-RNAi* does not seem to influence the locomotor abilities overtime. Notably, the inhibition of *Drp1* by expression of *Drp1-RNAi* acts to rescue the climbing ability lost by the RNA-interference of *Rbf* directed by the *Ddc-Gal4* transgene as determined in the non-linear fitting of the climbing curve by 95% confidence interval at a P-value=0.0001 (Figure 5.3B).

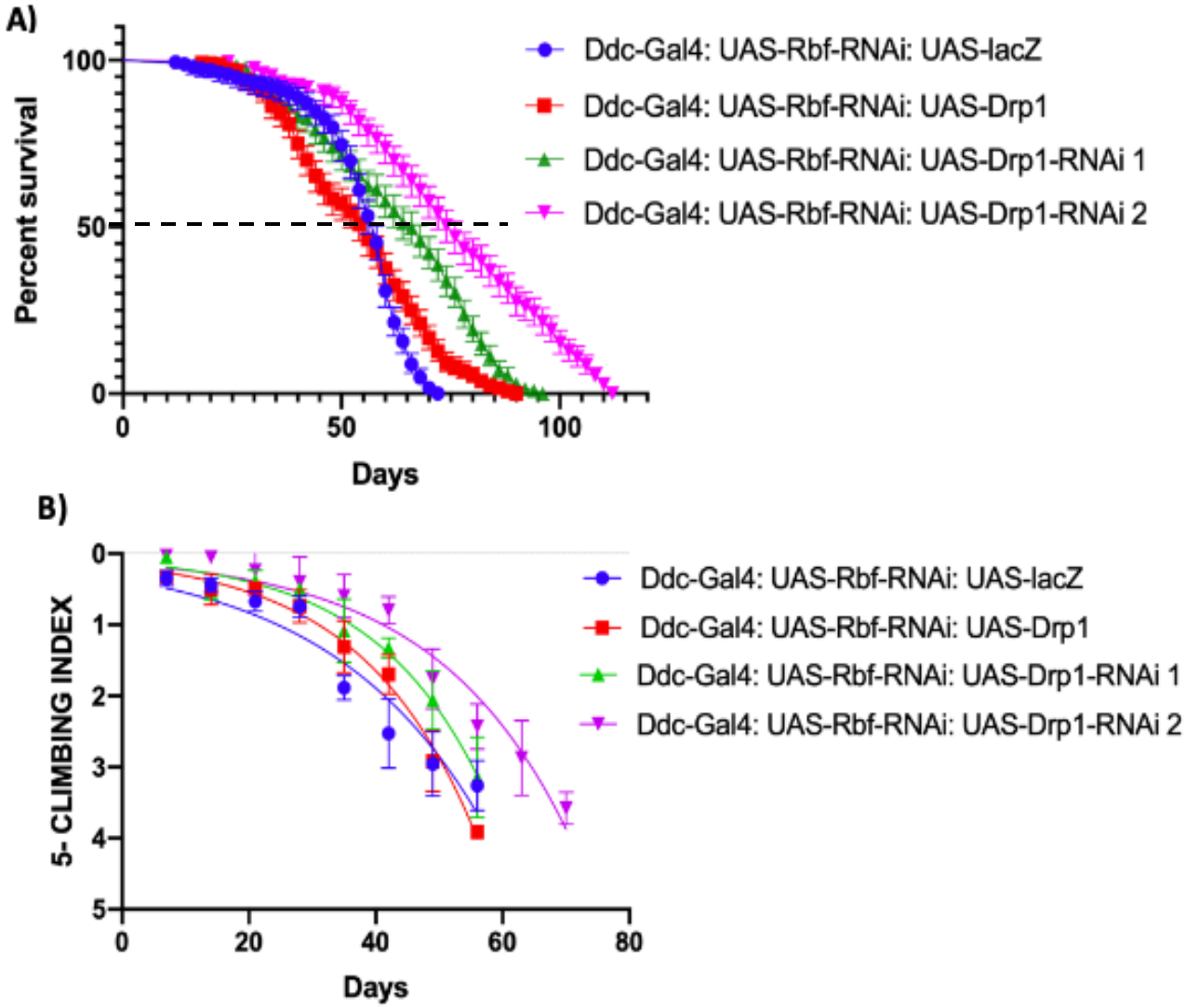

Figure 5.3: Altered *Drp1* expression coupled with *Ddc-Gal4$^{4.3D}$ Rbf-RNAi^{HMS03004}*. **A.** The graph of longevity assay generated by GraphPad prism8 with altered *Drp1* expression in *Ddc-Gal4 Rbf-RNAi^{HMS03004}* expressing flies. The overexpression of *Drp1* results in the median lifespan of 56 days (n=351), similar to 58 days of control (*lacZ/Rbf-RNAi^{HMS03004}*) determined by Log-rank Mantel-Cox test, with Bonferroni correction. The inhibition of *Drp1* in neurons using *Ddc-Gal4* transgene along with *Rbf-RNAi^{HMS03004}* results in an increased lifespan of 66 days (n=313) with UAS-*Drp1-RNAi1^{JF02762}* and lifespan of 76 days (n=322) with *UAS-Drp1-RNAi2^{HMC03230}* compares to 58 days of control done by Log-rank Mantel-Cox test, with Bonferroni correction. **B.** The GraphPad prism8 generated a graph of the climbing abilities of *Ddc-Gal4 Rbf-RNAi^{HMS03004}* flies when expressing *Drp1, Drp1 RNAi* and control. The climbing abilities of and *Drp1-RNAi* flies have significantly increased compared to control as determined in the non-linear fitting of the climbing curve by a 95% confidence interval (n=50).

Discussion

The cytosolic and nuclear role of the Rb/Rbf protein is crucial in cell differentiation and cell survival. The mutant or inactivated *Rb* gene is prevalent in some types of cancer, conversely increased expression of *Rb* is quite common in cancerous cells (Shi et al. 2000; Patel et al. 2020). Earlier, I have established (Chapter 4) that the overexpression and inhibition of *Rbf* in selected neurons of flies, has adverse effects and decrease median lifespan and climbing ability. Altered expression of Rb/*Rbf* homologues in mice has catastrophic effects, including lethality (Vooijs and Berns 1999; Lipinski and Jacks 1999). The overall function of Rb/Rbf is well conserved throughout evolution in worms, flies, and mammals (Van Den Heuvel and Dyson 2008). The crucial role of *Rbf* affects cellular health adversely when expression changes under normal conditions.

The directed expression of *Rbf* with *Drp1* resulted in the suppression of the *Drp1* overexpression phenotype of decreased longevity and age-dependent loss in climbing ability. The rescue of *Drp1* overexpression phenotype may suggest the activation of the *Rbf*-mediated cell proliferation pathway or inhibition of Drp1 induced apoptosis. The inhibition of *Rbf* in selected neurons that express *Drp1* did not enhance the phenotypes of decreased lifespan and age-dependent loss of climbing ability. A plausible explanation is that the toxic effects of excessive apoptosis due to *Drp1* overexpression is sufficient to generate the observed phenotypes (Willems et al. 2015; Nagdas and Kashatus 2017), and inhibition of *Rbf* activity does not confer an additional disadvantage. Alternatively, loss-of-*Rbf*-induced toxicity precede the effects of *Drp1*-induced toxicity, but the effect is not additive, as such, additional phenotypes may not be observable. The lifespan and climbing abilities of the flies that overexpress *Drp1*, or inhibit *Rbf*, individually are very close to

each other. The phenotypic effect of *Drp1* overexpression and *Rbf* inhibition together is not additive.

The role of *Rbf/Rb* in apoptosis is influenced by its interaction with multiple proteins. The mitochondrial fission protein Drp1 functions with Bcl-2 family proteins to promote mitochondrial fragmentation during apoptosis (Clerc et al. 2014; Wang et al. 2015; Zhang et al. 2016). In Drosophila, the Rbf protein regulates mitochondrial fragmentation hence apoptosis by promotion of excessive ROS production. The pro-apoptotic Debcl and Drp1 co-localize at the mitochondria, and their interactions can be disrupted by the overexpression of the anti-apoptotic *Buffy* (Clavier et al. 2015). The inhibition of *Drp1* in *Rbf-RNAi* background acted to rescue the phenotypes associated *Rbf* loss of function. This suggests that the inhibition of *Drp1*, may impede the molecular process which was responsible for *Rbf* inhibition PD phenotype. The inhibition of *Rbf* in *Drp1-RNAi* background has a phenotype that is very similar to *Drp1* inhibition alone. It is likely that Drp1 and Rbf function on the same biological process and, hence, show a similar outcome. Plausibly cytosolic Rbf functions downstream of Drp1 and is recruited by Drp1 on mitochondrial to promote cell death (Zhang et al. 2019). With the transcriptional activity of Rbf in mind, the Drp1 protein may function downstream of Rbf and has an epistatic effect over the *Rbf*-associated phenotypes.

The *Rbf* overexpression with *Drp1* inhibition slightly improved the lifespan but caused early onset in the climbing ability defect. The molecular mechanisms by which Rb/Rbf protein affects apoptosis and cell proliferation is fairly convoluted. It is important to understand that as a

transcription regulator, *Rbf* can promote things like cell proliferation and cell death under different molecular cues. Additionally, Rbf can localize in cytoplasm or mitochondria to maintain mitochondrial dynamics or apoptosis (Hilgendorf et al. 2013; Zhang et al. 2019). The total rescue of *Drp1* overexpression and partial recovery of Drp1 inhibition phenotype by *Rbf* overexpression is very interesting. In my experiments, the inhibition of *Rbf* is beneficial when combined with the inhibition of the mitochondrial fission protein *Drp1.* The numerous biological functions dependent upon the *Rbf* transcription regulator and the dynamic structure of mitochondria are obscure. The elucidation of the link to mitochondrial dysfunction remains challenging. The activity of Rb at the mitochondria is maybe an essential way to control for extremes of Rb expression leading to mitophagy, autophagy, cell death, organismal impaired or enhanced survival.

	Genotype	Median Lifespan	Lifespan increased/ Decreased	Climbing Increase/ Decrease
Control	*Ddc-Gal4$^{4.3D;}$ UAS-Drp1; UAS-lacZ*	58 days		
Experiment	*Ddc-Gal4$^{4.3D;}$ UAS-Drp1; UAS-Rbf*	74 days	Increased	Increased
	Ddc-Gal4$^{4.3D;}$ UAS-Drp1; UAS-Rbf-RNAi-1^{HMS03004}	56 days	Similar to control	Similar to control
	Ddc-Gal4$^{4.3D;}$ UAS-Drp1; UAS-Rbf-RNAi-2^{GL01293}	60 days	Similar to control	Similar to control
Control	*Ddc-Gal4$^{4.3D;}$ UAS-Drp1-RNAi; UAS-lacZ*	70 days		
Experiment	*Ddc-Gal4$^{4.3D;}$ UAS-Drp1-RNAi; UAS-Rbf*	74 days	Increased	Decreased
	Ddc-Gal4$^{4.3D;}$ UAS-Drp1-RNAi; UAS-Rbf-RNAi-1^{HMS03004}	72 days	Similar to control	Similar to control
	Ddc-Gal4$^{4.3D;}$ UAS-Drp1-RNAi; UAS-Rbf-RNAi-2^{GL01293}	70 days	Similar to control	Similar to control
Control	*Ddc-Gal$^{4.3D;}$ UAS-Rbf-RNAi; UAS- lacZ*	58 days		
	Ddc-Gal$^{4.3D;}$ UAS-Rbf-RNAi; UAS-Drp1	56 days	Similar to control	Similar to control
	Ddc-Gal$^{4.3D;}$ UAS-Rbf-RNAi; UAS-Drp1-RNAi1^{JF02762}	66 days	Increased	Increased
	Ddc-Gal$^{4.3D;}$ UAS-Rbf-RNAi; UAS-Drp1-RNAi2^{HMC03230}	76 days	Increased	Increased

Table 5. 1: Summary of the Result. The altered expression of *Rbf* genes directed by *Ddc-Gal4$^{4.3D}$ UAS-Drp1* and *Ddc-Gal4$^{4.3D}$ UAS-Drp1-RNAi* transgene on median lifespan and climbing ability of the critical class male flies. The effect of the altered expression of *Drp1* genes directed by *Ddc-Gal4$^{4.3D}$ UAS-Rbf-RNAi transgene* on median lifespan and climbing ability of the critical class male flies. The Cells with blue highlight denote control; Orange highlight denotes the decreased compared to control; Green highlights denote the increase compare to control, and yellow highlights indicate the resulting longevity, and climbing ability is very similar to control.

Conclusions

The Rbf protein does play major role in maintaining mitochondrial health transcriptionally. The Drp1 localizes in mitochondria and a fraction of Rbf localize in mitochondria to facilitate cell death. The decrease in lifespan and age-dependent loss in climbing ability observed in *Drp1* overexpression flies is rescued by *Rbf* overexpression. The inhibition of *Rbf* gene activity by the directed expression of an *RNAi* transgene in the selected neurons does not affect PD-like symptoms induced by *Drp1* overexpression or inhibition in Drosophila. Interaction or co-localization experiments are required to chart out the overall effect of cytosolic and nuclear role of Rbf. Additionally, it is important to elucidate the molecular changes associated with the loss of function of Rbf protein in development and function of dopaminergic neurons of Drosophila.

Bibliography

Ariss, M.M., Islam, A.B.M.M.K., Critcher, M., Zappia, M.P., and Frolov, M. V. 2018. Single cell RNA-sequencing identifies a metabolic aspect of apoptosis in Rbf mutant. Nat. Commun. **9**(1). Nature Publishing Group. doi:10.1038/s41467-018-07540-z.

Cassidy-Stone, A., Chipuk, J.E., Ingerman, E., Song, C., Yoo, C., Kuwana, T., Kurth, M.J., Shaw, J.T., Hinshaw, J.E., Green, D.R., and Nunnari, J. 2008. Chemical Inhibition of the Mitochondrial Division Dynamin Reveals Its Role in Bax/Bak-Dependent Mitochondrial Outer Membrane Permeabilization. Dev. Cell **14**(2): 193–204. doi:10.1016/j.devcel.2007.11.019.

Cereghetti, G.M., Stangherlin, A., Martins De Brito, O., Chang, C.R., Blackstone, C., Bernardi, P., and Scorrano, L. 2008. Dephosphorylation by calcineurin regulates translocation of Drp1 to mitochondria. Proc. Natl. Acad. Sci. U. S. A. **105**(41): 15803–15808. doi:10.1073/pnas.0808249105.

Chan, D.C. 2012. Fusion and Fission: Interlinked Processes Critical for Mitochondrial Health. Annu. Rev. Genet. **46**(1): 265–287. doi:10.1146/annurev-genet-110410-132529.

Clavier, A., Baillet, A., Rincheval-Arnold, A., Coléno-Costes, A., Lasbleiz, C., Mignotte, B., and Guénal, I. 2014. The pro-apoptotic activity of Drosophila Rbf1 involves dE2F2-dependent downregulation of diap1 and buffy mRNA. Cell Death Dis. **5**(9). Nature Publishing Group. doi:10.1038/cddis.2014.372.

Clavier, A., Ruby, V., Rincheval-Arnold, A., Mignotte, B., and Guénal, I. 2015. The Drosophila retinoblastoma protein, Rbf1, induces a Debcl- and Drp1-dependent mitochondrial apoptosis. J. Cell Sci. **128**(17): 3239–49. The Company of Biologists Ltd.

doi:10.1242/jcs.169896.
Clerc, P., Ge, S.X., Hwang, H., Waddell, J., Roelofs, B.A., Karbowski, M., Sesaki, H., and Polster, B.M. 2014. Drp1 is dispensable for apoptotic cytochrome c release in primed MCF10A and fibroblast cells but affects Bcl-2 antagonist-induced respiratory changes. Br. J. Pharmacol. **171**(8): 1988–1999. John Wiley and Sons Inc. doi:10.1111/bph.12515.
Cribbs, J.T., and Strack, S. 2007. Reversible phosphorylation of Drp1 by cyclic AMP-dependent protein kinase and calcineurin regulates mitochondrial fission and cell death. EMBO Rep. **8**(10): 939–44. European Molecular Biology Organization. doi:10.1038/sj.embor.7401062.
Du, W., and Searle, J. 2012. The Rb Pathway and Cancer Therapeutics. Curr. Drug Targets **10**(7): 581–589. Bentham Science Publishers Ltd. doi:10.2174/138945009788680392.
Dyson, N.J. 2016, July 1. RB1: A prototype tumor suppressor and an enigma. Cold Spring Harbor Laboratory Press. doi:10.1101/gad.282145.116.
Favaro, G., Romanello, V., Varanita, T., Andrea Desbats, M., Morbidoni, V., Tezze, C., Albiero, M., Canato, M., Gherardi, G., De Stefani, D., Mammucari, C., Blaauw, B., Boncompagni, S., Protasi, F., Reggiani, C., Scorrano, L., Salviati, L., and Sandri, M. 2019. DRP1-mediated mitochondrial shape controls calcium homeostasis and muscle mass. Nat. Commun. **10**(1): 2576. Nature Publishing Group. doi:10.1038/s41467-019-10226-9.
Ferecatu, I., Le Floch, N., Bergeaud, M., Rodríguez-Enfedaque, A., Rincheval, V., Oliver, L., Vallette, F.M., Mignotte, B., and Vayssière, J.L. 2009. Evidence for a mitochondrial localization of the retinoblastoma protein. BMC Cell Biol. **10**: 50. BioMed Central Ltd. doi:10.1186/1471-2121-10-50.
Githure, P.M., and Staveley, B.E. 2016. Bcl-2 homologue Debcl enhances α-synuclein-induced phenotypes in Drosophila. PeerJ **2016**(9). PeerJ Inc. doi:10.7717/peerj.2461.
Goyal, G., Fell, B., Sarin, A., Youle, R.J., and Sriram, V. 2007. Role of Mitochondrial Remodeling in Programmed Cell Death in Drosophila melanogaster. Dev. Cell **12**(5): 807–816. doi:10.1016/j.devcel.2007.02.002.
Hardwick, J.M., and Soane, L. 2013. Multiple functions of BCL-2 family proteins. Cold Spring Harb. Perspect. Biol. doi:10.1101/cshperspect.a008722.
Van Den Heuvel, S., and Dyson, N.J. 2008, September. Conserved functions of the pRB and E2F families. Nat Rev Mol Cell Biol. doi:10.1038/nrm2469.
Hilgendorf, K.I., Leshchiner, E.S., Nedelcu, S., Maynard, M.A., Calo, E., Ianari, A., Walensky, L.D., and Lees, J.A. 2013. The retinoblastoma protein induces apoptosis directly at the mitochondria. Genes Dev. **27**(9): 1003–1015. Cold Spring Harbor Laboratory Press. doi:10.1101/gad.211326.112.
Jagasia, R., Grote, P., Westermann, B., and Conradt, B. 2005. DRP-1-mediated mitochondrial fragmentation during EGL-1-induced cell death in C. elegans. Nature **433**(7027): 754–760. doi:10.1038/nature03316.
Jiao, W., Datta, J., Lin, H.M., Dundr, M., and Rane, S.G. 2006. Nucleocytoplasmic shuttling of the retinoblastoma tumor suppressor protein via Cdk phosphorylation-dependent nuclear export. J. Biol. Chem. **281**(49): 38098–38108. J Biol Chem. doi:10.1074/jbc.M605271200.
Jiao, W., Lin, H.M., Datta, J., Braunschweig, T., Chung, J.Y., Hewitt, S.M., and Rane, S.G. 2008. Aberrant nucleocytoplasmic localization of the retinoblastoma tumor suppressor protein in human cancer correlates with moderate/poor tumor differentiation. Oncogene **27**(22): 3156–3164. Oncogene. doi:10.1038/sj.onc.1210970.

Lipinski, M.M., and Jacks, T. 1999, December 20. The retinoblastoma gene family in differentiation and development. Nature Publishing Group. doi:10.1038/sj.onc.1203244.

Milet, C., Rincheval-Arnold, A., Moriéras, A., Clavier, A., Garrigue, A., Mignotte, B., and Guénal, I. 2014. Mutating RBF Can Enhance Its Pro-Apoptotic Activity and Uncovers a New Role in Tissue Homeostasis. PLoS One **9**(8): e102902. Public Library of Science. doi:10.1371/journal.pone.0102902.

Nagdas, S., and Kashatus, D.F. 2017. The Interplay between Oncogenic Signalling Networks and Mitochondrial Dynamics. Antioxidants **6**(2): 33. doi:10.3390/antiox6020033.

Nargund, A.M., Fiorese, C.J., Pellegrino, M.W., Deng, P., and Haynes, C.M. 2015. Mitochondrial and nuclear accumulation of the transcription factor ATFS-1 promotes OXPHOS recovery during the UPRmt. Mol. Cell **58**(1): 123–133. Cell Press. doi:10.1016/j.molcel.2015.02.008.

Oettinghaus, B., D'Alonzo, D., Barbieri, E., Restelli, L.M., Savoia, C., Licci, M., Tolnay, M., Frank, S., and Scorrano, L. 2016. DRP1-dependent apoptotic mitochondrial fission occurs independently of BAX, BAK and APAF1 to amplify cell death by BID and oxidative stress. Biochim. Biophys. Acta - Bioenerg. **1857**(8): 1267–1276. doi:10.1016/j.bbabio.2016.03.016.

Patel, J.M., Goss, A., Garber, J.E., Torous, V., Richardson, E.T., Haviland, M.J., Hacker, M.R., Freeman, G.J., Nalven, T., Alexander, B., Lee, L., Collins, L.C., Schnitt, S.J., and Tung, N. 2020. Retinoblastoma protein expression and its predictors in triple-negative breast cancer. npj Breast Cancer **6**(1): 1–6. Nature Research. doi:10.1038/s41523-020-0160-4.

Sebastián, D., Palacín, M., and Zorzano, A. 2017. Mitochondrial Dynamics: Coupling Mitochondrial Fitness with Healthyageing. Trends Mol. Med. **23**(3): 201–215. Elsevier Current Trends. doi:10.1016/J.MOLMED.2017.01.003.

Shi, Y.Z., Hui, A.M., Li, X., Takayama, T., and Makuuchi, M. 2000. Overexpression of retinoblastoma protein predicts decreased survival and correlates with loss of p16INK4 protein in gallbladder carcinomas. Clin. Cancer Res. **6**(10): 4096–100. Available from http://www.ncbi.nlm.nih.gov/pubmed/11051262 [accessed 9 March 2020].

Todd, A., and Staveley, B. 2012. Expression of Pink1 with α-synuclein in the dopaminergic neurons of Drosophila leads to increases in both lifespan and healthspan. Genet. Mol. Res. **11**(2): 1497–1502. doi:10.4238/2012.May.21.6.

Todd, A.M., and Staveley, B.E. 2004. Novel assay and analysis for measuring climbing ability in Drosophila. Drosoph. Inf. Serv. **87**: 101–108. Available from http://www.ou.edu/journals/dis/DIS87/4 - Techniques.pdf [accessed 6 October 2019].

Vooijs, M., and Berns, A. 1999, September 20. Developmental defects and tumor predisposition in Rb mutant mice. doi:10.1038/sj.onc.1202999.

Wang, P., Wang, P., Liu, B., Zhao, J., Pang, Q., Agrawal, S.G., Jia, L., and Liu, F.-T. 2015. Dynamin-related protein Drp1 is required for Bax translocation to mitochondria in response to irradiation-induced apoptosis. Oncotarget **6**(26): 22598–612. Impact Journals, LLC. doi:10.18632/oncotarget.4200.

Wen-Hwa, L., Bookstein, R., Hong, F., Young, L.J., Shew, J.Y., and Lee, E.Y.H.P. 1987. Human retinoblastoma susceptibility gene: Cloning, identification, and sequence. Science (80-.). **235**(4794): 1394–1399. Science. doi:10.1126/science.3823889.

Willems, P.H.G.M., Rossignol, R., Dieteren, C.E.J., Murphy, M.P., and Koopman, W.J.H. 2015, August 4. Redox Homeostasis and Mitochondrial Dynamics. Cell Press. doi:10.1016/j.cmet.2015.06.006.

Zhang, S., Che, L., He, C., Huang, J., Guo, N., Shi, J., Lin, Y., and Lin, Z. 2019. Drp1 and RB interaction to mediate mitochondria-dependent necroptosis induced by cadmium in hepatocytes. Cell Death Dis. **10**(7): 1–17. Nature Publishing Group. doi:10.1038/s41419-019-1730-y.

Zhang, Z., Liu, L., Wu, S., and Xing, D. 2016. Drp1, Mff, Fis1, and MiD51 are coordinated to mediate mitochondrial fission during UV irradiation-induced apoptosis. FASEB J. **30**(1): 466–476. FASEB. doi:10.1096/fj.15-274258.

Chapter 6: The *Buffy, Drp1* and *Rbf*-mediated rescue of *α-synuclein*-induced Parkinson Disease Models in *Drosophila melanogaster*

Abstract

Parkinson Disease (PD) is the second most common neurodegenerative disorder and is closely associated with the loss of DA neurons. Mutant forms of the α-*synuclein* gene were the first found to be associated with familial forms of PD. While the cellular functions of α-synuclein are not well understood; overexpression, mutation or post-translational protein modification can lead to the formation of LB, aggregates of a number of proteins with α-synuclein as a major component. The α-synuclein protein can greatly influence cellular function in ways that include dysfunction of the mitochondria, impairment of autophagy and failure to form the SNARE complex essential in vesicle formation. Several cellular mechanisms have been demonstrated to alleviate cellular dysfunction, including the participation of the anti-apoptotic Bcl-2 proteins and the mitochondrial fission protein, Drp1. The expression of *α-synuclein* in the selected neurons of flies directed by the *Ddc-Gal4* transgenes has provided a robust and very well-studied Drosophila model of PD characterized by locomotor defects and impairment to longevity. The co-expression of *Buffy* along with *α*-synuclein results in the rescue of these longevity and climbing defects. The altered expression of *Drp1* and *α-synuclein* in selected neurons offered an opportunity to highlight the role of *Drp1* in mitochondrial-dependent neurodegeneration and death. The directed inhibition of *Drp1* and the *α-synuclein* transgene directed by *Ddc-Gal4*$^{4.36}$ in Drosophila resulted in critical class flies with enhanced survival and improved climbing ability, whereas the overexpression of *Drp1* in the *α-synuclein*-induced Drosophila model of PD results in a much more severe climbing defect. Finally, the co-expression of the transcription factor *Rbf* along with *α-synuclein* counteracts the *α-synuclein*-induced phenotypes to increase the median lifespan and improve the associated loss of locomotor ability. Overall, these experiments suggest that the protein products of *Bcl-2, Drp1* and

Rbf genes function to protect mitochondria, either directly or indirectly, from the cellular dysfunction initiated by the altered expression of *α-synuclein*

Introduction

The gene encoding the α-*synuclein* protein was the first found to be associated with Parkinson Disease (PD). The protein product is a small soluble presynaptic nerve cell terminal protein with a somewhat elusive function. The histology of the PD brain and some other neurological disorders show abnormal aggregates of proteins, identified as Lewy Body, that contain α-synuclein as a major component (Recasens and Dehay 2014). LB are eosinophilic cytoplasmic inclusion with a dense core and surrounding fibrils that consist mainly of α-synuclein and are associated with other proteins including ubiquitin and neurofilament (Spillantini et al. 1997). The aberrant conformation of α-synuclein leads to the formation of an oligomeric species or protofibrils (Ingelsson 2016). The protofibrils are considered to be toxic and are believed to disrupt intracellular pathways to facilitate neuronal cell death. Mutant forms of the α-*synuclein* gene, found in some PD patients, include protein-altering point mutations and multiplications of gene copy numbers (Thomas and Beal 2011). Furthermore, post-translational modifications of the α-*synuclein* gene, protein product increase the aggregation of the protein (Thomas and Beal 2011; Zhang et al. 2019a). These protein alterations seem to cause the aggregation of insoluble proteins, which, eventually, may cause neurotoxicity and PD pathology.

The hypothesis that the α-synuclein protein acts to induce toxicity has not been supported completely. Cytoplasmic α-synuclein interacts with lipid vesicles that are rich in cardiolipins with

a composition that is very similar to the mitochondrial inner membrane (Zigoneanu et al. 2012) but has little affinity for vesicles with a composition that is similar to the cardiolipin-lacking mitochondrial inner membrane. Post-mortem analysis reveals that α-*syn*uclein is found to localize and accumulate at the mitochondria of the SNpc and striatum of PD subjects (Devi et al. 2008). One proposition is that mitochondrially-accumulated α-*synuclein* interacts with complex I to cause mitochondrial dysfunction (Devi et al. 2008). Normally, the affinity of α-synuclein for vesicles tend to depend upon the protein composition, curvature, fluidity, and surface charge (Kaur and Lee 2020); cardiolipin is important in maintaining the curvature of the membrane. The N-terminal of α-*synuclein* interacts with lipid vesicles (Zigoneanu et al. 2012); and the N and C-termini demonstrate affinity towards GM1-rich vesicles (Kaur and Lee 2020). The GM1 is a ganglioside that contains sialic acid residue, affects neuronal plasticity, neuronal repair and release of neurotrophins. Membrane-bound α-*synuclein* has a dynamic nature and shows conformation elasticity to facilitate exocytosis (Kaur and Lee 2020). The role of α-*synuclein* in the maintenance of cellular homeostasis and the adversities caused by the abnormal functions of pathogenic α-synuclein have proven to be very challenging to differentiate.

A very important aspect of this series of studies is that while the expression of human α-*sy*nuclein in selected neurons has been able to reproduce PD-like phenotypes in flies, *Drosophila melanogaster* lacks an identified α-*synuclein* orthologue (Feany and Bender 2000; Nagoshi 2018). The phenotypes associated with the expression of human α-*synuclein* in flies include locomotor dysfunction, the loss of dopaminergic (DA) neurons and accumulation of proteinaceous aggregates containing α-*synuclein* similar to LB. The upregulation of the molecular chaperone

Hsp70 mitigates the DA neuronal loss caused by the presence and activities of α-*synuclein* (Auluck et al. 2002). Investigation of the interactions of α-synuclein with other proteins will contribute to understand α-synuclein function and PD pathology. The molecular mechanism of α-*synuclein* function has not been elucidated, in rat PC12 cells the extracellular α-*synuclein* enhanced the pro-apoptotic gene expression and downregulated the expression of anti-apoptotic gene (Motyl et al. 2017). The overexpression of the anti-apoptotic Drosophila *Bcl-2* homologue, *Buffy*, or inhibition of pro-apoptotic *Bcl-2* homologue, *Debcl*, has been shown to suppress α-*synuclein*-induced PD phenotypes in flies (Githure and Staveley 2016a, 2016c). The upregulation of the autophagy pathway could be mediated by the phosphorylation of Bcl-2 family proteins to degrade dysfunctional α-synuclein species in mouse (Zhang et al. 2019b). Another hypothesized role of α-synuclein is that this protein can act to regulate the size of neuronal mitochondria through a currently undefined mechanism (Pozo Devoto and Falzone 2017). The overexpression of α-*synuclein* can reduce the proportion of elongated mitochondria due to the overexpression of the mitochondrial fusion protein in human neuroblastoma cells (Kamp et al. 2010). Of special note, α-*synuclein*-induced mitochondrial fragmentation is independent of the mitochondrial fission protein, Drp1, and can be altered by a pathogenic mutation in α-*synuclein* (Nakamura et al. 2011; Guardia-Laguarta et al. 2014). However, the inhibition of *Drp1*-rescued α-*synuclein*-induced models of PD in mammalian cell culture (Fan et al. 2019). This convoluted relationship reveals the complexity and sensitivity of a role for α-*synuclein* in this biological system.

The broad spectrum of α-synuclein potential functions encompass interaction with the cell cycle regulatory proteins. The treatment of PC12 cells with extracellular α-*synuclein* results in an

increase in calcium influx, a disturbance of mitochondrial function, an induction of oxidative stress and an expansion of CDK5(Cyclin Dependent Kinase 5) activity (Motyl et al. 2017). The CDK5-mediated phosphorylation of the Rb protein may be considered the first step in the initiation of neuronal cell death (Hamdane et al. 2005). The neuronal cell death observed in response to either treatment with dopamine or *β-amyloid* has been demonstrated to be dependent upon the expression of *E2F1* (Giovanni et al. 2000; Jordan-Sciutto et al. 2003). Notably, neuronal cell death due to the loss of *Rb* function can be rescued by the concurrent loss of *E2F1* (Jordan-Sciutto et al. 2003). The role of the cell cycle protein in PD is unclear, however an altered staining pattern for *Rb* in PD patients can be observed (Jordan-Sciutto et al. 2003). The aberrant phosphorylation of the Rb protein in DA neurons of the SNpc, altered activity of *E2F1,* and *E2F*-inducible proteins (Höglinger et al. 2007) can suggest that there may be a role for *Rb* in the activation of the cell cycle in DA neurons and in the processes that lead to neuronal cell death.

The role of mutation of the *α-synuclein* gene in the eventual production of the PD phenotypes is very well established. Here, I propose that the phenotypes that arise from the expression of *α-synuclein* is due to dysfunctional mitochondria and can be rescued through the appropriate regulation of this process. The role of *α-synuclein* in disruption of mitochondrial dynamics established *α-synuclein*-induced models of PD is attractive to investigate the role of *Bcl-2, Drp1* and other mitochondrial protection proteins. I have employed *Drosophila melanogaster* as a model organism to study the phenotypic effects of the interactions of the α-synuclein with other mitochondrial protection proteins. In these experiments, I exploited the *UAS-Gal4* system to direct the expression of the human *α-synuclein* gene in selected neuronal tissues using *Ddc-Gal4*$^{4.36}$

transgene. The expression of *α-synuclein* has led to PD phenotypes, compromised lifespan and the diminishment of climbing ability overtime. As well established in previous studies (Githure and Staveley 2016c), and strengthened by my experimental findings, the PD-like phenotypic effects of *α-synuclein* expression can be rescued by the co-expression of the anti-apoptotic Bcl-2 family protein gene, *Buffy*. In addition, I found that this phenotype can be suppressed by the overexpression of *Rbf* or partially rescued by alteration of the expression of the mitochondrial fission protein gene *Drp1.*

Materials and Methods

Drosophila stocks and media

The *UAS-Rbf RNAi1*^{HMS03004} (y[1] sc[*] v[1] sev[21]; P{y[+t7.7] v[+t1.8]=TRiP.HMS03004}attP2/TM3, Sb[1]); the *UAS-Rbf RNAi2*^{GL01293} (y[1] sc[*] v[1] sev[21]; P{y[+t7.7] v[+t1.8]=TRiP.GL01293}attP40); *UAS-Rbf* (w[*]; P{w[+mC]=UAS-Rbf.D}III); *UAS-Drp1* (y[1] w[*]; P{w[+mC]=FLAG-FlAsH-HA-*Drp1*}3, Ki[1]); the *UAS-Drp1-RNAi1*^{JF02762} (y[1] v[1]; P{y[+t7.7] v[+t1.8]=TRiP.JF02762}attP2}); and *UAS-Drp1-RNAi2*^{HMC03230} (y[1] v[1]; P{y[+t7.7] v[+t1.8]=TRiP.HMC03230}attP40); the *UAS-Buffy* (w[*]; P{w[+mC]=UAS-Buffy.S}E1); *UAS-Buffy-RNAi* (w[*]; P{w[+mC]=UAS-Buffy.RNAi}3); *UAS-Debcl* ^{EY05743} (y[1] w[67c23]; P{y[+mDint2] w[+mC]=EPgy2}Debcl[EY05743]); *Ddc-Gal4*$^{4.36}$(w[1118]; P{w[+mC]=Ddc-Gal4.L}Lmpt[4.36]; and *UAS-lacZ*$^{4-1-2}$ stocks were obtained from Bloomington Drosophila Stock Center at Indiana University, Bloomington, Indiana, USA. The *UAS-Debcl-RNAi*^{v47515} (w1118; P{GD 1637}v47515) stock were obtained from Vienna Drosophila Resource Center. The *UAS-α-synuclein* was generously provided by Dr. M. Feany of Harvard Medical School (Feany and Bender 2000). The

Ddc-Gal4/TM3, UAS-α-syn/CyO derivative line was generated through standard homologous recombination methods (Githure and Staveley 2016) and were used for expression of *α-synuclein* in selected neurons directed by the *Ddc-Gal4*$^{4.36}$ transgene. All flies were maintained on standard cornmeal, molasses, yeast, and agar media treated with propionic acid and methylparaben to inhibit fungal growth. Stocks were maintained on solid media for two to three weeks before transfer onto new media to re-culture. Stocks were maintained at room temperature (22°C ± 2°C) while crosses and experiments were carried out at 25°C.

Survival Assay

The virgin's females of *Ddc-Gal4-UAS-α-synuclein* genotype were collected every 8 to 12 hours for several days, and confirmed virgin female flies were then crossed with *UAS-lacZ, UAS-Rbf's, UAS-Rbf-RNAi's*, *UAS-Drp1, UAS-Drp1-RNAi's, UAS-Buffy, UAS-Buffy-RNAi, UAS-Debcl and UAS-Debcl-RNAi* males. The cohort of critical class male flies was collected upon eclosion. At least two hundred fifty flies were aged per genotype at a density of 20 or fewer flies per vial to avoid crowding on fresh media, which was replenished every two to five days. Flies were observed and scored every second day for the viability. Observations continue until all flies are dead. Longevity data analysis was performed with the GraphPad Prism version 8 (*graphpad.com*), and survival curves were compared through the log-rank (Mantel-Cox) test. Significance was determined at 95% confidence ($P \leq 0.05$) with Bonferroni correction.

Locomotor Analysis

Approximately 70 male flies of the critical class were collected over 24 hours from the crosses similar to survival assay and maintained as cohorts of 10 flies in each vial. Flies are scored for their

ability to climb over their lifetime, and flies were transferred to new food every two to five days. Every week, 50 males from every genotype were assayed for their ability to climb a 10 centimetres glass tube divided into five levels of 2 cm each, in 10 seconds, in 10 repetitions (Todd and Staveley 2004, 2012). The GraphPad Prism version 8 was used to analyze the data and generate the climbing curves, fitted via non-linear regression and compared using a 95% confidence interval with ($P \leq 0.05$)

Results

The expression of α-*synuclein* with *Ddc-Gal4*$^{4.36}$

In these experiments, the control *Ddc-Gal4*$^{4.36}$*; UAS-lacZ* critical class males were determined to have a median lifespan of 92 days (n=361). The directed expression of *α-synuclein* by the *Ddc-Gal4*$^{4.36}$ transgene results in decreased lifespan compared to the control shown (Figure 6.1A). The expression of *α-synuclein* resulted in median lifespans of 74 days in 331 flies, much lower compared to control flies (Figure 6.1A) as determined by log-rank (Mantel-Cox) test with a P-value at <0.0001. The expression of *α-synuclein* in neurons caused early onset of impairment in climbing ability. The non-linear fitting of the climbing curve shows the *α-synuclein* expression have compromised this locomotor ability phenotype compared to control at 95% CI (P-value <0.0001) (Figure 6.1B) (n=50).

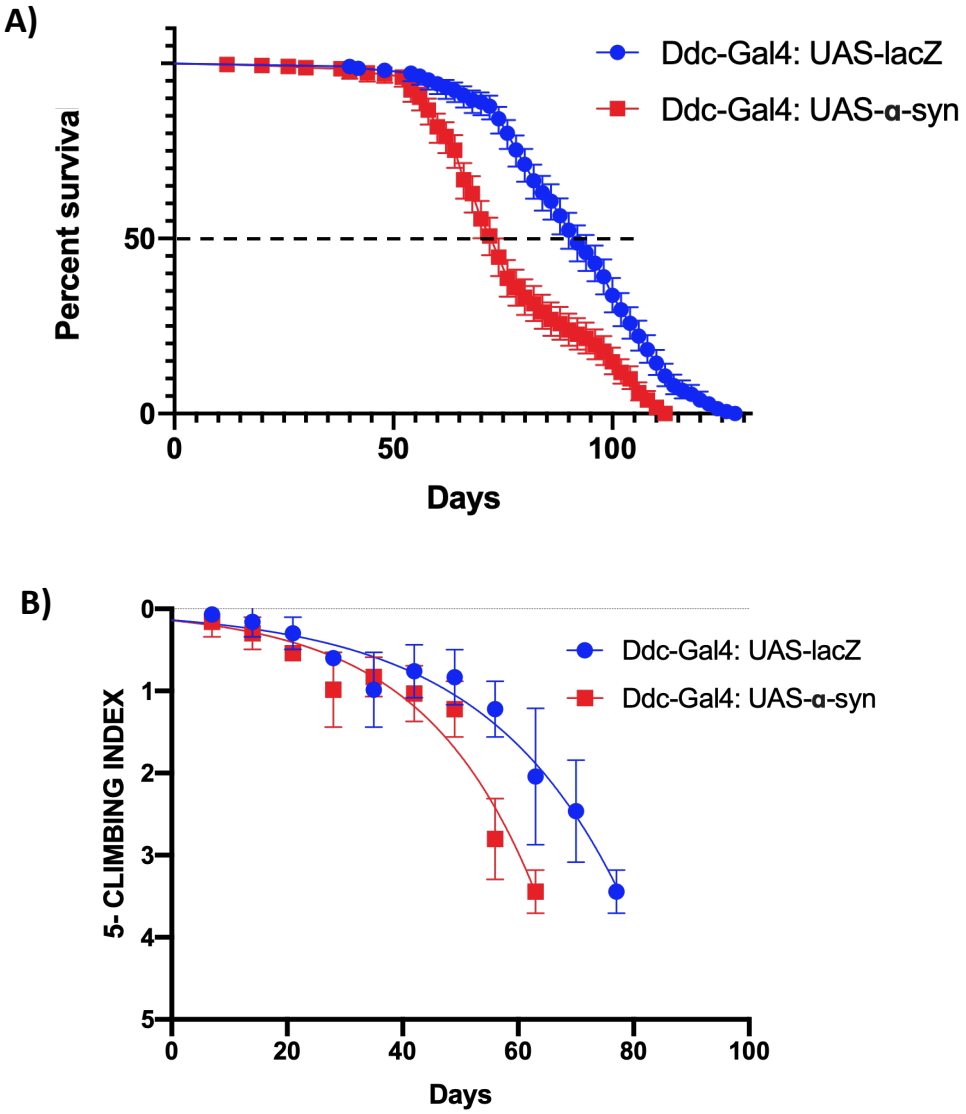

Figure 6.1: Altered *α-synuclein* expression with *Ddc-Gal4$^{4.36}$ transgene*. **A).** In the control, *Ddc-Gal4$^{4.36}$ UAS-lacZ* critical class males resulted in a median life span of 92 days (n=361). Expression of *α-synuclein* in *Ddc-Gal4$^{4.36}$ UAS-α-synuclein* transgene resulted in a median life span of 74 days (n=331), much lower compared to control as determined by the Log-rank Mantel-Cox test (P-value <0.0001) with Bonferroni correction. The graph of the longevity assay was generated by GraphPad prism8. **B).** The *Ddc-Gal4$^{4.36}$* flies express *UAS-lacZ in* control flies. The climbing abilities of flies with *α-synuclein* expression have decreased compared to control as determined in the non-linear fitting of the climbing curve by a 95% confidence interval (p<0.0001). The graph of longevity assay was generated by GraphPad prism8 non-linear regression curve (n=50).

The altered co-expression of *Buffy* and *Debcl* with *α-synuclein* via *Ddc-Gal4* $^{4.36}$

The expression of *α-synuclein* has led to the establishment of a number of Drosophila models of PD. In this experiment, the control *Ddc-Gal4*$^{4.36}$*; α-synuclein; UAS-lacZ* critical class males were determined to have a median lifespan of 78 days (n=257). The overexpression of *Buffy* in the *Ddc-Gal4; UAS-α-synuclein; UAS-Buffy* flies have a median lifespan of 88 days (n=375), much higher compared to control as determined by log-rank (Mantel-Cox) test with a P-value at <0.0001. The inhibition of *Buffy* in the *Ddc-Gal4; UAS-α-synuclein; UAS-Buffy-RNAi* critical class male flies have a median lifespan of 68 days in 370 flies, similar to the control (Figure 6.2A) as determined by log-rank (Mantel-Cox) test at a P-value at <0.0984. The overexpression of *Buffy* in neurons rescued the early onset of impairment in climbing ability of *Ddc-Gal4; UAS-α-synuclein* flies. The non-linear fitting of the climbing curve shows *Buffy* overexpression has rescued the climbing ability defect compared to control at a 95% CI (P-value <0.0001) (Figure 6.2B). The inhibition of *Buffy* in neurons caused early onset of impairment in climbing ability. The inhibition of *Buffy* by *Ddc-Gal4 UAS-α-synuclein; UAS-Buffy-RNAi* further contributes to loss of the climbing ability throughout the life of critical class flies compared to control at a 95% CI (P-value 0.0005). (Figure 6.2B).

The overexpression of *Debcl* in the *Ddc-Gal4; UAS-α-synuclein; UAS-Debcl*^{EY05743} flies have a median lifespan of 66 days in 253 flies, which is much less compared to control (Figure 6.2A) as determined by log-rank (Mantel-Cox) test at a P-value at <0.0001. The inhibition of *Debcl* in the *Ddc-Gal4 UAS-α-synuclein*; *UAS-Debcl-RNAi* ^{v47515} critical class male flies have a median lifespan of 86 days in 315 flies, much higher compared to control flies (Figure 6.2A) as determined by log-rank (Mantel-Cox) test with a P-value at <0.0001. The overexpression of *Debcl* by *Ddc-Gal4 UAS-α-synuclein; UAS-Debcl* ^{EY05743} further contributes to the impairment in the climbing ability defect compared to control at a 95% CI (P<0.0001). The inhibition of *Debcl* by *Ddc-Gal4 UAS-α-synuclein;*

UAS-Debcl-RNAi^{v47515} slightly increases the loss of the locomotor proficiency throughout the life of critical class flies compared to control at a 95% CI (P-value 0.0005) (Figure 6.2B) (n=50).

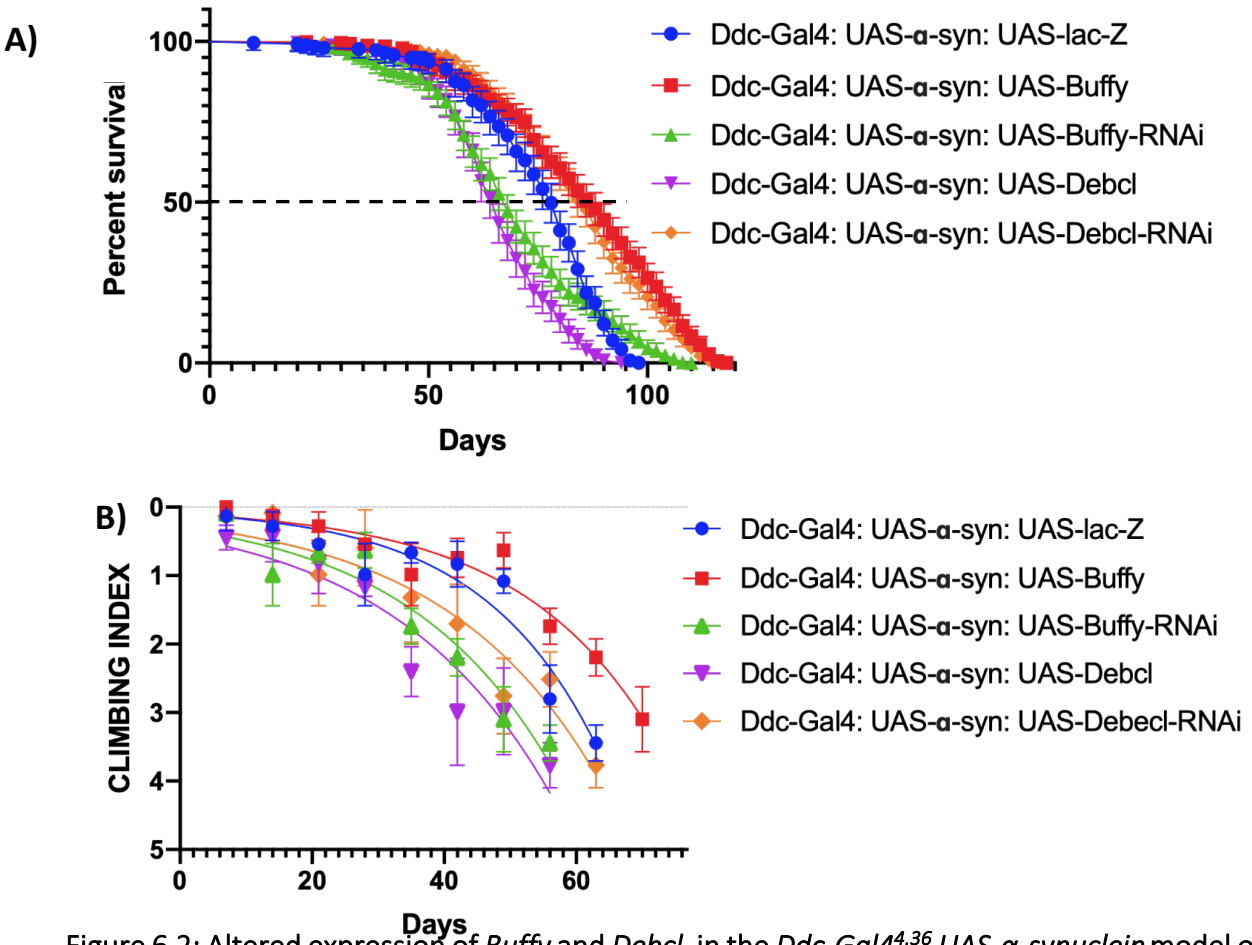

Figure 6.2: Altered expression of *Buffy* and *Debcl,* in the *Ddc-Gal4$^{4.36}$ UAS-α-synuclein* model of PD. **A)**. In the control, *Ddc-Gal4$^{4.36}$; UAS-α-synuclein; UAS-lacZ* critical class males resulted in a median life span of 78 days (n=257). The overexpression of *Buffy* results in a median lifespan of 88 days (n=375) compares control; the inhibition of *Buffy* directed by the *Ddc-Gal4$^{4.36}$; UAS-α-synuclein* transgene, result in the median lifespan of 68 (n=370) much less compared to control, determined by Log-rank Mantel-Cox test at P value <0.0001, with Bonferroni correction. The overexpression of *Debcl^{EY05743}* results in a median lifespan of 66 days (n=253) much less compares to control, determined by Log-rank Mantel-Cox test at P-value <0.0001; the inhibition of *Debcl* result in the median lifespan of 86 (n=315); much higher than control, determined by Log-rank Mantel-Cox test at p<0.0001, with Bonferroni correction. **B).** The GraphPad prism8 generated graph of the climbing abilities of *Ddc-Gal4-α-synuclein* flies with the expression of *Buffy, Buffy-RNAi, Debcl^{EY05743}, Debcl-RNAi^{v47515}* and control. The climbing abilities of flies overexpressing *Buffy* has rescued compared to control as determined in the non-linear fitting of the climbing curve by a 95% confidence interval (p<0.0001). The climbing ability of flies has further worsened by the expression of *UAS-Buffy-RNAi, UAS-Debcl^{EY05743}* and *UAS-Debcl-RNAi^{v47515}* as determined by the non-linear fitting of the climbing curve by a 95% confidence interval with p value at 0.0005, <0.0001 and 0.0005 respectively (n=50). The graph of longevity assay was generated by GraphPad prism8 non-linear regression curve.

The altered expression of the mitochondrial fission gene *Drp1 with α-synuclein* via *Ddc-Gal4$^{4.36}$*

The loss of function of *α-synuclein* leads to compromised lifespan and diminished climbing ability over time. The control *Ddc-Gal4$^{4.36}$; α-synuclein; UAS-lacZ* critical class males were determined to have a median lifespan of 78 days (n=257). The overexpression of *Drp1* along with *α-synuclein* expression *via Ddc-Gal4* results in flies with a median lifespan of 94 days, which is much higher compared to control in 282 flies (Figure 6.3A) as determined by log-rank (Mantel-Cox) test with a P-value at <0.0001. The inhibition of *Drp1* by the two RNAi transgenes, *UAS-Drp1-RNAi1^{JF02762}* and *UAS-Drp1-RNAi2^{HMC03230}*, results in longer median lifespans of 88 and 84 days, in approximately 250 flies, compared to the control (Figure 6.3A) as determined by log-rank (Mantel-Cox) test with a P-value at <0.0001. The overexpression of *Drp1* by *Ddc-Gal4 UAS-α-synuclein; UAS-Drp1* further contributes to loss of the climbing ability throughout the life of critical class flies compared to control at a 95% CI (P<0.0001). (Figure 6.3B). The inhibition of *Drp1* by *Ddc-Gal4 UAS-α-synuclein; UAS-Drp1-RNAi^{JF02762}* and *Ddc-Gal4 UAS-α-synuclein; UAS-Drp1-RNAi2^{HMC03230}* rescue the climbing ability defect compared to control at a 95% CI with P-value of 0.0003 and 0.0015 respectively (Figure6.3B) (n=50).

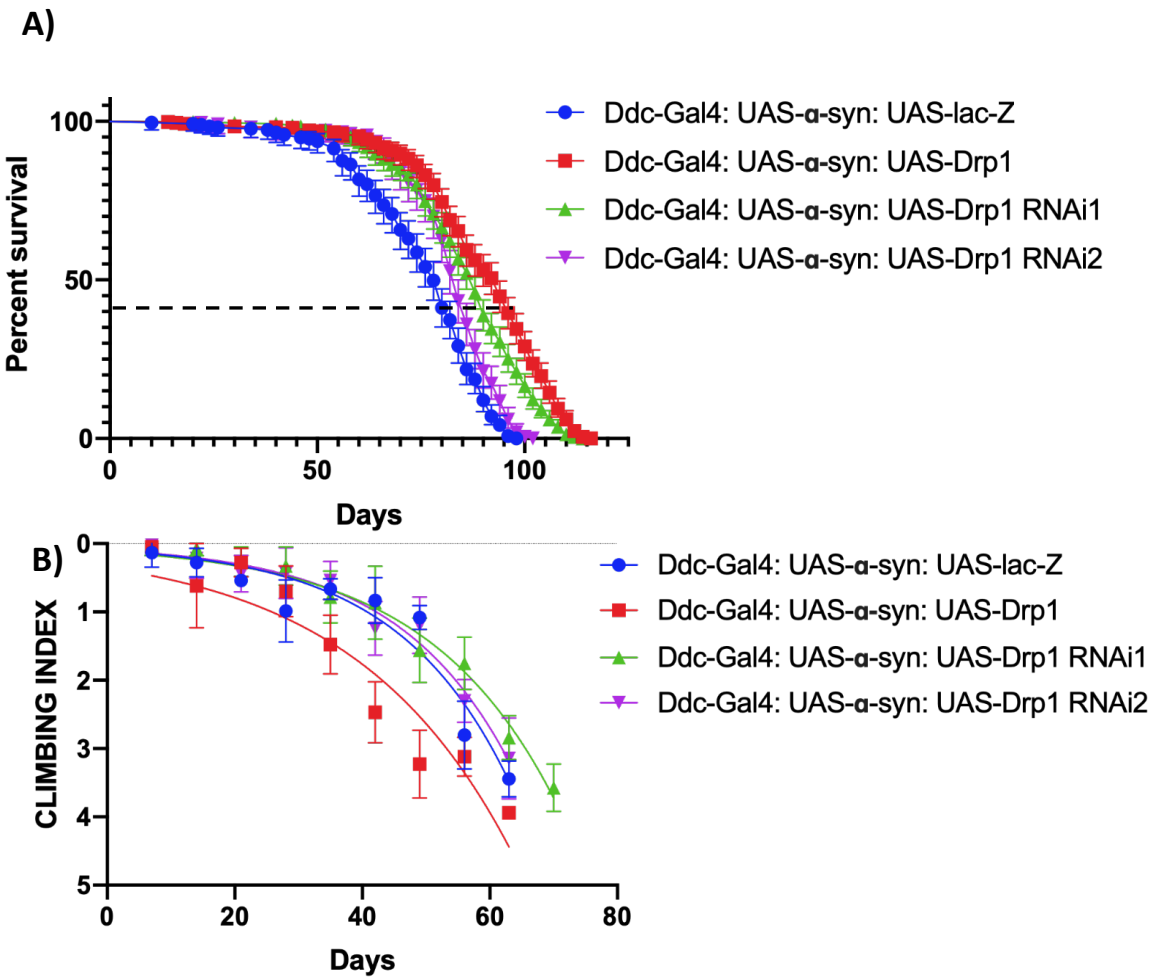

Figure 6.3: Altered expression of *Drp1,* in the *Ddc-Gal4$^{4.36}$ α-synuclein* model of PD. A). In the control, *Ddc-Gal4$^{4.36}$; UAS-α-synuclein; UAS-lacZ* critical class males produced a median life span of 78 days (n=257). The overexpression of *Drp1* results in the median lifespan of 94 days (n=382), much higher than control determined by the Log-rank Mantel-Cox test at P value <0.0001, with Bonferroni correction. The inhibition of *Drp1* by two RNAi lines directed by the *Ddc-Gal4$^{4.36}$ UAS-α-synuclein* transgene, result in the median lifespan of 88 and 84 days much higher compared to control, determined by Log-rank Mantel-Cox test at P-value <0.0001 (n~250), with Bonferroni correction. The graph of longevity assay was generated by GraphPad prism8. **B).** The GraphPad prism8 generated graph of the climbing abilities of *Ddc-Gal4 -α-synuclein* flies with the expression of *Drp1, Drp1-RNAi* and control. The climbing abilities of flies overexpressing *Drp1* has further compromised compared to control as determined in the non-linear fitting of the climbing curve by a 95% confidence interval (P-value <0.0001). The climbing ability of flies expressing *UAS-Drp1-RNAi's* has improved compared to control as determined by the non-linear fitting of the climbing curve at 95% confidence interval with P-value at 0.0003, 0.0015 (n=50). The graph of longevity assay was generated by GraphPad prism8 non-linear regression curve.

The altered expression of the *Rbf with α-synuclein* via *Ddc-Gal4$^{4.36}$*

The loss of function of *α-synuclein* leads to a compromised lifespan and a diminished climbing ability over time. The *Ddc-Gal4$^{4.36}$ UAS-α-synuclein UAS-lacZ* critical males were determined to have a median lifespan of 78 days in 257 flies. Overexpression of *Rbf* in the *Ddc-Gal4 UAS-α-synuclein* expressing flies results in the much-increased median life span of 100 days compared to the control in 376 flies as determined by log-rank (Mantel-Cox) test with a P-value at <0.0001. The two *UAS-Rbf-RNAi* transgenes, *UAS-Rbf-RNAi ^{HMS03004}* and *UAS-Rbf-RNAi2^{GL01293}*, when expressed along with *Ddc-Gal4 α-synuclein*, results in a median life span of 82 (n=327 flies) and 94 days (n=309 flies), respectively (Figure 6.4A) compared to control, as determined by log-rank (Mantel-Cox) test with a P-value at <0.0001. The overexpression of *Rbf* by *Ddc-Gal4 UAS-α-synuclein* rescues the decline in climbing ability compared to control at 95% CI with P-value < 0.0001. The inhibition of *Rbf* by *Ddc-Gal4 UAS-α-synuclein; UAS-Rbf-RNAi1 ^{HMS03004}* and *Ddc-Gal4 UAS-α-synuclein; UAS-Rbf-RNAi ^{GL01293}* further contributes to loss of the climbing ability throughout the life of critical class flies compared to control at a 95% CI with a P-value at <0.0001 and 0.0005 respectively (Figure 6.4B) (n=50).

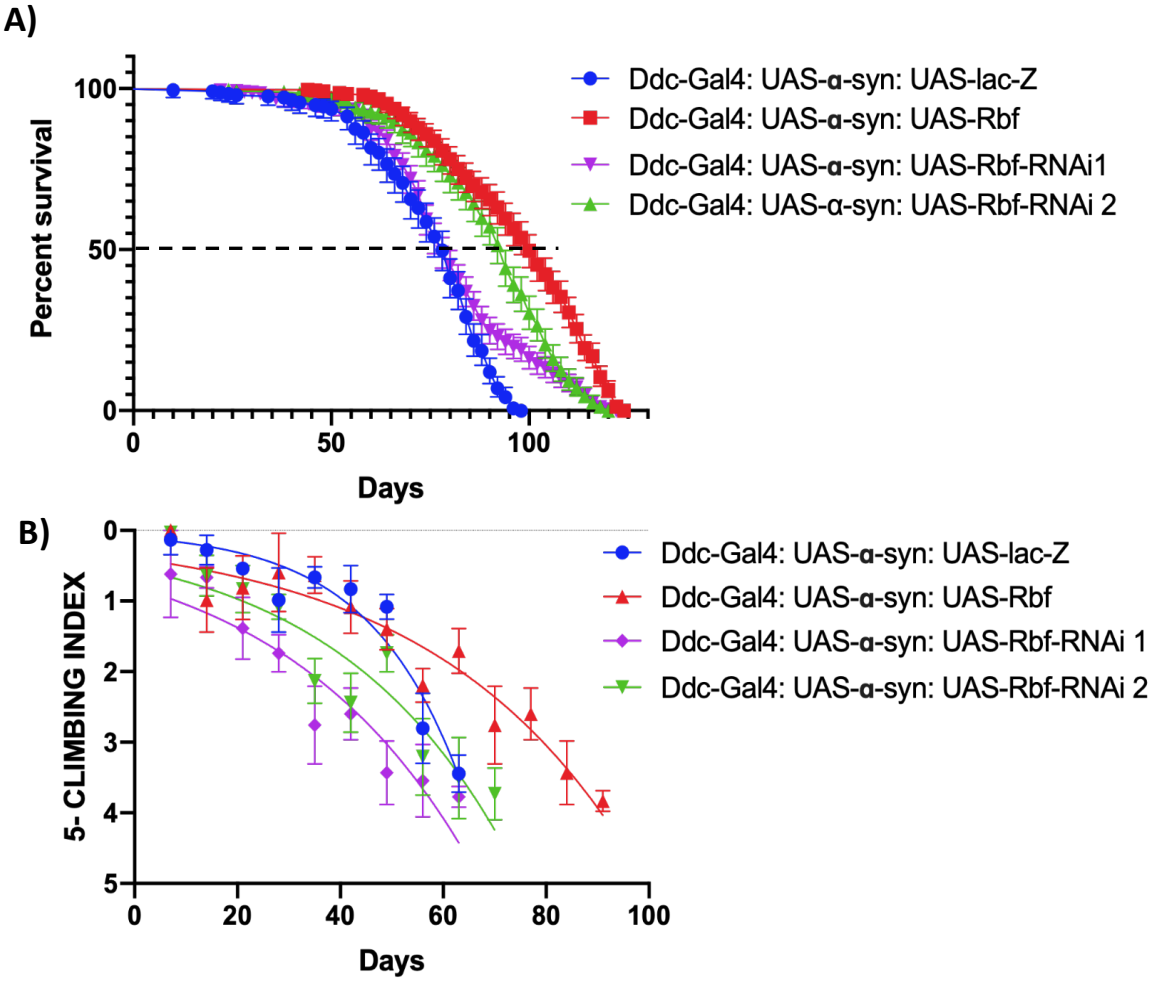

Figure 6.4: Altered expression of *Rbf,* in the *Ddc-Gal4$^{4.36}$ UAS-α-synuclein* model of PD. A). In the control, *Ddc-Gal4$^{4.36}$*; *UAS-α-synuclein UAS-lacZ* critical class males resulted in a median life span of 78 days (n=257). The overexpression of *Rbf* results in a median lifespan of 100 days (n=376), much higher compare to control determined by the Log-rank Mantel-Cox test at P-value of <0.0001, with Bonferroni correction. The inhibition of *Rbf* by two RNAi lines directed by the *Ddc-Gal4$^{4.36}$ UAS-α-synuclein* transgene, result in the median lifespan of 82 and 94 days higher compared to control, determined by Log-rank Mantel-Cox test at P value <0.0001 (n~250), with Bonferroni correction. The graph of longevity assay was generated by GraphPad prism8. **B).** The GraphPad prism8 generated a graph of the climbing abilities of *Ddc-Gal4 UAS-α-synuclein* flies when expressing *Rbf, Rbf-RNAi's* and control. The climbing abilities of flies overexpressing *Rbf* has improved compared to control as determined in the non-linear fitting of the climbing curve by a 95% confidence interval (P-value <0.0001). The climbing abilities of flies expressing *UAS-Rbf-RNAi's* has further compromised compared to control as determined in the non-linear fitting of the climbing curve by a 95% confidence interval with P-value of <0.0001 and 0.0005 (n=50). The graph of longevity assay was generated by GraphPad prism8 non-linear regression curve.

Discussion

The dysfunctional mitochondria in PD pathogenesis and the role of *α-synuclein* in the impairment of mitochondrial health is critical. The overexpression or mutation of *α-synuclein* in PD patients and models of PD has been well established (Singleton et al. 2003; Winkler et al. 2007; Ingelsson 2016). Here (see Table 6.1), the expression of *α-synuclein* directed through a *Ddc-Gal4*$^{4.36}$ transgene activity compromised lifespan and climbing ability similar to PD-like phenotypes observed in earlier experiments (Githure and Staveley 2016c; Dehay and Fernagut 2016). Likely, this is due to the induction of apoptosis in DA neurons as *α-synuclein* impairs exocytosis of neurotransmitter. This affects the neuronal communication by the disruption of membrane trafficking, the alteration of the synaptic vesicle pool, the inhibition the presynaptic SNARE complex protein and the reduction of the retrieval of endocytic synaptic vesicles (Bridi and Hirth 2018). The interactions with the mitochondrial complex I cause mitochondrial dysfunction (Devi et al. 2008). It can inhibit or alter various vesicular system including ER-Golgi transport, the ubiquitin-proteasome system, endosomal-lysosomal system, and autophagy in-turn promote apoptosis (Wang and Hay 2015). The disrupted pathways may indicate a protective mechanism initiated by *α-synuclein* to promote apoptosis and minimize the cellular damage. While the mechanism is unclear, the involvement of *α-synuclein* is evident in PD.

To rescue the phenotype induced by *α-synuclein* expression, I altered the expression of the anti-apoptotic Bcl-2 family member, *Buffy*. The overexpression of Buffy diminishes, and RNAi inhibition of *Buffy* enhances the *α-synuclein*-induced phenotypes of decreased median lifespan and early onset of climbing ability defect (Githure and Staveley 2016c). The role of *Buffy* in the protection against cellular impairment is well established in the rescue of PD phenotypes induced by various

other genes such as *Pink1, HtrA2, Bax-inhibitor-1, Pdxk, MICU1 homologue, Pi3K59F, porin, CG2076, GHITM* (Githure and Staveley 2016b, 2016c, 2016d, 2017a, 2017b, 2017c, 2017d). The inhibition of the *Buffy* antagonist, the pro-apoptotic Bcl-2 family member *Debcl,* (Quinn et al. 2003), acts to partially rescue these phenotypes. The cellular function of *Buffy* is to protect mitochondria from harm (Senoo-Matsuda et al. 2005; Githure and Staveley 2017a). Buffy's rescue effect signifies that the mitochondrial associated pro-cell survival Bcl-2 protein functions downstream of *α-synuclein* initiated cellular dysfunction.

The α-syn*uclein* protein has been demonstrated to interact with the mitochondrial membrane and other vesicular membranes: the *α-synuclein* mutant mouse models have endocytic deficits in synaptic vesicles (Vargas et al. 2014). The loss of α-syn*uclein* activity modifies the morphology of the mitochondria by modifying the Drp1 function at the mitochondrial membrane (Fan et al. 2019). To emphasize the importance of mitochondrial fission, the *α-synuclein*-induced impairment of autophagy and mitochondrial function in rat DA neuronal cells can be rescued by the inhibition of *Drp1* (Fan et al. 2019). My results show the novel rescue of *α-synuclein* expression phenotype by *Drp1* inhibition, increase in median lifespan and an enhanced climbing ability over-time. Importantly, the overexpression of this *Drp1* in selected neurons along with *α-synuclein* have resulted in a longer lifespan coupled with a severely impaired climbing ability. It implies that *α-synuclein* induced toxicity is pro-apoptotic mitochondrial fragmentation; we found this can be rescued by a decrease in the expression of *Drp1* and the pathway seems conserved between mammals and diptera.

To fully understand the consequences of direct or indirect interactions of *Rbf* and *α-synuclein* in the PD model, more experimental exploration is desirable. The overexpression of Rbf in the α-synuclein-dependent PD models results in an increased median lifespan and rescued climbing ability defects. The *α-synuclein* mediated increase in CDK5 activity and Rb inactivation seems to be conserved in flies and can be rescued by *Rb/Rbf* overexpression (Hamdane et al. 2005). The rise in CDK5 function heightens E2F transcription factor activity and may be an underlying mechanism in neuronal cell death (Futatsugi et al. 2012). The expression of the *Rbf-RNAi* transgenes produced a toxic effect that produced a consistent decrease in climbing ability over time. The toxic effect of *Rbf* inhibition seems similar to the consequences of the inactivation of *Rbf* which frees E2F transcription factor (Höglinger et al. 2007). The E2F transcription factor initiates transcription of pro-apoptotic genes in neuronal cells (Liu and Greene 2001; Höglinger et al. 2007). The molecular mechanism by which *Rbf* modifies the *α-synuclein* induced PD-like phenotypes seems to involve E2F mediated transcription of the apoptotic genes.

	Genotype	Median lifespan	Lifespan Increased/ Decreased	Climbing Ability Increased/ Decreased
Control	*Ddc-Gal4$^{4.36;}$ UAS-lac Z*	92 days		
Experiment	*Ddc-Gal4$^{4.36;}$ UAS-α-syn*	74 days	Decreased	Decreased
Control	*Ddc-Gal4$^{4.36;}$ UAS-α-syn; UAS-lacZ*	78 days		
Experiment	*Ddc-Gal4$^{4.36;}$ UAS-α-syn; UAS-Buffy*	88 days	Increased	Increased
	Ddc-Gal4$^{4.36;}$ UAS-α-syn; UAS-Buffy-RNAi	68 days	Decreased	Decreased
	Ddc-Gal4$^{4.36;}$ UAS-α-syn; UAS-Debcl^{EY05743}	66 days	Decreased	Decreased
	Ddc-Gal4$^{4.36;}$ UAS-α-syn; UAS-Debcl-RNAi^{v47515}	86 days	Increased	Decreased
Control	*Ddc-Gal4$^{4.36;}$ UAS-α-syn; UAS-lacZ*	78 days		
Experiment	*Ddc-Gal4$^{4.36;}$ UAS-α-syn; UAS-Drp1*	94 days	Increased	Decreased
	Ddc-Gal4$^{4.36;}$ UAS-α-syn; UAS-Drp1-RNAi-1^{JF02762}	88 days	Increased	Increased
	Ddc-Gal4$^{4.36;}$ UAS-α-syn; UAS-Drp1-RNAi-2^{HMC03230}	82 days	Increased	Increased
Control	*Ddc-Gal4$^{4.36;}$ UAS-α-syn; UAS-lacZ*	78 days		
Experiment	*Ddc-Gal4$^{4.36;}$ UAS-α-syn; UAS-Rbf*	100 days	Increased	Increased
	Ddc-Gal4$^{4.36;}$ UAS-α-syn; UAS-Rbf-RNAi-1^{HMS03004}	82 days	Increased	Decreased
	Ddc-Gal4$^{4.36;}$ UAS-α-syn; UAS-Rbf-RNAi-2^{GL01293}	94 days	Increased	Decreased

Table 6.1: Summary of the Results. The effect of the directed expression of *UAS-α-synuclein* by the *Ddc-Gal4$^{4.36}$* transgene on the median lifespan and climbing ability of the critical class male flies. The effect of the altered expression of *Buffy, Drp1* and *Rbf* genes directed by *Ddc-Gal4$^{4.36}$* along with *UAS-α-synuclein transgene* on median lifespan and climbing ability of the critical class male flies. The cells with blue highlight denote control; orange highlight denotes the decreased compared to control and green highlights denote the increase compare to control.

Conclusion

The aggregation of α-synuclein protein in DA neurons seems to promote the process of apoptosis. The overexpression of Buffy increases health span seems to protect mitochondria, by its anti-apoptotic properties and prevent neuronal cell death. To some extent, the mitochondrial fission protein Drp1 can influences the α-synuclein-induced PD phenotype. As well the Rbf protein, which is known to regulate cell cycle and play a role in apoptosis regulation, can alter the α-synuclein-induced phenotypes. The variation in the consequences of the altered expression of *Buffy, Drp1* and *Rbf* reveals the complexity of the cellular pathways that are transformed by the presence of α-synuclein aggregates in PD models.

Bibliography

Auluck, P.K., Chan, H.Y.E., Trojanowski, J.Q., Lee, V.M.Y., and Bonini, N.M. 2002. Chaperone suppression of α-synuclein toxicity in a Drosophila model for Parkinson's disease. Science (80-.). **295**(5556): 865–868. Science. doi:10.1126/science.1067389.

Bridi, J.C., and Hirth, F. 2018, February 19. Mechanisms of α-Synuclein induced synaptopathy in parkinson's disease. Frontiers Media S.A. doi:10.3389/fnins.2018.00080.

Dehay, B., and Fernagut, P.O. 2016, June 1. Alpha-synuclein-based models of Parkinson's disease. Elsevier Masson SAS. doi:10.1016/j.neurol.2016.04.003.

Devi, L., Raghavendran, V., Prabhu, B.M., Avadhani, N.G., and Anandatheerthavarada, H.K. 2008. Mitochondrial import and accumulation of α-synuclein impair complex I in human dopaminergic neuronal cultures and Parkinson disease brain. J. Biol. Chem. **283**(14): 9089–9100. doi:10.1074/jbc.M710012200.

Fan, R.Z., Guo, M., Luo, S., Cui, M., and Tieu, K. 2019. Exosome release and neuropathology induced by α-synuclein: New insights into protective mechanisms of Drp1 inhibition. Acta Neuropathol. Commun. **7**(1): 184. BioMed Central Ltd. doi:10.1186/s40478-019-0821-4.

Feany, M.B., and Bender, W.W. 2000. A Drosophila model of Parkinson's disease. Nature **404**(6776): 394–398. Nature Publishing Group. doi:10.1038/35006074.

Futatsugi, A., Utreras, E., Rudrabhatla, P., Jaffe, H., Pant, H.C., and Kulkarni, A.B. 2012. Cyclin-dependent kinase 5 regulates E2F transcription factor through phosphorylation of Rb protein in neurons. Cell Cycle **11**(8): 1603–1610. Taylor and Francis Inc. doi:10.4161/cc.20009.

Giovanni, A., Keramaris, E., Morris, E.J., Hou, S.T., O'Hare, M., Dyson, N., Robertson, G.S., Slack, R.S., and Park, D.S. 2000. E2F1 mediates death of B-amyloid-treated cortical neurons in a manner independent of p53 and dependent on Bax and caspase 3. J. Biol. Chem. **275**(16): 11553–11560. J Biol Chem. doi:10.1074/jbc.275.16.11553.

Githure, M.P., and Staveley, B.E. 2017a. Inhibition of mitochondrial calcium uptake 1 in Drosophila

neurons. Genet. Mol. Res. 16(1): 16019436. doi:10.4238/gmr16019436.
Githure, P.M., and Staveley, B.E. 2016a. Bcl-2 homologue Debcl enhances α-synuclein-induced phenotypes in Drosophila. PeerJ 2016(9). PeerJ Inc. doi:10.7717/peerj.2461.
Githure, P.M., and Staveley, B.E. 2016b. The HtrA2 Drosophila model of Parkinson's disease is suppressed by the pro-survival Bcl-2 Buffy. doi:10.1139/gen-2016-0069.
Githure, P.M., and Staveley, B.E. 2016c. The Bcl-2 homologue Buffy rescues α-synuclein-induced Parkinson disease-like phenotypes in Drosophila. BMC Neurosci. 17(1): 24. BioMed Central Ltd. doi:10.1186/s12868-016-0261-z.
Githure, P.M., and Staveley, B.E. 2016d. Loss of porin function in dopaminergic neurons of Drosophila is suppressed by Buffy. J. Biomed. Sci. 23(1): 84. BioMed Central. doi:10.1186/s12929-016-0300-1.
Githure, P.M., and Staveley, B.E. 2017b. A loss of Pdxk model of Parkinson disease in Drosophila can be suppressed by Buffy. BMC Res Notes 10: 205. doi:10.1186/s13104-017-2526-8.
Githure, P.M., and Staveley, B.E. 2017c. Bax-inhibitor-1 knockdown phenotypes are suppressed by Buffy and exacerbate degeneration in a Drosophila model of Parkinson disease. doi:10.7717/peerj.2974.
Githure, P.M., and Staveley, B.E. 2017d. Overexpression of Buffy enhances the loss of parkin and suppresses the loss of Pink1 phenotypes in Drosophila. Genome 60(3): 241–247. NRC Research Press. doi:10.1139/gen-2016-0165.
Guardia-Laguarta, C., Area-Gomez, E., Rüb, C., Liu, Y., Magrané, J., Becker, D., Voos, W., Schon, E.A., and Przedborski, S. 2014. α-synuclein is localized to mitochondria-associated ER membranes. J. Neurosci. 34(1): 249–259. J Neurosci. doi:10.1523/JNEUROSCI.2507-13.2014.
Hamdane, M., Bretteville, A., Sambo, A.V., Schindowski, K., Bégard, S., Delacourte, A., Bertrand, P., and Buée, L. 2005. p25/Cdk5-mediated retinoblastoma phosphorylation is an early event in neuronal cell death. J. Cell Sci. 118(6): 1291–1298. Company of Biologists Ltd. doi:10.1242/jcs.01724.
Höglinger, G.U., Breunig, J.J., Depboylu, C., Rouaux, C., Michel, P.P., Alvarez-Fischer, D., Boutillier, A.L., DeGregori, J., Oertel, W.H., Rakic, P., Hirsch, E.C., and Hunot, S. 2007. The pRb/E2F cell-cycle pathway mediates cell death in Parkinson's disease. Proc. Natl. Acad. Sci. U. S. A. 104(9): 3585–3590. National Academy of Sciences. doi:10.1073/pnas.0611671104.
Ingelsson, M. 2016, September 5. Alpha-synuclein oligomers-neurotoxic molecules in Parkinson's disease and other lewy body disorders. Frontiers Media S.A. doi:10.3389/fnins.2016.00408.
Jordan-Sciutto, K.L., Dorsey, R., Chalovich, E.M., Hammond, R.R., and Achim, C.L. 2003. Expression patterns of retinoblastoma protein in Parkinson disease. J. Neuropathol. Exp. Neurol. 62(1): 68–74. American Association of Neuropathologists Inc. doi:10.1093/jnen/62.1.68.
Kamp, F., Exner, N., Lutz, A.K., Wender, N., Hegermann, J., Brunner, B., Nuscher, B., Bartels, T., Giese, A., Beyer, K., Eimer, S., Winklhofer, K.F., and Haass, C. 2010. Inhibition of mitochondrial fusion by α-synuclein is rescued by PINK1, Parkin and DJ-1. EMBO J. 29(20): 3571–3589. European Molecular Biology Organization. doi:10.1038/emboj.2010.223.
Kaur, U., and Lee, J.C. 2020. Unroofing site-specific α-synuclein–lipid interactions at the plasma membrane. Proc. Natl. Acad. Sci.: 202006291. National Academy of Sciences. doi:10.1073/pnas.2006291117.
Liu, D.X., and Greene, L.A. 2001. Regulation of neuronal survival and death by E2F-dependent gene repression and derepression. Neuron 32(3): 425–438. Cell Press. doi:10.1016/S0896-

6273(01)00495-0.

Motyl, J., Wencel, P.L., Cieślik, M., Strosznajder, R.P., and Strosznajder, J.B. 2017. Alpha-synuclein alters differently gene expression of Sirts, PARPs and other stress response proteins: implications for neurodegenerative disorders. Mol. Neurobiol. **55**(1): 1–14. Humana Press Inc. doi:10.1007/s12035-016-0317-1.

Nagoshi, E. 2018, November 1. Drosophila models of sporadic parkinson's disease. MDPI AG. doi:10.3390/ijms19113343.

Nakamura, K., Nemani, V.M., Azarbal, F., Skibinski, G., Levy, J.M., Egami, K., Munishkina, L., Zhang, J., Gardner, B., Wakabayashi, J., Sesaki, H., Cheng, Y., Finkbeiner, S., Nussbaum, R.L., Masliah, E., and Edwards, R.H. 2011. Direct membrane association drives mitochondrial fission by the Parkinson disease-associated protein α-synuclein. J. Biol. Chem. **286**(23): 20710–20726. American Society for Biochemistry and Molecular Biology. doi:10.1074/jbc.M110.213538.

Pozo Devoto, V.M., and Falzone, T.L. 2017, September 1. Mitochondrial dynamics in Parkinson's disease: A role for α-synuclein? Company of Biologists Ltd. doi:10.1242/dmm.026294.

Quinn, L., Coombe, M., Mills, K., Daish, T., Colussi, P., Kumar, S., and Richardson, H. 2003. Buffy, a Drosophila Bcl-2 protein, has anti-apoptotic and cell cycle inhibitory functions. EMBO J. **22**(14): 3568–79. European Molecular Biology Organization. doi:10.1093/emboj/cdg355.

Recasens, A., and Dehay, B. 2014, December 18. Alpha-synuclein spreading in Parkinson's disease. Frontiers Media S.A. doi:10.3389/fnana.2014.00159.

Senoo-Matsuda, N., Igaki, T., and Miura, M. 2005. Bax-like protein Drob-1 protects neurons from expanded polyglutamine-induced toxicity in Drosophila. EMBO J. **24**(14): 2700–13. European Molecular Biology Organization. doi:10.1038/sj.emboj.7600721.

Singleton, A.B., Farrer, M., Johnson, J., Singleton, A., Hague, S., Kachergus, J., Hulihan, M., Peuralinna, T., Dutra, A., Nussbaum, R., Lincoln, S., Crawley, A., Hanson, M., Maraganore, D., Adler, C., Cookson, M.R., Muenter, M., Baptista, M., Miller, D., Blancato, J., Hardy, J., and Gwinn-Hardy, K. 2003. α-Synuclein Locus Triplication Causes Parkinson's Disease. Science (80-.). **302**(5646): 841. Science. doi:10.1126/science.1090278.

Spillantini, M.G., Schmidt, M.L., Lee, V.M.Y., Trojanowski, J.Q., Jakes, R., and Goedert, M. 1997. α-synuclein in Lewy bodies [8]. doi:10.1038/42166.

Thomas, B., and Beal, M.F. 2011, April 1. Molecular insights into Parkinson's disease. Faculty of 1000 Ltd. doi:10.3410/M3-7.

Vargas, K.J., Makani, S., Davis, T., Westphal, C.H., Castillo, P.E., and Chandra, S.S. 2014. Synucleins regulate the kinetics of synaptic vesicle endocytosis. J. Neurosci. **34**(28): 9364–9376. Society for Neuroscience. doi:10.1523/JNEUROSCI.4787-13.2014.

Wang, T., and Hay, J.C. 2015. Alpha-synuclein toxicity in the early secretory pathway: How it drives neurodegeneration in parkinsons disease. Frontiers Research Foundation. doi:10.3389/fnins.2015.00433.

Winkler, S., Hagenah, J., Lincoln, S., Heckman, M., Haugarvoll, K., Lohmann-Hedrich, K., Kostic, V., Farrer, M., and Klein, C. 2007. α-synuclein and Parkinson disease susceptibility. Neurology **69**(18): 1745–1750. Lippincott Williams and Wilkins. doi:10.1212/01.wnl.0000275524.15125.f4.

Zhang, J., Li, X., and Li, J. Da. 2019a, April 18. The Roles of Post-translational Modifications on α-Synuclein in the Pathogenesis of Parkinson's Diseases. Frontiers Media S.A. doi:10.3389/fnins.2019.00381.

Zhang, Y., Wu, Q., Zhang, L., Wang, Q., Yang, Z., Liu, J., and Feng, L. 2019b. Caffeic acid reduces A53T α-synuclein by activating JNK/Bcl-2-mediated autophagy in vitro and improves behaviour and protects dopaminergic neurons in a mouse model of Parkinson's disease. Pharmacol. Res. **150**. Academic Press. doi:10.1016/j.phrs.2019.104538.

Zigoneanu, I.G., Yang, Y.J., Krois, A.S., Haque, M.E., and Pielak, G.J. 2012. Interaction of α-synuclein with vesicles that mimic mitochondrial membranes. Biochim. Biophys. Acta - Biomembr. **1818**(3): 512–519. Elsevier. doi:10.1016/j.bbamem.2011.11.024.

Chapter 7: Altered expression of *tribbles* (*trbl)* in Drosophila models of Parkinson Disease

Abstract

Cellular stresses may induce Parkinson Disease (PD) and other neurodegenerative diseases. The substantial influence of the insulin receptor signalling pathway in neurodegenerative diseases has led to the trbl. The evolutionarily well-conserved gene trbl is activated during cellular insults, such as oxidative, metabolic, and neuron-specific stresses. Thus, the trbl protein is a pseudokinase and can act in cell survival to promote apoptosis and autophagy. The overexpression of *trbl* in *Drosophila melanogaster* neurons under the control of the *Ddc-Gal4* transgene decreases the lifespan and compromises climbing ability over time. The directed inhibition of *trbl* rescues the loss of *parkin*-dependent model of PD. Interestingly, the α-*synuclein* model of PD is rescued by the increased expression of *trbl*. The directed inhibition of *trbl* can enhance the PD-like phenotype generated by the loss of the *Drp1* to become more severe. Alteration of the expression of *trbl* in three different *Drosophila* models of PD revealed the complex relationship between this modulator of the insulin receptor signalling pathway and its regulators.

Introduction

The tribbles (trbl) family of proteins is evolutionarily conserved in metazoans (Eyers et al. 2017). The proteins encoded by the trbl homologues contain 1) a highly conserved central domain; 2) a non-conserved N-terminal domain; and 3) a C-terminal domain that includes binding sites for both COP-1 and MEK1. In structure, trbl is a pseudokinase adaptor protein that is characterized by the presence of a non-catalytic kinase region (Fischer et al. 2017). Pseudokinases are pseudo enzymes that lack key catalytic residues and, therefore, are catalytically inactive (Jacobsen and

Murphy 2017). While the general functions of pseudokinase proteins remain uncertain, apparently these proteins function in the mediation of protein-protein interaction; have an involvement in cell signalling through the allosteric regulation of the protein kinases activities; act in the direction of cellular localization; and take part in the assembly of signalling complexes. The trbl pseudokinase proteins are often located in the nucleus and function primarily as adaptor proteins to mediate a wide range of intracellular pathways.

Trib3, a human *trbl* homologue, regulates the function of the number of signalling pathways: 1) suppression of Akt phosphorylation; 2) transcriptional activation of CHOP; 3) promotion of ATF4 proteolysis; 4) interaction with MAPKK; and 5) mediation of the degradation of ACC (acetyl-coenzyme A) by E3 ubiquitin ligase (Yokoyama and Nakamura 2011). Abnormalities in insulin receptor signalling (IRS) have been linked to various human conditions and diseases, including neurodevelopmental disorders such as PD and Multiple Sclerosis and the trbl proteins play essential roles in this pathway (Fischer et al. 2017). The expression of *Trbl3* increases in response to a variety of stresses, including mitochondrial stress, endoplasmic reticulum stress, oxidative stress, metabolic stress and various neuronal stresses. The *trbl3* expression increases in PC12 cells when treated with dopaminergic toxins, 6-OHDA or MPP^+ (Aimé et al. 2015). The Trbl protein can be a part of an E3 ubiquitin ligase complex and functions in the ubiquitination of a number of proteins and organelles to initiate the degradation (Eyers et al. 2017). Depending on the molecular cue, the trbl proteins can act to promote both aspects of the processes of apoptosis and autophagy to alleviate neuronal stress.

The pathophysiology of PD is associated with abnormal accumulation of α-synuclein in the substantia nigra pars compacta (SNpc). The mutations of a-synuclein have been determined to

cause the excessive aggregation of Lewy Bodies (LB) and Lewy Neurites (LN) (Stefanis 2012). The α-*synuclein* associated models of PD show formation of proteinaceous inclusions, degeneration of dopaminergic (DA) neuron and the development of locomotion deficits over-time (Cheng et al. 2018). Another PD gene, parkin (park), encodes an E3-ubiquitin-ligase and is vital in regulating mitochondrial health. Parkin, along with Pink1, regulates the process of mitophagy. The role of the parkin extends to the degradation of misfolded proteins and the promotion of autophagy. Parkin acts to suppress dopaminergic toxicity induced by the activity of α-synuclein in Drosophila (Yang et al. 2003). The mitochondrial fission protein, Drp1, acts to assist the Parkin E3 ubiquitin ligase in the process of mitophagy and to support the segregation of depolarised mitochondria (Twig et al. 2008). The cellular stress caused by the presence of misfolded proteins in mitochondria and ER play pivotal roles in neurodegeneration (Bermales et al. 2012). In a concerted effort, Parkin, Drp1 and trbl respond to cellular stress due to the presence of misfolded proteins and promote the processes of autophagy and apoptosis in a manner dependent upon the molecular environment of the cell. The Parkin and Drp1 proteins interact with mitochondrial membrane proteins and have an important role in autophagy, a key step to alleviate stress caused by the accumulation of misfolded proteins.

Properties of the IRS pathway are highly conserved between mammals, including *Homo sapiens*, and insects, such as *Drosophila melanogaster*. *Drp1, trbl*, and *parkin* are highly conserved among these divergent species and appear to have very similar functions. Due to these properties, the effect of alterations in *trbl* expression in the *parkin-RNAi, Drp1-RNAi* and *α-synuclein*-dependent Drosophila models of PD was hypothesised to help elucidate the specific sub-cellular processes in humans and human-related diseases. This study aims to observe the effects of altered

expression of *trbl* under the control of the *Ddc-Gal4* and *GMR-Gal4* transgenes. Evidence of neuronal dysfunction is detected by analyzing the number of ommatidia, intra-ommatidial bristle number and ommatidial area of the *D. melanogaster* compound eye. The inhibition and overexpression of *trbl* by *Ddc-Gal4* in combination with *parkin-RNAi, Drp1-RNAi,* and the human *a-synuclein* transgenes will be analyzed using ageing and locomotion analysis. The inhibition of *trbl* in concert with *Ddc-Gal4*$^{4.3D}$ *UAS-parkin-RNAi* transgene resulted in an increased median lifespan and an enhanced ability to climb over time. The inhibition and overexpression of *trbl* along with *Drp1-RNAi* further augment the PD-like phenotypes. The overexpression of *trbl* along with the *a-synuclein* transgene increased the lifespan and climbing ability to a great degree. The purpose of this study is to further understand the role of trbl in *D. melanogaster* and to make implications of its role in the IRS and human-related diseases.

Materials and methods

Bioinformatic analysis

Protein sequences were obtained from the National Center of Biotechnology Information (NCBI) database *(https://www.ncbi.nlm.nih.gov/protein/).* The conserved domains and ATP binding regions were identified using the NCBI Conserved Domain Database *(https://www.ncbi.nlm.nih.gov/cdd/)*, and Eukaryotic Linear Motif *(http://elm.eu.org/).* Multiple sequence alignment was accomplished through the use of Clustal Omega *(https://www.ebi.ac.uk/Tools/msa/clustalo/)* to reveal the conservation of domains and further confirmed by TargetATPsite (*http://www.csbio.sjtu.edu.cn:8080/TargetATPsite/index.jsp).* The

conserved Catalytic loop, Mg^{2+} binding site, MEK-1 Binding site and COP-1 Binding site was identified from comparison to canonical kinase (Dobens and Bouyain 2012).

Drosophila stocks and media

The *Ddc-Gal4$^{4.36}$(w[1118]; P{w[+mC]=Ddc-Gal4.L}Lmpt[4.36]; Ddc-Gal4$^{4.3D}$(w[1118]; P{w[+mC]=Ddc-GAL4.L}4.3D); GMR-Gal4^{12}; UAS-lacZ^{4-1-2}; UAS-trbl-1* or *UAS-trbl.M (w[1118];P{w[+mC]=UASp-trbl.M}3), UAS-trbl-2* or *UAS-trbl^{EP3519} (w[1118];P{w[+mC]=EP}trbl[EP3519]/TM6B, Sb [1]), UAS-trbl-3* or *UAS-trbl^{EP1119} (w[1118];P{w[+mC]=EP}trbl[EP1119]/TM6B, Tb [1]), UAS-trbl-RNAi-1* or *UAS-trbl RNAi^{HMS04999} (y[1]sc[*]v[1];P{y[+7.7]v[+1.8]=TRiP.HMS04999}attP2), UAS-trbl-RNAi-2* or *UAS-trbl RNAi^{HMC04159} (y[1]sc[*]v[1];P{y[+7.7]v[+1.8]=TRiP.HMC04159}attP2), UAS-trbl-RNAi-3* or *UAS-trbl RNAi ^{GL01337} (y[1]sc[*]v[1];P{y[+7.7]v[+1.8]=TRiP.GL01337}attP2)* and the *UAS-Drp1-RNAi (y[1] v[1]; P{y[+t7.7] v[+t1.8]=TRiP.JF02762}attP2})*; stocks were obtained from Bloomington Drosophila Stock Center at Indiana University, Bloomington, Indiana, USA. The *UAS-parkin-RNAi* line was obtained from Dr. B. Lu (Yang et al. 2003, 2006). The *UAS-α-synuclein* was generously provided by Dr. M. Feany of Harvard Medical School (Feany and Bender 2000). The *Ddc-Gal4$^{4.3D}$ parkin-RNAi, Ddc-Gal4$^{4.3D}$Drp1-RNAi* and *Ddc-Gal4$^{4.36}$ α-synuclein* lines were produced through standard methods (M'angale and Staveley 2016). All flies were maintained on standard cornmeal/molasses/yeast/agar media treated with propionic acid and methylparaben to resist fungal growth. Stocks were kept at room temperature (22° ± 3° C), whereas crosses and experiments were maintained at 25°C.

Survival assay

Female virgins were collected every 8 to 12 hours for several days. The confirmed virgin flies were then crossed with *UAS-lacZ, UAS-trbl* and *UAS-trbl-RNAi* males. Critical class male progeny were collected from these matings until approximately 250 flies of each genotype were obtained. To avoid over-crowding, the flies were maintained in cohorts of 25 or less per vial on standard cornmeal/molasses/yeast/agar media. Flies were scored every second day for viability and were transferred to new food every two to five days. The scoring continued until all flies had died (Todd and Staveley 2004, 2012). The longevity data were analyzed using GraphPad Prism version 8 statistical software (*graphpad.com*), and survival curves were compared by the Mantel-Cox test. Significance were determined at a 95% confidence level ($P \leq 0.05$) with Bonferroni correction.

Locomotor analysis

The 70 critical class male flies were collected within 24 hours and maintained as cohorts of ten flies in each vial. The media was replenished twice a week. The climbing assay was performed as previously described according to a standard protocol (Todd and Staveley 2004, 2012). Briefly, every week 50 males were assayed, in groups of 10, for their ability to climb a glass tube divided into five levels of 2 cm each. The climbing index was calculated for each week using GraphPad prism version 8 statistical software. The climbing curve was fitted using nonlinear regression and determined at a 95% confidence interval ($P \leq 0.05$).

Biometric analysis of the *Drosophila melanogaster* eye

Female virgins of the *GMR-Gal4* genotype were collected every 8 to 12 hours for several days. Then, the confirmed virgins were crossed with the males of *UAS-lacZ*, *UAS-trbl* and *UAS-trbl1-RNAi*

genotypes. The resultant critical class male progeny were collected for each genotype. The collected flies were kept as cohorts of 10 flies or less upon fresh media and allowed to age for 3 to 4 days. The flies were prepared for scanning electron microscopy following the standard protocol established in our lab (Githure and Staveley 2017). Ommatidia and interommatidial bristle counts were performed on ten or more flies of each genotype using the National Institute of Health (NIH) ImageJ software. The ommatidium area was calculated by measuring the area of 5 distinct ommatidial "rosettes" per fly eye and then dividing by 7 to determine the mean area of each ommatidium; done on ten eyes of each genotype. The Biometric analysis was performed using GraphPad Prism version 8 statistical software. Significance were determined at 95% confidence level ($P \leq 0.05$).

Results:

Trbl is highly conserved among *Homo sapiens* and *Drosophila melanogaster*

The *trbl* protein sequence of *D. melanogaster* was sourced from NCBI Protein Database, and the conserved sequences were identified by using the NCBI Conserved Domain Database. NCBI protein Blast of trbl protein sequence of *D. melanogaster* (NP_524672.1) with the *H. sapiens,* identified the *trbl* homologue 2 (NP_067675.1), it has a protein sequence that is 39% identical and 58% similar. The multiple sequence alignment of the two proteins derived by Clustal Omega (Figure 7.1) shows a highly conserved Protein Kinase, catalytic domain. The well-conserved ATP binding domains were identified by NCBI CDD; 131-134, 139, 152, 154, 189, 264, 268-269 and 283-284 in *trbl* of *D. melanogaster* and 67-70, 76, 88, 90, 114, 175, 179-180 and 194-195 of *H. sapiens* (Table 7.1). The Catalytic loop, Mg^{2+} binding site, MEK-1 binding site and COP-1 binding site is well

conserved (Dobens and Bouyain 2012). As this protein is well conserved, it may be very likely that the functions may be very similar.

Conserved sequence	*D. melanogaster (trbl)*	*H. Sapiens (trbl3)*
ATP binding site	131-134	67-70
	139	76
	152	88
	154	90
	189	114
	264	175
	268-269	179-180
	283-284	194-195
Catalytic loop	263-269	174-180
$Mg2^{+}$ Binding site	281-284	192-195
MEK-1 binding site	391-397	302-308
COP-1 binding site	436-440	336-340

Table 7. 1: Tabulation of the canonical sequence of the conserved domains between the *Homo sapiens* trbl3 and *Drosophila melanogaster* trbl proteins.

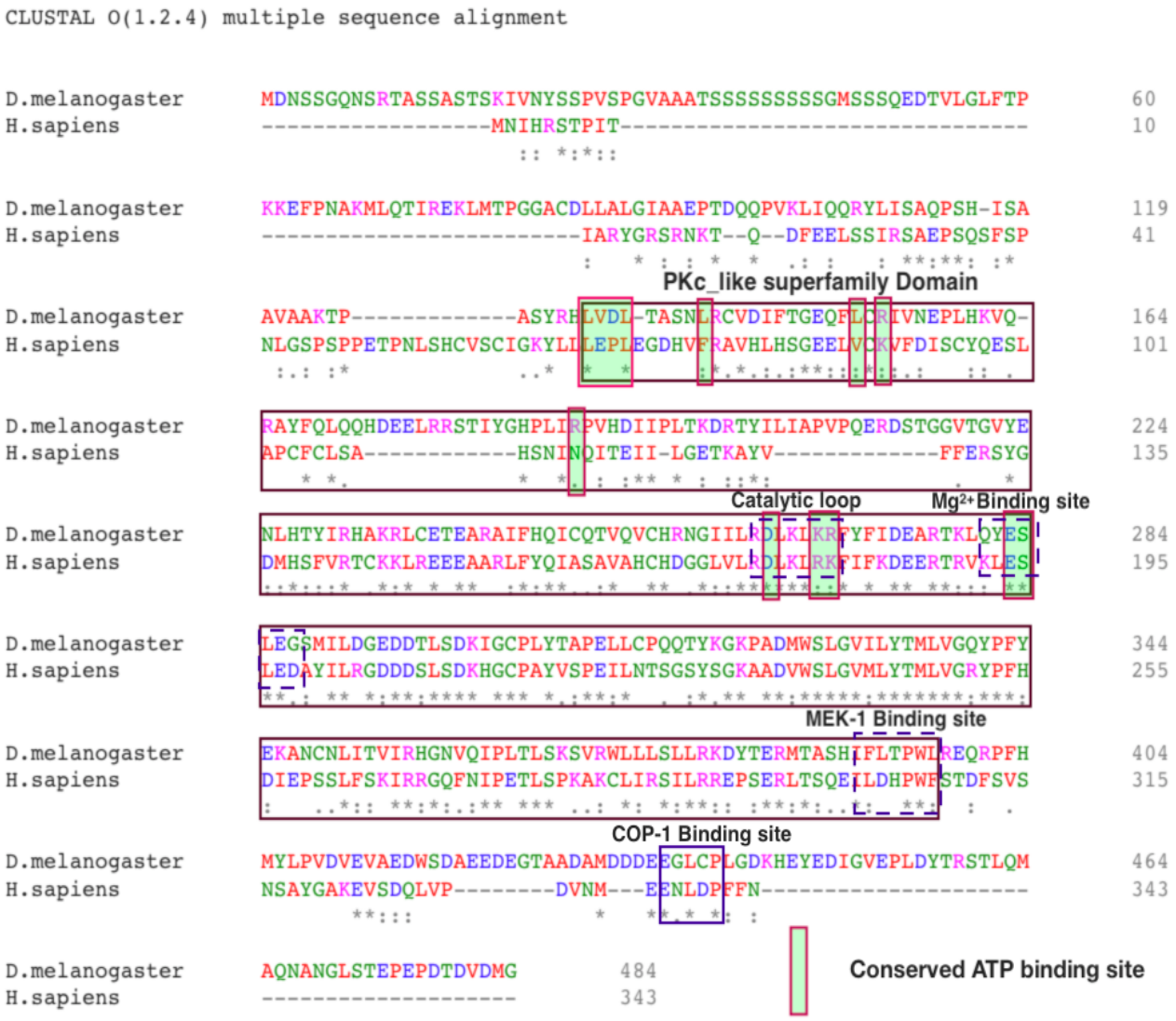

Figure 7.1: *Trbl* is evolutionarily conserved between Drosophila and humans. A Clustal Omega multiple sequence alignment (Sievers et al. 2011) of *D. melanogaster* trbl (NP_524672.1) with the *H. sapiens* (NP_067675.1) shows evolutionarily conserved domains identified using the NCBI Conserved Domain Database (CDD) and further confirmed by the Eukaryotic Linear Motif (ELM) resource. The well documented Mg^{2+} binding site, MEK-1 binding site, COP-1 binding site and ATP binding sites in *H. sapiens* and *D. melanogaster*. The asterisks indicate the residues that are identical; the colons indicate the conserved substitutions; and the dots indicate the semi-conserved substitutions. Colour differences indicate the chemical nature of amino acids: red indicates small hydrophobic (includes aromatic) residues; blue indicates acidic; magenta indicates basic; and green indicates basic with hydroxyl or amine groups.

The overexpression and inhibition of *trbl* directed by *Ddc-Gal4$^{4.3D}$*

As the control, *Ddc-Gal4$^{4.3D}$; UAS-lacZ* critical class males were determined to have a median lifespan of 68 days (n=340). The overexpression of *trbl* by *UAS-trbl-1.M*, *UAS-trbl-2^{EP3519}* and *UAS-trbl-3^{EP1119}* under the direction of the *Ddc-Gal4$^{4.3D}$* transgene produced median lifespans of 66 (n=259), 64 (n=254) and 54 (n=261) days, with last showing a significant decrease compared to the control with a P-value of 0.6594, 0.1590 and <0.0001 respectively, (Figure 7.2A) as determined by log-rank (Mantel-Cox). The inhibition of *trbl* by *UAS-trbl-RNAi1, UAS-trbl-RNAi2* and *UAS-trbl-RNAi3* under the direction of the *Ddc-Gal4$^{4.3D}$* transgene has a median lifespan of 78 (n=257), 70 (n=263) and 70 (n=268) days, increased compared to the control with a P-value <0.0001, 0.0280 and 0.0078 respectively (Figure 7.2B) as determined by log-rank Mantel-Cox test with Bonferroni correction. The overexpression and inhibition of *trbl* in neurons caused early onset of impairment in climbing ability. The non-linear fit of the climbing curve shows *trbl* overexpression lines has compromised the climbing ability phenotype compared to control at 95% CI (P-value <0.0001) (Figure 2C) (n=50). The non-linear fitting of the climbing curve shows *trbl* inhibition lines has compromised the climbing ability phenotype compared to control at 95% CI (P-value 0.0002, <0.0001 and 0.1163) (Figure 7.2C) (n=50).

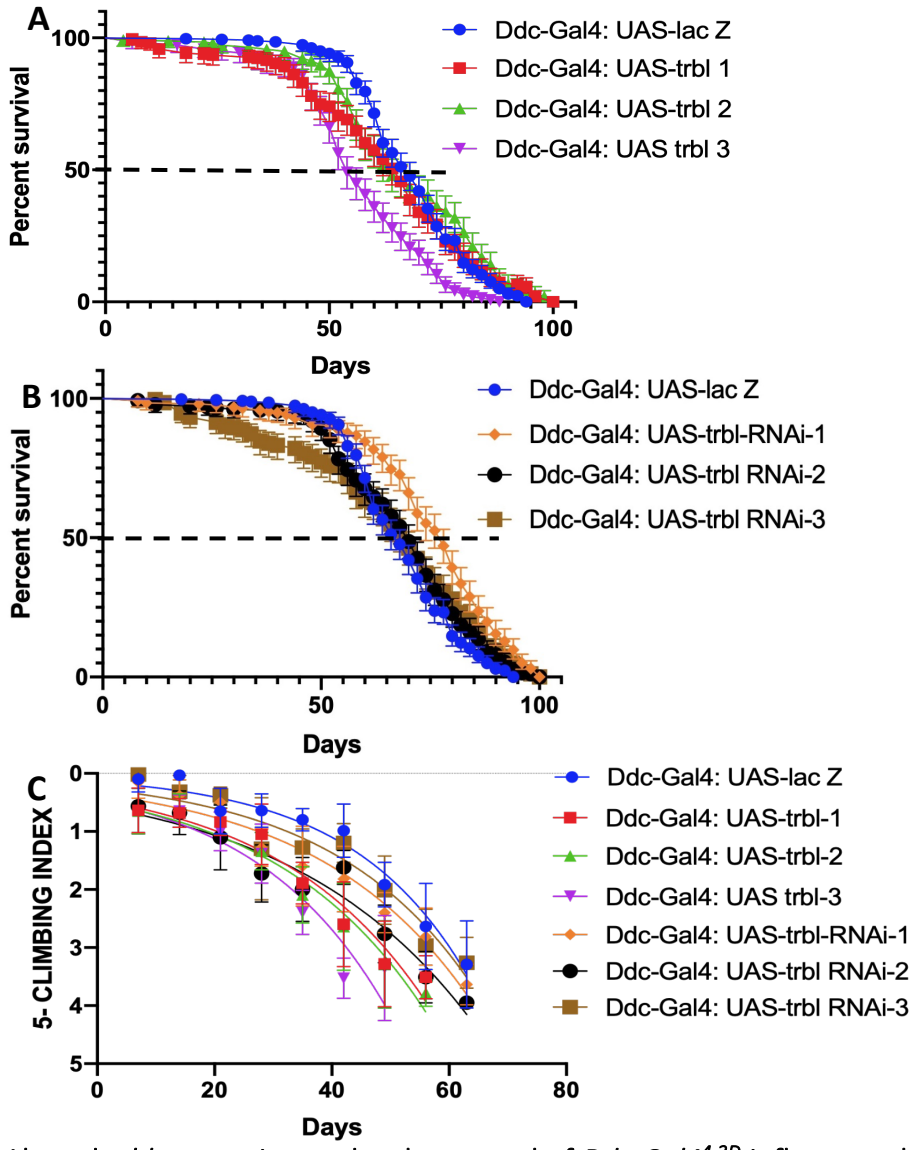

Figure 7. 2: Altered *trbl* expression under the control of *Ddc-Gal4$^{4.3D}$* influences the survival and climbing ability of flies. **A**. The GraphPad prism8 generated graph of the longevity assay for the expression of *trbl, trbl RNAi's* under the control of *Ddc-Gal4$^{4.3D}$* transgene. The overexpression results in decreased median lifespan of 66 days in *trbl.M(UAS-trbl-1)*, 64 days in *trbl^{EP3519}*(UAS-trbl-2) and 54 days in *trbl^{EP1119}* (UAS-trbl-3) compared to 68 days of control determined by Log-rank Mantel Cox test, with Bonferroni correction. **B.** The inhibition of *trbl* under the control of *Ddc-Gal4* transgene results in increased lifespan of 78 days with *UAS-trbl-RNAi-1(trbl-RNAi^{HMS04999})*, 70 days with *UAS-trbl-RNAi-2(*trbl-RNAi^{HMC04159}*)* and 70 days with *UAS-trbl-RNAi3(*trbl-RNAi^{GL01337}*)* compare to 68 days of control determined by Log-rank Mantel Cox test, with Bonferroni correction. **C**. The GraphPad prism8 generated graph of the climbing abilities of flies with overexpression of *trbl, trbl RNAi* and control. The non-linear fitting of the climbing ability of *trbl* overexpression and *trbl RNAi's* flies is less compared to control as determined at 95% confidence intervals. Error bars indicate the SEM and n=50.

The altered co-expression of *trbl* along with *parkin-RNAi* via *Ddc-Gal4$^{4.3D}$*

The loss of function of the *parkin* has led to the establishment of several Drosophila models of PD. In this experiment, the control *Ddc-Gal4$^{4.3D}$ UAS-parkin-RNAi UAS-lacZ* critical males were determined to have a median lifespan of 64 days (n=251). The overexpression of *trbl* by *UAS-trbl1* and *UAS-trbl-3* along with *UAS-parkin-RNAi* under the direction of the *Ddc-Gal4* transgene has a median lifespan of 66 (n=374) and 64 days (n=376), similar to control with a P-value of 0.8549 and 0.0512. However, the *UAS-trbl-2* along with *UAS-parkin-RNAi* under the direction of the *Ddc-Gal4* transgene has a median lifespan of 54 days (n=255), much less compare to the control with a P value of <0.0001 as determined by log-rank (Mantel-Cox) test with a Bonferroni correction (Figure 7.3A). The inhibition of *UAS-trbl-RNAi1, UAS-trbl-RNAi2* and *UAS-trbl-RNAi3* along with *UAS-parkin-RNAi under the direction of the Ddc-Gal4* transgene has a median lifespan 76 (n=287), 70 (n=319) and 70(n=324) days, increased compared to the control (Figure 3B) with a P value <0.0001 as determined by log-rank Mantel-Cox test with a Bonferroni correction. The non-linear fitting of the climbing curve shows *trbl* overexpression has further contributes to loss of the climbing ability throughout the life of critical class flies compared to control at 95% CI (p <0.0001) (Figure 7.3C). The inhibition of *trbl* by *UAS-trbl-RNAi2* and *UAS-trbl-RNAi3* along with *Ddc-Gal4 UAS-parkin-RNAi* has climbing curve similar to control at 95% CI (P value=0.0523 and 0.0577). The inhibition by *UAS-trbl-RNAi^{HMS04999}* has partially rescued the decline in climbing ability compared to control at 95% CI with P-value 0.0003 (Figure 7.3C) (n=50).

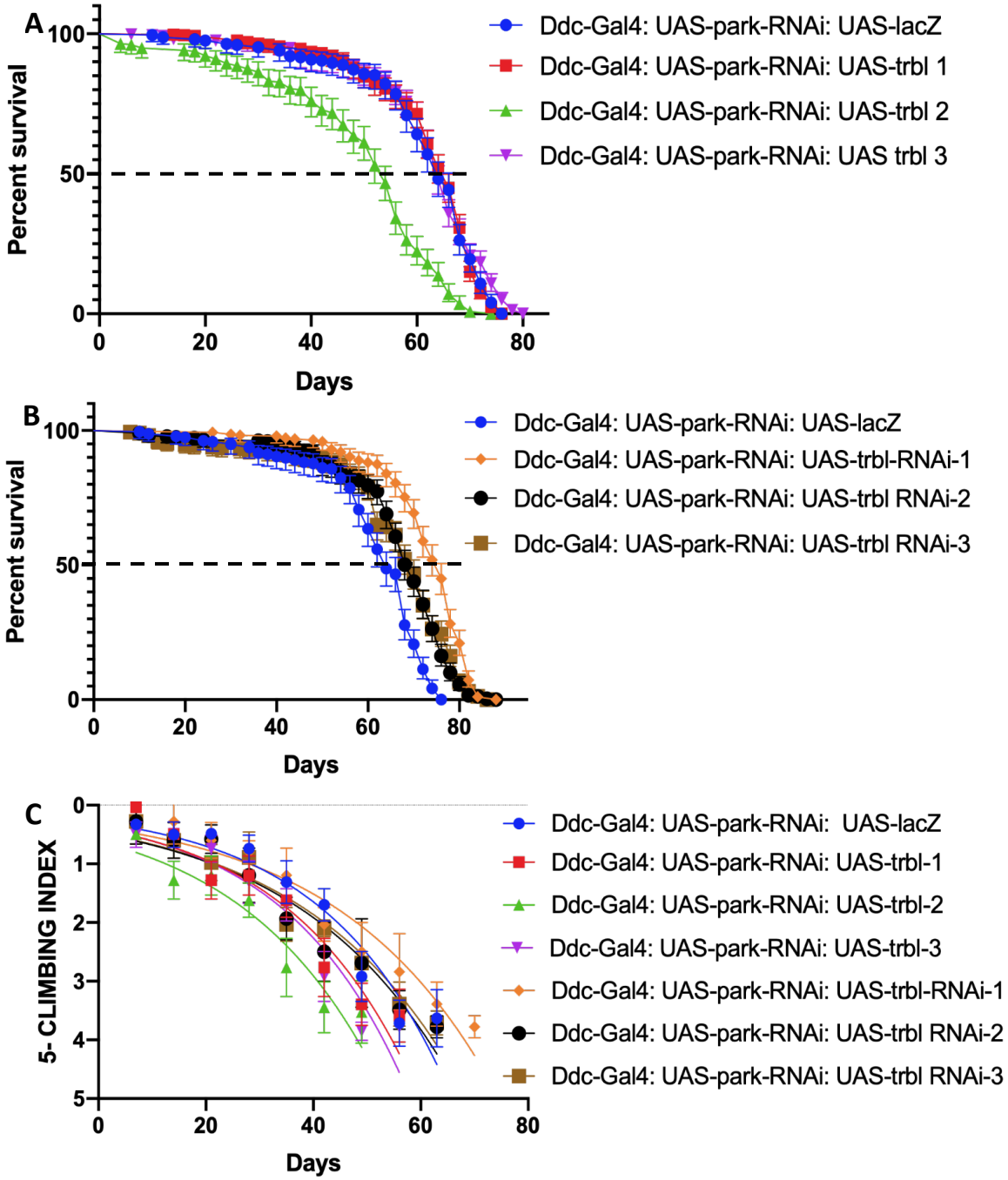

Figure 7.3: Altered *trbl* expression in the *Ddc-Gal4$^{4.3D}$ parkin-RNAi* model of PD. A. The graph of longevity assay generated by GraphPad prism8 with altered *trbl* expression in *Ddc-Gal4$^{4.3D}$ parkin-RNAi* expressing flies. The overexpression results in median lifespan of 66 days in *UAS-trbl.M(trbl-1)* and 64 days by UAS- *trbl^{EP1119}*(*trbl-3*) similar to 64 days of control (lacZ/Drp1-RNAi); the UAS-*trbl^{EP3519}*(trbl-2) has lifespan of 54 days much lower compared to control determined by Log-rank Mantel-Cox test, with Bonferroni correction. **B.** The inhibition of *trbl* under the control of *Ddc-Gal4 UAS-parkin-RNAi* transgene results in increased median lifespan of 76 days in UAS-*trblRNAi-1 (trbl-RNAi^{HMS04999}), 70 days in UAS-trbl-RNAi-2(*trbl-RNAi^{HMC04159}*)* and 70 days in *UAS-trbl-RNAi3(*trbl-RNAi^{GL01337}*)* compare to 64 days of control determined by Log-rank Mantel Cox test, with Bonferroni correction. **C**. The climbing abilities of flies with overexpression of *trbl's, trbl RNAi's* and control. The climbing abilities of trbl overexpression flies have decreased over time compared

to control as determined in nonlinear fitting of the climbing curve at 95% confidence interval. The climbing abilities of *trbl RNAi1* flies have partially rescued compare to control as determined in nonlinear fitting of climbing curve at 95% confidence interval. The climbing abilities of *trbl RNAi2* and *trbl-RNAi3* flies have no significant change over time compare to control as determined in nonlinear fitting of climbing curve at 95% confidence interval.

The altered co-expression of *trbl* along with *Drp1-RNAi* via *Ddc-Gal4$^{4.3D}$*

The control *Ddc-Gal4$^{4.3D}$; UAS-Drp1-RNAi; UAS-lacZ* critical class males were determined to have a median lifespan of 70 days (n=323). The overexpression of *trbl* by *UAS-trbl-1* and *UAS-trbl-3* along with *UAS-Drp1-RNAi* under the direction of the *Ddc-Gal4* transgene has a median lifespan of 70 (n=290) and 68 days (n=385), similar to control with a P-value of 0.06696 and 0.0625 respectively. However, the *UAS-trbl-2* along with *UAS-Drp1-RNAi* under the direction of the *Ddc-Gal4* transgene has a median lifespan of 56 days (n=253), much less compare to the control with a P-value of <0.0001 as determined by log-rank (Mantel-Cox) test with a Bonferroni correction (Figure 7.4A). The inhibition of *UAS-trbl-RNAi1, UAS-trbl-RNAi2* and *UAS-trbl-RNAi3* along with *UAS-Drp1-RNAi under the direction of the Ddc-Gal4* transgene has a median lifespan 56 (n=267), 56 (n=339) and 62 (n=346) days respectively, much less compared to the control (Figure 7.4B) with a P-value <0.0001 as determined by log-rank Mantel-Cox test with a Bonferroni correction.

The non-linear fit of the climbing curve shows *trbl* overexpression by *UAS-trbl-1.M* and *UAS- trbl-2* along with *Ddc-Gal4 UAS-Drp1-RNAi,* further contributes to loss of the climbing ability throughout the life of critical class flies compared to control at 95% CI (P-value= 0.0309 and <0.0001). The overexpression of *trbl* by *UAS-trbl-3^{EP1119}* under the direction of *Ddc-Gal4 UAS-Drp1-RNAi* has climbing curve similar to control at 95% CI (P value= 0.3710). The inhibition of *trbl* by *UAS-trbl-RNAi, UAS-trbl-RNAi2* and *UAS-trbl-RNAi3* along with *Ddc-Gal4 UAS-Drp1-RNAi*, further contributes to loss of the climbing ability throughout the life of critical class flies compared to control at 95% CI (P-value=<0.0001) (Figure 7.4C) (n=50).

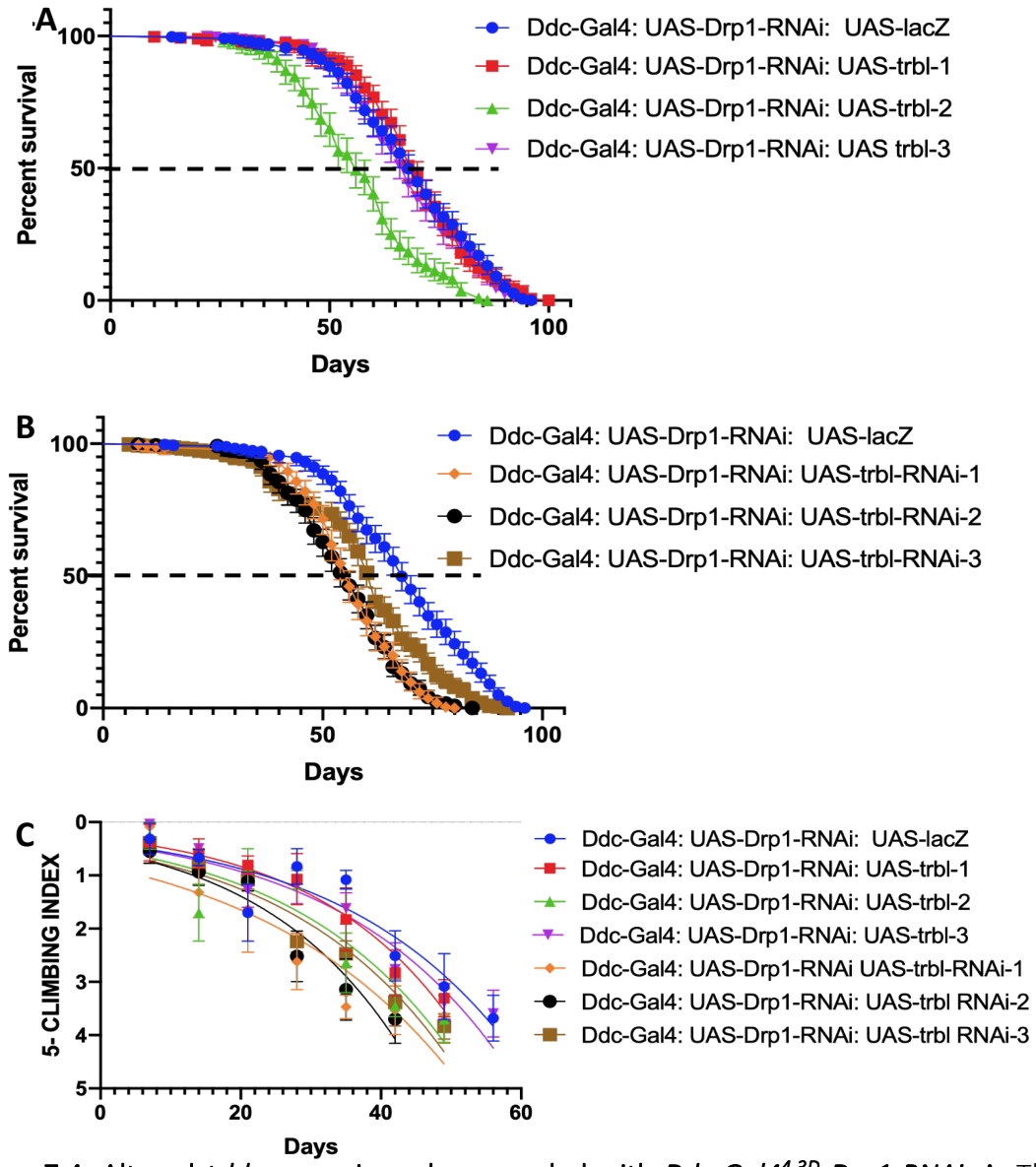

Figure 7.4: Altered *trbl* expression when coupled with *Ddc-Gal4$^{4.3D}$ Drp1-RNAi*. **A**. The graph of longevity assay generated by GraphPad prism8 with altered *trbl* expression in *Ddc-Gal4$^{4.3D}$ Drp1-RNAi* expressing flies. The overexpression results in median lifespan of 70 days by *UAS-trbl.M(trbl-1)* and 68 days by UAS- *trbl^{EP1119}*(*trbl-3*) similar to 68 days of control (lacZ/Drp1-RNAi); the UAS-*trbl^{EP3519}*(trbl-2) has lifespan of 56 days significantly lower than control determined by Log-rank Mantel-Cox test, with Bonferroni correction. **B.** The inhibition of *trbl* in neurons using *Ddc-Gal4$^{4.3D}$* transgene along with *Drp1-RNAi* results in decreased median lifespan of 56 days with *UAS-trbl-RNAi-1 (trbl-RNAi^{HMS04999}), 56 days with UAS-trbl-RNAi-2(*trbl-RNAi^{HMC04159}*)* and 62 days with *UAS-trbl-RNAi3(*trbl-RNAi^{GL01337}*)* compare to 68 days of control done by Log-rank Mantel Cox test, with Bonferroni correction. **C**. The GraphPad prism8 generated graph of the climbing abilities of flies with overexpression of *trbl, trbl RNAi* and control. The climbing abilities of trbl overexpression and *trbl RNAi* flies have significantly decreased over time compared to control as determined in nonlinear fitting of the climbing curve by 95% confidence interval.

The overexpression and inhibition of *trbl* with *Ddc-Gal4$^{4.36}$*

The control *Ddc-Gal4$^{4.36}$; UAS-lacZ* critical class males were determined to have a median lifespan of 92 days (n=361). The overexpression of *trbl* by *trbl1-.M*, *UAS-trbl-2^{EP3519},* and *UAS-trbl-3^{EP1119}* under the direction of *Ddc-Gal4$^{4.36}$* transgene has a median lifespan of 84 (n=307), 80 (n=256) and 76 (n=300) days, decreased compared to control with a P-value of <0.0001, 0.0002 and <0.0001 respectively, (Figure 7.5A) as determined by log-rank (Mantel-Cox). The inhibition of *trbl* by *UAS-trbl-RNAi1*^{HMS04999} under the direction of the *Ddc-Gal4* transgene has a median lifespan of 102 (n=342), increased compared to the control with a P-value 0.0002 (Figure 7.5B). The inhibition of *trbl* by *UAS-trbl-RNAi2*^{HMC04159} and *UAS-trbl-RNAi3*^{GL01337} under the direction of the *Ddc-Gal4$^{4.36}$* transgene has a median lifespan of 90 (n=300) and 92 days (n=301), similar to control with a P value of <0.0001 as determined by log-rank Mantel-Cox test with Bonferroni correction. The overexpression and inhibition of *trbl* in neurons caused early onset of impairment in climbing ability. The non-linear fitting of the climbing curve shows *trbl* overexpression lines has compromised the climbing ability phenotype compared to control at 95% CI (P-value <0.0001) (Figure 7.5C) (n=50). The non-linear fitting of the climbing curve shows *trbl* inhibition by *UAS-trbl-RNAi1^{HMS04999}, UAS-trbl-RNAi2^{HMC04159}* and *UAS-trbl-RNAi3^{GL01337}* lines has compromised the climbing ability phenotype compared to control at 95% CI (P-value <0.0001, <0.0001 and 0.0336) (Figure 7.5C) (n=50).

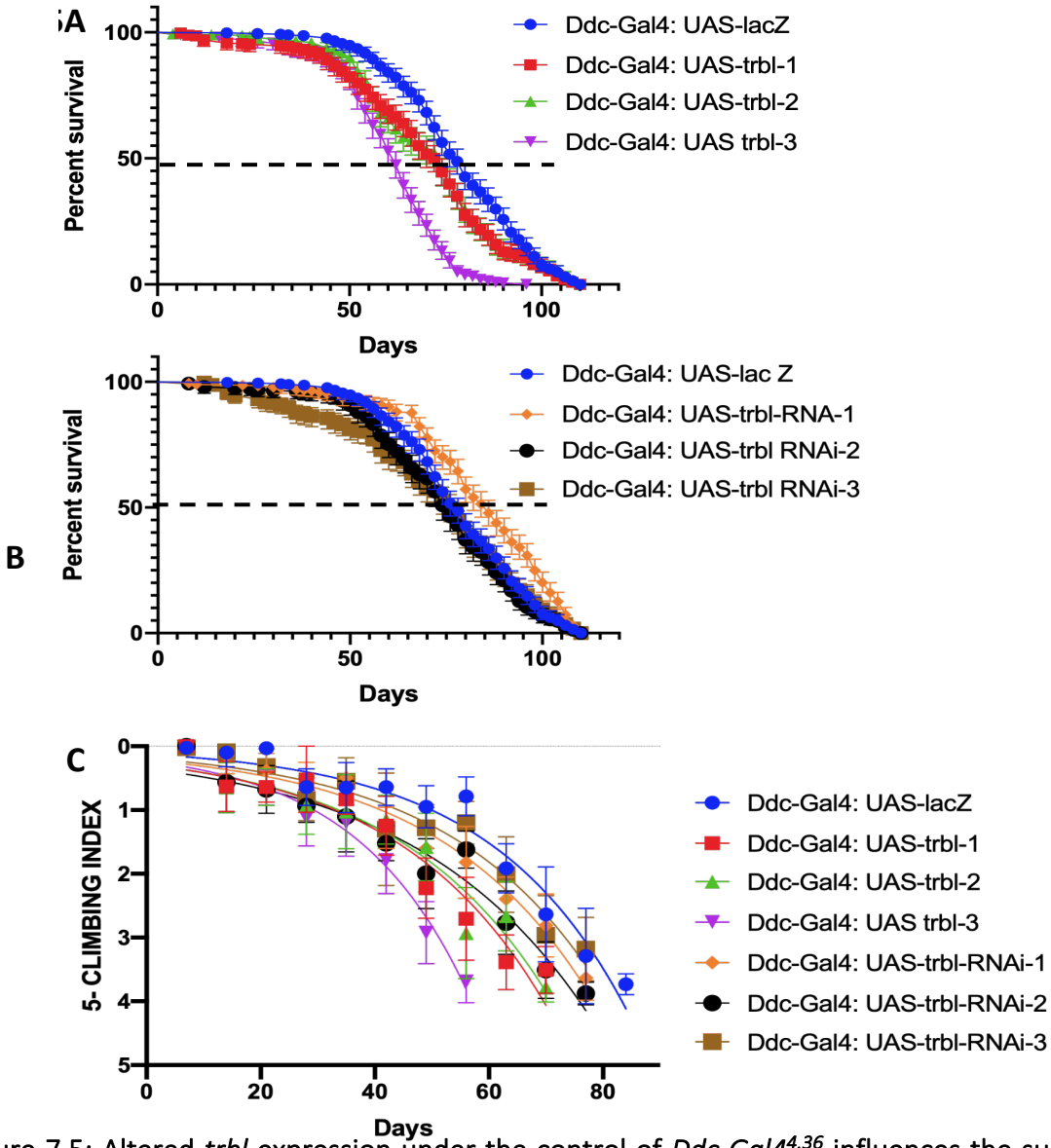

Figure 7.5: Altered *trbl* expression under the control of *Ddc-Gal4$^{4.36}$* influences the survival and climbing ability of flies. **A**. The GraphPad prism8 generated graph of the longevity assay for the expression of *trbl, trbl RNAi's* under the control of the *Ddc-Gal4$^{4.36}$* transgene. The directed expression results in decreased median lifespan of 84 days in *trbl.M(UAS-trbl-1)*, 80 days in *trbl^{EP3519}*(UAS-trbl-2) and 76 days in *trbl^{EP1119}* (UAS-trbl-3) compared to the control of 92 days determined by Log-rank Mantel Cox test, with Bonferroni correction. **B.** The directed inhibition results in median lifespan of 102 days in *UAS-trblRNAi1^{HMS04999}* increased compared to control; the directed inhibition by *UAS-trblRNAi2^{HMC04159}* and *UAS-trblRNAi3^{GL01337}* result in median lifespan of 90 and 92 days similar to the control determined by Log-rank Mantel Cox test, with Bonferroni correction. **C**. The GraphPad prism8 generated graph of the climbing abilities of flies with overexpression of *trbl, trbl-RNA's* and control. The non-linear fitting of the climbing ability of *trbl* overexpression and *trbl RNAi's* flies is less compared to control as determined by comparing the 95% confidence intervals. Error bars indicate the SEM and n=50.

The altered co-expression of *trbl* along with α-*synuclein* via *Ddc-Gal4*$^{4.36}$

For these experiments, the control *Ddc-Gal4*$^{4.36}$*; UAS-α-synuclein; UAS-lacZ* critical class males were determined to have a median lifespan of 78 days (n=374). The overexpression of *trbl* by *UAS-trbl1-.M*, *UAS-trbl-2*^{EP3519} and *UAS-trbl-3*^{EP1119} along with *UAS-α-synuclein* under the direction of the *Ddc-Gal4* transgene has a median lifespan of 98 (n=363), 104 (n=364) and 102 (371) days increased compared to control with a P value of <0.0001 as determined by log-rank (Mantel-Cox) test with a Bonferroni correction (Figure 7.6A). The inhibition of *trbl* by *UAS-trbl-RNAi1*^{HMS04999}*, UAS-trbl-RNAi2*^{HMC04159} and *UAS-trbl-RNAi3*^{GL01337} under the direction of the *Ddc-Gal4* transgene has a median lifespan of 80 (n=374), 78 (n=379) and 80 (n=346) days, very similar to the control with a P-value <0.0001, 0.0002 and 0.0150 respectively (Figure 7.6B) as determined by log-rank Mantel-Cox test with Bonferroni correction. The overexpression of *trbl* by *UAS-trbl-1.M*, *UAS-trbl-2*^{EP3519} and *UAS-trbl-3*^{EP1119} has partially rescue the decline in climbing ability compare to control at 95% CI with P-value <0.0001 (Figure 6C) (n=50). The inhibition of *trbl* by *UAS-trbl-RNAi1*^{HMS04999} and *UAS-trbl-RNAi3*^{GL01337} along with *Ddc-Gal4 UAS-α-synuclein-RNAi* has climbing curve similar to control at 95% CI (P-value= 0.0648 and 0.1485). The inhibition of *trbl* by *UAS-trbl-RNAi2*^{HMC04159} has partially rescued the decline in climbing ability compare to control at 95% CI with P-value <0.0001 (Figure 7.6C) (n=50).

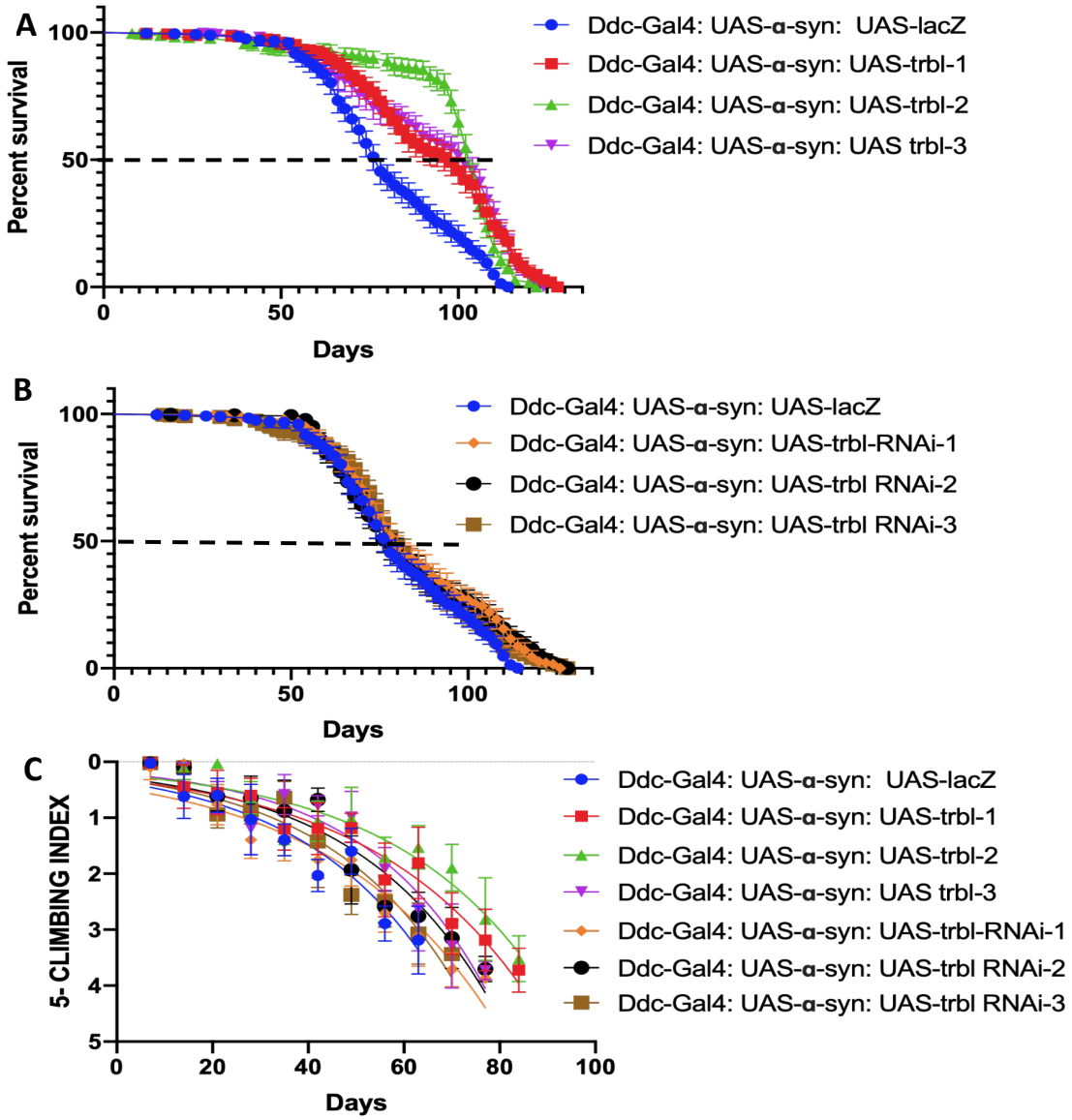

Figure 7.6: Altered *trbl* expression under the control of *Ddc-Gal4$^{4.36}$* with α-synuclein influences the survival and climbing ability of flies. **A**. The GraphPad prism8 generated graph of the longevity assay for the expression of *trbl, trbl RNAi's* under the control of *Ddc-Gal4$^{4.36}$ UAS-α-synuclein* transgene. The directed expression results in increased median lifespan of 98 days in *trbl.M-1*, 104 days in *UAS-trbl-2^{EP3519}* and 102 days in *UAS-trbl-3^{EP1119}* compared to the control of 78 days calculated by Log-rank Mantel Cox test, with Bonferroni correction. **B.** The inhibition of *trbl* under the control of *Ddc-Gal4$^{4.36}$ UAS-α-synuclein* transgene results in lifespan of 80 days with *UAS-trbl-RNAi-1^{HMS04999}*, 78 days with *UAS-trbl-RNAi-2^{HMC04159}* and 82 days with *UAS-trbl-RNAi-3^{GL01337}* similar to 78 days of control done by Log-rank Mantel Cox test, with Bonferroni correction. **C**. The GraphPad prism8 generated graph of the climbing abilities of flies with overexpression of *trbl, trbl RNA'si* and control. The climbing ability of *trbl* overexpression flies is increased compared to control as determined in nonlinear fitting of the climbing curve by 95% confidence interval. The climbing ability of *UAS-trbl-RNAi-1^{HMS04999} and UAS-trbl-RNAi-3^{GL01337}* flies is similar to control and

the climbing ability of *UAS-trbl-RNAi-2* ^{HMC04159} flies is rescued compared to control as determined in nonlinear fitting of the climbing curve by 95% confidence Interval.

The altered expression of *trbl* during development of eye via *GMR-Gal4*

In complementary experiments the inhibition and overexpression of *trbl*, directed by the *GMR-Gal4* transgene in the neuron-rich developing eye of flies influences eye development. The control *GMR-Gal4; UAS-lacZ* critical class males were determined to have an ommatidial count of 700.7 (n=15). The overexpression of *trbl* by *UAS-trbl-1.M*, *UAS-trbl-2*^{EP3519} and *UAS-trbl-3*^{EP1119} under the direction of the *GMR-Gal4* transgene has mean ommatidial count of 693.5, 693.8 and 698.4 respectively similar to control with a P-value of 0.3746, 0.3530 and 0.7438 as determined by unpaired T-test (Figure 7.7B). The inhibition of *trbl* by *UAS-trbl-RNAi1*^{HMS04999}, *UAS-trbl-RNAi2*^{HMC04159} and *UAS-trbl-RNAi3*^{GL01337} under the direction of the *GMR-Gal4* transgene has mean ommatidial count of 720.9, 720.8 and 729.7 respectively, higher compared to control with a P-value of 0.0016, 0.0134 and 0.0016 as determined by unpaired t-test (Figure 7.7B).

The control *GMR-Gal4; UAS-lacZ* critical class males were determined to have an interommatidial bristle count of 498.5 (n=15). The overexpression of trbl by *UAS-trbl-1.M*, *UAS-trbl-2*^{EP3519} and *UAS-trbl-3*^{EP1119} under the direction of the *GMR-Gal4* transgene has mean interommatidial bristle count of 492.6, 500.9 and 506.2 respectively similar to control with a P value of 0.6067, 0.8071 and 0.4160 as determined by unpaired T test (Figure 7.7C). The inhibition of *trbl* by *UAS-trbl-RNAi1*^{HMS04999}, *UAS-trbl-RNAi2*^{HMC04159} and *UAS-trbl-RNAi3*^{GL01337} under the direction of the *GMR-Gal4* transgene has mean interommatidial bristle count of 520.9, 518.8 and 520.2 respectively, higher compared to control with a P-value of 0.0127, 0.0422 and 0.0622 as determined by unpaired t-test (Figure 7.7C).

The control *GMR-Gal4; UAS-lacZ* critical class males were determined to have an ommatidial area of 200μm^2 (n=15). The overexpression of trbl by *UAS-trbl-1.M* under the direction of the *GMR-Gal4* transgene has mean ommatidium area of 202.1μm^2 similar to control with a P-value of

0.3984. The overexpression of trbl by *UAS-trbl-2*^{EP3519} and *UAS-trbl-3*^{EP1119} under the direction of the *GMR-Gal4* transgene has mean ommatidium area of 209.2µm^2 and 211.7µm^2 respectively, higher compare to control with a P-value of 0.0052 and <0.0001 as determined by unpaired T test (Figure 7.7D). The inhibition of trbl by *UAS-trbl-RNAi1*^{HMS04999}, *UAS-trbl-RNAi2*^{HMC04159} and *UAS-trbl-RNAi3*^{GL01337} under the direction of the *GMR-Gal4* transgene has mean ommatidium area of 212.1µm^2, 209.3µm^2 and 210.5µm^2 respectively, higher compare to control with a P value of 0.0002, 0.0154 and 0.0057 as determined by unpaired t-test (Figure 7.7D).

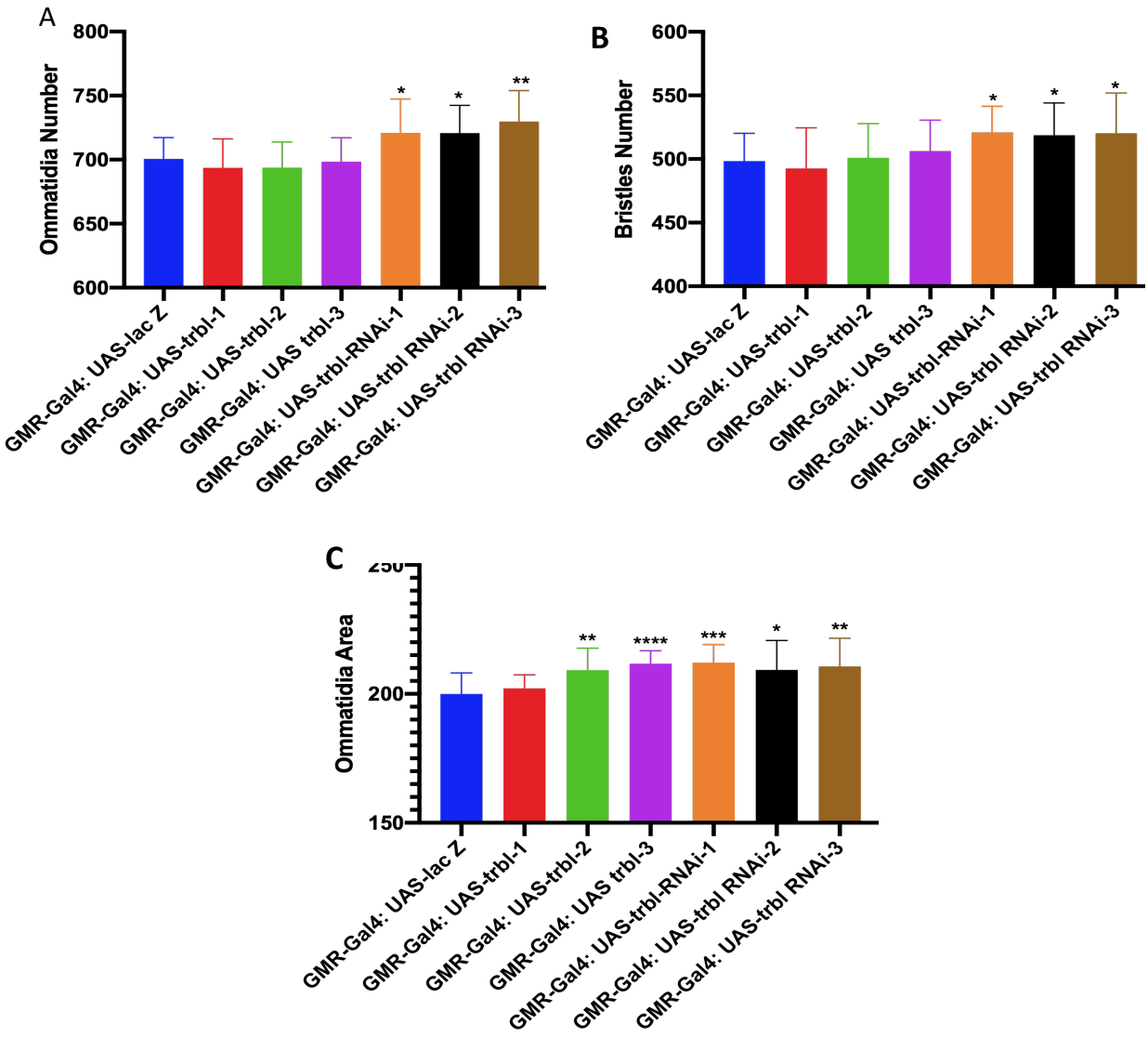

Figure 7.7: The phenotypic effects of altered *trbl* expression in *D. melanogaster* eye via *GMR-Gal4*. **A.** The ommatidia number for control is 700±17.8, the overexpression of *trbl* results in ommatidial count similar to control. The ommatidium counts of the trbl-RNAI-expressing flies were higher compared to control as determined by unpaired t-test. **B.** The interommatidial bristle count for the control is 498±21; for the overexpression of trbl the interommatidial bristle count is similar to control and interommatidial bristle count of inhibition lines are higher in the three RNAi transgenes as determined by unpaired t-test. **C.** The ommatidium area of trbl for the control is 200±9.1um^2. The ommatidium area of the *trbl* expression transgene *GMR-Gal4 UAS-trbl-3* and the inhibition RNAi transgenes are significantly higher than control as determined by unpaired t-test.

Discussion

The mechanism of *trbl* function as a pseudokinases is still uncertain, and it is thought that pseudokinases are involved in the regulation of the activities of protein kinases, through subcellular localization (Jacobsen and Murphy, 2017). However, it has been established that trbl plays an important role in diverse cellular processes. The level of trbl protein increases during starvation and after exercise in mammals; trbl can block Akt activation and reduce tissue growth in diabetic mice and human cell culture (Schwarzer et al. 2006; Lima et al. 2009; Fischer et al. 2017). The expression of *trbl* increases in DA neurons of the mice and rat PD model and promote cell death (Aimé et al. 2015). I found increasing *trbl* expression under control of the *Ddc-Gal4* transgene results in a decrease in longevity, likely by blocking the Akt protein kinase activation. Trbl inhibit Akt and promotes activation of the transcription factor foxo, which often leads to growth arrest and cell apoptosis (Saleem and Biswas 2017). The 4-PBA (4-phenyl butyric acid) and aFGF (acidic fibroblast growth factor) can alleviate the PD-like symptoms induced by 6-ODHA by decreasing the expression of trbl3 gene (Zhong et al. 2019). I found, the overexpression of trbl decreased the median lifespan, partly explaining the pro-apoptotic role of the trbl pseudokinase. The ommatidia and bristle numbers that arise with the GMR-Gal4-directed overexpression are significantly less than the trbl-RNAi-expressing critical class males. Thus, Trbl can regulate the function of IRS pathway at different levels and contribute to cellular homeostasis.

The ER stress seems to increase neuronal cell death with the specific activity of *trbl3*. The expression of *trbl3* is significantly higher in PD and AD patients (Aimé et al. 2015; Saleem and Biswas 2017). The expression of *trbl3* in amyloid-β treated neurons inhibits the activation of Akt, leading to the transcription enhancement activity of *foxo* in the promotion of the transcription of the pro-apoptotic *Bcl-2* family genes and enhanced *trbl3* expression. Trbl3 is required for

autophagosome formation in autophagy (Saleem and Biswas 2017). Although, evidence of the interaction between trbl and parkin was not available, I found that the overexpression of trbl further decreases the median lifespan of *parkin-RNAi* flies to suggest a cellular dysfunction or an increase in cell death. The co-inhibition of *parkin* and *trbl* under the control of the Ddc-Gal4 transgene result in flies that live longer than controls. Thus, I anticipate the toxic phenotypic effects produced by the expression of *parkin-RNAi* can be rescued by the inhibition of *trbl*. The molecular dynamics of trbl and parkin interaction is not clear but are likely the antagonist of each-other.

Overexpression of *trbl* activates *Bax* (pro-apoptotic Bcl-2 family protein), induces loss of mitochondrial membrane potential and initiates caspase-dependent apoptosis (Lin et al. 2007). The overexpression and inhibition of *trbl* under the control of *Ddc-Gal4* in combination with *Drp1-RNAi* seem to have decreased longevity or have no effect. The co-inhibition of *trbl* and *Drp1* may increase the cellular stress to promote cell death. The increased expression of *trbl* ameliorated the α-synuclein induced PD phenotypes in flies and increased the median lifespan and climbing abilities. Increased expression of *trbl* seems to deal with the cellular stress caused by α-synuclein–containing protein aggregates when other pathways function normally.

	Genotype	Median lifespan	Lifespan increased/ Decreases	Climbing Increased/ Decreased
Control	*Ddc-Gal4$^{4.3D;}$ UAS-lac Z*	68 days		
Experiment	*Ddc-Gal4$^{4.3D;}$ UAS-trbl.M*	66 days	Similar to control	Decreased
	Ddc-Gal4$^{4.3D;}$ UAS- trbl^{EP3519}	64 days	Similar to control	Decreased
	Ddc-Gal4$^{4.3D;}$ UAS- trbl^{EP1119}	54 days	Decreased	Decreased
	Ddc-Gal4$^{4.3D;}$UAS-trbl-RNAi^{HMS04999}	78 days	Increased	Decreased
	Ddc-Gal4$^{4.3D;}$ UAS-trbl-RNAi^{HMC04159}	70 days	Increased	Decreased
	Ddc-Gal4$^{4.3D;}$ UAS-trbl-RNAi^{GL01337}	70 days	Increased	Similar to control
Control	*Ddc-Gal4$^{4.3D;}$ UAS-park-RNAi; UAS-lacZ*	64 days		
Experiment	*Ddc-Gal4$^{4.3D;}$ UAS-park-RNAi; UAS-trbl.M*	66 days	Similar to control	Decreased
	Ddc-Gal4$^{4.3D;}$ UAS-park-RNAi; UAS- trbl^{EP3519}	54 days	Decreased	Decreased
	Ddc-Gal4$^{4.3D;}$ UAS-park-RNAi; UAS- trbl^{EP1119}	64 days	Similar to control	Decreased
	Ddc-Gal4$^{4.3D;}$ UAS-park-RNAi; UAS-trbl-RNAi^{HMS04999}	76 days	Increased	Increased
	Ddc-Gal4$^{4.3D;}$ UAS-park-RNAi; UAS-trbl-RNAi^{HMC04159}	70 days	Increased	Decreased
	Ddc-Gal4$^{4.3D;}$ UAS-park-RNAi; UAS-trbl-RNAi^{GL01337}	70 days	Increased	Decreased
Control	*Ddc-Gal4$^{4.3D;}$ UAS-Drp1-RNAi; UAS-lacZ*	68 days		
Experiment	*Ddc-Gal4$^{4.3D;}$ UAS-Drp1-RNAi; UAS-trbl.M*	70 days	Similar to control	Decreased
	Ddc-Gal4$^{4.3D;}$ UAS-Drp1-RNAi; UAS- trbl^{EP3519}	56 days	Decreased	Decreased
	Ddc-Gal4$^{4.3D;}$ UAS-Drp1-RNAi; UAS- trbl^{EP1119}	68 days	Similar to control	Similar to control
	Ddc-Gal4$^{4.3D;}$ UAS-Drp1-RNAi; UAS-trbl-RNAi^{HMS04999}	56 days	Decreased	Decreased
	Ddc-Gal4$^{4.3D;}$ UAS-Drp1-RNAi; UAS-trbl-RNAi^{HMC04159}	56 days	Decreased	Decreased
	Ddc-Gal4$^{4.3D;}$ UAS-Drp1-RNAi; UAS-trbl-RNAi^{GL01337}	62 days	Decreased	Decreased

Control	*Ddc-Gal4$^{4.36;}$ UAS-lac Z*	92 days		
Experiment	*Ddc-Gal4$^{4.36;}$ UAS-trbl.M*	84 days	Decreased	Decreased
	Ddc-Gal4$^{4.36;}$ UAS- trbl^{EP3519}	80 days	Decreased	Decreased
	Ddc-Gal4$^{4.36;}$ UAS- trbl^{EP1119}	76 days	Decreased	Decreased
	Ddc-Gal4$^{4.36;}$ UAS-trbl-RNAi^{HMS04999}	102 day	Increased	Decreased
	Ddc-Gal4$^{4.36;}$ UAS-trbl-RNAi^{HMC04159}	90 days	Similar to control	Decreased
	Ddc-Gal4$^{4.36;}$ UAS-trbl-RNAi^{GL01337}	92 days	Similar to control	Decreased
Control	*Ddc-Gal4$^{4.36;}$ UAS-α-syn; UAS-lacZ*	78 days		
Experiment	*Ddc-Gal4$^{4.36;}$ UAS- α-syn; UAS-trbl.M*	98 days	Increased	Increased
	Ddc-Gal4$^{4.36;}$ UAS-α-syn; UAS-trbl^{EP3519}	104 day	Increased	Increased
	Ddc-Gal4$^{4.36;}$ UAS-α-syn; UAS-trbl^{EP1119}	102 day	Increased	Increased
	Ddc-Gal4$^{4.36;}$ UAS-α-syn; UAS-trbl-RNAi^{HMS04999}	80 days	Similar to control	Similar to control
	Ddc-Gal4$^{4.36;}$ UAS-α-syn; UAS-trbl-RNAi^{HMC04159}	78 days	Similar to control	Increased
	Ddc-Gal4$^{4.36;}$ UAS-α-syn; UAS-trbl-RNAi^{GL01337}	80 days	Similar to control	Similar to control

Table 7.2: Summary of the Results. The effect of the altered expression of *trbl* directed by *Ddc-Gal4$^{4.3D}$*, *Ddc-Gal4$^{4.3D}$UAS-parkin-RNAi*, *Ddc-Gal4$^{4.3D}$ UAS-Drp1-RNAi*, *Ddc-Gal4$^{4.36}$* and *Ddc-Gal4$^{4.36}$ UAS-α-synuclein* transgene on median lifespan and climbing ability of the critical class male flies. The Cells with blue highlight denote control; Orange highlight denotes the decreased compared to control Green highlights denote the increase compared to control, and yellow highlights denote the resulting longevity and climbing ability is very similar to control.

Conclusion

Trbl activates during different categories of cellular stresses and alleviates the consequences through the promotion of autophagy or apoptosis. The diverse effects of *trbl* overexpression and inhibition in different PD models: *trbl* inhibition partially rescues the *parkin-RNAi* PD phenotype, *trbl* inhibition worsen the *Drp1-RNAi* PD phenotype and *trbl* overexpression rescues the *α-synuclein* induced PD phenotype are due to the multiple pathways and their overall effect in each scenario.

Bibliography

Aimé, P., Sun, X., Zareen, N., Rao, A., Berman, Z., Volpicelli-Daley, L., Bernd, P., Crary, J.F., Levy, O.A., and Greene, L.A. 2015. Trib3 is elevated in Parkinson's disease and mediates death in Parkinson's disease models. J. Neurosci. **35**(30): 10731–10749. Society for Neuroscience. doi:10.1523/JNEUROSCI.0614-15.2015.

Bermales, S., Soto, M.M., and McCullagh, E. 2012, April 25. Unfolded protein stress in the endoplasmic reticulum and mitochondria: A role in neurodegeneration. Frontiers. doi:10.3389/fnagi.2012.00005.

Cheng, J., Lu, Q., Song, L., and Ho, M.S. 2018, November 1. α-Synuclein Trafficking in Parkinson's Disease: Insights From Fly and Mouse Models. SAGE Publications Inc. doi:10.1177/1759091418812587.

Dobens, L.L., and Bouyain, S. 2012. Developmental roles of tribbles protein family members. Dev. Dyn. **241**(8): 1239–1248. John Wiley & Sons, Ltd. doi:10.1002/dvdy.23822.

Eyers, P.A., Keeshan, K., and Kannan, N. 2017, April 1. Tribbles in the 21st Century: The Evolving Roles of Tribbles Pseudokinases in Biology and Disease. Elsevier Ltd. doi:10.1016/j.tcb.2016.11.002.

Fischer, Z., Das, R., Shipman, A., Fan, J.Y., Pence, L., Bouyain, S., and Dobens, L.L. 2017. A Drosophila model of insulin resistance associated with the human TRIB3 Q/R polymorphism. DMM Dis. Model. Mech. **10**(12): 1453–1464. Company of Biologists Ltd. doi:10.1242/dmm.030619.

Githure M'angale, P., and Staveley, B.E. 2016. Bcl-2 homologue Debcl enhances a-synuclein-induced phenotypes in Drosophila. PeerJ. doi:10.7717/peerj.2461.

Githure, P.M., and Staveley, B.E. 2017. Overexpression of Buffy enhances the loss of parkin and suppresses the loss of Pink1 phenotypes in Drosophila. Genome **60**(3): 241–247. NRC Research Press. doi:10.1139/gen-2016-0165.

Jacobsen, A. V., and Murphy, J.M. 2017, June 15. The secret life of kinases: Insights into noncatalytic signalling functions from pseudokinases. Portland Press Ltd. doi:10.1042/BST20160331.

Lima, A.F., Ropelle, E.R., Pauli, J.R., Cintra, D.E., Frederico, M.J.S., Pinho, R.A., Velloso, L.A., and De Souza, C.T. 2009. Acute exercise reduces insulin resistance-induced TRB3 expression and amelioration of the hepatic production of glucose in the liver of diabetic mice. J. Cell. Physiol. **221**(1): 92–97. J Cell Physiol. doi:10.1002/jcp.21833.

Lin, K.R., Lee, S.F., Hung, C.M., Li, C.L., Yang-Yen, H.F., and Yen, J.J.Y. 2007. Survival factor withdrawal-induced apoptosis of TF-1 cells involves a TRB2-Mcl-1 axis-dependent pathway. J. Biol. Chem. **282**(30): 21962–21972. J Biol Chem. doi:10.1074/jbc.M701663200.

Saleem, S., and Biswas, S.C. 2017. Tribbles pseudokinase 3 induces both apoptosis and autophagy in amyloid-β-induced neuronal death. J. Biol. Chem. **292**(7): 2571–2585. American Society for Biochemistry and Molecular Biology Inc. doi:10.1074/jbc.M116.744730.

Schwarzer, R., Dames, S., Tondera, D., Klippel, A., and Kaufmann, J. 2006. TRB3 is a PI 3-kinase dependent indicator for nutrient starvation. Cell. Signal. **18**(6): 899–909. Cell Signal. doi:10.1016/j.cellsig.2005.08.002.

Sievers, F., Wilm, A., Dineen, D., Gibson, T.J., Karplus, K., Li, W., Lopez, R., McWilliam, H., Remmert, M., Söding, J., Thompson, J.D., and Higgins, D.G. 2011. Fast, scalable generation of high-quality protein multiple sequence alignments using Clustal Omega. Mol. Syst. Biol. **7**. Mol Syst Biol. doi:10.1038/msb.2011.75.

Stefanis, L. 2012. α-Synuclein in Parkinson's disease. Cold Spring Harb. Perspect. Med. **2**(2). Cold Spring Harbor Laboratory Press. doi:10.1101/cshperspect.a009399.

Todd, A., and Staveley, B. 2012. Expression of Pink1 with α-synuclein in the dopaminergic neurons of Drosophila leads to increases in both lifespan and healthspan. Genet. Mol. Res. **11**(2): 1497–1502. doi:10.4238/2012.May.21.6.

Todd, A.M., and Staveley, B.E. 2004. Novel assay and analysis for measuring climbing ability in Drosophila. Drosoph. Inf. Serv. **87**: 101–108. Available from http://www.ou.edu/journals/dis/DIS87/4 - Techniques.pdf [accessed 6 October 2019].

Twig, G., Elorza, A., Molina, A.J.A., Mohamed, H., Wikstrom, J.D., Walzer, G., Stiles, L., Haigh, S.E., Katz, S., Las, G., Alroy, J., Wu, M., Py, B.F., Yuan, J., Deeney, J.T., Corkey, B.E., and Shirihai, O.S. 2008. Fission and selective fusion govern mitochondrial segregation and elimination by autophagy. EMBO J. **27**(2): 433–446. doi:10.1038/sj.emboj.7601963.

Wang, P., Wang, P., Liu, B., Zhao, J., Pang, Q., Agrawal, S.G., Jia, L., and Liu, F.-T. 2015. Dynamin-related protein Drp1 is required for Bax translocation to mitochondria in response to irradiation-induced apoptosis. Oncotarget **6**(26): 22598–612. Impact Journals, LLC. doi:10.18632/oncotarget.4200.

Yang, Y., Gehrke, S., Imai, Y., Huang, Z., Ouyang, Y., Wang, J.W., Yang, L., Beal, M.F., Vogel, H., and Lu, B. 2006. Mitochondrial pathology and muscle and dopaminergic neuron degeneration caused by inactivation of Drosophila Pink1 is rescued by Parkin. Proc. Natl. Acad. Sci. U. S. A. **103**(28): 10793–10798. doi:10.1073/pnas.0602493103.

Yang, Y., Nishimura, I., Imai, Y., Takahashi, R., and Lu, B. 2003. Parkin suppresses dopaminergic neuron-selective neurotoxicity induced by Pael-R in Drosophila. Neuron **37**(6): 911–924. Cell Press. doi:10.1016/S0896-6273(03)00143-0.

Yokoyama, T., and Nakamura, T. 2011. Tribbles in disease: Signalling pathways important for cellular function and neoplastic transformation. Cancer Sci. **102**(6): 1115–1122. John Wiley & Sons, Ltd. doi:10.1111/j.1349-7006.2011.01914.x.

Zareen, N., Biswas, S.C., and Greene, L.A. 2013. A feed-forward loop involving Trib3, Akt and FoxO mediates death of NGF-deprived neurons. Cell Death Differ. **20**(12): 1719–1730. Nature Publishing Group. doi:10.1038/cdd.2013.128.

Zhong, X., Wang, B., Zhang, G., Yuan, Y., Hu, X., Xiong, J., Zheng, P., Liu, Y., Xu, K., Xiao, J., Wu, Y., and Ye, J. 2019. Autophagy activation is involved in acidic fibroblast growth factor ameliorating Parkinson's disease via regulating tribbles homologue 3. Front. Pharmacol. **10**. Frontiers Media S.A. doi:10.3389/fphar.2019.01428.

Chapter 8: Potential interactions of *foxo* inhibition in *Drp1*, *Rbf*, *Parkin* and *α-synuclein* models of PD

Abstract

The activities of the insulin receptor signalling (IRS) pathway are essential for the proper maintenance of cellular homeostasis. The *foxo* transcription factor, a crucial downstream target of IRS, regulates many signalling pathways that are key to cellular health, including mitochondrial health. The health of the mitochondrial network is maintained directly by members of the Bcl-2 family of proteins and other proteins that participate in quality control such as Pink1, parkin and Drp1. The directed inhibition of *foxo* via expression of *foxo-RNAi*, in combination in *α-synuclein* or *parkin*-induced models of PD directed by the *Ddc-Gal4* transgene, can rescue the PD-like phenotypes and increase median lifespans. Further, I exploited our novel models of *Drp1* overexpression, *Drp1* inhibition and *Rbf* inhibition guided by *Ddc-Gal4* to study the changes in phenotypes due to the *foxo-RNAi*-induced inhibition. The inhibition of *foxo* in the *Drp1*-induced PD model effectively rescues the PD-like phenotypes that influence longevity and locomotor activities. The phenotypes that mimic PD produced through the inhibition of *Drp1* and *Rbf* were not altered through the inhibition of *foxo*. These results suggest a network of regulatory pathways that may be directly or indirectly controlled by the foxo transcription factor.

Introduction

Parkinson Disease (PD) is among the most common neurodegenerative diseases and is characterized, through post-mortem analyses, by the loss of dopaminergic (DA) neurons from the SNpc region of the brains of patients. Often, the loss of DA neurons is linked closely to the dysfunction of the neuronal mitochondria. The extremely diverse cell signalling pathways and sub-cellular mechanisms that are responsible for the protection of mitochondria include several complex processes such as mitophagy and apoptosis. The transcription factors, encoded by *foxo,*

can act to influence multiple cellular processes that include insulin receptor signalling (IRS), a number of stress responses, energy metabolism, autophagy (and the mitochondrial-specific subtype, mitophagy), cellular differentiation and programmed cell death (Greer and Brunet 2005). When the IRS pathway is activated, this series of events is responsible for the export of the foxo transcription factor from the nucleus to cytoplasm, to physically remove the protein from the nuclear locations of transcriptional activity (Greer and Brunet 2007). The activity of *foxo* provides stress resistance, during diverse cellular stresses, and enhanced longevity through the transcription of responsible genes (Kramer et al. 2003; Martins et al. 2016). However, the overexpression of *foxo* can be toxic and unregulated expression lead to tumourigenesis (Huang and Tindall 2007). Interestingly, aggregates of the α-synuclein protein constitute a major component of the Lewy Bodies and Lewy Neurites observed in an array of degenerative pathological conditions, especially notable in PD (Recasens and Dehay 2014). In human cell culture, the foxo3a protein has an important role in cell death induced by α-synuclein (Angelova et al. 2018). The protective role of *foxo* in stress conditions could be reversed through the overexpression of *foxo* and the removal of the source of stress.

The *foxo* transcription factors can regulate an array of signal transduction pathways. The expression of *foxo* has been found to alter the phosphorylation of the mitochondrial fission protein Drp1 in endothelial cells (Shi et al. 2018). The inhibition of *Drp1* can rescue damage to the mitochondrial network and creation of excessive mitochondrial reactive oxygen species (mtROS) production (Shi et al. 2018). The foxo transcription factors can regulate some aspects of mitochondrial dynamics by activation of the ROCK1 (rho-associated, coiled-coil-containing protein

kinase 1) transcription factor (Shi et al. 2018). In addition, foxo can activate the transcription of *Pink1* to regulate the *Pink1/parkin*-dependent process of mitophagy (Mei et al. 2009; Li et al. 2017; Bartolomé et al. 2017). In turn, the Pink1 protein recruits the parkin E3 ubiquitin ligase to the cytoplasm face of the mitochondrial membrane to prepare for ubiquitination (Thomas et al. 2014). The role of the parkin E3 ubiquitin ligase is not limited to mitophagy, and parkin functions in other cellular protective pathways, in addition to mitophagy. In mammalian cell culture, the foxo proteins can activate the transcription of pro-apoptotic Bcl-2 family members such as *Bim,* and *bnip3* and, indirectly, suppress the expression of pro-survival *Bcl-XL* (Fu and Tindall 2008). However, a direct foxo-mediated activation of the Bcl-2 family genes have not been characterized in drosophila, as of yet. Further experimentation is desirable to pursue a more complete understanding of the mechanisms by which foxo may regulate the drosophila Bcl-2 family of proteins. Nevertheless, with the current state of knowledge, *foxo* may be critical in the regulation of mitochondrial dynamics, mitophagy and apoptosis.

Alterations to the IRS can play key roles in development and in disease. The essential function of *foxo* in the IRS pathway has been established through genetic and biochemical evidence (Puig and Tjian 2005). Rbf has been reported to target genes of multiple pathways including members of the IRS pathway (Acharya et al. 2012). In part, the transcription regulator Rbf, the fly version of the human pRb protein, is responsible for the G1/S transition and acts in the regulation of various cellular processes that include DNA replication, DNA repair, cell cycle, transcription, oncogenesis, tumour suppression and apoptosis (Chakraborty *et al*., 2007; Classon and Harlow, 2002). Rbf is a component of the DREAM complex (dimerization partner, RB-like, E2F and multi-vulval class B), a multi-protein complex, that can act as transcription activator or

repressor dependent upon the cellular environment (Ariss *et al.,* 2018). Determination of the extent of the influence of *Rbf* and *foxo* upon the cellular signal transduction pathways that support cellular homeostasis promises to be very informative.

In my experiments, I exploited the *UAS-Gal4* system to direct the expression and inhibition of the *foxo* gene in selected neuronal tissues directed by the *Ddc-Gal4*$^{4.3D}$ and *Ddc-Gal4*$^{4.36}$ transgenes. Notably, the overexpression of *foxo* is lethal when expressed in these tissues when using the *Ddc-Gal4* transgenes. Along with *UAS-foxo-RNAi*, I combined each of the *UAS-Drp1, UAS-Drp1-RNAi, UAS-Rbf-RNAi, UAS-parkin-RNAi* and *UAS-α-synuclein* transgenes to study the influence of the loss of *foxo* function upon median lifespan and climbing ability over time in a number of PD models. The inhibition of *foxo* suppressed or rescued the phenotypes generated through 1) the inhibition of *parkin*; 2) the ectopic expression of human *α-synuclein*; and 3) the overexpression of *Drp1* under the control of the *Ddc-Gal4* transgene.

Material and Methods

Drosophila Stocks and media

Drosophila stocks and culture media: The *UAS-lacZ*$^{4-1-2}$; *UAS-Drp1 (y[1] w[*]; P{w[+mC]=FLAG-FlAsH-HA-Drp1}3, Ki[1]), UAS-Drp1-RNAi1*^{JF02762} *(y[1] v[1]; P{y[+t7.7]v[+t1.8]=TRiP.JF02762}attP2});* the *UAS-Rbf RNAi1*^{HMS03004} *(y[1] sc[*] v[1] sev[21]; P{y[+t7.7] v[+t1.8]=TRiP.HMS03004}attP2/TM3, Sb[1]); Ddc-Gal4*$^{4.3D}$*(w[1118]; P{w[+mC]=Ddc-GAL4.L}4.3D)* and *Ddc-Gal4*$^{4.36}$*(w[1118]; P{w[+mC]=Ddc=Gal4.L}Lmpt[4.36])* stocks were obtained from the Bloomington Drosophila Stock Center at Indiana University, Bloomington, Indiana, USA. The *UAS-parkin-RNAi* line was obtained from Dr. B. Lu (Yang et al. 2003, 2006). The *UAS-α-synuclein* was generously provided by Dr. M.

Feany of Harvard Medical School (Feany and Bender 2000). The *Ddc-Gal4 UAS-Drp1, Ddc-Gal4 UAS-Drp1-RNAi, Ddc-Gal4 UAS-Rbf RNAi, Ddc-Gal4 UAS-parkin-RNAi,* and *Ddc-Gal4 UAS-α-synuclein* lines were produced through standard methods (M'Angale and Staveley, 2016). All flies were maintained on standard cornmeal/molasses/yeast/agar media treated with propionic acid and methylparaben to resist fungal growth. Stocks were kept at room temperature (22° ± 3° C), whereas crosses and experiments were maintained at 25°C.

Survival assay

Female virgins of the *Ddc-Gal4 UAS-Drp1; Ddc-Gal4 UAS-Drp1-RNAi; Ddc-Gal4 UAS-α-synuclein; Ddc-Gal4 UAS-Rbf-RNAi1, Ddc-Gal4 UAS-parkin-RNAi,* genotype was collected every 8 to 12 hours for several days. The confirmed virgin flies were then crossed with *UAS-lacZ* and *UAS-foxo-RNAi* males. Critical class male progeny was collected from mating's until approximately 250 flies of each genotype were obtained. To avoid over-crowding, the flies were maintained in cohorts of 25 or less per vial on standard cornmeal/molases/yeast/agar media. Flies were scored every second day for viability and were transferred to new food every two to five days. Scoring continued until all flies had died (Todd and Staveley 2004, 2012)). Longevity data were analyzed using GraphPad Prism version 8 statistical software (*graphpad.com*), and survival curves were compared by Mantel-Cox test. Significance were determined at 95% confidence level ($P \leq 0.05$).

Locomotor analysis

The 70 critical class male flies were collected within a 24-hour period and maintained as cohorts of 10 flies in each vial. The food was replenished twice every week. The climbing assay was performed according to a standard protocol (Todd and Staveley 2004, 2012). Every week 50 males

were assayed, in groups of 10, for their ability to climb a glass tube divided into 5 levels of 2 cm each. The climbing index was calculated for each week using GraphPad prism version 8 statistical software. The climbing curve was fitted using non-linear regression and determined at a 95% confidence interval ($P \leq 0.05$).

Results and Discussion

Inhibition of the expression of *foxo* via *Ddc-Gal4$^{4.3D}$* and *Ddc-Gal4$^{4.36}$* transgenes

In these experiments, the control *Ddc-Gal4$^{4.3D}$; UAS-lacZ* critical class males were determined to have a median lifespan of 68 days (n=340). The directed inhibition of *foxo* in the *Ddc-Gal4$^{4.3D}$* transgene results in lifespan similar to control. The expression of *foxo-RNAi* resulted in a median lifespan of 72 days (n=266), similar to the control (Figure 8.1A) as determined by log-rank (Mantel-Cox) test at a P-value at 0.3067. The non-linear fit of the climbing curves demonstrates the expression of *foxo-RNAi* have compromised the climbing ability phenotype compared to the control at 95% CI (P-value 0.0003) (Figure 8.1B) (n=50).

In these experiments, the control *Ddc-Gal4$^{4.36}$; UAS-lacZ* critical class males were determined to have a median lifespan of 92 days (n=361). The expression of *foxo-RNAi* under *Ddc-Gal4$^{4.36}$* control resulted in median lifespans of 96 days (n=359), similar to the control (Figure 8.1C) as determined by log-rank (Mantel-Cox) test at a P-value at 0.0917. The non-linear fit of the climbing curve shows *foxo-RNAi* expression has increased the compromise in climbing ability compared to control at 95% CI (P-value 0.0157) (Figure 8.1D) (n=50).

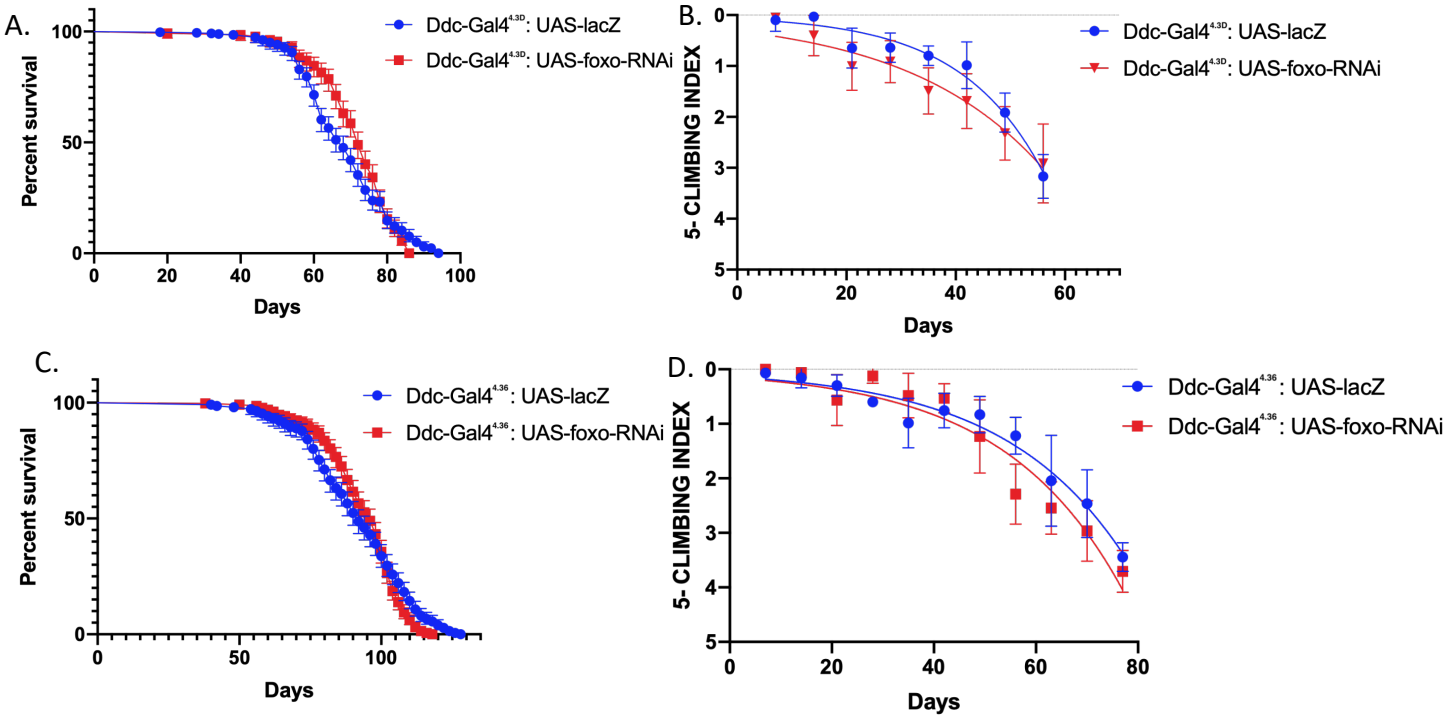

Figure 8.1: *RNA interference* of *foxo* directed by the *Ddc-Gal4$^{4.3D}$* and *Ddc-Gal4$^{4.36}$* transgenes affects longevity and motor function. The expression of *foxo-RNAi* transgene in the *Ddc-Gal4*-expressing neurons results in lifespan and locomotor function similar to control. **A.** The inhibition of *foxo* in the *Ddc-Gal4$^{4.3D}$*-expressing neurons results in similar lifespan of 72 days compared to 68 days of control flies expressing the *lacZ* transgene. The genotypes are *Ddc-Gal4/UAS-lacZ* and *Ddc-Gal4/UAS-foxo-RNAi*. Longevity is shown as percent survival ($P < 0.05$, determined by the Log-rank (Mantel–Cox) test and $N > 250$). **B.** The inhibition of *foxo* in the *Ddc-Gal4$^{4.36}$* expressing neurons results in similar lifespan of 96 days when compared to 92 days of control flies expressing the lacZ transgene. The genotypes are *Ddc-Gal4/UAS-lacZ* and *Ddc-Gal4/UAS-foxo*-RNAi. Longevity is shown as percent survival ($P < 0.05$, determined by the Log-rank (Mantel–Cox) test and $N > 250$). **C and D.** The inhibition of foxo in these neurons resulted in further decrease in climbing ability as determined by nonlinear fitting of the climbing curves and comparing the 95% CI. The genotypes are *Ddc-Gal4/UAS-lacZ* and *Ddc-Gal4/UAS-foxo-RNAi*. Error bars indicate standard error of the mean and $N = 50$.

Inhibition of the expression of *foxo* along with *Drp1* overexpression via *Ddc-Gal4$^{4.3D}$ transgene*

The control *Ddc-Gal4; UAS-Drp1; UAS-lacZ* critical class males were determined to have a median lifespan of 58 days (n=254). In comparison, the directed inhibition of *foxo* in the *Ddc-Gal4; UAS-Drp1; UAS-foxo* critical class individuals results in a median lifespan of 70 days (n=324), with a P-value of <0.0001 when compared to the control as determined by the log-rank (Mantel-Cox) test (Figure 8.2A). The non-linear fit of the climbing curve shows *foxo* inhibition has rescued the climbing ability defect compared to control at 95% CI (P-value <0.0001) (Figure 8.2B).

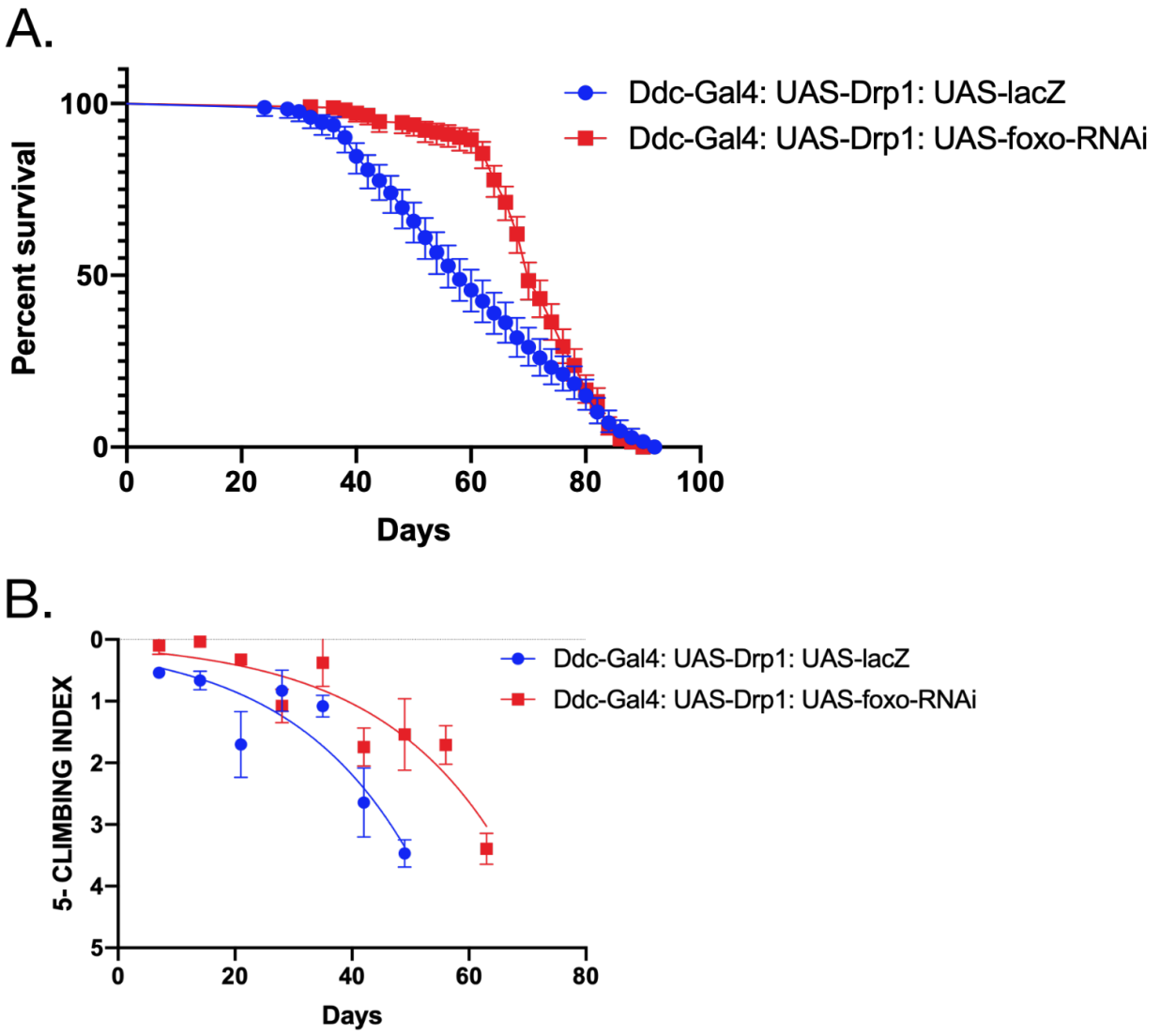

Figure 8.2: RNA interference of *foxo* along with the expression of *Drp1* directed by *Ddc-Gal4*$^{4.3D}$. The expression of *foxo-RNAi* by the *Ddc-Gal4* expressing neurons coupled with *UAS-Drp1 results* in an enhanced lifespan and locomotor function compared to the control. **A.** The inhibition of *foxo* in the *Ddc-Gal4 UAS-Drp1*-expressing neurons results in lifespan of 70 days compared to 58 days of control flies expressing the *lacZ* transgene. The genotypes are *Ddc-Gal4/UAS-Drp1/UAS-lacZ* and *Ddc-Gal4/UAS-Drp1/UAS-foxo-RNAi*. Longevity is shown as percent survival ($P < 0.05$, determined by the Log-rank (Mantel–Cox) test and $N > 300$). **B** The inhibition of *foxo* in these neurons resulted in slight improvement in climbing ability as determined by nonlinear fitting of the climbing curves and comparing the 95% CI. The genotypes are *Ddc-Gal4/UAS-Drp1/UAS-lacZ* and *Ddc-Gal4/UAS-Drp1/UAS-foxo-RNAi*. Error bars indicate standard error of the mean and N = 50.

Inhibition of *foxo* expression along with *UAS-Drp1-RNAi* via *Ddc-Gal4*$^{4.3D}$

The control *Ddc-Gal4; UAS-Drp1-RNAi; UAS-lacZ* critical class males were determined to have a median lifespan of 70 days (n=323). The directed inhibition of *foxo* in the *Ddc-Gal4; UAS-Drp1-RNAi; UAS-lacZ* transgene results in median lifespan of 67 days slightly decreased compared to the control (Figure 8.3A) with a P-value of <0.0001 as determined by log-rank (Mantel-Cox) test at a P-value <0.0001. The non-linear fitting of the climbing curve shows *foxo* inhibition does not affect the climbing ability defect compared to control at 95% CI (P-value 0.3827) (Figure 8.3B).

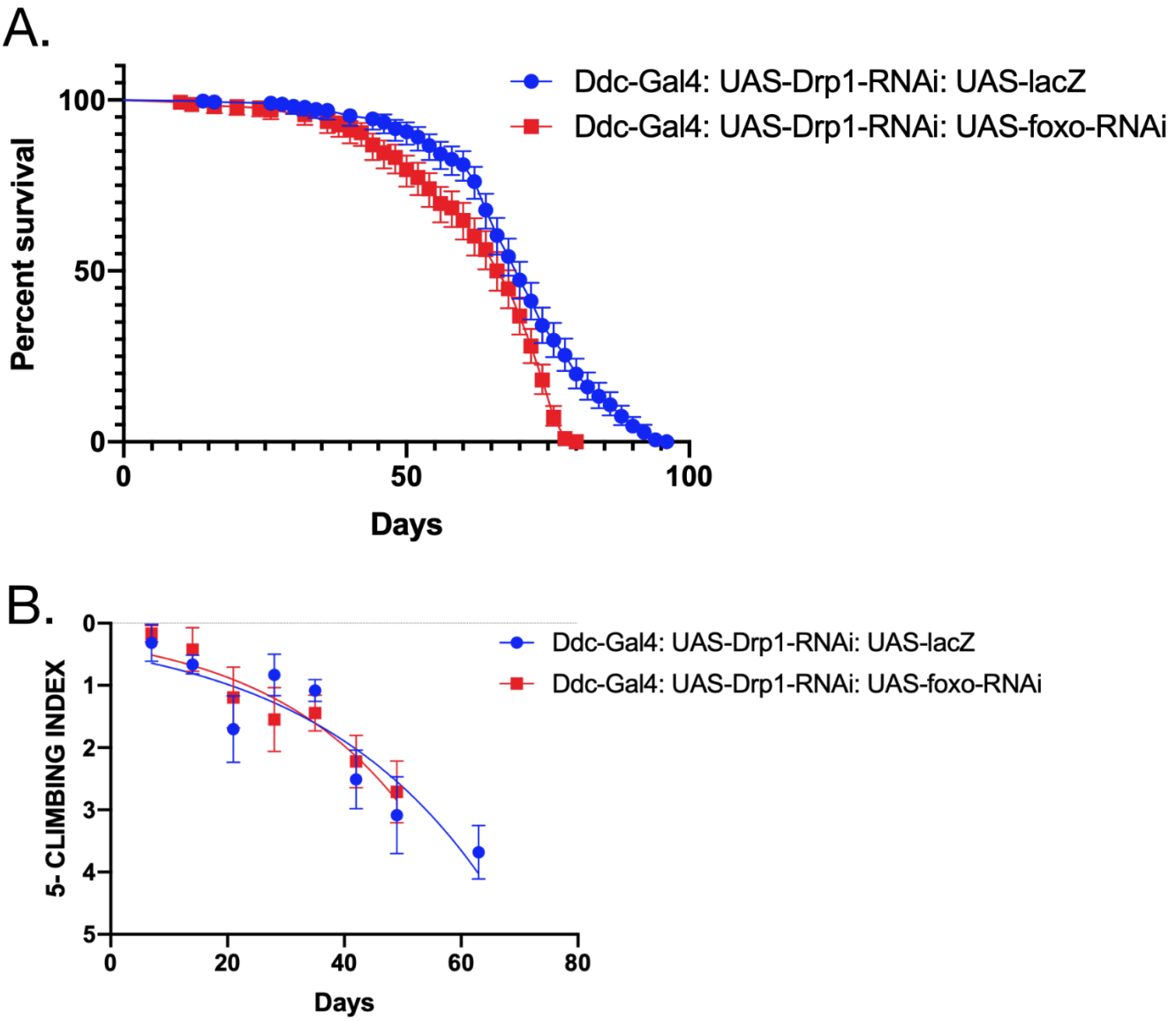

Figure 8.3: RNA interference of both *foxo* and *Drp1* expression directed by *Ddc-Gal4$^{4.3D}$*. The expression of *foxo-RNAi* along with *Drp1-RNAi* in the *Ddc-Gal4$^{4.3D}$* expressing neurons results in a slightly decreased lifespan compared to the control. **A.** The inhibition of *foxo* and *Drp1* by *Ddc-Gal4* -expressing neurons results in a lifespan of 67 days compared to 70 days of control flies expression of the *lacZ* transgene. The genotypes are *Ddc-Gal4/UAS-Drp1-RNAi/UAS-lacZ* and *Ddc-Gal4/UAS-Drp1-RNAi/UAS-foxo-RNAi*. Longevity is shown as percent survival ($P < 0.05$, determined by the Log-rank (Mantel–Cox) test and $N > 300$). **B** The inhibition of *foxo* in these neurons does not diminish the climbing defect significantly as determined by non-linear fitting of the climbing curves and comparing the 95% CI. The genotypes are *Ddc-Gal4/UAS-Drp1-RNAi/UAS-lacZ* and *Ddc-Gal4/UAS-Drp1-RNAi/UAS-foxo-RNAi*. Error bars indicate standard error of the mean and $N = 50$.

Inhibition the expression of *foxo* and *Rbf* via *Ddc-Gal4*$^{4.3D}$

The control *Ddc-Gal4; UAS-Rbf-RNAi; UAS-lacZ* critical class males were determined to have a median lifespan of 58 days (n=351). The directed inhibition of *foxo* in the *Ddc-Gal4; UAS-Rbf-RNAi results* in median lifespan of 62 days (n=314) compared to control (Figure 8.4A) with a P-value of <0.0001 as determined by log-rank (Mantel-Cox) test. The non-linear fitting of the climbing curve shows *foxo* inhibition does not affect the climbing ability defect compared to control at 95% CI (P-value 0.3389) (Figure 8.4B).

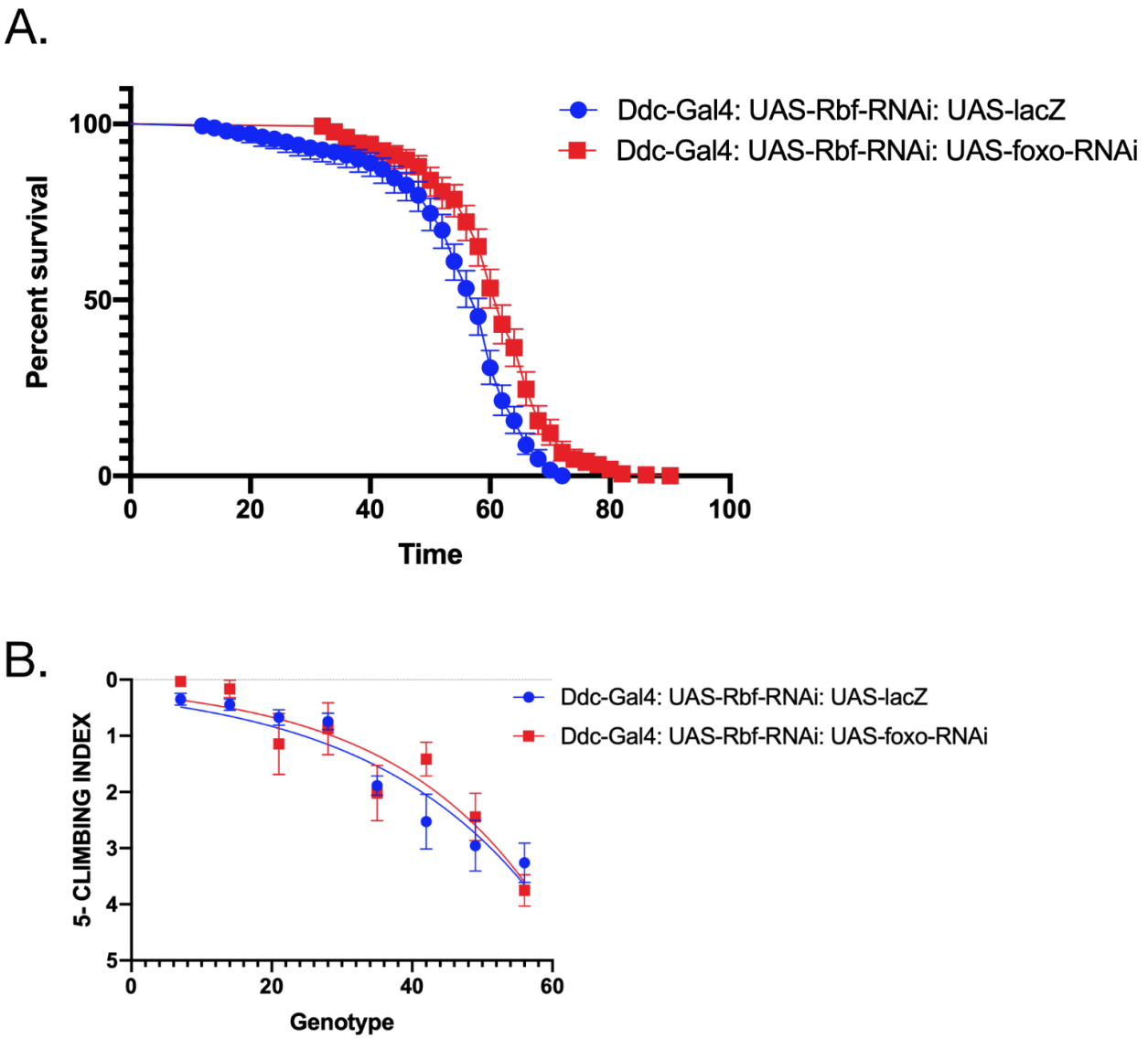

Figure 8.4: RNA interference of *foxo* along with the expression of *Rbf* directed by *Ddc-Gal4$^{4.3D}$*. The expression of *foxo-RNAi* lines in the Ddc-Gal4 UAS-Rbf expressing neurons results in increase lifespan compare to control. **A.** The inhibition of *foxo* in *the Ddc-Gal4 UAS-Rbf*-expressing neurons results in lifespan of 62 days compared to 58 days of control flies with expression of the *lacZ* transgene. The genotypes are *Ddc-Gal4/UAS-Rbf/UAS-lacZ* and *Ddc-Gal4/UAS-Rbf/UAS-foxo-RNAi*. Longevity is shown as percent survival ($P < 0.05$, determined by the Log-rank (Mantel–Cox) test and $N > 300$). **B** The inhibition of *foxo* in these neurons resulted in no significant difference in climbing ability as determined by nonlinear fitting of the climbing curves and comparing the 95% CI. The genotypes are *Ddc-Gal4/UAS-Rbf/UAS-lacZ* and *Ddc-Gal4/UAS-Rbf/UAS-foxo-RNAi.* Error bars indicate standard error of the mean and $N = 50$.

Inhibition the expression of *foxo* along with *UAS-parkin-RNAi* via *Ddc-Gal4$^{4.3D}$*

The control *Ddc-Gal4; UAS-parkin-RNAi; UAS-lacZ* critical class males were determined to have a median lifespan of 62 days (n=275). The directed inhibition of *foxo* in the *Ddc-Gal4; UAS-parkin-RNAi;* transgene results in median lifespan of 68 days (n=384) compared to control (Figure 8.5A) with a P-value of <0.0001 as determined by log-rank (Mantel-Cox) test (Figure 5A) The non-linear fitting of the climbing curve shows *foxo* inhibition has ameliorated the climbing ability defect compared to control at 95% CI (P-value of 0.0135) (Figure 8.5B).

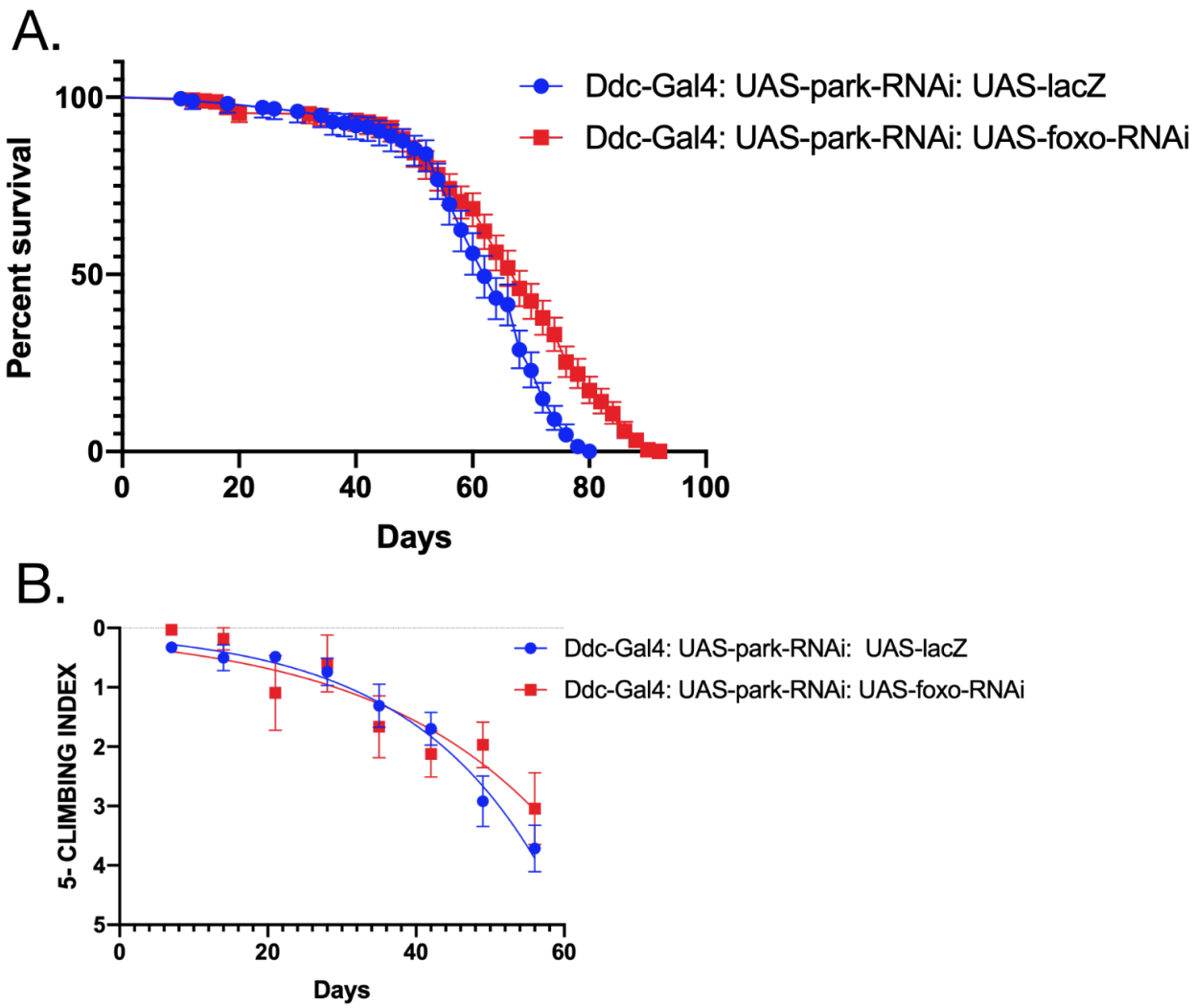

Figure 8.5: RNA interference of both *foxo* and *parkin* expression directed by *Ddc-Gal4$^{4.3D}$*. The expression of *foxo-RNAi* lines in the Ddc-Gal4 UAS-parkin-RNAi expressing neurons results in increase lifespan compare to control. **A.** The inhibition of *foxo* in the *Ddc-Gal4 UAS-parkin-RNAi*-expressing neurons results in lifespan of 68 days compared to 62 days of control flies expressing the *lacZ* transgene. The genotypes are Ddc-Gal4/UAS-parkin-RNAi/UAS-lacZ and Ddc-Gal4/UAS-parkin-RNAi/UAS-foxo-RNAi. Longevity is shown as percent survival ($P < 0.05$, determined by the Log-rank (Mantel–Cox) test and $N > 300$). **B** The inhibition of foxo in these neurons resulted in no significant difference in climbing ability as determined by nonlinear fitting of the climbing curves and comparing the 95% CI. The genotypes are Ddc-Gal4/UAS-parkin-RNAi/UAS-lacZ and Ddc-Gal4/UAS-parkin-RNAi/UAS-foxo-RNAi. Error bars indicate standard error of the mean and N = 50

Inhibition of the expression of *foxo* along with *α-synuclein* expression via *Ddc-Gal4$^{4.36}$ transgene*

The control *Ddc-Gal4; UAS-α-synuclein; UAS-lacZ* critical class males were determined to have a median lifespan of 78 days (n=257). The directed inhibition of *foxo* in the *Ddc-Gal4; UAS-α-synu; UAS-lacZ* transgene results in median lifespan of 112 days (n=405) much higher compared to control with a P-value of <0.0001 as determined by log-rank (Mantel-Cox) test (Figure 8.6A). The non-linear fitting of the climbing curve shows *foxo* inhibition rescued the climbing ability defect compared to control at 95% CI (P-value <0.0001) (Figure 8.6B)

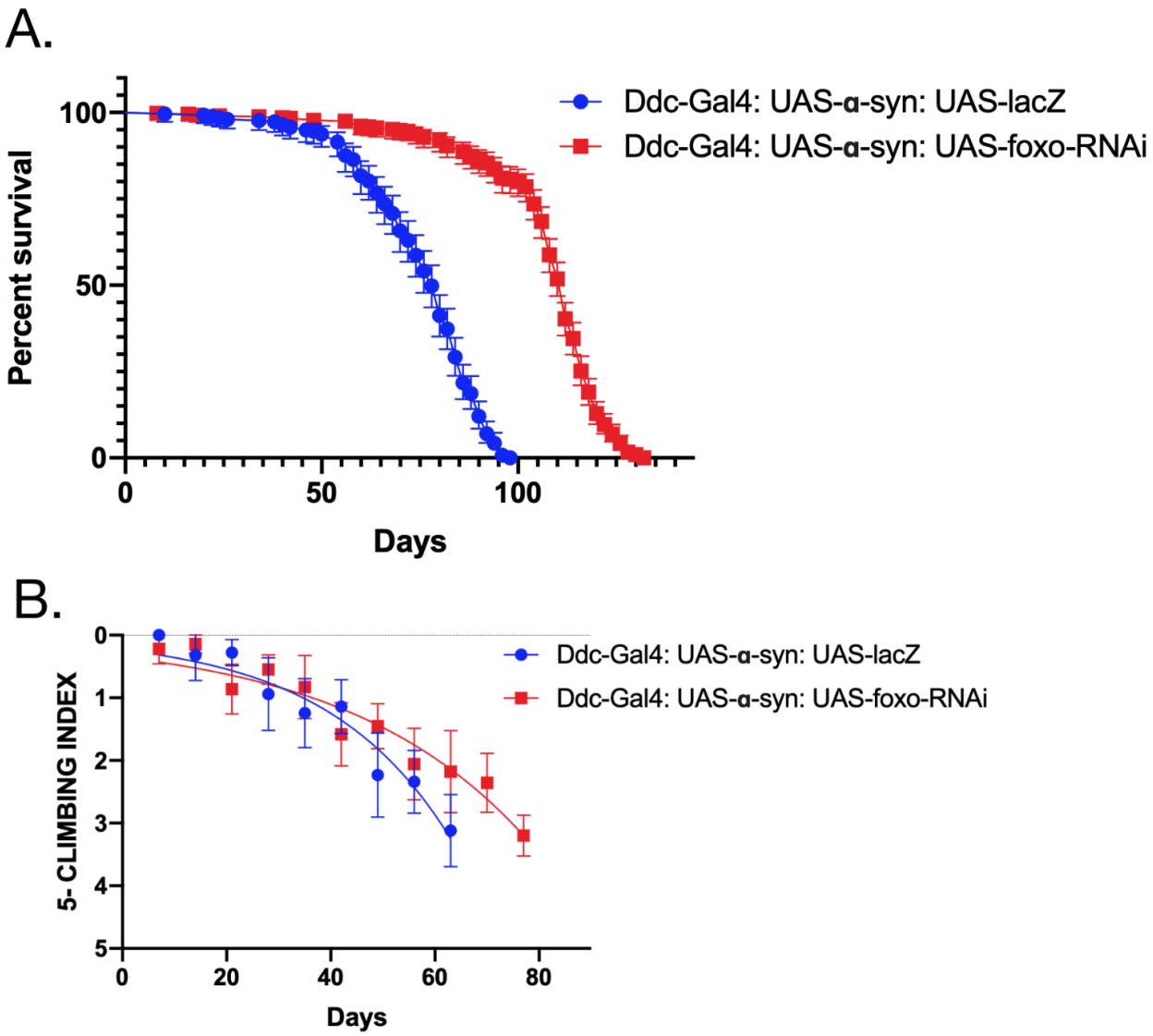

Figure 8.6: RNA interference of *foxo* along with the expression of *α-synuclein* directed by *Ddc-Gal4*$^{4.3D}$. The expression of *foxo-RNAi* lines in the *Ddc-Gal4 UAS-α-synuclein* expressing neurons results in increase lifespan compare to control. **A.** The inhibition of *foxo* in the *Ddc-Gal4 UAS-α-synuclein*-expressing neurons results in lifespan of 112 days compared to 78 days of control flies expressing the lacZ transgene. The genotypes are *Ddc-Gal4/UAS-α-syn*/UAS-lacZ and *Ddc-Gal4/UAS-α-syn/UAS-foxo-RNAi*. Longevity is shown as percent survival ($P < 0.05$, determined by the Log-rank (Mantel–Cox) test and $N > 300$). **B.** The inhibition of foxo in these neurons resulted in significant improvement in climbing ability as determined by nonlinear fitting of the climbing curves and comparing the 95% CI. The genotypes are *Ddc-Gal4/UAS-α-syn/UAS-lacZ* and *Ddc-Gal4/UAS-α-syn/UAS-foxo-RNAi*. Error bars indicate standard error of the mean and $N = 50$.

Discussion

Acute stress can cause *foxo* to activate the transcription of pro-apoptotic genes (Fu and Tindall 2008). My results indicate that loss of *foxo* in the *Ddc-Gal4*-expressing neurons do not alter median lifespan. The overexpression of *foxo* by the *Ddc-Gal4* transgene was found to be lethal. Notably, the Foxo transcription factor plays a central role in neuroprotection and protects against axonal tract degeneration in mammalian models (Hwang et al. 2018). The overexpression of *Foxo* is not always toxic and it is a bona-fide tumour suppressor and helps in alleviating different cellular stresses. The IRS is dependent on foxo, Rbf and other transcription factors (Wei et al. 2016). The co-inhibition of *foxo* and *Rbf* by RNAi transgenes directed by *Ddc-Gal4* can result in an increase to median lifespan and little effect upon the compromised climbing ability. The molecular mechanism behind the pro-cell survival affects is anticipated to be increase in homeostasis.

The suppression of *foxo* along with the overexpression of *Drp1* directed by the *Ddc-Gal4* transgene can rescue the median lifespan and climbing ability defects caused by *Drp1* overexpression. Studies have shown that *foxo* can activate *Drp1* by mediating its phosphorylation at S616 in mice (Shi et al. 2018), which can explain the inhibition of *foxo* rescued the *Drp1* overexpression phenotype and likely the pathway is conserved between flies and mammals. The co-suppression of *foxo* and *Drp1* decreases the median lifespan of *Drp1-RNAi* lines. The inhibition of *foxo* likely further increases the mitochondrial network connectivity and lose the survival advantage over *Drp1-RNAi* alone. One of the main functions of *foxo* is the stress response and hyper-elongated mitochondrial network increase cellular stress (Das and Chakrabarti 2020). The hyper-elongated mitochondria inhibit mitophagy and prolonged fusion can cause apoptosis (Das and Chakrabarti 2020). The inhibition of *foxo* and *Drp1* disturb the hemostasis balance and adversely affect the flies health-span.

Foxo is known to induced apoptosis in DA neurons under oxidative stress. In mammals foxo1 promotes mitophagy via Pink1/parkin pathway (Li et al. 2017). In flies, *foxo* overexpression has prevented the parkin mutant dependent DA neuronal loss (Tain et al. 2009). Surprisingly the inhibition of foxo seems to increase the homeostasis and rescue the *parkin*-dependent model of PD assumed by increased health span of the flies. This reiterates the diverse role of *foxo,* that it can protect DA neurons when stress is low and initiate apoptosis during high oxidative stress (Webb and Brunet 2014). The suppression of *foxo* also rescue the *α-synuclein* induced PD phenotype of compromised longevity and climbing defect in flies. Previous finding shows dominant negative *foxo* has protective effect against acute oxidative stress caused by *α-synuclein* in mammalian cell culture by increasing the number of autophagosomes (Pino et al. 2014). Presumably, the effect of *foxo* inhibition is similar in flies and mammals. Future study needs to investigate the importance of expression level of mitochondrial protection proteins (Pink1, parkin, Drp1) and their direct and indirect relationship with *foxo* transcription factor.

	Genotype	Median lifespan	Lifespan Increased/ Decreased	Climbing Increase/ Decrease
Control	*Ddc-Gal$^{4.3D;}$ UAS-lac Z*	68 days		
Experiment	*Ddc-Gal$^{4.3D;}$ UAS-foxo-RNAi*	72 days	Similar to control	Decreased
Control	*Ddc-Gal$^{4.36;}$ UAS-lac Z*	92 days		
Experiment	*Ddc-Gal$^{4.36;}$ UAS-foxo-RNAi*	96 days	Similar to control	Decreased
Control	*Ddc-Gal$^{4.3D;}$ UAS-Drp1; UAS-lac Z*	50 days		
Experiment	*Ddc-Gal$^{4.3D;}$ UAS-Drp1; UAS-foxo-RNAi*	70 days	Increased	Increased
Control	*Ddc-Gal$^{4.3D;}$ UAS-Drp1-RNAi; UAS-lac Z*	70 days		
Experiment	*Ddc-Gal$^{4.3D;}$ UAS-Drp1-RNAi; UAS-foxo-RNAi*	67 days	Decreased	Similar to control
Control	*Ddc-Gal$^{4.3D;}$ UAS-Rbf-RNAi; UAS-lac Z*	58 days		
Experiment	*Ddc-Gal$^{4.3D;}$ UAS-Rbf-RNAi; UAS-foxo-RNAi*	62 days	Increased	Similar to control
Control	*Ddc-Gal$^{4.3D;}$ UAS-park-RNAi; UAS-lac Z*	62 days		
Experiment	*Ddc-Gal$^{4.3D;}$ UAS-park-RNAi; UAS-foxo-RNAi*	68 days	Increased	Increased
Control	*Ddc-Gal$^{4.36;}$ UAS-α-syn; UAS-lac Z*	78 days		
Experiment	*Ddc-Gal$^{4.36;}$ UAS-α-syn; UAS-foxo-RNAi*	112 days	Increased	Increased

Table 8. 1: Summary of the Results. The effect of the directed inhibition of *UAS-foxo-RNAi* in the *Ddc-Gal4$^{4.3D}$*, *Ddc-Gal4$^{4.36}$*, *Ddc-Gal4$^{4.3D}$UAS-Drp1*, *Ddc-Gal4$^{4.3D}$ UAS-Drp1-RNAi*, *Ddc-Gal4$^{4.3D}$ UAS-Rbf-RNAi*, *Ddc-Gal$^{4.3D;}$ UAS-parkin-RNAi* and *Ddc-Gal4$^{4.36}$ UAS-α-synuclein* transgene on the median lifespan and climbing ability of the critical class male flies. The Cells with blue highlight denote control; Orange highlight denotes the decreased compared to control and Green highlights denote the increase compare to control.

Conclusion

The foxo transcription factor respond differently to various molecular cues. The overexpression of *Drp1*-induced PD phenotypes is rescued by the inhibition of *foxo*. The inhibition of *foxo* rescued the *parkin*-induced PD-phenotypes strongly associated with a compromised level of mitochondrial health due to reduced mitophagy. The flies that express *α-syn*to induce PD-like phenotype via *Ddc-Gal4* was rescued by inhibition of the expression of *foxo.* We anticipate *foxo* inhibition may increase the number of autophagosomes and alleviate the *α-synuclein*-induced stress. The suppression of *foxo* can ameliorate the *Rbf*-induced longevity phenotype but does not affect climbing defect. These results demonstrate the multi-faceted mechanisms involved in the regulation by *foxo* through downstream targets and the potential to lead to aspects of the aetiology of PD.

Bibliography

Acharya, P., Negre, N., Johnston, J., Wei, Y., White, K.P., Henry, R.W., and Arnosti, D.N. 2012. Evidence for Autoregulation and Cell Signalling Pathway Regulation From Genome-Wide Binding of the Drosophila Retinoblastoma Protein. G3 Genes, Genomes, Genet. **2**(11): 1459–1472. doi:10.1534/g3.112.004424.

Angelova, D.M., Jones, H.B.L., and Brown, D.R. 2018. Levels of a-and b-synuclein regulate cellular susceptibility to toxicity from a-synuclein oligomers. FASEB J.: 995–1006. doi:10.1096/fj.201700675R.

Bartolomé, A., García-Aguilar, A., Asahara, S.-I., Kido, Y., Guillén, C., Pajvani, U.B., and Benito, M. 2017. MTORC1 Regulates both General Autophagy and Mitophagy Induction after Oxidative Phosphorylation Uncoupling. Mol. Cell. Biol. **37**(23). American Society for Microbiology. doi:10.1128/mcb.00441-17.

Das, R., and Chakrabarti, O. 2020, April 1. Mitochondrial hyperfusion: A friend or a foe. Biochemical Society Transactions. Portland Press Ltd. doi:10.1042/BST20190987.

Fu, Z., and Tindall, D.J. 2008, April 7. FOXOs, cancer and regulation of apoptosis. NIH Public Access. doi:10.1038/onc.2008.24.

Greer, E.L., and Brunet, A. 2005, November 14. FOXO transcription factors at the interface between longevity and tumor suppression. doi:10.1038/sj.onc.1209086.

Greer, E.L., and Brunet, A. 2007. FOXO transcription factors in ageing and cancer. Acta Physiol. **192**(1): 19–28. Blackwell Publishing Ltd. doi:10.1111/j.1748-1716.2007.01780.x.

Huang, H., and Tindall, D.J. 2007, August 1. Dynamic FoxO transcription factors. The Company of Biologists Ltd. doi:10.1242/jcs.001222.

Hwang, I., Oh, H., Santo, E., Kim, D.Y., Chen, J.W., Bronson, R.T., Locasale, J.W., Na, Y., Lee, J., Reed, S., Toth, M., Yu, W.H., Muller, F.L., and Paik, J. 2018. FOXO protects against age-progressive axonal degeneration.ageing Cell **17**(1). Blackwell Publishing Ltd. doi:10.1111/acel.12701.

Kramer, J.M., Davidge, J.T., Lockyer, J.M., and Staveley, B.E. 2003. Expression of Drosophila FOXO regulates growth and can phenocopy starvation. BMC Dev. Biol. **3**: 1–14. BioMed Central Ltd. doi:10.1186/1471-213X-3-5.

Li, W., Du, M., Wang, Q., Ma, X., Wu, L., Guo, F., Ji, H., Huang, F., and Qin, G. 2017. FoxO1 Promotes Mitophagy in the Podocytes of Diabetic Male Mice via the PINK1/Parkin Pathway. Endocrinology **158**(7): 2155–2167. Narnia. doi:10.1210/en.2016-1970.

Martins, R., Lithgow, G.J., and Link, W. 2016, April 1. Long live FOXO: Unraveling the role of FOXO proteins inageing and longevity. Blackwell Publishing Ltd. doi:10.1111/acel.12427.

Mei, Y., Zhang, Y., Yamamoto, K., Xie, W., Mak, T.W., and You, H. 2009. FOXO3a-dependent regulation of Pink1 (Park6) mediates survival signalling in response to cytokine deprivation. Proc. Natl. Acad. Sci. **106**(13): 5153–5158. doi:10.1073/pnas.0901104106.

Pino, E., Amamoto, R., Zheng, L., Cacquevel, M., Sarria, J.C., Knott, G.W., and Schneider, B.L. 2014. FOXO3 determines the accumulation of α-synuclein and controls the fate of dopaminergic neurons in the substantia nigra. Hum. Mol. Genet. **23**(6): 1435–1452. Oxford Academic. doi:10.1093/hmg/ddt530.

Puig, O., and Tjian, R. 2005. Transcriptional feedback control of insulin receptor by dFOXO/FOXO1. Genes Dev. **19**(20): 2435–2446. Cold Spring Harbor Laboratory Press. doi:10.1101/gad.1340505.

Recasens, A., and Dehay, B. 2014, December 18. Alpha-synuclein spreading in Parkinson's disease. Frontiers Media S.A. doi:10.3389/fnana.2014.00159.

Shi, Y., Fan, S., Wang, D., Huyan, T., Chen, J., Chen, J., Su, J., Li, X., Wang, Z., Xie, S., Yun, C., Li, X., and Tie, L. 2018. FOXO1 inhibition potentiates endothelial angiogenic functions in diabetes via suppression of ROCK1/Drp1-mediated mitochondrial fission. Biochim. Biophys. Acta - Mol. Basis Dis. **1864**(7): 2481–2494. Elsevier B.V. doi:10.1016/j.bbadis.2018.04.005.

Tain, L.S., Mortiboys, H., Tao, R.N., Ziviani, E., Bandmann, O., and Whitworth, A.J. 2009. Rapamycin activation of 4E-BP prevents parkinsonian dopaminergic neuron loss Europe PMC Funders Group. Nat Neurosci **12**(9): 1129–1135. doi:10.1038/nn.2372.

Thomas, R.E., Andrews, L.A., Burman, J.L., Lin, W.-Y., and Pallanck, L.J. 2014. PINK1-Parkin Pathway Activity Is Regulated by Degradation of PINK1 in the Mitochondrial Matrix. PLoS Genet. **10**(5): e1004279. Public Library of Science. doi:10.1371/journal.pgen.1004279.

Todd, A., and Staveley, B. 2012. Expression of Pink1 with α-synuclein in the dopaminergic neurons of Drosophila leads to increases in both lifespan and healthspan. Genet. Mol. Res. **11**(2): 1497–1502. doi:10.4238/2012.May.21.6.

Todd, A.M., and Staveley, B.E. 2004. Novel assay and analysis for measuring climbing ability in Drosophila. Drosoph. Inf. Serv. **87**: 101–108. Available from http://www.ou.edu/journals/dis/DIS87/4 - Techniques.pdf [accessed 6 October 2019].

Webb, A.E., and Brunet, A. 2014. FOXO transcription factors: key regulators of cellular quality control. Trends Biochem. Sci. **39**(4): 159–69. NIH Public Access. doi:10.1016/j.tibs.2014.02.003.

Wei, Y., Gokhale, R.H., Sonnenschein, A., Montgomery, K.M., Ingersoll, A., and Arnosti, D.N. 2016. Complex cis-regulatory landscape of the insulin receptor gene underlies the broad expression of a central signalling regulator. Development **143**(19): 3591–3603. Company of Biologists. doi:10.1242/dev.138073.

Chapter 9: Altered expression of *Drp1, Buffy, Debcl, Rbf, Pink1, parkin and trbl* in the developing Drosophila eye alters the characteristic *foxo* phenotype

Abstract

The insulin receptor signalling pathway maintains cellular homeostasis. The transcription factor, foxo, is a crucial downstream target of IRS and regulates numerous cellular pathways to sustain cellular health. The health of mitochondria is essential for maintaining cellular health and homeostasis. Pink1, parkin, Drp1 and members of the Bcl-2 family of proteins are the direct regulators of mitochondrial health and other proteins such as Rbf and trbl have an indirect role. The transcription factor foxo indirectly regulates mitochondrial dynamics and cellular homeostasis. The expression of foxo directed by the GMR-Gal4 transgene during the development of the Drosophila eye produces a robust phenotype characterized by reduced numbers of ommatidia and inter-ommatidial bristles to provide a biological system to study genetic interactions. The directed inhibition of Pink1 or Rbf1 ameliorates the foxo-induced eye phenotype in Drosophila. Alteration of the expression of both anti-apoptotic and pro-apoptotic Bcl-2 protein genes has either no effect or makes the characteristic phenotype more severe. Modification of the expression of the pseudo-kinase gene trbl has mixed effects on the foxo eye phenotype. These results implies that the developmental eye defect of foxo transcription factor can be modified by different downstream regulators like Pink1 and Rbf.

Introduction

Parkinson disease (PD) is a progressive motor disorder characterized by the loss of dopaminergic (DA) neurons in the SNPc of the brain. The cell death of DA neurons seems to be the consequence of the dysfunction of cell signalling pathways, primarily those that produce dysfunctional mitochondria and eventually cause intrinsic apoptosis. The transcription factor *foxo* influences stress responses and regulates multiple cellular processes such as insulin receptor signalling (IRS),

energy metabolism, autophagy (and the subtype, mitophagy), cellular differentiation and cell death (Greer and Brunet 2005). The IRS pathway acts to sequester and incapacitate the foxo transcription factor by translocating it from the nucleus to the cytoplasm (Greer and Brunet 2007). During different cellular stresses, foxo is responsible for the transcription of a specific set of genes to provide resistance to stress (Kramer et al. 2003). The overexpression of *foxo* can be toxic and upregulation can lead to tumourigenesis (Huang and Tindall 2007). The directed expression of *foxo* in developing eye of drosophila generates a phenotype that is characterized by a reduced number of ommatidia and complete or nearly complete loss of interommatidial bristles (Kramer et al. 2003; Todd and Staveley 2013). The overall effect of foxo on the outcome of organismal survival can vary from cell survival to cell death, depending on the cellular requirement and molecular cues.

The foxo transcription factors influence an array of signal transduction pathways. The expression of foxo can lead to the phosphorylation and activation of the mitochondrial fission protein Drp1 in endothelial cells (Shi et al. 2018). The activity of foxo can regulate mitochondrial dynamics through the activation of the ROCK1 (rho-associated, coiled-coil-containing protein kinase 1) transcription factor (Shi et al. 2018). Foxo can regulate the process of Pink1/parkin-mediated mitophagy through the control of the expression of *Pink1* (Mei et al. 2009; Li et al. 2017; Bartolomé et al. 2017). The Pink1 protein can act to recruit the parkin E3 ubiquitin ligase to the surface of the mitochondrial membrane to induce the ubiquitination of mitochondrial proteins (Thomas et al. 2014). Not limited to mitophagy, Parkin can function in other cell protective pathways (Panicker et al. 2017). In mammalian cell culture, the foxo protein can activate the transcription of pro-apoptotic Bcl-2 family genes, such as *Bim* and *Binp3,* and can indirectly suppress the expression of pro-survival such as *Bcl-xL* (Fu and Tindall 2008). However, direct foxo mediated activation of Bcl-

2 family protein is not established in drosophila. More experiments are required to understand the mechanisms of Bcl-2 protein regulation in drosophila. The pseudo-kinase-encoding gene tribbles (trbl) has shown to decrease phosphorylation of the foxo protein (Das et al. 2014). Although not active as a kinase, the protein product of trbl functions as an adaptor molecule in important signalling pathways that include those that lead to the deactivation of both the foxo and Akt proteins (Yokoyama and Nakamura 2011). Overall, this evidence supports the hypothesis that foxo may be the central regulator of pathways that control the cellular decision between cell survival and cell death.

The transcription factor Rbf is the fly version of the human pRb protein and plays essential role in G1/S transition and the regulation of various cellular processes that include DNA replication, DNA repair, cell cycle, transcription, oncogenesis, tumour suppression and apoptosis (Classon and Harlow 2002; Chakraborty et al. 2007). Rbf is a component of the DREAM complex (dimerization partner, RB-like, E2F and multi-vulval class B), a multiprotein complex, that can act as a transcription activator or repressor depending upon the cellular environment (Ariss et al. 2018). The Rbf is reported to target IRS pathway genes in drosophila (Acharya et al. 2012) and the *foxo* protein is regulated by IRS pathway (Puig and Tjian 2005). Determination of the extent of Rbf and foxo upon cellular pathways in cellular homeostasis will be very informative.

Experimentally, the role of foxo overexpression in the developing eye phenotype can be quite informative. However, little is known about the activities that can to alleviate the “foxo” phenotype. Here I propose that the phenotype primarily results from the initiation of excessive apoptosis due to the elevated level of the foxo and can be rescued by the specific regulation of this process. The role of dysfunction mitochondrial, IRS, and other regulatory protein-encoding

genes suggests that they might be candidates to rescue the foxo eye phenotype. I employed Drosophila melanogaster as a model organism to study the phenotypic effects of the interactions of the foxo with the mitochondrial protection genes, which can alter apoptosis. In my experiments, I exploited the *UAS-Gal4* system to direct the expression and inhibition of the foxo gene in developing eye using *GMR-Gal4*. The overexpression of foxo has led to disrupted eye phenotype. I altered the expression of *Drp1, Buffy, Debcl, Rbf, Pink1, parkin* and *trbl* in *GMR-Gal4 UAS-foxo* transgene to observe effects upon the foxo eye phenotype.The inhibition of *Pink1* can rescue the *foxo* phenotype in support of previous observations (Todd and Staveley 2013), the phenotypic effects can be lessened by inhibiting the transcription regulator gene, Rbf or pseudo-kinase, trbl. In addition, I found the phenotype is made more severe by the directed overexpression of either *Buffy* or *Drp1. Pink1* and *Rbf* alleviate the phenotype, but *Buffy* and *Drp1* don't.

Material and Methods

Drosophila Stocks and media

Drosophila stocks and culture media: The *GMR-Gal4*^{12}; *UAS-lacZ*$^{4-1-2}$; *UAS-Drp1 (y[1] w[*]; P{w[+mC]=FLAG-FlAsH-HA-Drp1}3, Ki[1]), UAS-Drp1-RNAi1*^{JF02762} *(y[1] v[1]; P{y[+t7.7]v[+t1.8]=TRiP.JF02762}attP2}), UAS-Drp1-RNAi2*^{HMC03230} *(y[1] v[1]; P{y[+t7.7]v[+t1.8]=TRiP.HMC03230}attP40), UAS-Buffy (w[*]; P{w[+mC]=UAS-Buffy.S}E1); UAS-Buffy-RNAi (w[*], P{w[+mC]=UAS-Buffy.RNAi}3), UAS-Debcl*^{EY05743} *(y[1] w[67c23], P{y[+mDint2 w[+mC]=EPgy2}Debcl[EY05743]),* the *UAS-Rbf (*w[*]; P{w[+mC]=UAS-Rbf.D}III), the *UAS Rbf RNAi1*^{HMS03004} *(y[1] sc[*] v[1] sev[21]; P{y[+t7.7] v[+t1.8]=TRiP.HMS03004}attP2/TM3, Sb[1])*, the *UAS Rbf RNAi2*^{GL01293} *(y[1] sc[*] v[1] sev[21]; P{y[+t7.7] v[+t1.8]=TRiP.GL01293}attP40), UAS-trbl-1 or UAS-trbl.M (w[1118];P{w[+mC]=UASp-trbl.M}3*), *UAS-trbl-2 or UAS-trbl*^{EP3519}

(w[1118];P{w[+mC]=EP}trbl[EP3519]/TM6B, Sb [1]), UAS-trbl-3 or UAS-trbl^{EP1119} *(w[1118];P{w[+mC]=EP}trbl[EP1119]/TM6B, Tb [1]), UAS-trbl-RNAi-1 or UAS-trbl RNAi*^{HMS04999} *(y[1]sc[*]v[1];P{y[+7.7]v[+1.8]=TRiP.HMS04999}attP2), UAS-trbl-RNAi-2 or UAS-trbl RNAi*^{HMC04159} *(y[1]sc[*]v[1];P{y[+7.7]v[+1.8]=TRiP.HMC04159}attP2)* and the *UAS-trbl-RNAi-3 or UAS-trbl RNAi* ^{GL01337} *(y[1]sc[*]v[1];P{y[+7.7]v[+1.8]=TRiP.GL01337}attP2)* stocks were obtained from Bloomington Drosophila Stock Center at Indiana University, Bloomington, Indiana, USA. The *UAS-Debcl-RNAi*^{v47515} (*w1118; P{GD 1637}v47515*) and *UAS-foxo-RNAi* (P{KK108590}VIE-260B) was obtained from Vienna Drosophila Resource Center. The *UAS-foxo* line is described (Kramer *et al*., 2003) and the *GMR-Gal4 UAS-foxo,* line was produced through standard methods (M'Angale and Staveley, 2016). All flies were maintained on standard cornmeal/molasses/yeast/agar media treated with propionic acid and methylparaben to resist fungal growth. Stocks were kept at room temperature (22° ± 3° C), whereas crosses and experiments were maintained at 25°C.

Biometric analysis of the *Drosophila melanogaster* eye

Female virgins of the *GMR-Gal4-UAS-foxo* genotype were collected every 8 to 12 hours for several days. The confirmed virgins were then crossed with the males of *UAS-lacZ*, *UAS-Drp1, UAS-Drp1-RNAi1*^{JF02762}*, UAS-Drp1-RNAi2*^{HMC03230}*, UAS-Buffy, UAS-Buffy-RNAi, UAS-Debcl* ^{EY05743}*, UAS-Debcl-RNAi*^{v47515}*, UAS-Rbf*, *UAS-Rbf RNAi1*^{HMS03004}, *UAS-Rbf RNAi2* ^{GL01293}*, UAS-trbl.M-1, UAS-trbl*^{EP3519}*-2, UAS-trbl*^{EP1119}*-3*, *UAS-trbl RNAi-1*^{HMS04999}, *UAS-trbl RNAi-2*^{HMC04159} and the *UAS-trbl RNAi-3* ^{GL01337} genotypes. Critical class male progeny was collected for each genotype. The collected flies were kept as cohorts of 10 flies or less upon fresh media and allowed to age for 3 to 4 days. The flies were prepared for scanning electron microscopy following the standard protocol (Githure and Staveley 2017). Ommatidia, interommatidial bristle counts and eye disruption area was calculated

on 15 or more flies of each genotype using National Institute of Health (NIH) ImageJ software. The disrupted eye area was calculated through the determination of the area of eye without ommatidium; done on 15 eyes of each genotype (Lipsett and Staveley 2014). The Biometric analysis was performed using GraphPad Prism version 8 statistical software. Significance was determined at 95% confidence level ($P \leq 0.05$).

Results and Discussion

The overexpression and inhibition of *foxo* during eye development directed by *GMR-Gal4*

The inhibition and overexpression of *foxo*, directed by the *GMR- Gal4* transgene in the neuron-rich developing eye of flies can influence development. The control *GMR-Gal4; UAS-lacZ* critical class males were determined to have an ommatidial count of 703 (n=15). The overexpression of *foxo* directed by the *GMR-Gal4* has mean ommatidial count of 335.8, much less compared to control with P value <0.0002 as determined by unpaired t-test (Figure 9.1B). The directed expression of *foxo-RNAi* directed by the *GMR-Gal4* has mean ommatidial count of 718, higher compared to control with P-value <0.0484 as determined by unpaired t-test. The control *GMR-Gal4; UAS-lacZ* critical class males were determined to have an interommatidial bristle count of 536 (n=10). The overexpression of *foxo* directed by *GMR-Gal4* transgene has mean interommatidial bristle count of 4.333 (P-value<0.0001), very low compare to control flies as determined by an unpaired t-test. The RNAi-dependent inhibition of *foxo* directed by *GMR-Gal4* transgene has mean interommatidial bristle count of 548.3 (P-value 0.3202), similar to control as determined by an unpaired t-test. The disrupted eye area of *foxo* is 2932um^2, compared to the *lacZ* control flies, which does not have detectable regions of disrupted ommatidia and/or bristle

as shown in Figure 9.1B (iii) as determined by unpaired t-test with P-values <0.0001. The decrease in the interommatidial bristle number is consistent with the reduction of ommatidial numbers produced through overexpression of the *foxo* transgene compared to control.

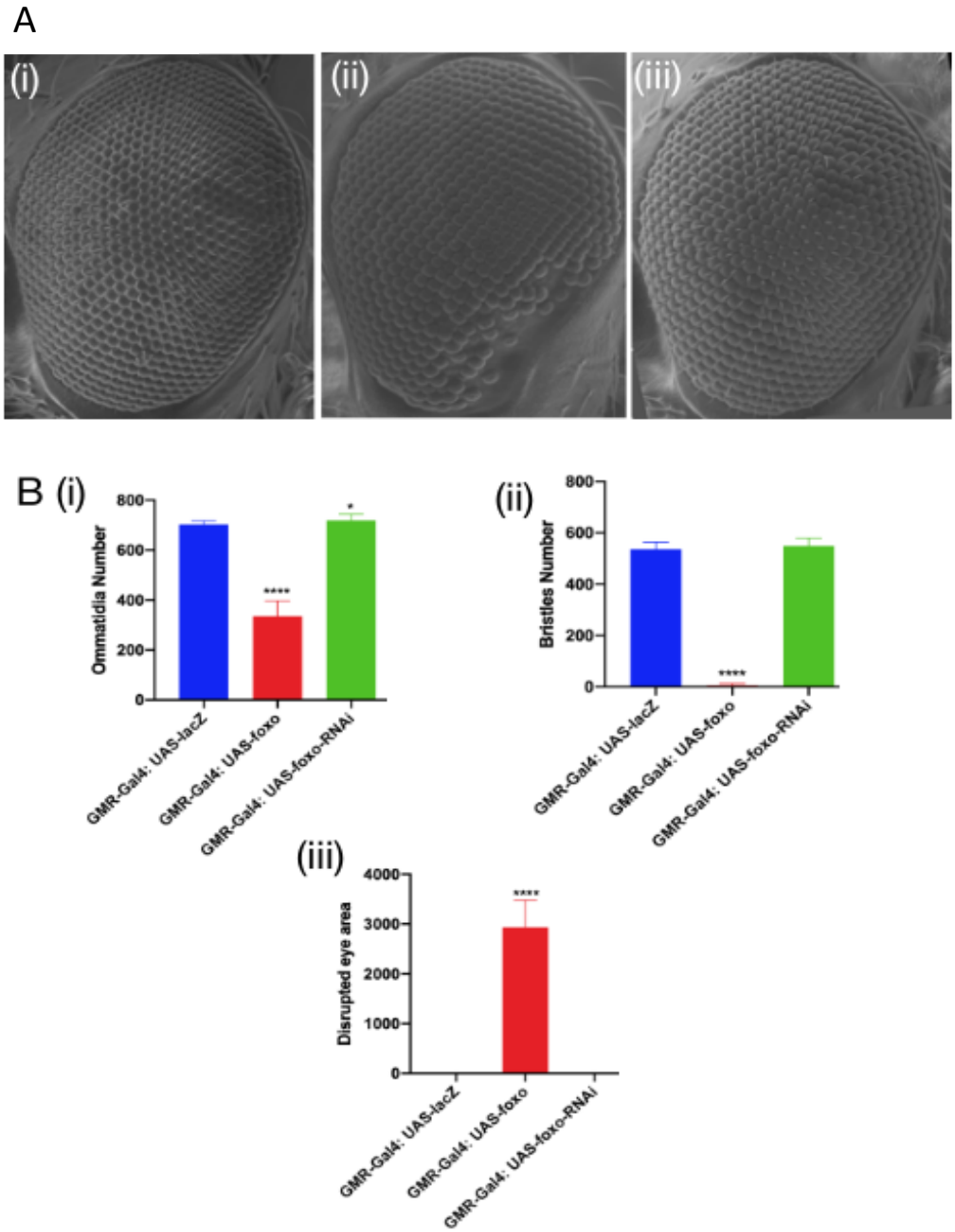

Figure 9.1: The phenotypic effects of altered *foxo* expression in *D. melanogaster* eye. A. Scanning electron micrograph of the altered *foxo* expression under the control of *GMR-Gal4* transgene. The genotypes are (a) *GMR-Gal4/UAS-lacZ* (Control); (b) *GMR-Gal4/UAS-foxo*; (c) *GMR-Gal4/UAS-foxo-RNAi*. **B.** The mean ommatidial count for control is 703; the expression of *foxo* results in 335.8 ommatidia, decreased compared to control. The mean ommatidial number of *foxo-RNAi* is 518.8, a slight increase compares to control. **C.** The mean interommatidial bristle count for the control is 536, and the expression lines have almost no interommatidial bristle. The mean interommatidial bristle count of *foxo-RNAi* line is 548.3 similar to control. **D.** There is no detectable areas of disruption in the eyes of the control and *foxo-RNAi* but *foxo* overexpression line has very large disrupted eye area without ommatidium.

Effects of *Drp1* and *Drp1-RNAi* expression directed by *GMR-Gal4* on the *foxo* eye phenotype

The control *GMR-Gal4; UAS-foxo UAS-lacZ* critical class males were determined to have mean ommatidial count of 377.9 (n=15). The overexpression of *Drp1* along with *foxo* directed by the *GMR-Gal4* has mean ommatidial count of 317.8, much less compared to control with P-value <0.0031 as determined by unpaired t-test (Figure 9.2B i). The inhibition of *Drp1* by *Drp1-RNAi's* along with *foxo* directed by the *GMR-Gal4* has mean ommatidial count of 416.4 (P-value 0.1300) and 375 (P-value=0.8497), similar to control as determined by unpaired t-test (Figure 9.2B i).

The control *GMR-Gal4; UAS-foxo UAS-lacZ* critical class males were determined to have mean interommatidial bristle count of 4.846 (n=15). The overexpression of *Drp1* along with *foxo* directed by the *GMR-Gal4* has no interommatidial bristle, much less compared to control with P-value <0.0001 as determined by unpaired t-test (Figure 9.2B ii). The inhibition of *Drp1* by *Drp1-RNAi's* along with *foxo* directed by the *GMR-Gal4* has mean interommatidial bristle count of 1.769 (P-value 0.0219) and 0.3846 (P-value 0.0016), much less compared to control with P-value <0.0001 as determined by unpaired t-test (Figure 9.2B ii)

The control *GMR-Gal4; UAS-foxo UAS-lacZ* critical class males were determined to have 2932 μm^2 (n=15) mean disrupted eye area of. The overexpression of *Drp1* along with *foxo* directed by the *GMR-Gal4* has 6240 μm^2 mean disrupted eye area, much less compared to control with P-value <0.0001 as determined by unpaired t-test (Figure 9.2B iii). The inhibition of *Drp1* by *Drp1-RNAi's* along with *foxo* directed by the *GMR-Gal4* has 2293μm^2(P-value=0.0145) and 3059μm^2(P-value=0.6575) mean disrupted eye area, decrease compared to control as determined by unpaired t-test (Figure 9.2B iii). Out of the two RNAi lines the *Drp1-RNAi1* has much increase in ommatidia number and decrease in disrupted eye area. The decrease in the interommatidial bristle number

and reduction of ommatidial count is consistent with increase in disrupted eye area produced through overexpression of *Drp1* and *foxo* compare to control (Figure 9.2B iii).

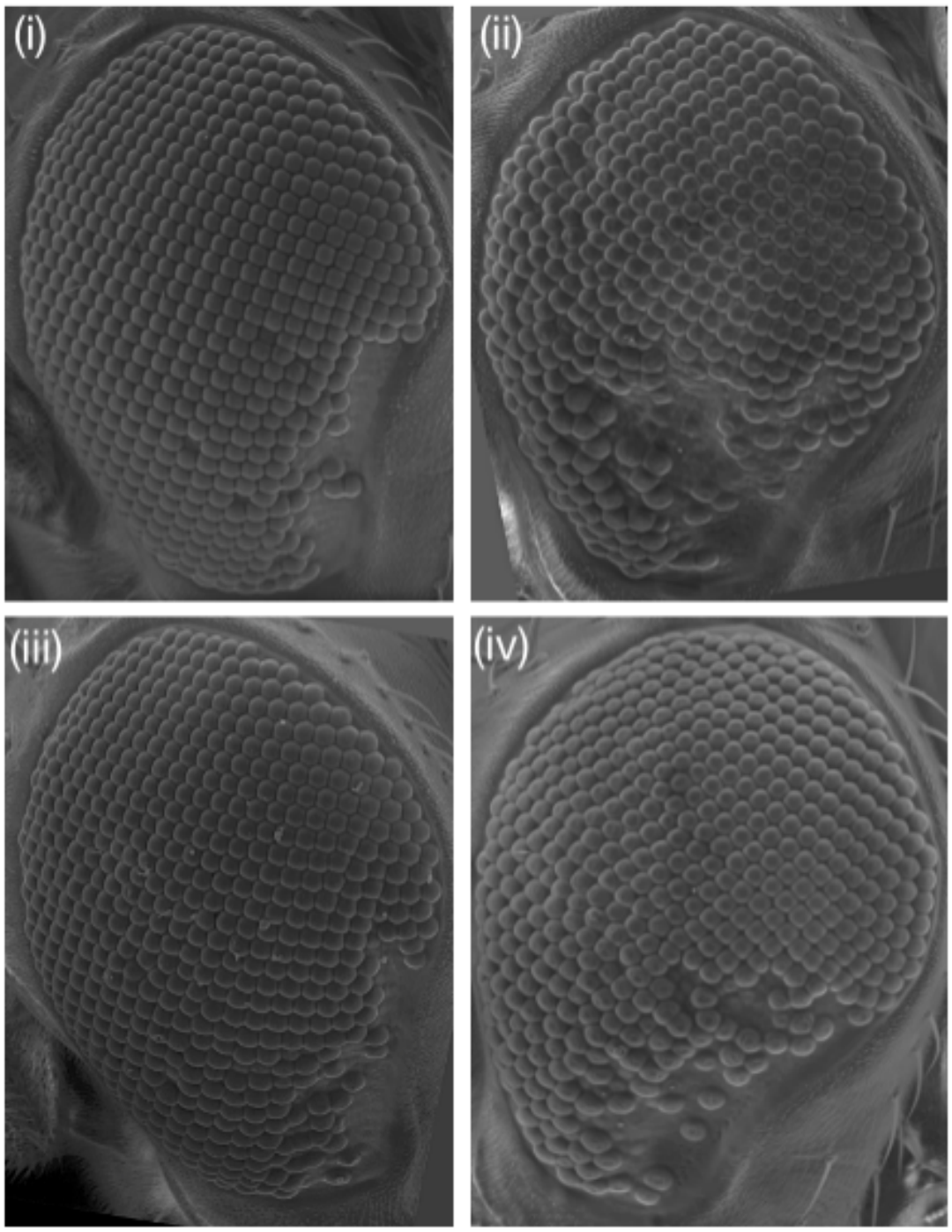
(i)
(ii)
(iii)
(iv)

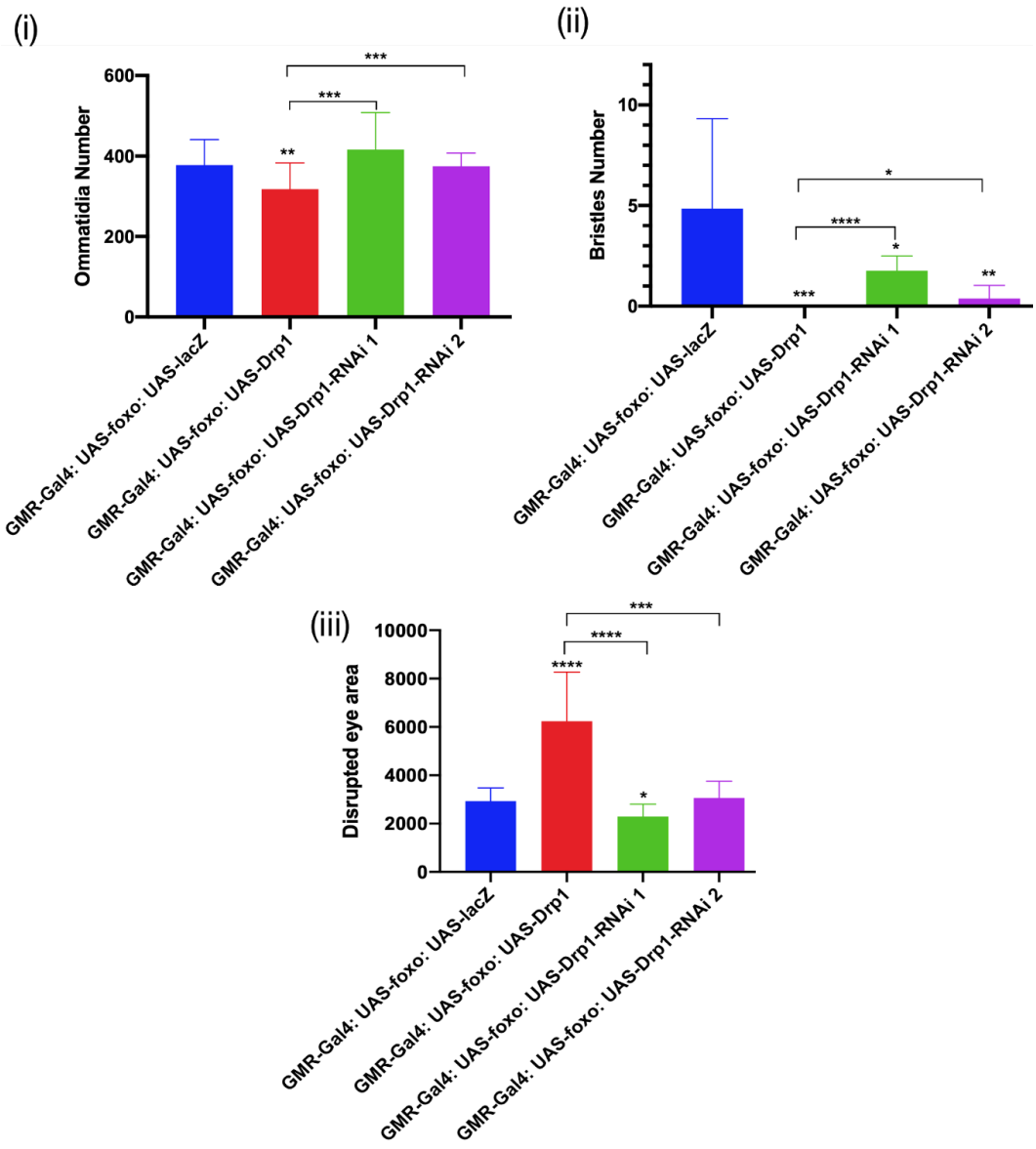

Figure 9.2: The phenotypic effects of altered *Drp1* expression on *foxo* eye phenotype. A. Scanning electron micrograph of the altered *Drp1* expression under the control of *GMR-Gal4/UAS-foxo* transgene. The genotypes are (a) *GMR-Gal4/UAS-lacZ/UAS-foxo* (Control); (b) *GMR-Gal4/UAS-foxo/UAS-Drp1*; (c) *GMR-Gal4/UAS-foxo/UAS-Drp1-RNAi1*; (d) *GMR-Gal4/UAS-foxo/UAS-Drp1-RNAi2*. **B.** The mean ommatidia number for control is 377.9; the expression of *Drp1* results in 317.8 ommatidia, decreased compared to control. The mean ommatidial count of *Drp1-RNAi* lines is 416.4 and 375 slight increases compare to control. **C.** The mean interommatidial bristle count for the control is 4.846, and the Drp1 expression lines has no interommatidial bristle. The mean interommatidial bristle count of *Drp1-RNAi* line is 1.769 and 0.3846 slight decrease compare to control. **D.** There disrupted eye for the control is 2932µm^2, and the Drp1 expression lines results in 6240µm^2 increased compare to control. The disrupted eye area of *Drp1-RNAi* line is 2293µm^2 and 3059µm^2 compare to control.

Effect of altered expression of *Buffy* and *Debcl* via *GMR-Gal4* on the *foxo* eye phenotype

The control *GMR-Gal4; UAS-foxo UAS-lacZ* critical class males were determined to have mean ommatidial count of 354.5 (n=15). The overexpression of *Buffy* along with *foxo* directed by the *GMR-Gal4* has mean ommatidial count of 345.8, similar to control with P-value 0.6716 as determined by unpaired t-test (Figure 9.3B i). The inhibition of *Buffy* along with *foxo* directed by the *GMR-Gal4* has mean ommatidial count of 152.1, similar to control with P-value <0.0001 as determined by unpaired t-test (Figure 9.3B i).

The control *GMR-Gal4; UAS-foxo UAS-lacZ* critical class males were determined to have mean interommatidial bristle count of 5.929 (n=15). The overexpression of *Buffy* along with *foxo* directed by the *GMR-Gal4* has no interommatidial bristle, much less compared to control with P-value <0.0022 as determined by unpaired t-test (Figure 9.3B ii). The inhibition of *Buffy* along with *foxo* directed by the *GMR-Gal4* has mean interommatidial bristle count of 3, similar to control with P-value <0.0528 as determined by unpaired t-test (Figure 9.3B ii).

The control *GMR-Gal4; UAS-foxo UAS-lacZ* critical class males were determined to have mean disrupted eye area of 52942µm^2 (n=15). The overexpression of *Buffy* along with *foxo* directed by the *GMR-Gal4* has 16647µm^2 disrupted eye area, much less compared to control with P-value <0.0001 as determined by unpaired t-test (Figure 9.3B iii). The inhibition of *Buffy* along with *foxo* directed by the *GMR-Gal4* has 4671µm^2 disrupted eye area, increased compared to control with P-value 0.0019 as determined by unpaired t-test (Figure 9.3B iii).

The control *GMR-Gal4; UAS-foxo UAS-lacZ* critical class males were determined to have mean ommatidial count of 354.5 (n=15). The overexpression of *Debcl* along with *foxo* directed by the *GMR-Gal4* has mean ommatidial count of 1.938, none compare to control with P-value <0.0001 as determined by unpaired T-test (Figure 9.3B i). The inhibition of *Debcl* along with *foxo* directed

by the *GMR-Gal4* has mean ommatidial count of 164.9, much less to control with P-value <0.0001 as determined by unpaired t-test (Figure 9.3B i).

The control *GMR-Gal4; UAS-foxo UAS-lacZ* critical class males were determined to have mean interommatidial bristle count of 5.929 (n=15). The overexpression of *Debcl* along with *foxo* directed by the *GMR-Gal4* has interommatidial bristle count of 8.143, similar to control with P-value 0.1480 as determined by unpaired t-test (Figure 9.3B ii). The inhibition of *Debcl* along with *foxo* directed by the *GMR-Gal4* has no interommatidial bristle, less compared to control with P-value 0.0022 as determined by unpaired t-test (Figure 9.3B ii).

The control *GMR-Gal4; UAS-foxo UAS-lacZ* critical class males were determined to have mean disrupted eye area of 52942µm^2 (n=15). The overexpression of *Debcl* along with *foxo* directed by the *GMR-Gal4* has 33325µm^2 disrupted eye area, much higher compared to control with P-value <0.0001 as determined by unpaired t-test (Figure 9.3B iii). The inhibition of *Debcl* along with *foxo* directed by the *GMR-Gal4* has 13082µm^2 disrupted eye area, increased compared to control with P-value <0.0001 as determined by unpaired t-test (Figure 9.3B iii).

9

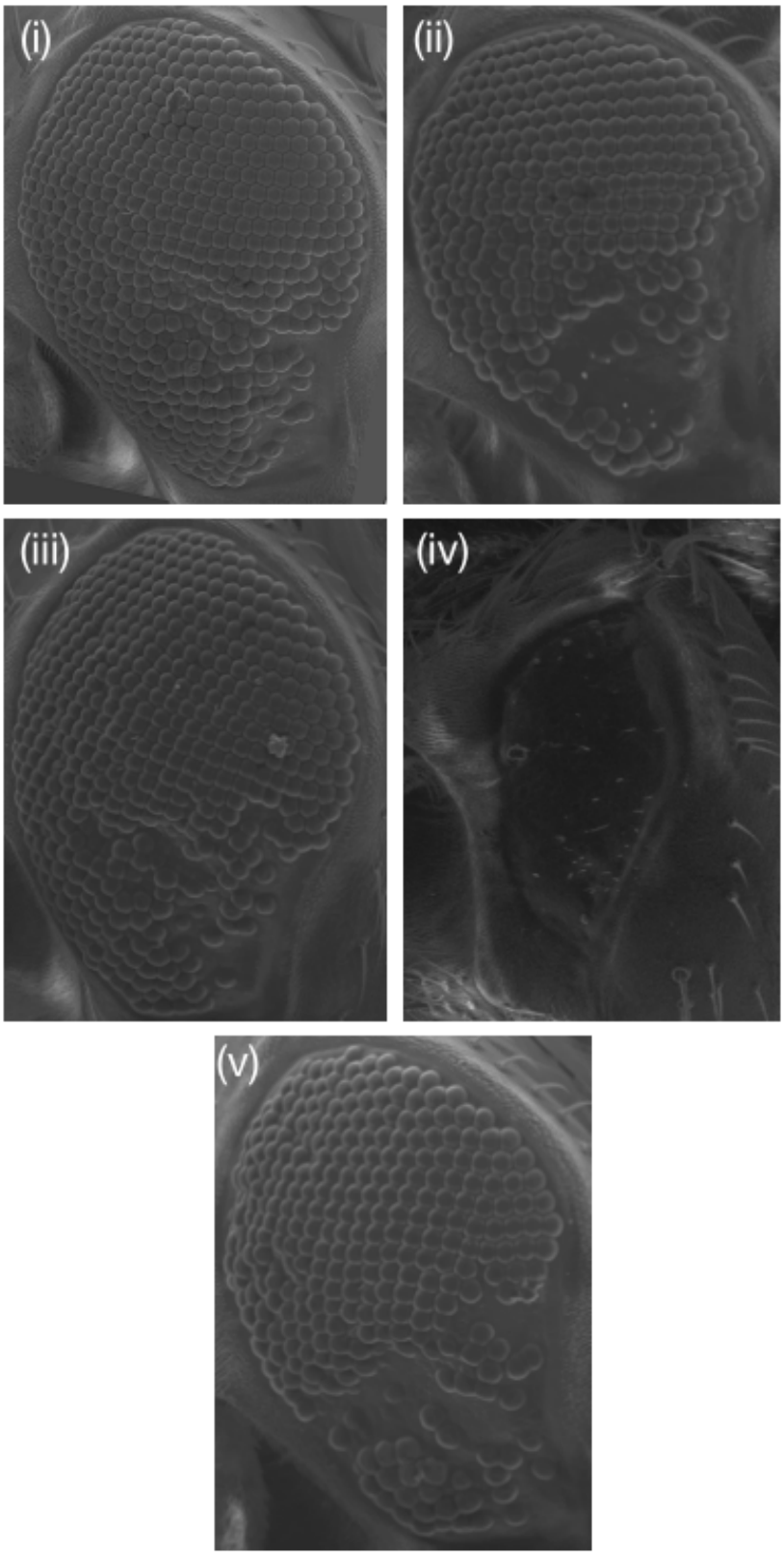

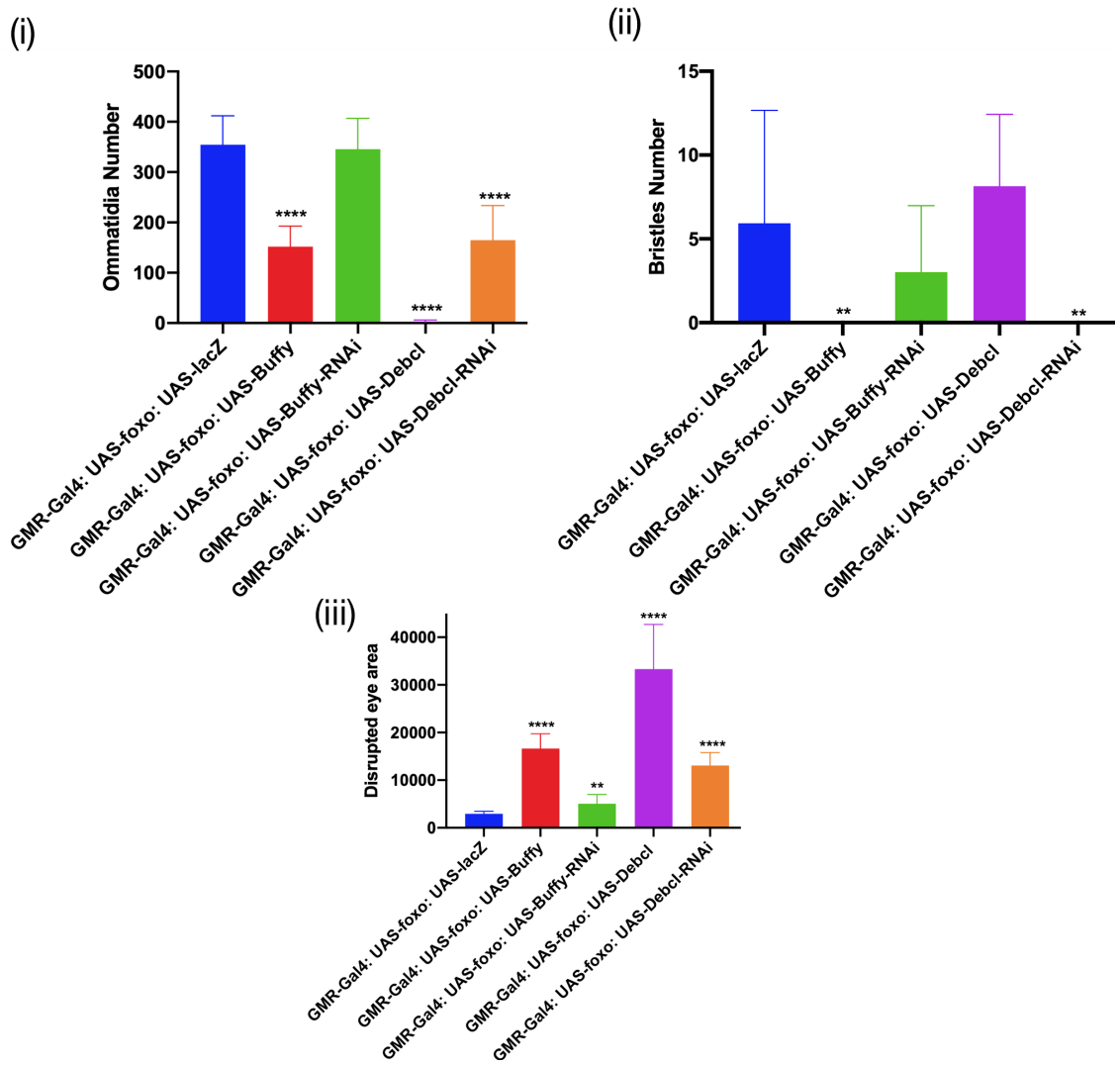

Figure 9.3: The phenotypic effects of altered *bcl-2* expression on *foxo* eye phenotype. A. Scanning electron micrograph of the altered *buffy* and *Debcl* expression under the control of *GMR-Gal4/UAS-foxo* transgene. The genotypes are (a) *GMR-Gal4/UAS-lacZ/UAS-foxo* (Control); (b) *GMR-Gal4/UAS-foxo*/UAS-Buffy; (c) *GMR-Gal4/UAS-foxo/UAS-Buffy-RNAi*; (d) *GMR-Gal4/UAS-foxo*/UAS-Debcl; (e) *GMR-Gal4/UAS-foxo/UAS-Debcl-RNAi*. **B.** The mean ommatidia number for control is 335.8; the expression of *Buffy* results in 152.1 and Debcl-RNAi results in 164.9 ommatidia, decreased compared to control. The mean ommatidial count of *Buffy-RNAi* lines is similar compare to control. The overexpression of Debcl has no district ommatidia. **C.** The interommatidial bristle count for the control is 5.929, and the *Buffy* and *Debcl-RNAi* expression lines have no interommatidial bristle. The interommatidial bristle count of *Buffy-RNAi* and *Debcl* line is similar to control. **D.** There disrupted eye for the control is 2943um^2, and the *Buffy* expression lines results in 16647um^2 and *Debcl-RNAi* results in 1308um^2, increased compare to control. The disrupted eye area of *Buffy-RNAi* lines is 4671um^2 increased compare to control. The total eye area of Debcl is disrupted accounting for 33325um^2 increased compare to control

Effect of overexpression and inhibition on *Rbf* on *foxo* eye phenotype via *GMR-Gal4*

The control *GMR-Gal4; UAS-foxo UAS-lacZ* critical class males were determined to have mean ommatidial count of 457.8 (n=15). The overexpression of *Rbf* along with *foxo* directed by the *GMR-Gal4* has mean ommatidial count of 404.4, less compared to control with P-value 0.0100 as determined by unpaired t-test (Figure 9.4B i). The inhibition of *Rbf* by *Rbf-RNAi's* along with *foxo* directed by the *GMR-Gal4* has mean interommatidial bristle count of 592 and 603.5, much higher to control with P-value <0.0001 as determined by unpaired t-test (Figure 9.4B ii).

The control *GMR-Gal4; UAS-foxo UAS-lacZ* critical class males were determined to have mean interommatidial bristle count of 5.929 (n=15). The overexpression of *Rbf* along with *foxo* directed by the *GMR-Gal4* has mean interommatidial bristle count of 0.5, less compared to control with P-value 0.0068 as determined by unpaired t-test (Figure 9.4B ii). The inhibition of *Rbf* by *UAS-Rbf-RNAi1* and *UAS-Rbf-RNAi2* along with *foxo* directed by the *GMR-Gal4* has mean interommatidial bristle count of 49.71 and 17.93 respectively, much higher to control with P-value <0.0001 as determined by unpaired t-test (Figure 9.4B ii).

The control *GMR-Gal4; UAS-foxo UAS-lacZ* critical class males were determined to have 2902µm^2 mean disrupted eye area (n=15). The overexpression of *Rbf* along with *foxo* directed by the *GMR-Gal4* has 2662µm^2 mean disrupted eye area, similar to control with P-value 0.3584 as determined by unpaired t-test (Figure 9.4B i). The inhibition of *Rbf* by *Rbf-RNAi1* and *Rbf-RNAi2* along with *foxo* directed by the *GMR-Gal4* has 493.3µm^2 and 558.4µm^2 mean disrupted eye area respectively, much less compared to control with P-value <0.0001 as determined by unpaired t-test (Figure 9.4B iii)

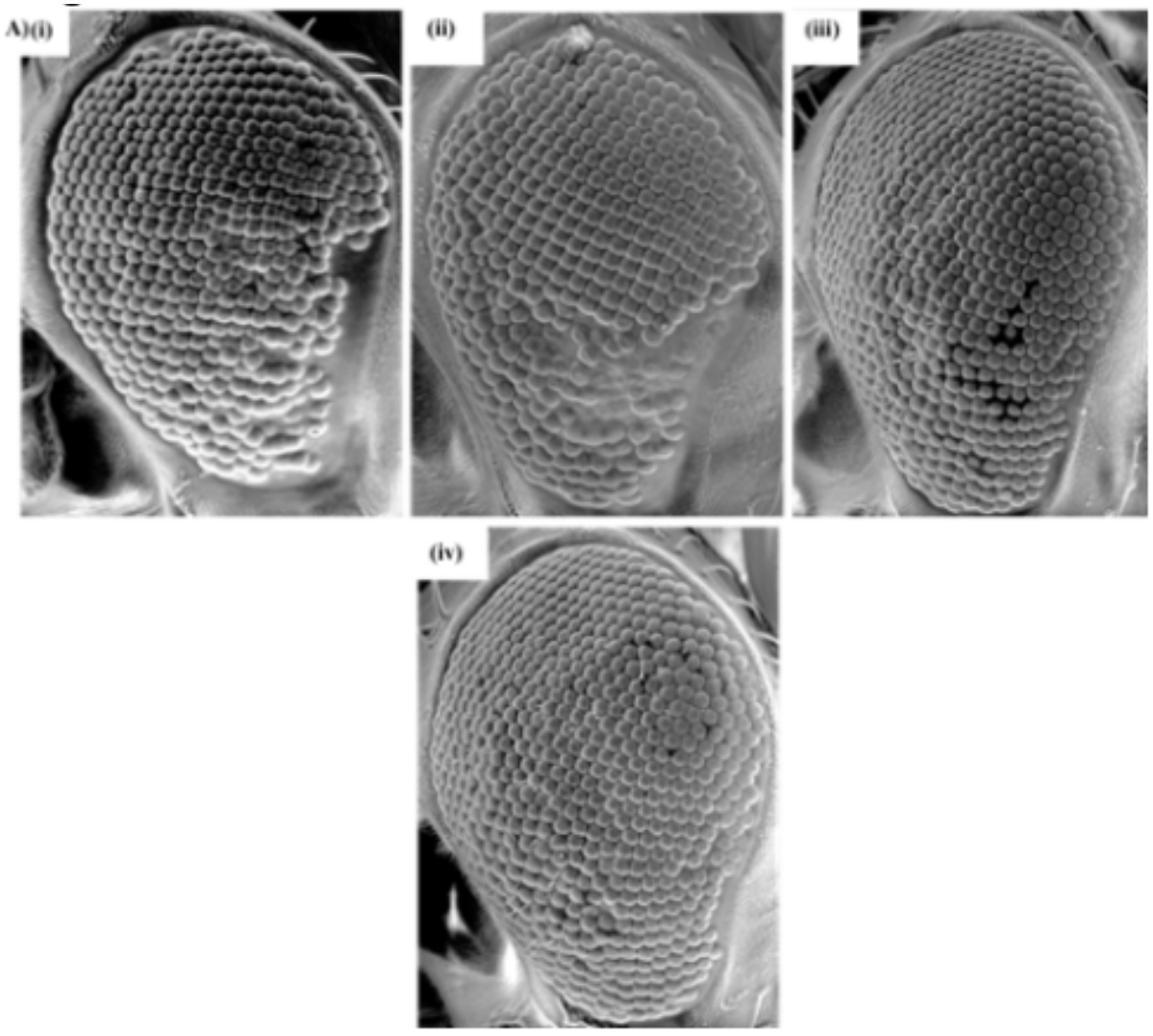
A)(i)
(ii)
(iii)
(iv)

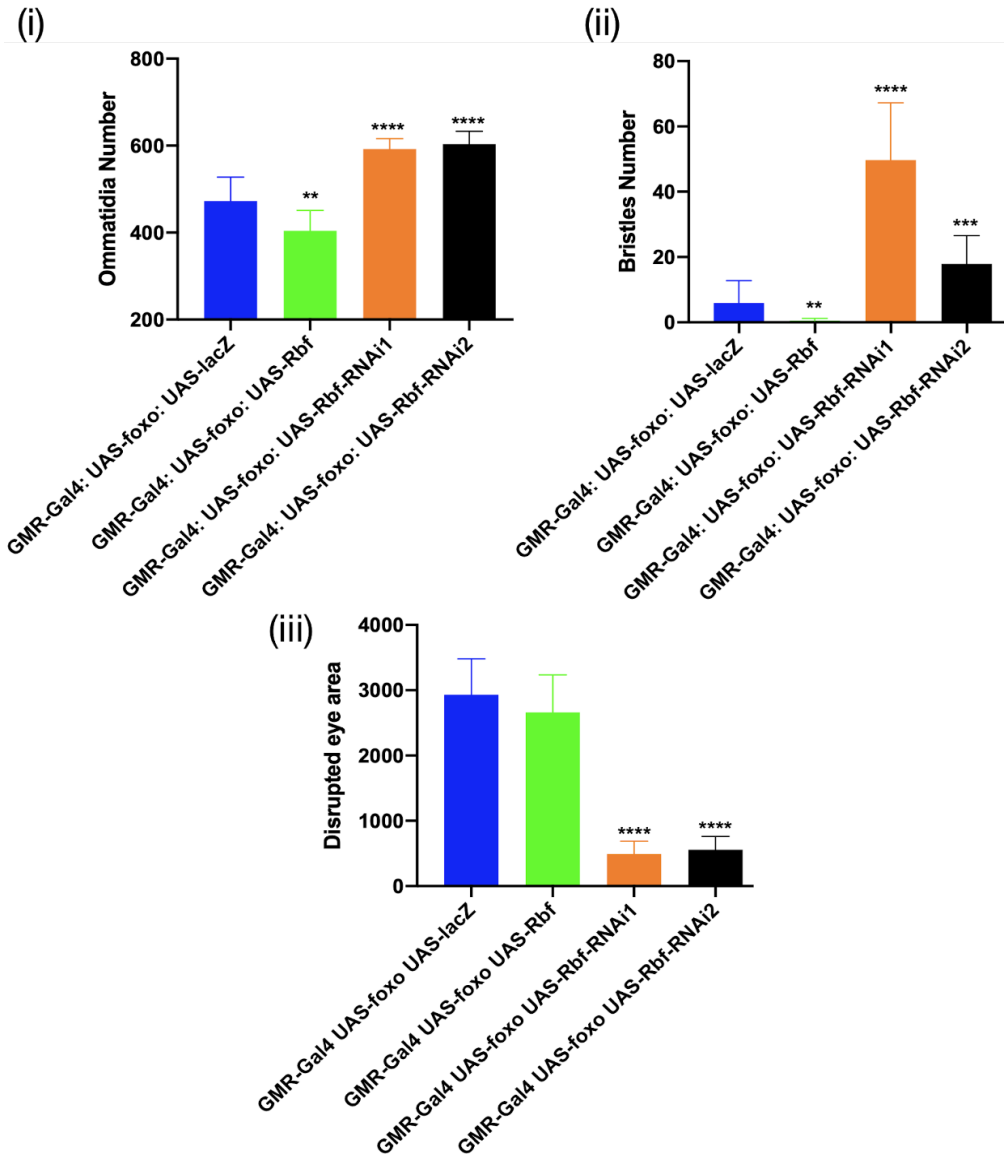

Figure 9.4: The phenotypic effects of altered *Rbf* expression on *foxo* eye phenotype. A. Scanning electron micrograph of the altered *Drp1* expression under the control of *GMR-Gal4/UAS-foxo* transgene. The genotypes are (a) *GMR-Gal4/UAS-lacZ/UAS-foxo* (Control); (b) *GMR-Gal4/UAS-foxo*/UAS-Rbf; (c) *GMR-Gal4/UAS-foxo/UAS-Rbf-RNAi1*; (d) *GMR-Gal4/UAS-foxo/UAS-Rbf-RNAi2*. **B.** The mean ommatidia number for control is 457.8; the expression of *Rbf* results in 404.4 ommatidia, decreased compared to control. The mean ommatidial count of *Rbf-RNAi* lines is 592 and 603.5 increase compare to control. **C.** The mean interommatidial bristle count for the control is 5.929, and the *Rbf* expression lines have almost no interommatidial bristle. The mean interommatidial bristle count of *Rbf-RNAi* line is 49.71 and 17.93 increase compare to control. **D.** There disrupted eye for the control is 2902µm^2, and the *Rbf* expression lines results in 2662µm^2 similar compare to control. The disrupted eye area of *Rbf-RNAi* lines was 493.3µm^2 and 558.4µm^2 much less compared to control.

Effect of overexpression and inhibition on *Pink1* on *foxo* eye phenotype via *GMR-Gal4*

The control *GMR-Gal4; UAS-foxo UAS-lacZ* critical class males were determined to have mean ommatidial count of 386.4 (n=15). The overexpression of *Pink1* along with *foxo* directed by the *GMR-Gal4* has mean ommatidial count of 318.8, less compared to control with P-value 0.0010 as determined by unpaired t-test (Figure 9.5B i). The inhibition of *Pink1* along with *foxo* directed by the *GMR-Gal4* has mean ommatidial count of 616.1, much higher compared to control with P-value <0.0001 as determined by unpaired t-test (Figure 9.5B i).

The control *GMR-Gal4; UAS-foxo; UAS-lacZ* critical class males were determined to have mean interommatidial bristle count of 6.800 (n=15). The overexpression of *Pink1* along with *foxo* directed by the *GMR-Gal4* has mean interommatidial bristle count of 3.643, less compared to control with P-value 0.0113 as determined by unpaired t-test (Figure 9.5B ii). The inhibition of *Pink1* along with *foxo* directed by the *GMR-Gal4* has mean interommatidial bristle count of 247.9, much higher compared to control with P-value <0.0001 as determined by unpaired t-test (Figure 9.5B ii).

The control *GMR-Gal4; UAS-foxo UAS-lacZ* critical class males were determined to have 2573µm^2 mean of disrupted eye are (n=15). The overexpression of *Pink1* along with *foxo* directed by the *GMR-Gal4* has 3419µm^2 mean of disrupted eye area, similar to control with P-value 0.0515 as determined by unpaired t-test (Figure 9.5B ii). The inhibition of *Pink1* along with *foxo* directed by the *GMR-Gal4* has no disrupted eye area, much less compared to control with P-value <0.0001 as determined by unpaired t-test (Figure 9.5B iii).

Effect of overexpression and inhibition on *parkin* on *foxo* eye phenotype via *GMR-Gal4*

The control *GMR-Gal4; UAS-foxo UAS-lacZ* critical class males were determined to have mean ommatidial count of 386.4 (n=15). The overexpression of *parkin* along with *foxo* directed by the *GMR-Gal4* has mean ommatidial count of 218.1, less compared to control with P-value <0.0001 as determined by unpaired t-test (Figure 9.5B i). The inhibition of *parkin* along with *foxo* directed by the *GMR-Gal4* has mean ommatidial count of 262.6, much less compared to control with P-value <0.0001 as determined by unpaired t-test (Figure 9.5B i).

The control *GMR-Gal4; UAS-foxo; UAS-lacZ* critical class males were determined to have mean interommatidial bristle count of 6.800 (n=15). The overexpression of *parkin* along with *foxo* directed by the *GMR-Gal4* has mean interommatidial bristle count of 1.133, less compared to control with P-value <0.0001 as determined by unpaired t-test (Figure 9.5B ii). The inhibition of *parkin* along with *foxo* directed by the *GMR-Gal4* has mean interommatidial bristle count of1.867, much lower compared to control with P-value 0.0003 as determined by unpaired t-test (Figure 9.5Bii). The control *GMR-Gal4; UAS-foxo UAS-lacZ* critical class males were determined to have 2573µm^2 mean of disrupted eye are (n=15). The overexpression of *parkin* along with *foxo* directed by the *GMR-Gal4* has 2998µm^2 mean of disrupted eye area, similar to control with P-value 0.2440 as determined by unpaired t-test (Figure 9.5B ii). The inhibition of *parkin* along with *foxo* directed by the *GMR-Gal4* has 3040µm^2 mean of disrupted eye area, similar to control with P-value 0.2064 as determined by unpaired t-test (Figure 9.5B iii).

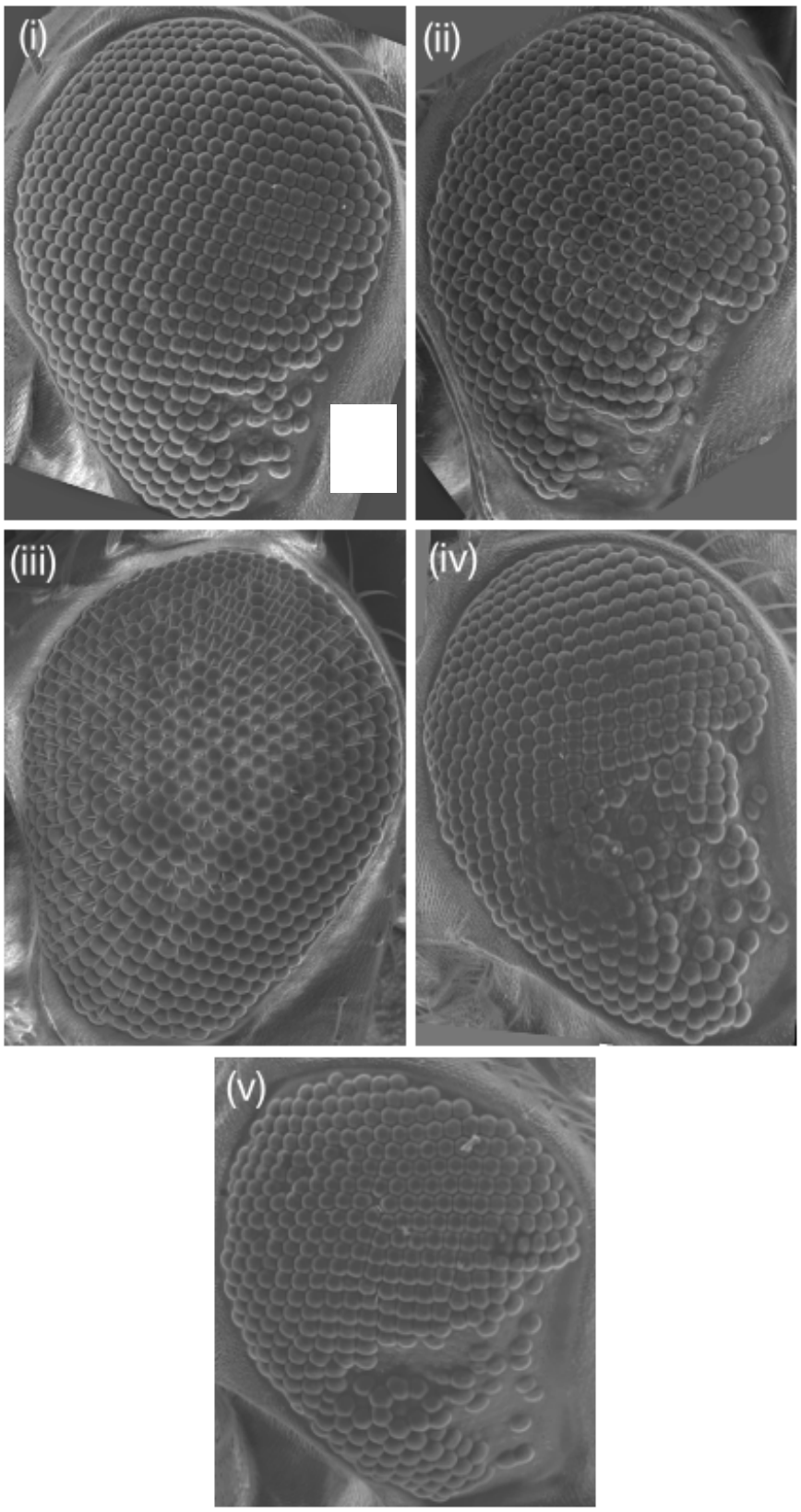
(i)
(ii)
(iii)
(iv)
(v)

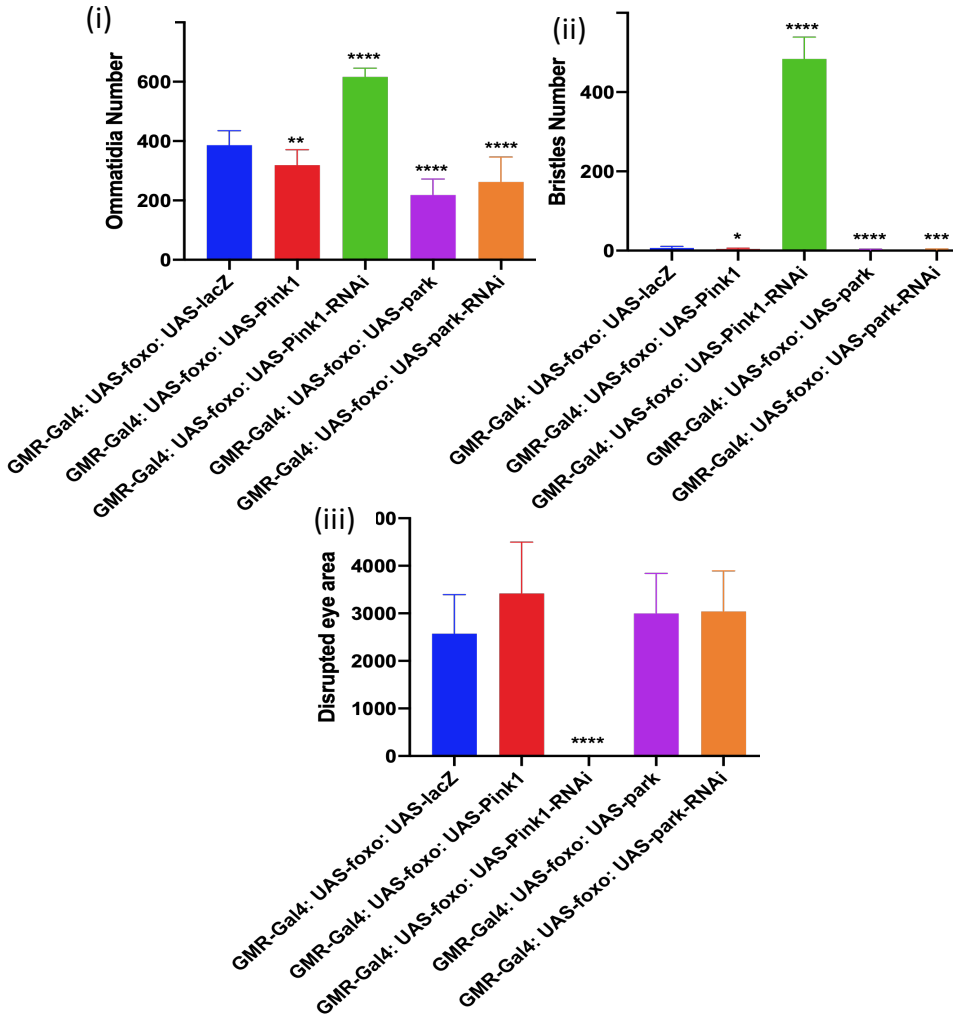

Figure 9.5: The phenotypic effects of altered *Pink1 and parkin* expression on *foxo* eye phenotype. **A**. Scanning electron micrograph of the altered *Drp1* expression under the control of *GMR-Gal4/UAS-foxo* transgene. The genotypes are (a) *GMR-Gal4/UAS-lacZ/UAS-foxo* (Control); (b) *GMR-Gal4/UAS-foxo*/UAS-Pink1; (c) *GMR-Gal4/UAS-foxo/UAS-Pink1-RNAi*; (d) *GMR-Gal4/UAS-foxo*/UAS-parkin; (e) *GMR-Gal4/UAS-foxo/UAS-parkin-RNAi*. **B.** The ommatidia number for control is 381 median ommatidia per eye; the expression of *Pink1* results in 321 and *parkin* results in 218.1 ommatidia per eye, much less compared to control. The mean ommatidial count of *Pink1-RNAi* is 616.1 much higher compare to control. The mean ommatidia count of *parkin-RNAi* is 262.6 decreased compare to control. **C.** The interommatidial bristle count for the control is 6.8; the expression of *Pink1* results in 3.643, *parkin* results in 1.133, and *parkin-RNAi* result in 1.867 bristle decreased compared to control. The interommatidial bristle count of *Pink1-RNAi* was 247.9 increase compare to control. **D.** The disrupted eye for the control is 2573µm^2, the *Pink1* expression lines results in 3419µm^2, and *parkin* results in 2998µm^2, and *parkin-RNAi* results in 3040µm^2 similar to control. There is no disrupted eye area in *Pink1-RNAi* lines which is decrease compare to control.

Effect of overexpression and inhibition on *trbl* via *GMR-Gal4* on the *foxo* eye phenotype

Alteration of the expression of *trbl* in the in the developing eye of *GMR-Gal4 UAS-foxo* flies influences the characteristic *foxo* phenotype. The ommatidial count are much lower with *trbl* overexpression, in two out of three transgenes when analyzed for 15 flies of each genotype. The mean of ommatidial count produced by the *UAS-trbl-1, UAS-trbl-2* and *UAS-trbl-3* transgene was 141.4 (P value<0.0001), 425.4 (P value=0.0.0273) and 122 (P value<0.0001) respectively, compared to 363.1 of control flies as determined by an unpaired t-test. Out of the three genotypes, *UAS-trbl-2* expression produced few visible bristles which were much less compared to control. The disrupted eye area of *UAS-trbl-1, UAS-trbl-2* and *UAS-trbl-3* transgene was, 12926µm^2 (P-value<0.0001), 3514µm^2 (P-value=0.2538) and 15153µm^2 (P-value<0.0001) respectively, compared to 2932µm^2 of the control flies as determined by an unpaired t-test.

The mean of ommatidia count produced by the *UAS-trbl-RNAi-1, UAS-trbl-RNAi-2* and *UAS-trbl-RNAi-3* transgene was much lower except *UAS-trbl-RNAi-1* at, 274.6 (P-value<0.0139), 495.1 (P value<0.0001) and 460 (P value<0.0001) compared to 363.1 of control flies as determined by an unpaired t-test. The mean of bristle count produced through inhibition by *the UAS-trbl-RNAi1, UAS-trbl-RNAi2* and *UAS-trbl-RNAi3* transgene was much less at, 0 (P-value<0.0001), 1.923 (P-value=0.0452) and 1.077 (P-value=0.0074) compared to 4.846 median bristles per eye of control flies as determined by an unpaired t-test. The disrupted eye area *of UAS-trbl-1, UAS-trbl-2* and *UAS-trbl-3* transgene were similar to control except UAS-trbl-1, 14080µm^2 (P value<0.0001), 3004µm^2 (P-value=0.8915) and 3091µm^2 (P-value=0.6558) respectively compared to 2932µm^2 of control flies as determined by an unpaired t-test Figure 9.6B(iii).

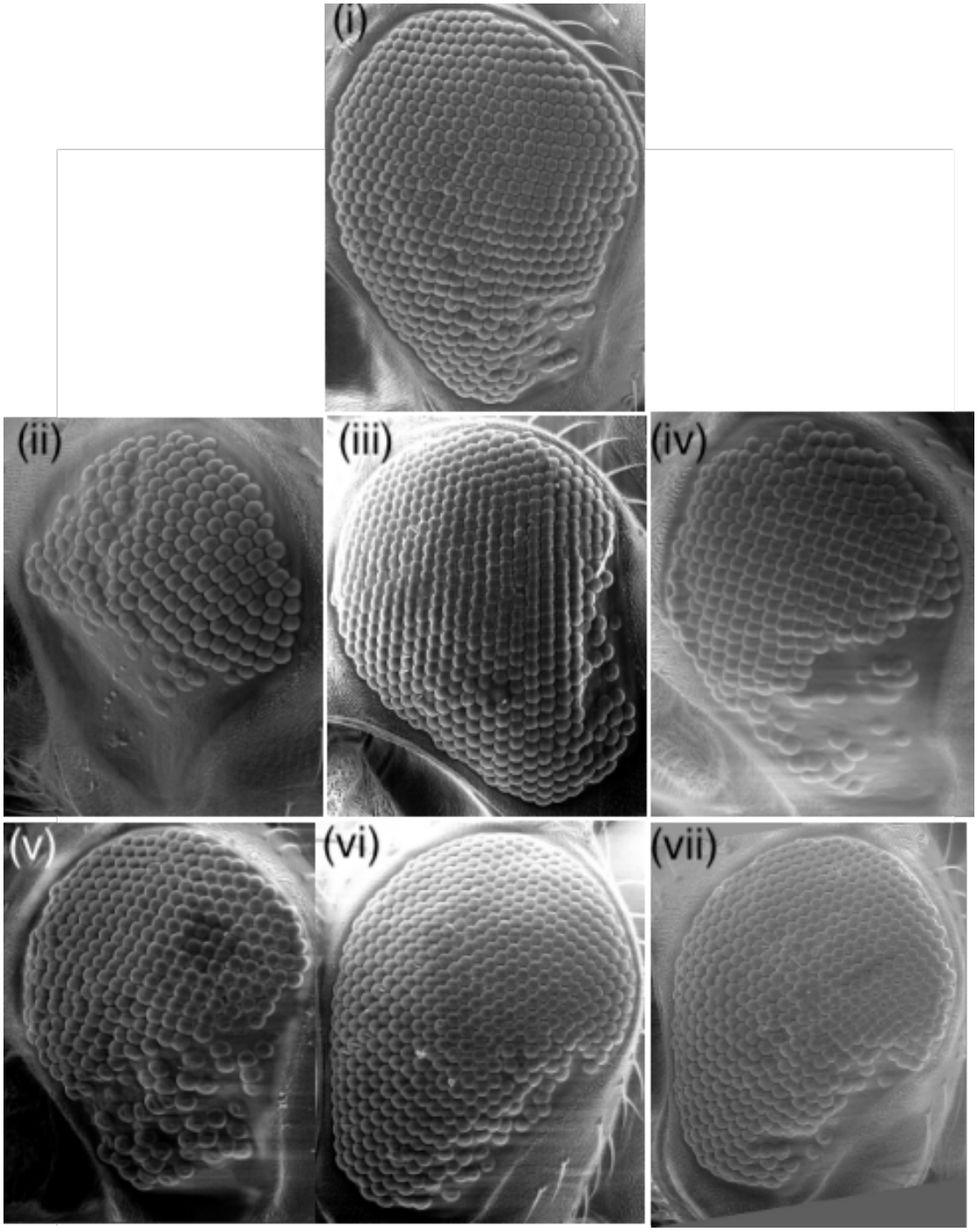
(i)
(ii)
(iii)
(iv)
(v)
(vi)
(vii)

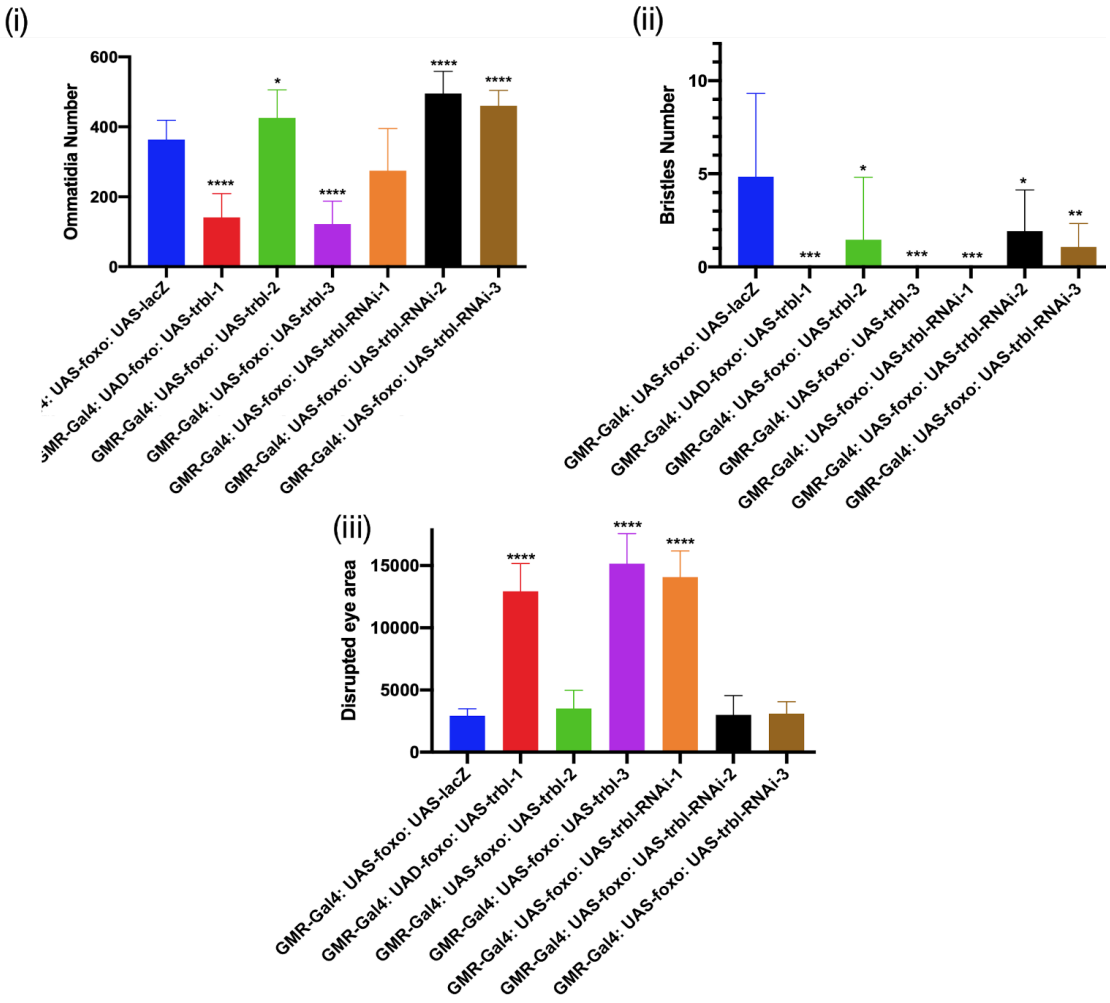

Figure 9.6: The phenotypic effects of altered *trbl and trbl-RNAi* expression upon the *foxo* eye phenotype. A. Scanning electron micrograph of the altered *Drp1* expression under the control of *GMR-Gal4/UAS-foxo* transgene. The genotypes are (a) *GMR-Gal4/UAS-lacZ/UAS-foxo* (Control); (b) *GMR-Gal4/UAS-foxo*/UAS-trbl1; (c) *GMR-Gal4/UAS-foxo*/UAS-trbl2; (d) *GMR-Gal4/UAS-foxo/UAS-trbl3*; (e) *GMR-Gal4/UAS-foxo/UAS-trbl-RNAi1*; (f) *GMR-Gal4/UAS-foxo/UAS-trbl-RNAi2*; (g) *GMR-Gal4/UAS-foxo/UAS-trbl-RNAi3*. **B.** The ommatidia number for the control is 363.1; the expression of the three *trbl* transgenes result in 141.4, 425.4 and 122 ommatidia, a decrease with two of three transgenes compared to the control. The mean ommatidial counts of *trbl-RNAi* transgenes is 274.6, 495.1 and 460 increased in two out of three lines compared to control. **C.** The mean number of interommatidial bristles for the control is 4.846, the expression of *trbl* results in 0, 1.42 and 0 bristles, a decrease compared to the control. The number of interommatidial bristles of *trbl-RNAi* is 0, 1.923 and 1.077 decreased compare to control. **D.** The disrupted eye for the control is 2932µm^2, the *trbl* expression lines results in 12926µm^2, 3514µm^2 and 15153µm^2 increased on two out of three lines compared to control. and *trbl-RNAi* results in 14080µm^2, 3004µm^2 and 3091µm^2 decreased in two out of three lines compared control.

Discussion

The directed expression of *foxo* in the developing fly eye produces a characteristic phenotype consisting of decreased numbers of ommatidia and interommatidial bristles (Kramer et al. 2003). Acute stress can cause foxo to activate the transcription of pro-apoptotic protein genes (Fu and Tindall 2008). The directed inhibition of foxo through RNAi (UAS-foxo-RNAi) transgenes led to a slight increase in the number of ommatidia and inter-ommatidial bristles. The increase in the ommatidia and bristle count could be due to hormesis effect of foxo inhibition during eye development. The expression of foxo-RNAi in different transgenes, which give PD-like characteristics in drosophila, helped us investigate the possible link between the genes and their respective phenotypes. Foxo plays a central role in neuroprotection and protects against axonal tract degeneration in mammalian models (Hwang et al. 2018). *Foxo* overexpression is not always toxic and acts as a bona-fide tumour suppressor and helps in alleviation of cellular stresses.

Pink1 is the direct downstream target of foxo (Mei et al. 2009; Li et al. 2017; Bartolomé et al. 2017). The directed expression of the *Pink1-RNAi* results in the suppression of the *foxo* overexpression eye phenotype. Hence, the directed expression of *Pink1-RNAi* and loss of *Pink1* function confers the advantage through inhibition of downstream signalling. The expression of *parkin-RNAi* does not rescue the phenotype, which supports the importance of separate roles for Pink1 and parkin apart from their collaboration in the initiation of mitophagy (Seirafi et al. 2015). The activities of the foxo protein can be altered by the directed expression of *PI3K*, *Akt* or other upstream regulators (Greer and Brunet 2005; Hay 2011). In mammals, Akt modulates the mitochondrial-mediated apoptosis through inactivation of the pro-apoptotic Bcl-2 family protein, Bad (Song et al. 2009). The role of Bcl-2 family proteins in the maintenance of mitochondrial health and the regulation of apoptosis is well established. The overexpression of anti-apoptotic *Buffy*

along with the expression of *foxo* in developing eye result in the enhancement of the foxo eye phenotype. The tumour-suppression signal by the excess foxo abrogates the anti-apoptotic effect of *Buffy* overexpression. We established that overexpression of pro-apoptotic *Debcl*, along with the excess foxo gives a novel eye phenotype; lose all ommatidial structure likely due to excessive pro-apoptotic signalling. Thus, foxo protein seems vital in the regulation of the IRS and maintenance of homeostasis.

The IRS is dependent on foxo, Rbf and other transcription factors (Wei et al. 2016). The directed overexpression of *Rbf* along with *foxo* causes the phenotype to become more severe. The directed expression of foxo along with the inhibition of Rbf through UAS-Rbf RNAi suppresses the eye phenotype. Similarly, the suppression of foxo rescued the Rbf inhibition induced phenotype in selected neurons (Chapter 8). The molecular mechanism behind the pro-cell survival effects is apparently increased homeostasis.

While the trbl/trbl3 protein binds to Akt to block Akt-mediated IRS in flies and mammals (Qi et al. 2006), unexpectedly it decreases the total levels of foxo protein in flies (Das et al. 2014). In my results, two out of three trbl overexpression lines enhance the foxo eye phenotype, contrary to the synergistic activities that allow trbl and Akt to degrade the foxo protein (Das et al. 2014). The two of three trbl-RNAi transgenes ameliorate the foxo eye phenotype. Furthermore, the intermediate results in my data strongly support the role of trbl in regulating foxo-mediated pathways.

Conclusion

The inhibition of Pink1 suppresses the foxo eye phenotype that is strongly associated with excessive apoptosis. In comparison, the inhibition of parkin does not affect the foxo overexpression phenotype, which indicates the existence of two important and distinct

mechanisms for Pink1 and parkin in relation to foxo. The suppression of Rbf increases homeostasis and ameliorates the foxo eye phenotype. The mixed results of trbl and foxo altered expression highlights the complexity of trbl-induced Akt and foxo regulation mechanisms and its adverse effects of misregulation. These results demonstrate the multi-faceted mechanisms involved in the foxo regulation and its downstream targets, sometimes leading to the etiology of PD

Bibliography

Acharya, P., Negre, N., Johnston, J., Wei, Y., White, K.P., Henry, R.W., and Arnosti, D.N. 2012. Evidence for Autoregulation and Cell Signalling Pathway Regulation From Genome-Wide Binding of the Drosophila Retinoblastoma Protein. G3 Genes, Genomes, Genet. **2**(11): 1459–1472. doi:10.1534/g3.112.004424.

Ariss, M.M., Islam, A.B.M.M.K., Critcher, M., Zappia, M.P., and Frolov, M. V. 2018. Single cell RNA-sequencing identifies a metabolic aspect of apoptosis in Rbf mutant. Nat. Commun. **9**(1). Nature Publishing Group. doi:10.1038/s41467-018-07540-z.

Bartolomé, A., García-Aguilar, A., Asahara, S.-I., Kido, Y., Guillén, C., Pajvani, U.B., and Benito, M. 2017. MTORC1 Regulates both General Autophagy and Mitophagy Induction after Oxidative Phosphorylation Uncoupling. Mol. Cell. Biol. **37**(23). American Society for Microbiology. doi:10.1128/mcb.00441-17.

Chakraborty, S., Khare, S., Dorairaj, S.K., Prabhakaran, V.C., Prakash, D.R., and Kumar, A. 2007. Identification of genes associated with tumorigenesis of retinoblastoma by microarray analysis. Genomics **90**(3): 344–353. doi:10.1016/j.ygeno.2007.05.002.

Classon, M., and Harlow, E. 2002, December. The retinoblastoma tumour suppressor in development and cancer. doi:10.1038/nrc950.

Das, R., Sebo, Z., Pence, L., and Dobens, L.L. 2014. Drosophila tribbles antagonizes insulin signalling-mediated growth and metabolism via interactions with akt kinase. PLoS One **9**(10): 109530. Public Library of Science. doi:10.1371/journal.pone.0109530.

Fu, Z., and Tindall, D.J. 2008, April 7. FOXOs, cancer and regulation of apoptosis. NIH Public Access. doi:10.1038/onc.2008.24.

Githure, P.M., and Staveley, B.E. 2017. Overexpression of Buffy enhances the loss of parkin and suppresses the loss of Pink1 phenotypes in Drosophila. Genome **60**(3): 241–247. NRC Research Press. doi:10.1139/gen-2016-0165.

Greer, E.L., and Brunet, A. 2005, November 14. FOXO transcription factors at the interface between longevity and tumor suppression. doi:10.1038/sj.onc.1209086.

Greer, E.L., and Brunet, A. 2007. FOXO transcription factors in ageing and cancer. Acta Physiol. **192**(1): 19–28. Blackwell Publishing Ltd. doi:10.1111/j.1748-1716.2007.01780.x.

Hay, N. 2011, November. Interplay between FOXO, TOR, and Akt. NIH Public Access. doi:10.1016/j.bbamcr.2011.03.013.

Huang, H., and Tindall, D.J. 2007, August 1. Dynamic FoxO transcription factors. The Company of Biologists Ltd. doi:10.1242/jcs.001222.

Hwang, I., Oh, H., Santo, E., Kim, D.Y., Chen, J.W., Bronson, R.T., Locasale, J.W., Na, Y., Lee, J., Reed,

S., Toth, M., Yu, W.H., Muller, F.L., and Paik, J. 2018. FOXO protects against age-progressive axonal degeneration.ageing Cell **17**(1). Blackwell Publishing Ltd. doi:10.1111/acel.12701.

Kramer, J.M., Davidge, J.T., Lockyer, J.M., and Staveley, B.E. 2003. Expression of Drosophila FOXO regulates growth and can phenocopy starvation. BMC Dev. Biol. **3**: 1–14. BioMed Central Ltd. doi:10.1186/1471-213X-3-5.

Li, W., Du, M., Wang, Q., Ma, X., Wu, L., Guo, F., Ji, H., Huang, F., and Qin, G. 2017. FoxO1 Promotes Mitophagy in the Podocytes of Diabetic Male Mice via the PINK1/Parkin Pathway. Endocrinology **158**(7): 2155–2167. Narnia. doi:10.1210/en.2016-1970.

Lipsett, D.B., and Staveley, B.E. 2014. A Blueberry Extract Supplemented Diet Partially Restores α-Synuclein-Dependent Lifespan Loss and Developmental Defects in Drosophila. doi:10.4236/apd.2014.32002.

Mei, Y., Zhang, Y., Yamamoto, K., Xie, W., Mak, T.W., and You, H. 2009. FOXO3a-dependent regulation of Pink1 (Park6) mediates survival signalling in response to cytokine deprivation. Proc. Natl. Acad. Sci. **106**(13): 5153–5158. doi:10.1073/pnas.0901104106.

Panicker, N., Dawson, V.L., and Dawson, T.M. 2017, September 15. Activation mechanisms of the E3 ubiquitin ligase parkin. Portland Press Ltd. doi:10.1042/BCJ20170476.

Puig, O., and Tjian, R. 2005. Transcriptional feedback control of insulin receptor by dFOXO/FOXO1. Genes Dev. **19**(20): 2435–2446. Cold Spring Harbor Laboratory Press. doi:10.1101/gad.1340505.

Qi, L., Heredia, J.E., Altarejos, J.Y., Screaton, R., Goebel, N., Niessen, S., MacLeod, I.X., Liew, C.W., Kulkarni, R.N., Bain, J., Newgard, C., Welson, M., Evans, R.M., Yates, J., and Montminy, M. 2006. TRB3 links the E3 ubiquitin ligase COF1 to lipid metabolism. Science (80-.). **312**(5781): 1763–1766. Science. doi:10.1126/science.1123374.

Seirafi, M., Kozlov, G., and Gehring, K. 2015, June 1. Parkin structure and function. Blackwell Publishing Ltd. doi:10.1111/febs.13249.

Shi, Y., Fan, S., Wang, D., Huyan, T., Chen, J., Chen, J., Su, J., Li, X., Wang, Z., Xie, S., Yun, C., Li, X., and Tie, L. 2018. FOXO1 inhibition potentiates endothelial angiogenic functions in diabetes via suppression of ROCK1/Drp1-mediated mitochondrial fission. Biochim. Biophys. Acta - Mol. Basis Dis. **1864**(7): 2481–2494. Elsevier B.V. doi:10.1016/j.bbadis.2018.04.005.

Thomas, R.E., Andrews, L.A., Burman, J.L., Lin, W.-Y., and Pallanck, L.J. 2014. PINK1-Parkin Pathway Activity Is Regulated by Degradation of PINK1 in the Mitochondrial Matrix. PLoS Genet. **10**(5): e1004279. Public Library of Science. doi:10.1371/journal.pgen.1004279.

Todd, A.M., and Staveley, B.E. 2013. Pink1 and parkin demonstrate multifaceted roles when co-expressed with Foxo. **2**(1): 5–10. doi:10.4236/apd.2013.21002.

Wei, Y., Gokhale, R.H., Sonnenschein, A., Montgomery, K.M., Ingersoll, A., and Arnosti, D.N. 2016. Complex cis-regulatory landscape of the insulin receptor gene underlies the broad expression of a central signalling regulator. Development **143**(19): 3591–3603. Company of Biologists. doi:10.1242/dev.138073.

Yokoyama, T., and Nakamura, T. 2011. Tribbles in disease: Signalling pathways important for cellular function and neoplastic transformation. Cancer Sci. **102**(6): 1115–1122. John Wiley & Sons, Ltd. doi:10.1111/j.1349-7006.2011.01914.x.

Chapter 10: Summary and Future Direction

The Drosophila mitochondria fission protein is pro-survival

The Dynamin superfamily of genes encodes a highly conserved family of proteins that are present in the cytoplasm of all eukaryotic organisms, including plants, mammals, and yeast. Drp1 is responsible for the process of the fission of mitochondria in eukaryotic cells (Bleazard et al. 1999; Hu et al. 2017) [Chapter1 and 2]. Mitochondrial dysfunction underlies important mechanisms implicated in the pathogenesis of PD (McLelland et al. 2014). When altered, genes that function in the maintenance of mitochondria health, have been demonstrated to cause neurodegeneration due to mitochondrial dysfunction (McLelland et al. 2014). With these observations as a basis, I pursued the hypothesis that the expression of the *Drp1* gene can change mitochondrial dynamics to affect mitochondrial function which, in turn, may influence greatly phenotypes that contribute to models of neurodegenerative disease and ageing. Cellular stress, such as hypoxia in mice (Kim et al. 2011) and rifampicin in human hepatocyte lines (Li et al. 2019), increased the prevalence of mitochondrial fragmentation through translocation Drp1 to mitochondria. The hyperactivity of Drp1 is a cellular response against increased stress promoted cell death (Kim et al. 2011; Pradeep et al. 2014; Zemirli et al. 2018; Li et al. 2019). The overexpression of *Drp1* in selected neurons, decreases median lifespan and climbing ability over time [Chapter 2]. My study found the overexpression of *Drp1* results in a PD-like phenotype and is detrimental for Drosophila healthspan. The gain of function may likely activate the downstream signal transduction pathways to initiate mechanisms associated with cell death as do some aspects of cellular stress in mammals (Pradeep et al. 2014) (Figure 10.1). The complex aspects of mitochondrial fission controlled by *Drp1/DMN1* seem to be very well conserved between mammals and flies.

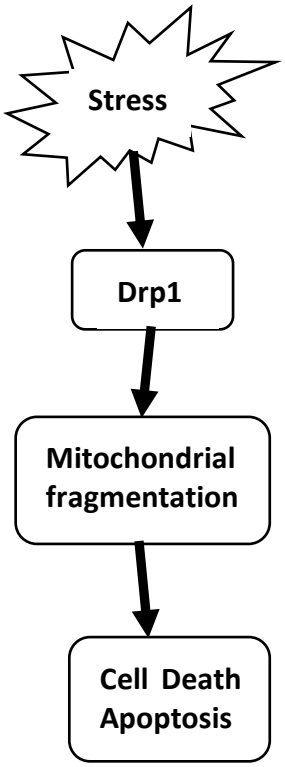

Figure 10.1: Diagrammatic representation of the effect of cellular and envoirmental stress on Drp1 and mitochondria. The overall effect of either cellular stresses or the overexpression of *Drp1* seems to be well conserved between flies and mammals.

Drp1 influences the Bcl-2 protein induced apoptosis

Apoptosis is one of the main mechanisms implicated in the neuronal loss of PD (Erekat 2018). The post-mortem and in vitro studies confirm the vital role of apoptosis in the degeneration of dopaminergic (DA) neurons. In my study, I altered the expression of Drp1, mitochondrial fission protein-encoding gene, in the DA neurons and the developing eye (Chapter 2). Manipulations in the neurons resulted in flies with compromised survival and locomotor functions. The overexpression or inhibition of *Drp1* may alter the mitochondrial function which leads to consequences that range from an enhanced homeostasis to the facilitation of apoptosis (Frank et al. 2001; Hu et al. 2017; Rana et al. 2017). The *Drp1*-dependent phenotypes may be modified through changes to the expression of Bcl-2 family of genes. I obtained strong evidence that the

overexpression of *Buffy* or *Debcl* inhibition can amend the phenotypes that result from the overexpression of *Drp1*. These interactions suggest a strong involvement of the Bcl-2 family of proteins in the degeneration of DA neurons during PD pathogenesis (Van der Heide and Smidt 2013; Robinson et al. 2018; Erekat 2018). Mitochondria undergo extensive fission during apoptosis (Desagher and Martinou 2000) and the Drp1 protein is essential for the release of cytochrome c from the inner mitochondrial membrane (Breckenridge et al. 2008; Clerc et al. 2014). In humans, the pro-apoptotic Bcl-2 protein, Bax co-localizes with Drp1 (Karbowski et al. 2002) but the consequence of this interaction remains unclear. Proposed models of Bax and Drp1 function suggest that these proteins may co-operate to carry out mitochondrial apoptosis (Martinou and Youle 2011; Maes et al. 2019). However, the role of Drp1 in apoptosis is dependent upon mitochondrial fission activity and remains the subject of active investigation. In drosophila, the Drp1 and Debcl proteins are found to co-localize on mitochondrial membrane and act to promote apoptosis (Clavier et al. 2015). In mammalian cell culture, another Bcl-2 protein, Bcl-$x_{L,}$ can induce Drp1-dependent mitochondrial fission; as the GTPase activity of Drp1 is increased *in vitro* and the formation of synaptic vesicle cluster is mediated in the presence of this protein (Li et al. 2008; Berman et al. 2009). In addition, studies reveal that the phenotypes associated with alterations to the expression of the inner mitochondrial protein gene *GHITM* can be suppressed by the expression of *Buffy* (Githure and Staveley 2016b). The GHITM protein contains a Bax-inhibitor motif and is involved in the regulation of mitochondrial morphology, and downregulation of GHITM causes mitochondrial fragmentation and apoptosis (Willems et al. 2015). The interaction points of *Buffy, Debcl* and *Drp1* are remaines to be determined by further studies and will possibly find out the role of Drp1 in inner mitochondrial protein homeostasis.

The transcription activity of *Rbf* has been demonstrated to decrease the transcription of *Buffy* and promotes the activation of the JNK pathway in flies (Clavier et al. 2015). However, the role of Rbf is much more complex than simply the regulation of the JNK pathway and the overall cell death or cell survival signalling can be identified by the phenotypic expressions. Buffy is the only anti-apoptotic Bcl-2 family protein in drosophila and gives a survival advantage over multiple pro-apoptotic proteins (Githure and Staveley 2016a, 2017a, 2017b) (Figure 10.2). However, alterations in the expression of *Buffy* in the *Drp1* inhibition neurons only partially modify the phenotype, shows cell survival is extremely sensitive of mitochondrial dynamics (Chapter 3). I altered the expression of Buffy and Debcl separately to observe the phenotypes produced in the common background of Rbf inhibition (Chapter 4). The expression of *Buffy* and *Debcl-RNAi* provided an advantage to survival and seems to amplify the cell survival signals in an *Rbf* inhibition background. The pro-survival effect of Buffy is well established (Githure and Staveley 2016a, 2017a, 2017b) and gives survival advantage to neurons under condition of *Rbf* inhibition.

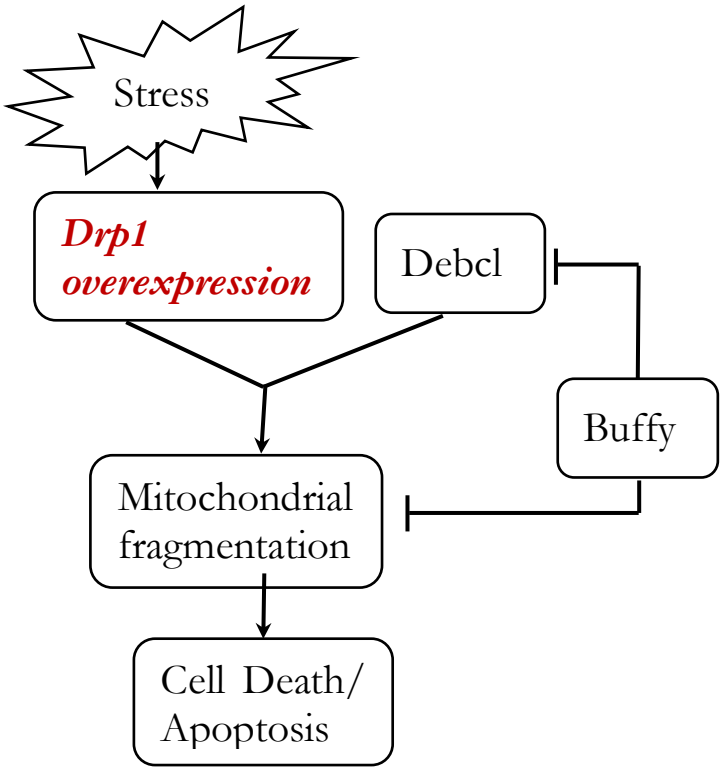

Figure 10.2: Diagrammatic representation of the interpretation of the interactions of *Drp1*, *Buffy* and *Debcl* upon mitochondria under stress in flies.

Drp1 effect on the *Parkin* and *α-synuclein* models of PD

To protect the cell, the process of mitophagy is utilized to remove dysfunctional mitochondria. The Pink1/Parkin cell signalling transduction pathway believed to be responsible primarily for the turnover of defective mitochondria via mitophagy. I utilized PD models (*Parkin* and *α-synuclein*) to investigate the effect of the overexpression or inhibition of *Drp1*. In the *parkin* loss of function critical class, the overexpression of *Drp1* has acted to enhance the phenotypes (Chapter 2). This finding indicates the involvement of Drp1 in a pro-apoptotic signalling mechanism, which may be initiated by the production of excess *Drp1* protein, coupled with a diminished presence of the parkin protein. These observations are consistent with studies that found that parkin may ubiquitinylate the Drp1 protein to promote degradation and that the inhibition of the parkin E3

ubiquitin ligase activity may impair the ubiquitination of substrates to cause of neuronal degradation effect in PD (Willems et al. 2015). The inhibition of *Drp1* can result in the suppression of the loss of *parkin*-induced phenotypes which may indicate an improvement in cellular homeostasis (Chapter 2); the pathway appears to be very well-conserved between mammals and diptera. The *Drp1* inhibition may prevent the toxic aspects of the inhibition of *parki*n signalling to provide an advantage in survival. As to the possibility that the Drp1 and parkin proteins interact in a direct manner remains to be elucidated, this relationship can serve as therapeutic target. The Drp1 inhibition suppresses the MPTP-induced reduction in DA neurons and alleviates the behavioral deficits induced by MPTP in mice (Filichia et al. 2016). Mutations of Pink and parkin have been found to increase the mitochondrial localization of Drp1 in Drosophila (Poole et al. 2010). The *parkin*-knockout mouse embryonic fibroblasts (MEFs) increase the mitochondrial fission in *Drp1* knockout cells (Roy et al. 2016) and is consistent with the hypothesis that the *Pink1* and *parkin* mutations result in an increase in the localization of the Drp1 protein to the mitochondria in Drosophila (Poole et al. 2010). The most plausible interpretation may be that this mechanism may act to achieve a healthy balance between the amounts of the parkin and Drp1 proteins on the surface of mitochondria in neurons.

The *α-synuclein*-induced PD model in Drosophila is a robust model for the study of neuronal degeneration and programmed cell death (Feany and Bender 2000). The loss of function of *Drp1* alleviates the compromised longevity and climbing defects in the *α-synuclein*-induced PD model (Chapter 6). This survival enhancement may be due to the inhibition of *Drp1* and was demonstrated both in *Pink1* deletion and MPTP-treated mice models of PD (Rappold et al. 2014;

Filichia et al. 2016). This is consistent with results of the expression of a-synuclein in combination with *Drp1* inhibition, as predicted from experiments in mammalian cell culture (Fan et al. 2019). The inhibition of *Drp1* produces a discontinuation of the translocation of p53 to the mitochondria and the subsequent activation of BAX and PUMA-mediated apoptotic pathway (Filichia et al. 2016). The PD related proteins including parkin, Pink1 and α-synuclein regulate the mitochondrial function with the assistance of Drp1 (Yang et al. 2008; Kamp et al. 2010; Liu et al. 2011; Filichia et al. 2016). The overexpression of *Drp1* along with expression of *α-synuclein* in the DA neurons has been shown to counteract the *α-synuclein*-induced longevity phenotypes but further impairs the climbing abilities of the flies throughout the life of the organisms (Chapter 6). In general, cellular stress increases the *Drp1* localization on mitochondria to promote mitophagy or apoptosis depending on the cellular environment (Pradeep et al. 2014). The *Drp1* assists different pathways to maintain mitochondrial health and cellular homeostasis.

The expression of *Rbf* in an *α-synuclein*-induced PD model in Drosophila rescues the phenotype (Chapter 6). The Rbf induced protection could be by initiating apoptosis which decrease the cellular stress caused by the accumulation of the *α-synuclein* protofibrils. This survival enhancement by *Rbf* overexpression was demonstrated in other PD models in Drosophila that included the mitochondrial *parkin-RNAi* model (Chapter 5), Drp1 expression and Drp1 inhibition models (Chapter 4). However, the expression of *Rbf* without the co-expression of the other genes of interest in the selected DA neurons compromised lifespan and climbing ability. Rbf can regulate cell proliferation and apoptosis depending on the cellular signalling (Tanaka-Matakatsu et al.

2009). The inhibition of the transcriptional regulator *Rbf* in DA neurons resulted in shortened lifespan and a precocious loss in climbing ability

Direct and indirect regulatory partners of Drp1

Drp1 functions through interactions with a number of proteins to cooperatively regulate the process of mitochondrial fission. The inhibition of *Drp1* through the directed expression of *UAS-Drp1-RNAi* transgenes can lead to an increased lifespan coupled with diminished climbing abilities over time. The reduced climbing abilities during interference of the expression of *Drp1* seems to be consequence of the disruption of a number of complex sub-cellular relationships. I have evaluated the potential of protein partners that are less known for their regulatory relationship to *Drp1* and to the health of the mitochondrial population. The Rb protein functions with Drp1 to promote mitochondrial-dependent cell death induced by cadmium in hepatocytes and the inhibition of *Drp1* acts to counteract the effects of mitochondrial mediated cell death induced by the Rb protein (Zhang et al. 2019). I found that the phenotypes produced by co-inhibition of *Drp1* and *Rbf* are very similar to the consequences of the inhibition of *Drp1* (Chapter 2 and Chapter 5) and the phenotypes of *Drp1* overexpression and *Rbf* inhibition are very close (Chapter 2 and Chapter 5). Although this information may not be enough to chart-out the regulatory relationship between the two proteins, I have established that overexpression of *Rbf* can rescue the phenotypes caused by *Drp1* overexpression in flies (Chapter 4). The mechanism of action for this protection is not established, however the expression of *Rbf* may reduce the potential of cellular stress caused by the *Drp1* overexpression. The effect of *Rbf* overexpression is beneficial for cell which is undergoing excessive mitochondrial fission.

The *foxo*-induced Drosophila eye phenotype

The overexpression of *Drp1* in selected neurons results in a compromised lifespan along with defects in climbing abilities over time (Chapter 2). The suppression of *foxo* in the background of directed overexpression of *Drp1* can increase the lifespan and climbing ability, perhaps as *foxo* may activate the Drp1-mediated fission, inhibition of *foxo* may be beneficial for cell survival under these experimental conditions (Shi et al. 2018). The inhibition of *foxo* along with loss of *Drp1* can result in a decrease in the median lifespan. Inhibition of *Drp1* may provide a limited survival advantage and the inhibition of *foxo* may increase the overall stress to result in cell death. Regardless, the survival advantage of *Drp1* inhibition is limited and likely helps cell survival by diminishment and delay of apoptotic signals.

The loss of *foxo* function, in combination with the inhibition of *Rbf* activities may increase lifespan (Chapter 8) as *Rbf* is involved in insulin receptor signalling (Acharya et al. 2012), a complex relationship may exist between these two components. Additionally, the inhibition of *Rbf* expression seems to ameliorate the *foxo*-induced disrupted eye phenotype (Chapter 9). These experiments suggest either a direct or indirect involvement of *Rbf* or *foxo* in these processes. Finally, when the expression of *foxo* is inhibited in the *α-synuclein*-induced Drosophila model of PD, this gave a dramatic survival advantage to flies (Chapter 8). My result support the hypothesis that reduced *foxo* function may provide protection against the well-demonstrated toxicity observed to be induced by *α-synuclein*. The transcription activity of *foxo/FoxO3a* plays a pivotal role in *α-synuclein*-induced toxicity.

Limitations of the study

The limitation of our study is that the experimental design could have some technical flaws. We overexpressed and inhibited the homologues of *H. sapiens* genes implicated for neurodegeneration using the UAS-Gal4 and RNAi system. The transgenes employed have been previously characterized by other groups; however, I did not assay the expression of these transgenes personally. I did express overexpression and inhibition line together to see if the results were similar to control, but a protein assay would have given more certainty to the expression levels. I did utilize more than one *RNAi* for the *Drp1*, *Rbf* and *trbl* for expression analysis which helps alleviate this effect in these datasets. Our results provided us with the phenotype which traditionally signifies degenerations and decreased homeostasis. However, we did not quantify the expression level of these genes by quantitative methods such as PCR, RT-PCR or western blotting. We implied that phenotypic effects were due to the excessive mitochondrial fission or excessive apoptosis, giving reference to the previous studies, but no molecular staining or assay was done to verify these interpretations. Molecular work to assay the amount of protein expression in these cases would help to explain some of the unexpected effects witnessed in these experiments.

Future directions

For the most part, I believe that my studies have helped put into perspective the pro-survival advantages that result from inhibition of the Dynamin 1-like protein homologue *Drp1* in Drosophila. The experiments presented in this thesis anticipate that Drp1 has an active role in maintaining mitochondrial homeostasis. Further investigations should focus on studies into the potential interactions between *Drp1* and other genes of interest. The understanding of sensitivity

of cells following the loss and gain of *Drp1* expression is crucial to the potential utilization of this protein as a target of therapeutic approaches in the treatment of a wide range of human conditions. The evaluation of multiple approaches to control of *Drp1* may be required to determine the optimum conditions of Drp1 expression that favour cell survival. One important area of research may centre upon the incompletely understood relationship between the Drp1 protein and the Bcl-2 family of proteins. Apparently, Drp1 functions in tandem with the Debcl protein to promote cell death. Studies of specific protein interactions are desirable to help come to a clear understanding of the roles of *Rbf*, *Drp1* and the *Bcl-2*-related genes in the regulation of mitochondrial health. Finally, further investigation into the interaction between Drp1 and parkin is required to more fully understand the effects that the overexpression of *Drp1* has upon flies when *parkin* is inhibited or when human *α-synuclein* is expressed to produce phenotypes that model of PD. As the survival benefit of inhibition of *Drp1* is subtle and *Drp1* expression provides a survival advantage, such interaction studies should help us to differentiate the molecular mechanisms that contribute to the *parkin* loss of function and the ectopic *alpha-synuclein* "gain of function" Drosophila models of PD and, consequently a fuller understanding of the role of altered *Drp1* expression at the level of molecular cell biology.

Bibliography

Acharya, P., Negre, N., Johnston, J., Wei, Y., White, K.P., Henry, R.W., and Arnosti, D.N. 2012. Evidence for Autoregulation and Cell Signalling Pathway Regulation From Genome-Wide Binding of the Drosophila Retinoblastoma Protein. G3 Genes, Genomes, Genet. **2**(11): 1459–1472. doi:10.1534/g3.112.004424.

Angelova, D.M., Jones, H.B.L., and Brown, D.R. 2018. Levels of a-and b-synuclein regulate cellular susceptibility to toxicity from a-synuclein oligomers. FASEB J.: 995–1006. doi:10.1096/fj.201700675R.

Berman, S.B., Chen, Y.B., Qi, B., McCaffery, J.M., Rucker, E.B., Goebbels, S., Nave, K.A., Arnold, B.A., Jonas, E.A., Pineda, F.J., and Hardwick, J.M. 2009. Bcl-x L increases mitochondrial fission,

fusion, and biomass in neurons. J. Cell Biol. **184**(5): 707–719. J Cell Biol. doi:10.1083/jcb.200809060.

Bleazard, W., McCaffery, J.M., King, E.J., Bale, S., Mozdy, A., Tieu, Q., Nunnari, J., and Shaw, J.M. 1999. The dynamin-related GTPase Dnm1 regulates mitochondrial fission in yeast. Nat. Cell Biol. **1**(5): 298–304. Macmillan Magazines Ltd. doi:10.1038/13014.

Breckenridge, D.G., Kang, B.-H., Kokel, D., Mitani, S., Staehelin, L.A., and Xue, D. 2008. Caenorhabditis elegans drp-1 and fis-2 regulate distinct cell-death execution pathways downstream of ced-3 and independent of ced-9. Mol. Cell **31**(4): 586–97. NIH Public Access. doi:10.1016/j.molcel.2008.07.015.

Chan, F.K.M., and Baehrecke, E.H. 2012, January 20. RIP3 finds partners in crime. Cell Press. doi:10.1016/j.cell.2011.12.020.

Chang, C.-R., and Blackstone, C. 2007. Cyclic AMP-dependent Protein Kinase Phosphorylation of Drp1 Regulates Its GTPase Activity and Mitochondrial Morphology. J. Biol. Chem. **282**(30): 21583–21587. doi:10.1074/jbc.C700083200.

Chang, C.R., and Blackstone, C. 2010. Dynamic regulation of mitochondrial fission through modification of the dynamin-related protein Drp1. *In* Annals of the New York Academy of Sciences. Blackwell Publishing Inc. pp. 34–39. doi:10.1111/j.1749-6632.2010.05629.x.

Chistiakov, D.A., Sobenin, I.A., Revin, V. V., Orekhov, A.N., and Bobryshev, Y. V. 2014. Mitochondrial aging and age-related dysfunction of mitochondria. Hindawi Publishing Corporation. doi:10.1155/2014/238463.

Clavier, A., Ruby, V., Rincheval-Arnold, A., Mignotte, B., and Guénal, I. 2015. The Drosophila retinoblastoma protein, Rbf1, induces a Debcl- and Drp1-dependent mitochondrial apoptosis. J. Cell Sci. **128**(17): 3239–49. The Company of Biologists Ltd. doi:10.1242/jcs.169896.

Clerc, P., Ge, S.X., Hwang, H., Waddell, J., Roelofs, B.A., Karbowski, M., Sesaki, H., and Polster, B.M. 2014. Drp1 is dispensable for apoptotic cytochrome c release in primed MCF10A and fibroblast cells but affects Bcl-2 antagonist-induced respiratory changes. Br. J. Pharmacol. **171**(8): 1988–1999. John Wiley and Sons Inc. doi:10.1111/bph.12515.

Cribbs, J.T., and Strack, S. 2007. Reversible phosphorylation of Drp1 by cyclic AMP-dependent protein kinase and calcineurin regulates mitochondrial fission and cell death. EMBO Rep. **8**(10): 939–44. European Molecular Biology Organization. doi:10.1038/sj.embor.7401062.

Cribbs, J.T., and Strack, S. 2009. Chapter 13 Functional Characterization of Phosphorylation Sites in Dynamin-Related Protein 1. NIH Public Access. doi:10.1016/S0076-6879(09)05013-7.

Desagher, S., and Martinou, J.C. 2000, September 1. Mitochondria as the central control point of apoptosis. Trends Cell Biol. doi:10.1016/S0962-8924(00)01803-1.

Erekat, N.S. 2018. Apoptosis and its Role in Parkinson's Disease. *In* Parkinson's Disease: Pathogenesis and Clinical Aspects. Codon Publications. pp. 65–82. doi:10.15586/codonpublications.parkinsonsdisease.2018.ch4.

Estaquier, J., and Arnoult, D. 2007. Inhibiting Drp1-mediated mitochondrial fission selectively prevents the release of cytochrome c during apoptosis. Cell Death Differ. **14**(6): 1086–1094. Nature Publishing Group. doi:10.1038/sj.cdd.4402107.

Fan, R.Z., Guo, M., Luo, S., Cui, M., and Tieu, K. 2019. Exosome release and neuropathology induced by α-synuclein: New insights into protective mechanisms of Drp1 inhibition. Acta Neuropathol. Commun. **7**(1): 184. BioMed Central Ltd. doi:10.1186/s40478-019-0821-4.

Feany, M.B., and Bender, W.W. 2000. A Drosophila model of Parkinson's disease. Nature 404(6776): 394–398. Nature Publishing Group. doi:10.1038/35006074.

Filichia, E., Hoffer, B., Qi, X., and Luo, Y. 2016. Inhibition of Drp1 mitochondrial translocation provides neural protection in dopaminergic system in a Parkinson's disease model induced by MPTP. Sci. Rep. 6: 32656. Nature Publishing Group. doi:10.1038/srep32656.

Frank, S., Gaume, B., Bergmann-Leitner, E.S., Leitner, W.W., Robert, E.G., Catez, F., Smith, C.L., and Youle, R.J. 2001. The Role of Dynamin-Related Protein 1, a Mediator of Mitochondrial Fission, in Apoptosis. Dev. Cell 1(4): 515–525. doi:10.1016/S1534-5807(01)00055-7.

Githure, P.M., and Staveley, B.E. (n.d.). Overexpression of Buffy enhances the loss of parkin and suppresses the loss of Pink1 phenotypes in Drosophila. doi:10.1139/gen-2016-0165.

Githure, P.M., and Staveley, B.E. 2016a. The Bcl-2 homologue Buffy rescues α-synuclein-induced Parkinson disease-like phenotypes in Drosophila. BMC Neurosci. 17(1): 24. BioMed Central Ltd. doi:10.1186/s12868-016-0261-z.

Githure, P.M., and Staveley, B.E. 2016b, October. The inhibition of CG2076, the GHITM homologue in neurons of Drosophila Melanogaster can be rescued by Buffy. Available from https://www.researchgate.net/publication/313476508_The_inhibition_of_CG2076_the_GHITM_homologue_in_neurons_of_Drosophila_Melanogaster_can_be_rescued_by_Buffy [accessed 20 September 2020].

Githure, P.M., and Staveley, B.E. 2017a. Bax-inhibitor-1 knockdown phenotypes are suppressed by Buffy and exacerbate degeneration in a Drosophila model of Parkinson disease. doi:10.7717/peerj.2974.

Githure, P.M., and Staveley, B.E. 2017b. A loss of Pdxk model of Parkinson disease in Drosophila can be suppressed by Buffy. BMC Res Notes 10: 205. doi:10.1186/s13104-017-2526-8.

Guo, X., Sesaki, H., and Qi, X. 2014. Drp1 stabilizes p53 on the mitochondria to trigger necrosis under oxidative stress conditions in vitro and in vivo. Biochem. J. 461(1): 137–146. Portland Press Ltd. doi:10.1042/BJ20131438.

Han, X.J., Lu, Y.F., Li, S.A., Kaitsuka, T., Sato, Y., Tomizawa, K., Nairn, A.C., Takei, K., Matsui, H., and Matsushita, M. 2008. CaM kinase Iα-induced phosphorylation of Drp1 regulates mitochondrial morphology. J. Cell Biol. 182(3): 573–585. J Cell Biol. doi:10.1083/jcb.200802164.

He, B., Lu, N., and Zhou, Z. 2009, December. Cellular and nuclear degradation during apoptosis. NIH Public Access. doi:10.1016/j.ceb.2009.08.008.

Heide Van der, L.P., and Smidt, M.P. 2013, April. The BCL2 code to dopaminergic development and Parkinson's disease. Trends Mol Med. doi:10.1016/j.molmed.2013.02.003.

Hu, C., Huang, Y., and Li, L. 2017, January 13. Drp1-dependent mitochondrial fission plays critical roles in physiological and pathological progresses in mammals. MDPI AG. doi:10.3390/ijms18010144.

Ingerman, E., Perkins, E.M., Marino, M., Mears, J.A., McCaffery, J.M., Hinshaw, J.E., and Nunnari, J. 2005. Dnm1 forms spirals that are structurally tailored to fit mitochondria. J. Cell Biol. 170(7): 1021–7. Rockefeller University Press. doi:10.1083/jcb.200506078.

Kamp, F., Exner, N., Lutz, A.K., Wender, N., Hegermann, J., Brunner, B., Nuscher, B., Bartels, T., Giese, A., Beyer, K., Eimer, S., Winklhofer, K.F., and Haass, C. 2010. Inhibition of mitochondrial fusion by α-synuclein is rescued by PINK1, Parkin and DJ-1. EMBO J. 29(20): 3571–3589. European Molecular Biology Organization. doi:10.1038/emboj.2010.223.

Karbowski, M., Lee, Y.-J., Gaume, B., Jeong, S.-Y., Frank, S., Nechushtan, A., Santel, A., Fuller, M., Smith, C.L., and Youle, R.J. 2002. Spatial and temporal association of Bax with mitochondrial fission sites, Drp1, and Mfn2 during apoptosis. J. Cell Biol. **159**(6): 931–8. The Rockefeller University Press. doi:10.1083/jcb.200209124.

Kim, H., Scimia, M.C., Wilkinson, D., Trelles, R.D., Wood, M.R., Bowtell, D., Dillin, A., Mercola, M., and Ronai, Z.A. 2011. Fine-Tuning of Drp1/Fis1 Availability by AKAP121/Siah2 Regulates Mitochondrial Adaptation to Hypoxia. Mol. Cell **44**(4): 532–544. Mol Cell. doi:10.1016/j.molcel.2011.08.045.

Labrousse, A.M., Zappaterra, M.D., Rube, D.A., and Van der Bliek, A.M. 1999. C. elegans dynamin-related protein DRP-1 controls severing of the mitochondrial outer membrane. Mol. Cell **4**(5): 815–826. Cell Press. doi:10.1016/S1097-2765(00)80391-3.

Lackner, L.L., Horner, J.S., and Nunnari, J. 2009. Mechanistic analysis of a dynamin effector. Science **325**(5942): 874–7. American Association for the Advancement of Science. doi:10.1126/science.1176921.

Legesse-Miller, A., Massol, R.H., and Kirchhausen, T. 2003. Constriction and Dnm1p Recruitment Are Distinct Processes in Mitochondrial Fission. Mol. Biol. Cell **14**(5): 1953–1963. doi:10.1091/mbc.e02-10-0657.

Li, F., Zhou, J., Li, Y., Sun, K., and Chen, J. 2019. Mitochondrial Damage and Drp1 Overexpression in Rifampicin- and Isoniazid-induced Liver Injury Cell Model. J. Clin. Transl. Hepatol. **7**(X): 1–6. Xia & He Publishing. doi:10.14218/jcth.2018.00052.

Li, H., Alavian, K.N., Lazrove, E., Mehta, N., Jones, A., Zhang, P., Licznerski, P., Graham, M., Uo, T., Guo, J., Rahner, C., Duman, R.S., Morrison, R.S., and Jonas, E.A. 2013. A Bcl-x L -Drp1 complex regulates synaptic vesicle membrane dynamics during endocytosis. Nat. Cell Biol. **15**(7): 773–785. doi:10.1038/ncb2791.

Li, H., Chen, Y., Jones, A.F., Sanger, R.H., Collis, L.P., Flannery, R., McNay, E.C., Yu, T., Schwarzenbacher, R., Bossy, B., Bossy-Wetzel, E., Bennett, M.V.L., Pypaert, M., Hickman, J.A., Smith, P.J.S., Hardwick, J.M., and Jonas, E.A. 2008. Bcl-xL induces Drp1-dependent synapse formation in cultured hippocampal neurons. Proc. Natl. Acad. Sci. U. S. A. **105**(6): 2169–2174. Proc Natl Acad Sci U S A. doi:10.1073/pnas.0711647105.

Liu, W., Acín-Peréz, R., Geghman, K.D., Manfredi, G., Lu, B., and Li, C. 2011. Pink1 regulates the oxidative phosphorylation machinery via mitochondrial fission. Proc. Natl. Acad. Sci. U. S. A. **108**(31): 12920–12924. Proc Natl Acad Sci U S A. doi:10.1073/pnas.1107332108.

Maes, M.E., Grosser, J.A., Fehrman, R.L., Schlamp, C.L., and Nickells, R.W. 2019. Completion of BAX recruitment correlates with mitochondrial fission during apoptosis. Sci. Rep. **9**(1). Nature Publishing Group. doi:10.1038/s41598-019-53049-w.

Martinou, J.C., and Youle, R.J. 2011, July 19. Mitochondria in Apoptosis: Bcl-2 Family Members and Mitochondrial Dynamics. Dev Cell. doi:10.1016/j.devcel.2011.06.017.

McLelland, G.L., Soubannier, V., Chen, C.X., McBride, H.M., and Fon, E.A. 2014. Parkin and PINK1 function in a vesicular trafficking pathway regulating mitochondrial quality control. EMBO J. **33**(4): 282–295. doi:10.1002/embj.201385902.

Mears, J.A., Lackner, L.L., Fang, S., Ingerman, E., Nunnari, J., and Hinshaw, J.E. 2011. Conformational changes in Dnm1 support a contractile mechanism for mitochondrial fission. Nat. Struct. Mol. Biol. 18(1): 20–26. Nature Publishing Group. doi:10.1038/nsmb.1949.

Parsons, M.J., and Green, D.R. 2010. Mitochondria in cell death. Essays Biochem. 47: 99–114.

Portland Press Limited. doi:10.1042/bse0470099.
Poole, A.C., Thomas, R.E., Yu, S., Vincow, E.S., and Pallanck, L. 2010. The Mitochondrial Fusion-Promoting Factor Mitofusin Is a Substrate of the PINK1/Parkin Pathway. PLoS One **5**(4): e10054. Public Library of Science. doi:10.1371/journal.pone.0010054.
Pradeep, H., Sharma, B., and Rajanikant, G.K. 2014. Drp1 in Ischemic Neuronal Death: An Unusual Suspect. Curr. Med. Chem. **21**(19): 2183–2189. Bentham Science Publishers Ltd. doi:10.2174/09298673216613122820351 3.
Rana, A., Oliveira, M.P., Khamoui, A. V., Aparicio, R., Rera, M., Rossiter, H.B., and Walker, D.W. 2017. Promoting Drp1-mediated mitochondrial fission in midlife prolongs healthy lifespan of Drosophila melanogaster. Nat. Commun. **8**(1): 1–14. Nature Publishing Group. doi:10.1038/s41467-017-00525-4.
Rappold, P.M., Cui, M., Grima, J.C., Fan, R.Z., De Mesy-Bentley, K.L., Chen, L., Zhuang, X., Bowers, W.J., and Tieu, K. 2014. Drp1 inhibition attenuates neurotoxicity and dopamine release deficits in vivo. Nat. Commun. **5**(1): 1–13. Nature Publishing Group. doi:10.1038/ncomms6244.
Robinson, E.J., Aguiar, S.P., Kouwenhoven, W.M., Starmans, D.S., von Oerthel, L., Smidt, M.P., and van der Heide, L.P. 2018. Survival of midbrain dopamine neurons depends on the Bcl2 factor Mcl1. Cell Death Discov. **4**(1). Springer Nature. doi:10.1038/s41420-018-0125-7.
Roy, M., Itoh, K., Iijima, M., and Sesaki, H. 2016. Parkin suppresses Drp1-independent mitochondrial division. Biochem. Biophys. Res. Commun. **475**(3): 283–8. NIH Public Access. doi:10.1016/j.bbrc.2016.05.038.
Schmitt, K., Grimm, A., Dallmann, R., Oettinghaus, B., Restelli, L.M., Witzig, M., Ishihara, N., Mihara, K., Ripperger, J.A., Albrecht, U., Frank, S., Brown, S.A., and Eckert, A. 2018. Circadian Control of DRP1 Activity Regulates Mitochondrial Dynamics and Bioenergetics. Cell Metab. **27**(3): 657-666.e5. Cell Press. doi:10.1016/j.cmet.2018.01.011.
Shi, Y., Fan, S., Wang, D., Huyan, T., Chen, J., Chen, J., Su, J., Li, X., Wang, Z., Xie, S., Yun, C., Li, X., and Tie, L. 2018. FOXO1 inhibition potentiates endothelial angiogenic functions in diabetes via suppression of ROCK1/Drp1-mediated mitochondrial fission. Biochim. Biophys. Acta - Mol. Basis Dis. **1864**(7): 2481–2494. Elsevier B.V. doi:10.1016/j.bbadis.2018.04.005.
Taguchi, N., Ishihara, N., Jofuku, A., Oka, T., and Mihara, K. 2007. Mitotic phosphorylation of dynamin-related GTPase Drp1 participates in mitochondrial fission. J. Biol. Chem. **282**(15): 11521–11529. doi:10.1074/jbc.M607279200.
Tanaka-Matakatsu, M., Xu, J., Cheng, L., and Du, W. 2009. Regulation of apoptosis of rbf mutant cells during Drosophila development. Dev. Biol. **326**(2): 347–356. Academic Press Inc. doi:10.1016/j.ydbio.2008.11.035.
Willems, P.H.G.M., Rossignol, R., Dieteren, C.E.J., Murphy, M.P., and Koopman, W.J.H. 2015. Cell Metabolism Perspective Redox Homeostasis and Mitochondrial Dynamics. Cell Metab. **22**: 207–218. doi:10.1016/j.cmet.2015.06.006.
Yan, J., Liu, X.H., Han, M.Z., Wang, Y.M., Sun, X.L., Yu, N., Li, T., Su, B., and Chen, Z.Y. 2015. Blockage of GSK3β-mediated Drp1 phosphorylation provides neuroprotection in neuronal and mouse models of Alzheimer's disease. Neurobiol.ageing **36**(1): 211–227. Elsevier Inc. doi:10.1016/j.neurobiolaging.2014.08.005.
Yang, Y., Ouyang, Y., Yang, L., Beal, M.F., McQuibban, A., Vogel, H., and Lu, B. 2008. Pink1 regulates mitochondrial dynamics through interaction with the fission/fusion machinery. Proc. Natl.

Acad. Sci. U. S. A. **105**(19): 7070–7075. Proc Natl Acad Sci U S A. doi:10.1073/pnas.0711845105.

Zemirli, N., Morel, E., and Molino, D. 2018, February 13. Mitochondrial dynamics in basal and stressful conditions. MDPI AG. doi:10.3390/ijms19020564.

Zhang, S., Che, L., He, C., Huang, J., Guo, N., Shi, J., Lin, Y., and Lin, Z. 2019. Drp1 and RB interaction to mediate mitochondria-dependent necroptosis induced by cadmium in hepatocytes. Cell Death Dis. **10**(7): 1–17. Nature Publishing Group. doi:10.1038/s41419-019-1730-y.

Zhao, G., Cao, K., Xu, C., Sun, A., Lu, W., Zheng, Y., Li, H., Hong, G.L., Wu, B., Qiu, Q.M., and Lu, Z. 2017. Crosstalk between mitochondrial fission and oxidative stress in paraquat-induced apoptosis in mouse alveolar type II cells. Int. J. Biol. Sci. **13**(7): 888–900. Ivyspring International Publisher. doi:10.7150/ijbs.18468.